# Oxford Brookes University

# PhD thesis

# Metastatic cell responses to anticancer therapy: The possible role of cancer stem cells

**Raheem Abd Zaid Abed AL-Abedi**

**A thesis submitted in partial fulfilment of the requirements of Oxford Brookes University for the degree of Doctor of Philosophy**

**December 2018**

## Acknowledgement

Foremost, I would like to give my gratefully thank to my first supervisor Professor Munira Kadhim for here suggestion excellent project, and for her continuous support, help, guide and contribution to my PhD thesis. So, I would like to say the biggest thank for her. Extremely thank for my second supervisor Professor Susan Brooks for suggestion the excellent project, for help, the guidance of research and contribution to my thesis. I can't get imagination how I lucky to have excellent advisors and monitors for my thesis.

Beside my supervisors I would like to give extremely thankful for Dr Ammar Mayah for help and guidance in the exosome's isolation and characterisation, I also would like to thank him for wise advice and support all the time during my PhD. Avery special tank goes to Mrs Deborah Lord for her help and advice whenever I asked her. Huge thank goes to other people in genomic instability and cell communication group, Dr Scott Bright, Dr Eman Elbakrawy, Dr Seda Tunkay-Cagaty, Miss Jessica Horsburgh, Miss Brittany Almond for help supports and wise advice whatever I asked them.

Grateful thank for the people in the Gray institution, University of Oxford, Dr Mark Hill Dr James Thompson Mr Luke Bird and Miss Amy Elliott for irradiation. Extremely thank goes for my colleague Mr Sunny Vijen to guide me using qPCR. Special thanks go to Professor Dave Carter for offering using Flow cytometry. Great thank also goes to Dr Genevieve Melling and Miss Migena Tushe for guiding me using flow cytometry. Grateful thank to the home country for offering the scholarship and for funding this project.

Lastly and not the last, I would like to thank my family for help, support and encourage me all the time to target my goal. All the time they believe that I can target this biggest challenge, so I would like to say big thanks for them and dedicate this work for my lovely family.

Thank you very much

*Raheem*

## List of abbreviations

°C Degrees Celsius

ALHD1 Aldehyde dehydrogenase -1

Asp Asparagine

AXL AXL receptor tyrosine kinase

BCSCs Breast cancer stem cells

BM Basement membrane

BSA Bovine serum albumin

CCCM Control cell condition media

CDKN Cyclin-dependent kinase inhibitor

cDNA Complementary deoxyribonucleic acid

CHRK1 Checkpoint kinase 1

CHRK2 Checkpoint kinase 2

CSCs Cancer stem cells

CT scan Computed tomography scan

$dH_2O$ Distilled water

DMEM Dulbecco's Modified Eagle's Medium

DMSO Dimethyl sulfoxide

DNA Deoxyribonucleic Acid

Dnmts DNA methyltransferases

DPX Distyrene, a plasticizer, and xylene

DSB Double strand breaks

dsDNA Double-stranded DNA

DTT DL-dithiothreitol

E-cad E-cadherin

ECM Extracellular matrix

EDTA Ethylenediaminetetraacetic acid

EGF Epidermal growth factor

ENT Epithelial-mesenchymal transition

ER Oestrogen receptor

ESR1 Oestrogen receptor 1

ESR2 Oestrogen receptor 2

EVs Extracellular vesicles

Exo Exosome
FCS Foetal calf serum
GEMM genetically engendering mouse model
GJ Gap junction
GJIC Gap junction intercellular communication
Gy Gray
HBECs Human bronchial epithelial cell
hEs human embryonic stem cell
HMLE Human mammary epithelial cells
HMPA High melting point agar
HPA *Helix pomatia* agglutinin
HR Homologous recombination
hr Hour
ICCM Irradiated cells conditioned media
IL Interleukin
IR Ionizing radiation
ITGB4 integrin subunit beta 4
KCl Potassium chloride
LET Linear energy transfer
LMPA Low melting point agar
M Molar
MAPK Mitogen-activated protein kinase
MEM Minimum essential medium
mg Milligram
mins Minutes
miRNA microRNA
ml Millilitre
mm Millimetre
mM Millimolar
MMPs Matrix metalloproteases
mtDNA mitochondrial DNA
MW Molecular weight
N/S Not significant

ng Nanogram

nm Nanometre

NO Nitric oxide

NTEs Non-target effects

OH Hydroxyl group

p p-value

P/S penicillin-streptomycin

PBS Phosphate buffered saline

PD Population doubling

PDGFR platelet-derived growth factor receptor

PHA-L *Phaseolus vulgaris* leukoagglutinin

PIPES piperazine-N,N′-bis(2-ethanesulfonic acid)

PLAU plasminogen activator urokinase

PNA Peptide nucleic acid

PR progesterone receptors

PVDF polyvinylidene difluoride

qEV qNano extracellular vesicles

qPCR Quantitative polymerase chain reaction

REM Radiation absorbent dose

RIPA Radioimmunoprecipitation assay buffer

RNA Ribonucleic acid

ROS Reactive oxygen species

rpm Revolutions per minute

S Significant

SEM Standard error of the mean

Ser Serine

SI International system of units

$SLe^a$ Sialyl Lewis$^a$

$SLe^x$ Sialyl Lewis$^x$

SNA *Sambucus nigra* agglutinin

SPI Plexin-semaphorin-integrin

ST Sialyl T

STn Sialyl Tn

Sv Sievert
T Ag T antigen
TAM tumour associated macrophage
TBS Tris-buffered saline
TBST Tris-buffered saline with Tween twenty
TF Thomsen-Friedenreich antigen
TGF-β Transforming growth factor-beta
TGF-βR1 transforming growth factor-beta receptor 1
Thr Threonine
Tn Tn antigen
TNBC Triple negative breast cancer
TNF-α Tumour necrosis factor-alpha
uPA urokinase-type plasminogen activator
VEGF Vascular endothelial growth factor
Vim Vimentin
µg Microgram
µl Microlitre
µm Micrometer

**Publications and conferences**

**Publications**

1- Raheem A A AL-Abedi ; Ammar H J Mayah ; Susan A Brooks ; Munira A Kadhim; Ionising radiation altered cell surface glycosylation: promote invasive capacity of breast cancer cells. (Manuscript paper in preparation).

2- Raheem A A AL-Abedi ; Ammar H J Mayah ; Susan A Brooks ; Munira A Kadhim; The role of microvesicle/exosomes in the invasions of breast cancer cells. (Manuscript paper in preparation).

**Conferences**

2018 Raheem A A AL-Abedi ; Ammar H J Mayah ; Susan A Brooks ; Munira A Kadhim; Metastatic cells response to anti-cancer therapy: possible role of cancer

stem cells.  postgraduate symposium, Oxford Brookes University postgraduate symposium, Oxford Brookes University (Poster).

2017 Raheem  A A  AL-Abedi ;  Ammar H J Mayah ;  Susan A Brooks ; Munira A Kadhim; Metastatic cells response to anti-cancer therapy: possible role of cancer stem cells.  postgraduate symposium, Oxford Brookes University (Talk).

2017 Raheem  A A  AL-Abedi ;  Ammar H J Mayah ;  Susan A Brooks ; Munira A Kadhim: Exosomes derived from irradiated cancer cells enhance invasive capacity of unirradiated cells.; ARR Conference: Improving Radiotherapy Response through Radiation; 26 – 28 June at St Hilda's College, Oxford, (Poster).

2017 Raheem  A A  AL-Abedi ;  Ammar H J Mayah ;  Susan A Brooks ; Munira A Kadhim: Ionising radiation enhance metastasis/invasiveness capacity of unirradiated cells. Seed and Soil: In Vivo Models of Metastasis Berlin, Germany: 27 - 29 November 2017, (Poster).

2016 Raheem  A A  AL-Abedi ;  Ammar H J Mayah ;  Susan A Brooks ; Munira A Kadhim: Exosomes derived from irradiated cancer cells enhance invasive capacity of unirradiated cells. UK EV 13 December 2016, Oxford Brookes University, Oxford, UK. 10 January 2016, (Talk).

**Abstract**

Metastasis is a multistep process, by which cancer cells dissociate from the initial site and travel to form new secondary tumours at distant sites. This process has been reported to require epithelial-mesenchymal transition (EMT), by which the epithelial cancer cells convert to a mesenchymal form, associated with increasing levels of vimentin and decrease in E-cadherin markers. Cancer metastasis is also associated with aberrations in cells' glycosylation such as Tn antigen which can be detected by *Helix pomatia* agglutinin (HPA) lectin extract from *Helix pomatia* snails.

Radiotherapy could have an effect on cancer metastasis; by stimulating regulation signalling including ROS, TGF-β, E-cadherin and vimentin. This signalling can promote cancer cells to change from the epithelial to mesenchymal form. The cells behaviour could be mediated by the production of extracellular vesicles/exosomes from irradiated cells, which may have an impact on unirradiated cells. To date, the role of direct and bystander effect of ionising irradiation on the cancer cells glycosylation, EMT markers and invasiveness has not yet been investigated.

Therefore, a study has been established to determine the direct effect, and if the progeny of cancer cells that survive a therapeutic dose of X-radiation show differences in aberrant glycosylation associated with metastasis, EMT markers and their ability to invade compared to unirradiated cells. The study also aims to investigate the bystander effect of extracellular vesicle/exosomes in the invasion of breast cancer cells. The molecular mechanisms that could be involved in the invasion of breast cancer cells following irradiation or exosome transfer were also investigated.

In this study, both cells directly exposed to a therapeutic dose of ionising radiation and unirradiated recipient cells treated with exosomes from irradiated cells showed an increase in vimentin immunopositivity, HPA positivity, a decrease in the E-cadherin immunopositivity and a significant increase in the invasive capacity of the cells. The study also showed that breast cancer cells treated with a single dose of ionising irradiation induce invasion of breast cancer cells *in vitro*. The findings were further confirmed using qPCR and western blot for examination

of selected genes and proteins that have an effect on the invasion of cancer cells following direct ionising irradiation or bystander effect of exosomes and may have an impact on cancer metastasis. The study also showed that exosomes isolated from irradiated cells carried a high quantity of TGF-β protein and specific miRNA which have an impact on the invasion of cancer cells. This study concludes that single therapeutic dose of ionising irradiation induces invasion of cancer cell *in vitro*. In addition, exosomes and its compounds that were isolated from irradiated cell condition media can promote invasion of breast cancer cells, and that could have an implication on cancer therapy in the future.

Contents

## List of figures

## List of tables

# Chapter 1: Introduction

## 1. Introduction

Breast cancer is a common type of cancer in women worldwide (Gangopadhyay *et al.*, 2013). Based on the histological category, breast cancer can be classified into luminal and basal subtypes, represented by cell lines MCF-7 and MDA-MB-231 respectively. Breast cancer can also be classified into luminal A and luminal B. A Luminal A, which is characterised by lower levels of proliferation-related genes and higher levels of oestrogen receptor (ER). Meanwhile, a luminal B subtype, characterised by higher levels of a proliferative index and human epidermal growth factor receptor 2 (HER2) gene expression (Yersal and Barutca, 2014). ER, progesterone receptor (PR) and (HER2) have also been used to subdivide basal breast cancer cells into two types, triple-negative breast cancer (TNBC) cells (lacking of ER, PR and HER2 receptors) and non-TNBC cells (List *et al.*, 2014; Graudenzi *et al.*, 2017).

There is also another classification category based on the stage of the cancer cell, stages 0 to IV. Stage 0 is a small and localised tumour, in which cells are unable to invade and metastasise to other parts of the body. Meanwhile, a tumour in stage IV is malignant and metastasised (Vuong *et al.*, 2014). Much evidence has shown that a small population of cells in the tumour bulk is responsible for cancer initiation, resistance to radiotherapy, metastasis and recurrence (Wang *et al.*, 2013a; Gangopadhyay *et al.*, 2013; Krause *et al.*, 2017). These cells exhibit cancer stem cell characteristics (Al-Hajj *et al.*, 2003; Li *et al.*, 2007; Zhu *et al.*, 2012).

### 1.1 Cancer metastasis

Metastasis is a complex and multistep process in which cancer cells dissociate from a primary tumour and transfer through the lymph or bloodstream to make a new secondary cancer growth in distant site (Cappello, Barresi and Martorana, 2000; Kozlowski, Kozlowska and Kocki, 2015; Wright *et al.*, 2017), as shown in Figure 1.1.

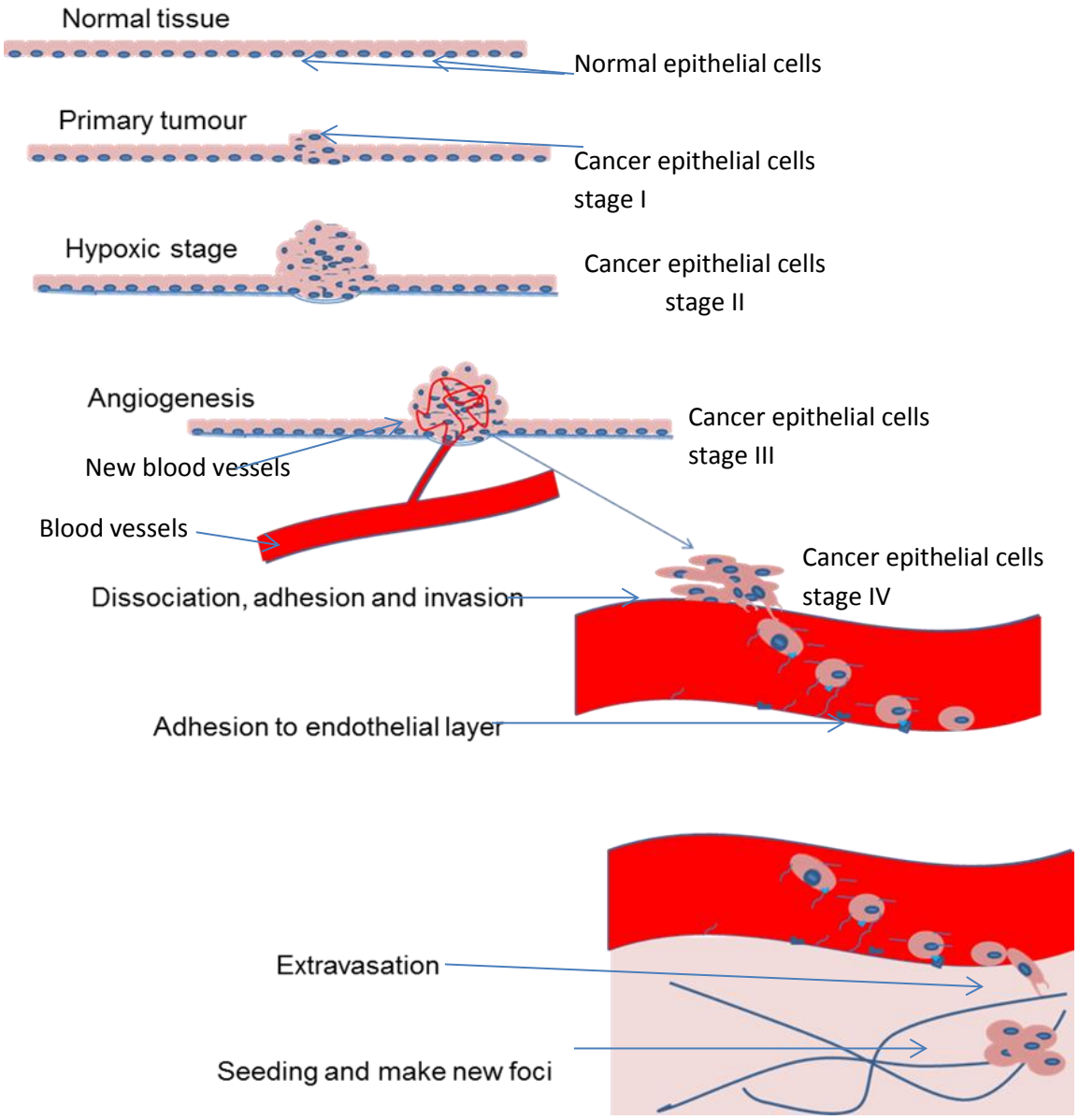


*Figure 1.1 A schematic diagram showing stages of cancer cell metastasis*

The complexity of metastasis includes angiogenesis, epithelial mesenchymal transition (EMT), dissociation from cancer mass, adhesion and invasion of the basement membrane and extracellular matrix, migration frequently through blood and lymph vessels, adhesion to the endothelial layer of vessels, seeding the metastasis cells in the new organ and proliferation of cancer cells to form secondary cancer (Barnhill and Lugassy, 2004). The work described in this thesis focusses particularly on invasion and EMT, and they are described in detail in Sections 1.2 and 1.3. It also investigates the relationship between ionising radiation, EMT, glycosylation and invasion of cancer cells.

### 1.1.1 Angiogenesis and hypoxia

Oxygen and nutrition are delivered to cancer cells by diffusion when the tumour size is less than 2 mm. Otherwise, cells will be in a hypoxic environment (Gimbrone *et al.*, 1972). A tumour under hypoxic conditions can induce vasculogenesis factors; platelet-derived growth factor (PDGF), and vesicular endothelial growth factor I and II (VEGF-I, and VEGF-II) and VEGF-R1, VEGF-R2, Ang-1, and Ang-2 (Berger and Lavie, 2011). Therefore, new blood vessels are generated and pass through the cancer mass (Reviewed by Muz *et al.*, 2015).

### 1.1.2 Dissociation and invasion of cancer cells to the surrounding tissues

It has been reported that cancer cells in a hypoxic environment can exhibit EMT characteristics (Kidd, Shumaker and Ridge, 2014), including downregulation in epithelial markers such as E-cadherin and overexpression of mesenchymal markers, vimentin and N-cadherin (Zhang *et al.*, 2018). The decrease in the expression of E-cadherin causes a reduction in cell-cell attachment, as well as a loss of the polarity of the cells (Zheng *et al.*, 2009). Moreover, an increase in the vimentin cytoskeleton promotes cells to change from epithelial to mesenchymal shape. These changes can help cells to dissociate from the original cancer mass and move (Mendez, Kojima and Goldman, 2010). However, cancer cells need to develop other mechanisms, including the production of enzymes and transcription factors which can help cancer cells to break down the basement membrane and extracellular matrix. Consequently, cancer cells invade and enter the lymphatic and blood vessels preparing to invade and metastasise as described in more detail below in Section 1.2.

### 1.1.3 Adhesion of cancer cells to the endothelial cells

Once cancer cells reach the blood vessels in the target organ, specific interactions can develop between the cancer cells and the endothelial cells. During this interaction, it is believed that cancer cells employ molecular mechanisms similar to those used in leukocyte adhesion and extravasation in the inflammatory response (Barthel *et al.*, 2007). In the paradigm of leukocyte adhesion and extravasation, Sanchez-Madrid and Barreiro (2009) have reported that rolling of leukocytes on the endothelial cells mediated selectin-carbohydrate interaction. This step is followed by activation of integrin, consequently mediating

firm adhesion between leukocytes and endothelial cells. Once leucocytes adhere firmly to the endothelial cells, they begin to extravasate by the aid of vimentin and actin intermediate filaments protein by forming pseudopodia (Sanchez-Madrid and Barreiro, 2009).

### 1.1.4 Seeding of cancer cells in a new environment

Hence cancer cells have extravasated and seeded in the target organ; they then start to change the microenvironment and interact with other cells such as fibroblast cells to block the maturation and function of professional antigen-presenting cells (APCs). Consequently, cancer cells evade the immune system by being protected from NK cells (Rodriguez, Zea and Ochoa, 2003; Amo *et al.*, 2014). It has also been reported that the same signalling involved in the maintenance and development of primary cancer can keep up the growth, proliferation and differentiation of secondary cancer (Hanahan and Weinberg, 2011).

## 1.2 Invasion of cancer cells into the cell membrane and extracellular matrix

As described above in Section 1.1.2, the dissociation, invasion and migration of cancer cells represent the key steps of cancer metastasis. The dissemination of cancer cells from the cancer mass requires loss- of cell-cell attachment, that can be regulated by abrogation of catenin and E-cadherin in the membranes of the cancer cells (Baum, Settleman and Quinlan, 2008). It has been reported that alteration in catenin expression in a primary tumour influences the loss of cell-cell adhesion and induces migration and envision of A-498 and GRC1 kidney cancer cells (Yang *et al.*, 2017). Moreover, downregulation of E-cadherin has also been reported to be associated with cancer metastasis. In this instance, Petrova, Schecterson and Gumbiner (2016) demonstrated that the metastasis of 4T1-hE human mammary cancer cells to the lungs of mice was influenced by reduced E-cadherin adhesive function. Therefore, loss or downregulation of E-cadherin promotes cells to be more motile and move.

Sahai (2005) and Stichel *et al.* (2017) have highlighted the most common mechanisms that explain the motility of cancer cells. These mechanisms include a cluster of cancer cell migration, a sheath of cells motility and mesenchymal-like cells motility. These mechanisms need to be regulated by growth factors, such as

transforming growth factor-β (TGF-β), matrix metalloproteinases (MMPs) and urokinase-type plasminogen activator (uPA) and uPA receptor. Consequently, these regulate the various physiological activities of cancer cells such as EMT, adhesion of cancer cells to the basement membrane (BM), and degradation of BM and extracellular matrix (ECM) by proteolytic enzymes (reviewed by Brooks *et al.*, 2010). Breakdown of BM and ECM can facilitate migration and invasion of cancer cells. The invasion and migration of cancer cells through the BM and ECM until they reach the blood or lymph vessels can be directed by active and passive mechanisms (Bockhorn, Jain and Munn, 2007; Hamill, Paller and Jones, 2010). In the active form of invasion and migration, cancer cells can utilise elements of the cytoskeleton such as laminin and vimentin to produce pseudopodia/ lamellipodia, and direct cells toward the endothelial cells of capillaries (Hamill, Paller and Jones, 2010). In the passive mechanism, cancer cells can enter the blood vessels as a result of damaging of capillaries, due to the pressures of unusual growth of cancer cells which produce mechanical damage (Bockhorn, Jain and Munn, 2007).

It has been demonstrated that the crosstalk between cancer cells, ECM and the adjacent normal cells/ tissues can contribute to the development of cancer in the microenvironment (Van Slambrouck *et al.*, 2009). Activation of TGF- β and MMP in the cancer microenviroment can promote cancer cell motility and invasion (Reviewed by Brooks *et al.*, 2010). The adhesion and invasion of cancer cells to the BM and ECM can maintain a microenvironment where cancer cells can destroy the BM and ECM and move. During the invasion, cancer cells have to attach primarily to the integrin family of adhesion receptors and create integrin–integrin adhesion (Van Slambrouck *et al.*, 2009).

The integrin protein is mainly composed of 18 α and 8 β subunits. Both α and β subunits are composed of several domains with flexible links between them. Each subunit has a binding site, spin helix (calf) and a structured short cytoplasmic tail. The β subunit constitutes of βI domain, hybrid and plexin-semaphorin-integrin (SPI), laminin-epidermal growth factor (EGF), βI tail and cytoplasmic N-terminal domain (Campbell and Humphries, 2011), as illustrated in Figure 1.2.

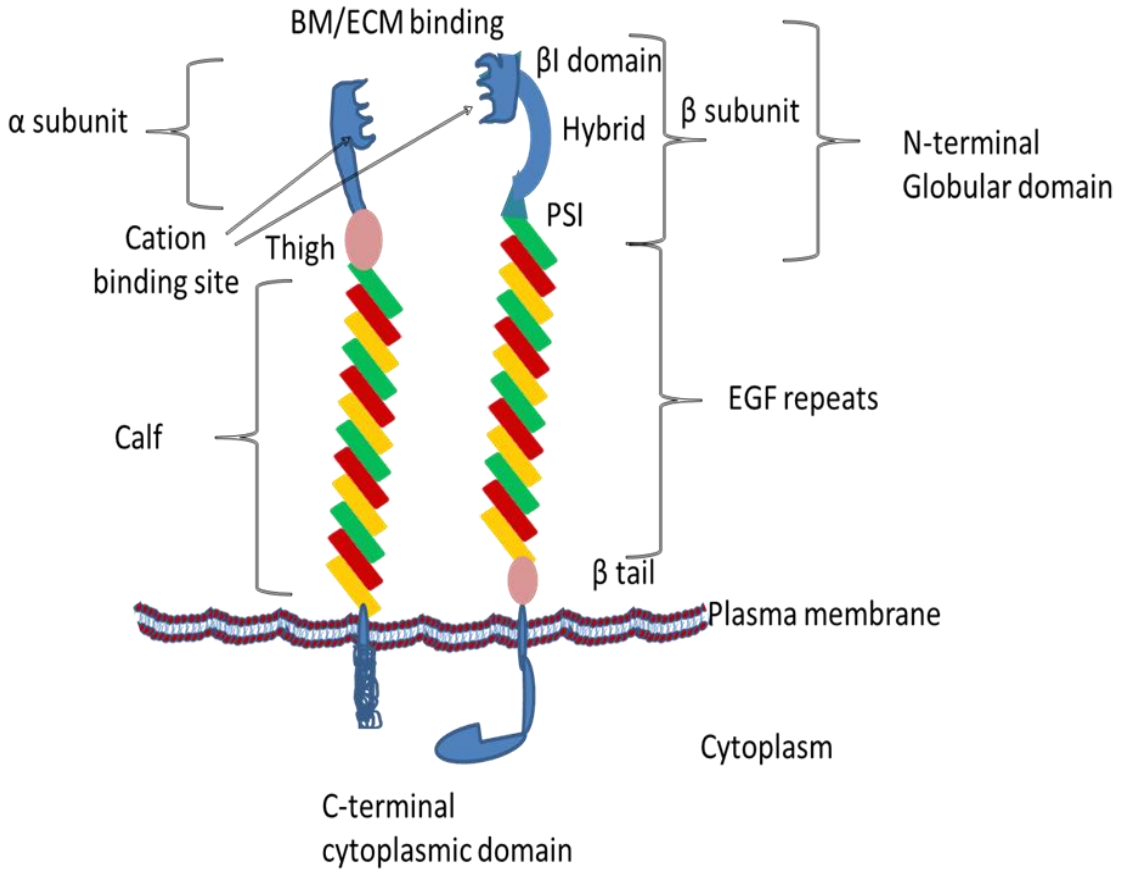


*Figure 1.2 A schematic structure of an integrin*

Meng *et al.* (2010) studied the interaction between Matrigel component and the integrin. Matrigel is a semisolid collagenous substance extracted from Engelbreth-Holm-Swarm mouse sarcoma, which is composed mainly of laminin, collagen IV, heparan sulphate proteoglycans and entactin (Hughes, Postovit and Lajoie, 2010). Integrins can interact with the ECM and EM components by interacting with collagen IV, laminin and actin. However, cells can utilise the integrin receptors that are located outside the cell membrane to adhere to the Matrigel component in *vitro*. For instance, Meng *et al.* (2010) demonstrated that various types of integrin were found in H1 human embryonic stem cells (hEs). Using an antibody blocking assay, they showed that only $\alpha_2\beta_1$, $\alpha_6$, $\beta_1$ and $\alpha_v\beta_3$ integrin subunits have a significant role in the adhesion of H1 cells to Matrigel. They also showed that the AG-10 peptide (a domain derived from COOH-terminal of laminin111 $\alpha_1$ chain) promoted adhesion of hEs to Matrigel.

Much evidence suggests that integrin β1 is highly expressed in invasive cancer cells, including TNBC cells (Feldman *et al.*, 1991; Lee *et al.*, 2011; Czarnomysy *et al.*, 2017). It has also been reported that integrin β1 expression was elevated in metastatic cancer cells. For example, integrin β1 was highly expressed in TNBC cells and was associated with the invasion and migration of MDA-MB-231 and HS578T breast cancer cells (Yin *et al.*, 2016). They compare the expression of integrin β1 in three TNBCs, MDA-MB-231, HS578T, and MDA-MB-468 to that the M10 normal mammary epithelial cell line. They showed a high expression of integrin β1 in MDA-MB-231, HS578T compared to M10 cells. Knockdown of the integrin β1 reduced the invasion of MDA-MB-231 and HS578T to Matrigel (Yin *et al.*, 2016). The other evidence supported the role of integrin β1 in the adhesion and invasion of cancer cells was observed by Czarnomysy *et al.* (2017). They showed that MDA-MB-231 breast cancer cells treated with cisplatin and echistatin (types of cancer chemotherapy drugs) induced apoptosis, and this was associated with downregulation of integrin β1 and decreased collagen biosynthesis.

Moreover, the correlation between the sialylation of integrin β1 receptor and ECM collagen have been explored by Lin *et al.* (2002). They reported that treating MDA-MB-435 breast cancer cells with ST6GalNAc-I cDNA, promoted adhesion of the cells to collagen IV. ST6GalNAc-I as described in Section 1.5.9, mediated synthesis of sTn antigen in the integrin β1 receptor. Therefore, sTn antigen could play a crucial role in the adhesion of cancer cells to the ECM *in vitro* and *in vivo* Lin *et al.* (2002).

## 1.3 Epithelial-mesenchymal transition

As described previously in section 1.1.2, adhesion and invasion of cancer cells to the EM and ECM is associated with a change in the shape of cells from epithelial to mesenchymal. Therefore, the role of EMT in cancer cell metastasis will be described in this section. EMT is frequently associated with the loss of apical-basal polarisation, which can enhance the ability of cells to migrate from the initial site (Hanahan and Weinberg, 2011). This process can be distinguished in three biological contexts: embryogenesis, wound healing and cancer metastasis (Kalluri and Weinberg, 2009).

In the context of cancer progression and metastasis, EMT plays a crucial role in the metastatic cascade, which can involve the enhancing of mesenchymal cell properties that increase the resistance of cells to apoptosis, reduce cell-cell interactions and enhance migration and invasiveness (Kondaveeti, Guttilla Reed and White, 2015). Moreover, genetic and epigenetic factors are associated with the EMT process; these include transcriptional factors, mRNA, miRNA, and post-transitional modification, such as O-linked glycosylation, N-linked glycosylation and methylation (Lange *et al.*, 2014).

### 1.3.1 The role of E-cadherin in the EMT and cancer metastasis

E-cadherin is a cell membrane adhesion protein which is responsible for keeping up the normal structure of epithelial tissues by maintaining the polarity of epithelial cells and increasing cell-cell adhesion (Tiwari *et al.*, 2012). Conversely, a decrease in expression of E-cadherin can cause a disturbance in tissue organisation. Interestingly, blocking E-cadherin in mammalian cells encourages EMT through remodelling cell-cell contacts (Zhu, Leber and Andrews, 2001). Moreover, low levels of E-cadherin have been observed in many types of tumours with high rates of metastasis. (Baum, Settleman and Quinlan, 2008). Several genetic and epigenetic factors can contribute to E-cadherin dysfunction in metastatic cancer such as helix-loop-helix transcriptional factors (Twist and E12/E47) and zinc finger factors including, Snail family transcriptional repressor 1 and 2 (*SNAIL1* and *SNAIL2)* also known as *SLUG*. These factors are also regulated by EMT inducer factors, such as transforming growth factor-beta receptor 1 TGF-βR1, ER1 and 2 ER2 which are also able to inhibit expression of E-cadherin (Huber, Kraut and Beug, 2005; Zhao, Wu and Zhou, 2011). On the other hand, over-expression of the *SNAIL1* gene can induce mesenchymal markers such as N-cadherin and vimentin, which have important roles in the metastatic behaviour of cancer cells (Baum, Settleman and Quinlan, 2008; Chaffer, Thompson and Williams, 2007; Warzecha and Carstens, 2012).

### 1.3.2 The role of vimentin in the EMT and cancer metastasis

Vimentin is a type III intermediate filament, which plays an essential role in maintaining cell architecture. It has been reported that vimentin can be produced by mesenchymal cells in normal conditions. Nevertheless, it can also be produced under pathological conditions (Brzozowa *et al.*, 2015; Vuoriluoto *et al.*,

2011). Moreover; vimentin also contributes to the promotion of hypoxia-inducible factor-1 (HIF1), which play a critical role in tumour formation through its involvement in angiogenesis (Kidd, Shumaker and Ridge, 2014). The accumulative literature reports that overexpression of vimentin is associated with various aggressive tumour types, including in breast cancer, colon cancer, malignant melanoma and central nervous system tumours (Tezcan and Gunduz, 2014; Zhu *et al.*, 2011a). Down-regulation of vimentin can inhibit cell motility and invasion of MCF-7 and MDA-MB-231 breast cancer cells (Ogunbolude *et al.*, 2017).

Furthermore, immunohistochemistry shows that the level of vimentin was elevated in high stage breast carcinomas (Vuoriluoto *et al.*, 2011). Vimentin can be down-regulated by inhibiting expression of genes linked with breast cancer motility and invasions such as the AXL receptor tyrosine kinase *AXL* (Asiedu *et al.*, 2014), plasminogen activator urokinase *PLAU*, and integrin subunit beta 4 *ITGB4* (Kawakami *et al.*, 2015; Stewart *et al.*, 2016). In addition, vimentin can be upregulated by the *SLUG* transcription factor, consequently inducing migration of MDA-MB-231 breast cancer cells (Vuoriluoto *et al.*, 2011).

### 1.3.3 Role of transcription factors in EMT and cancer metastasis

TGF-β is one of the most abundant cytokines secreted by tumour and stromal cells in the microenvironment of cancer. It controls various factors contributing to the invasion and metastasis of cancer cells (Massague, 2008; Chen *et al.*, 2018). The contradictory fact about TGF-β as a promoter or inhibitor of cancer progression has been the subject of intensive studies. For example, TGF-β from an inflammatory microenvironment can inhibit proliferation of KSC mice pancreatic cancer cells by targeting Snail and Sox4 transcription factors and inducing apoptosis (David *et al.*, 2016). However, TGF-β can promote angiogenesis, EMT and metastasis of lung cancer (Yu *et al.*, 2015).

Despite extensive studies into the role of TGF-β in EMT and cancer metastasis, the relationship between glycosylation, EMT and TGF-β, explored in this thesis has not previously been studied. TGF-β can control the expression of vimentin and E-cadherin associated with EMT and invasion of cancer cells (Yen *et al.*, 2017). The expression and activation of TGF-β can be controlled by extrinsic

factors such as ionising radiation (IR), and be described in Section1.6.1.i. The expression of TGF-β can also be controlled by the intrinsic factors such as P38 mitogen-activated protein kinases (P38MAPK), extracellular signal-regulated kinase (ERK), and c-Jun N-terminal kinase (JNK), transcription factors (Xiao *et al.*, 2008). It has also been reported that, in addition to the role of TGF-β in EMT, it can induce cancer stem cell (CSC) characteristics in TGF-β treated MCF-7 cells' (Pirozzi *et al.*, 2011).

SLUG, SNAIL and ZEB are other transcription factors which contribute to the progression of cancer by promoting invasion and metastasis of cancer cells. These transcription factors also can contribute to inhibition p53 and apoptosis pathway and induce cancer stem cell-like characteristic of A4 ovarian cancer cell line (Kurrey *et al.*, 2009). SLUG and SNAIL have a role in the metastasis of cancer cells by inhibition of E-cadherin, causing an increase in dissociation and movement of breast cancer cells (Storci *et al.*, 2010). ZEB transcription factor was reported to have a role in metastasis of cervical carcinoma, and that was associated with negative regulation of E-cadherin and an increase in the expression of N-cadherin (Ma *et al.*, 2015). An increase in ZEB2 expression was reported associated with an increase in the invasion and metastatic of gastric cancer cells to the lymph node (Dai *et al.*, 2012). Matrix metalloproteinase (MMP) transcription factor was documented to contribute to the regulation of EMT, migration and invasion of nasopharyngeal cancer (Yan *et al.*, 2015). MMP can mediate cancer metastasis via degradation of the basement membrane and extracellular matrix and induction of cancer cells migration and invasion (Nguyen *et al.*, 2016).

TWIST transcription factor also has a role in EMT and cancer invasion and metastasis. It has been reported that TWIST1 expression correlated with cancer lymph node metastasis, and that was associated with an increase in vimentin and a decrease in E-cadherin expression (Lv *et al.*, 2016). Moreover, TWIST can promote methylation in colorectal cancer by controlling in the expression of E-cadherin and induce EMT and cancer invasion and metastasis (Galvan *et al.*, 2015). Furthermore, overexpression of TWIST was associated with increased CD44 and decrease CD24 expression in breast cancer stem cells and that also

associated with EMT and an increase in breast cancer cells invasion (Vesuna *et al.*, 2009).

### 1.3.4 Role of miRNA in EMT and cancer metastasis

miRNA is short single strand noncoding RNA between 21-25 nucleotide located in the 3 prime UTR region of the gene which produces hairpin shape precursors, and act as activators or inhibitor of the target gene or protein (Zaravinos *et al.*, 2012). The mechanisms of miRNA synthesis can be described as the following. The sequence of DNA in 3 prime at the beginning of the gene is transcript to produce pri-miRNA. This pri-miRNA is processed in the nucleus by a class 2 RNA enzyme (Drosha). The precursors of miRNA are transported to the cytoplasm by the aid of exportin-5. miRNA precursors where they undergo further processing by Dicer, an RNase III-type protein enzyme to produce mature miRNA. The mature miRNA is loaded into Argonaute protein to produce an active form of miRNA for silencing gene (Wahid *et al.*, 2010).

In animal cells, miRNA can play a crucial role in the function of the gene by targeted degradation of the synthetic mRNA (Xuan *et al.*, 2015). In cancer cells, miRNA can target genes and proteins associated with EMT and invasion. For example, downregulation of Let-7a miRNA was associated with high metastasis in nasopharyngeal carcinoma (Wu *et al.*, 2015). On the other hand, a high level of miRNA Let-7a can inhibit the migration invasion and metastasis of human colon cancer by targeting Rhotekin protein (Li *et al.*, 2016a). miR-30a can target cyclin E3 expression and inhibit migration and invasion of prostate cancer (Zhang *et al.*, 2016). miR-30a also can target TGF-β and suppressing EMT and invasion of HMrSV5 a human peritoneal mesothelial cell line (Zhou *et al.*, 2013). It has been reported that miR-200a has a crucial role in cancer metastasis by downregulation of ZEB transcription factor, vimentin and N-cadherin and an increase in the expression of E-cadherin in PANC-1human pancreatic adenocarcinoma cell (Lu *et al.*, 2014). Conversely, miR-9a can induce EMT and cancer cells migration and invasion via targeting SOX7. MiR-9a upregulated by TGF-β-1 and that was associated with an increase in the invasion of non-small-cell lung cancer (NSCLC) cells (Han *et al.*, 2017).

## 1.4. Cancer stem cells

CSCs are a small population of cells within the cancer mass, which have the ability of self-renewal and can proliferate to initiate a tumour. A mutation in the normal stem and progenitor cells and other microenvironment and macroenvironment factors such as IR can induce the onset of CSCs development. These cells can generate new pro-genitor CSC leading to initiating the bulk of cancer cells (Cabrera, Hollingsworth and Hurt, 2015).

CSC can be identified by using cell surface markers, miRNA and the expression of transcription factors (Kurth *et al.*, 2015). CSCs exhibit specific surface markers, such as CD24, CD34, CD38, CD44, CD90, CD133 and aldehyde dehydrogenase -1 (ALDH-1). These markers have been used to distinguish CSCs from other cell types, and also from other cancer cells (Al-Hajj *et al.*, 2003; Li *et al.*, 2007; Zhu *et al.*, 2012). For example, human pancreatic CSCs are $CD44^{+}/CD24^{+}$ (Zhu *et al.*, 2012), meanwhile breast CSCs are $CD44^{+}/CD24^{-}$ (Al-Hajj *et al.*, 2003).

Transcription factors including TGF-β, Wnt, Notch, Sox2, Oct4, platelet-derived growth factor receptor (PDGFR) and Janus kinase/signal transducers and activators of transcription (JAK/STAT) all play a crucial role in maintaining the self-renewal of stem cells. These factors and their signalling pathways have usually been used as cancer stem cell markers (Lee *et al.*, 2017). miRNAs, including miR34a, miR-200 family and Let-7, can be considered as other factors that contribute to the stemness of CSCs (Li *et al.*, 2012; Takahashi, Miyazaki and Ochiya, 2014).

CSCs activity can be regulated by intrinsic and extrinsic factors including miRNAs, histone modification, DNA methylation, microenvironment and immune signalling (Munoz, Iliou and Esteller, 2012). miRNAs can play a central role in the characterisation of CSCs. For example, Boo *et al.* (2017) have used next-generation sequencing of miRNA to quantify the expression of miRNA in spheroids of MDA-MB-231 and MCF-7 breast cancer cells. They found that miR15b, miR-34a, miR-148a, miR-628 and miR-196b from the total miRNA profile were expressed in spheroid of both cell lines. These results highlight the involvement of these miRNA in preserving CSC characteristics. Unique miRNAs - miR-181, miR-204 and miR-205- have been found in MDA-MB-231 basal-like

breast cancer cells spheroids. Meanwhile, -miR-30c, miR-125 and miR-760- have been found only in MCF-7 luminal-like breast cancer spheroids (Boo *et al.*, 2017).

miRNAs have been reported to play an essential role in CSCs tumourigenicity and metastasis (Takebe *et al.*, 2011). miRNAs can target genes that regulate EMT, migration, invasion and metastasis of CSCs. Accordingly, miRNAs can positively and negatively control tumour development and metastasis (Zhou *et al.*, 2015).

Transcription factors that regulate EMT have also been shown to play a crucial role in the stemness, invasion and metastasis of cancer cells. Cancer cells undergoing EMT which produce transcription factors, such as snail, ZEB and Twist, can also exhibit CSC characteristics (Wellner *et al.*, 2009; Casas *et al.*, 2011; Hahn *et al.*, 2013). In addition to its role in EMT, Snail can induce CSC phenotypic properties in colorectal carcinoma cells (Hwang *et al.*, 2011). It can promote stemness, self-renewal, tumourigenicity and radio-resistance, with a potential increase in the invasiveness and metastasis of cancer cells. ZIB transcription factor has also been implicated in the stemness and invasion of colorectal cancer. ZEB can inhibit the expression of several miRNAs, including miR-183, miR-200c and miR-203. These miRNAs repress expression of CSC-inducing factors (Sox2 and KIf4). Inhibition of expression of ZEB notably does not only associate with a decrease in the invasion nonetheless also inhibits the stemness and self-renewal of CSCs (Wellner *et al.*, 2009).

Moreover, Twist is known to have a role in the EMT of stem cell-like cells (stem cell progenitor cells), by directing the expression of CD24 in breast cancer cells (Vesuna *et al.*, 2009). Vesuna *et al*. (2009) have generated and used two cell lines, MCF10/Twist and MCF-7/Twist as a model; they also used parent cell lines MCF-10, MCF-7 and MDA-MB-231. They have demonstrated that the MCF-10, MCF-7 cells do not exhibit $CD44^{+}/CD24^{-}$ expression. Conversely, MCF10/Twist and MCF-7/Twist can show a low level of $CD44^{+}/CD24^{-}$. In addition, they have stated that MDA-MB-231 cells demonstrate a high percentage of $CD44^{+}/CD24^{-}$ cells compared to MCF10/Twist and MCF-7/Twist. Moreover, the study above reported that knockdown of Twist expression in the three experimental cell lines

MCF-10/Twist, MCF-7/Twist and MDA-MB-231 can decrease the percentage of $CD44^+/CD24^-$ cells in comparison to the parental cells (Vesuna *et al.*, 2009).

It has been reported that treating lung and breast cancer cells with TGF-β does not only induce transcription factors association with EMT, but also can promote CSC markers, including Sox2, Oct4 and Kif4 in LC31 primary lung cancer cell line (Pirozzi *et al.*, 2011) and $CD44^+/CD24^-$ in MCF-7 breast cancer (Park *et al.*, 2016).

### 1.4.1 Cancer stem cell markers

As described in the previous section, many markers are associated with CSCs. However, the most popular and well-known markers are CD44 and CD24 (Al-Hajj *et al.*, 2003). Therefore, these two markers have been selected for the study presented in this thesis and are described below.

#### *1.4.1. i CD44*

CD44 is a cell surface transmembrane glycoprotein, which can interact with extracellular ligands causing adhesion, invasion and metastasis of cancer cells. It is a universal marker that has been identified to isolate cancer stem cells. It can be utilised alone to identify cancer stem cells or in combination with other markers such as CD24 (Yan, Zuo and Wei, 2015). CD44 can mediate the hyaluronan-adhesion (HA) dependent pathway (Legras *et al.*, 1997; Zoller, 2015; Lee-Sayer *et al.*, 2018). Catterall, Jones and Turner (1999) examined four human ovarian cancer cell lines which differ in the CD44 content and glycosylation. They found that adhesion of these cells is frequently associated with high-profile of CD44 and high concentration of HA (Catterall, Jones and Turner, 1999). Moreover, high amounts of modified T antigen on CD44 is also observed in prostate cancer-initiating cells (Li *et al.*, 2017a) and breast cancer stem cells (Phillips, McBride and Pajonk, 2006).

#### *1.4.1.ii CD24*

CD24 is a cell surface glycoprotein linked to glycosylphosphatidylinositol, and it was first discovered in mice as a heat-stable antigen (Fang *et al.*, 2010; Shi *et al.*, 2012). CD24 is mainly expressed in B lymphocyte cells in humans. However, CD24 has also been found as a ligand for P-selectin on endothelial cells (Zheng *et al.*, 2011). Moreover, CD24 can promote cancer cell proliferation and adhesion

to laminin, collagen and fibronectin (Yeung *et al.*, 2010; Muraro *et al.*, 2012). CD24 has also been found highly expressed in aggressive tumours such as ovarian and colorectal cancer in stage three and four compared to those in stage one and two (Kim *et al.*, 2009; Nakamura *et al.*, 2017). High levels of CD24 are frequently associated with an increase in the migration, invasion, and metastasis of MCF-7 breast cancer cells (Jing *et al.*, 2018). CD24 has also been found at a high level in breast cancer clinical specimens compared to normal tissues (Jing *et al.*, 2018). In contrast, a low level of CD24 expression has been documented in breast cancer stem cells (Bensimon *et al.*, 2013). CD24 was identified as a cancer stem cell marker in colorectal and ovarian cancer (Nosrati *et al.*, 2016; Zhou *et al.*, 2018).

CD24 is a glycoprotein which can be induced by TGF-β. Therefore, the glycosylation of CD24 could play an important role in cancer metastasis. For example, TGF-β-mediated CD24 can increase EMT markers in human CRC colorectal cell line (Okano *et al.*, 2014). Thus, CD44 and CD24 can play an essential role in CSCs identification and EMT regulation.

## 1.5 Glycosylation

Glycosylation is a conventional process in mammalian cells that modifies proteins in the endoplasmic reticulum and Golgi apparatus (Patrie, Roth and Kohler, 2013; Almeida and Kolarich, 2016). The mechanisms of glycan processing and secretion have been well reported. Glycosylation is a post-translational alteration of the protein (Boscher, Dennis and Nabi, 2011; Varelas, Bouchie and Kukuruzinska, 2014; Oliveira-Ferrer, Legler and Milde-Langosch, 2017). Glycosylation has an essential role in the physiological and developmental process of organisms (Ungar, 2009; Sprovieri and Martino, 2018). However, in most cases, the exact functions of cellular glycans are still incompletely understood.

Glycosylation can be divided into two types, either N-linked glycosylation when the sugar is linked to an asparagine residue, or O-linked glycosylation when the sugar is attached to a serine or threonine of the polypeptide chain (Patrie, Roth and Kohler, 2013).

### 1.5.1 N-Linked glycosylation

N-linked glycosylation is a process initiated in the endoplasmic reticulum by which the glycan is linked to the amine group of the asparagine (Asp.) residue of a protein (Park *et al.*, 2015). N-glycosylation is one of the most important post-translational modifications of protein which is involved in protein folding, trafficking, targeting and secretion (Stanley and Okajima, 2010). N-glycosylation plays a critical role in cellular functions including cell-cell communication, cell survival, cellular immune responses and proliferation (Varki *et al.*, 2008). Dysregulation of N-glycosylation is reported to be associated with pathologies, including cancer (Varki, Kannagi and Toole, 2009). Cancer development and progression are related to dramatic changes in cell polarisation, integrity and cytoskeleton rearrangement (Beavon, 2000) that are associated with glycosylation aberrations, including that of N-glycosylation (Chugh *et al.*, 2016). Glycosylation of cell surface proteins is mediated by a set of glycosyltransferases. The activity of transferases can be altered in cancer compared to the normal cells. For example, an increase in the GlcNAc transferase V expression in cancer cells causes an increase in the amount of polylactosamine chains on the cell surface proteins. Which can increase the branching and elongation of N-glycans, particularly β1, 6 branchings (Demetriou *et al.*, 1995). Increased β 1, 6 branchings can be detected by PHA-L lectin binding (Dennis, Granovsky and Warren, 1999a). PHA-L is a lectin extracted from *Phaseolus vulgaris* (common bean) and can detect β 1, 6 branched N-glycans in breast and colon cancer (Dennis, Granovsky and Warren, 1999b). Increased β1,6 branching and polylactosamine chains have also been reported to be associated with lymph node metastasis of breast cancer (Handerson *et al.*, 2005).

### 1.5.2 O-linked glycosylation

O-linked glycosylation occurs when the first monosaccharide (most usually GalNAc) of the glycan connects to the hydroxyl group of an amino acid residue, usually serine (Ser) or threonine (Thr) through an O-glycosidic linkage (Brooks *et al.*, 2008). O-linked glycosylation is initiated in the cis-Golgi apparatus, in which UDP-GalNAc: polypeptide N-acetylgalactosaminyltransferases (GalNAc-Ts) catalyse the transfer of GalNAc to a Ser or Thr residue on the protein chain, resulting in the synthesis of GalNAc-O-Ser/Thr, Tn (Gill *et al.*, 2013). Then Gal,

GalNAc and GlcNAc, and sialic acid residues will be added to Tn forming four common core structures (Tran and Ten Hagen, 2013), as shown in Figure 1.3. The most frequent extension of Tn antigen in the mammals is core 1, or T antigen. These antigens are catalysed by a β1,3-galactosyltransferase enzyme, which can add a galactose in a β1,3 –linkage to the GalNAc (Ju *et al.*, 2002). On the other hand, Tn antigen can be extended by adding GlcNAc in a β1, 3-linkage through the action of the 1, 3-N-acetylglucosaminyltransferase 6. These two types of structures (core1 and core 3) can further be extended to form more complicated core structures (core 2 and core 4). Synthesis of these structures is catalysed by 1,6-N-acetylglucosaminyltransferases (Tran and Ten Hagen, 2013). They can also be extended by adding monosaccharides such as GlcNAc, galactose, fucose and sialic acid (Gill *et al.*, 2013) as shown in Figure 1.3.

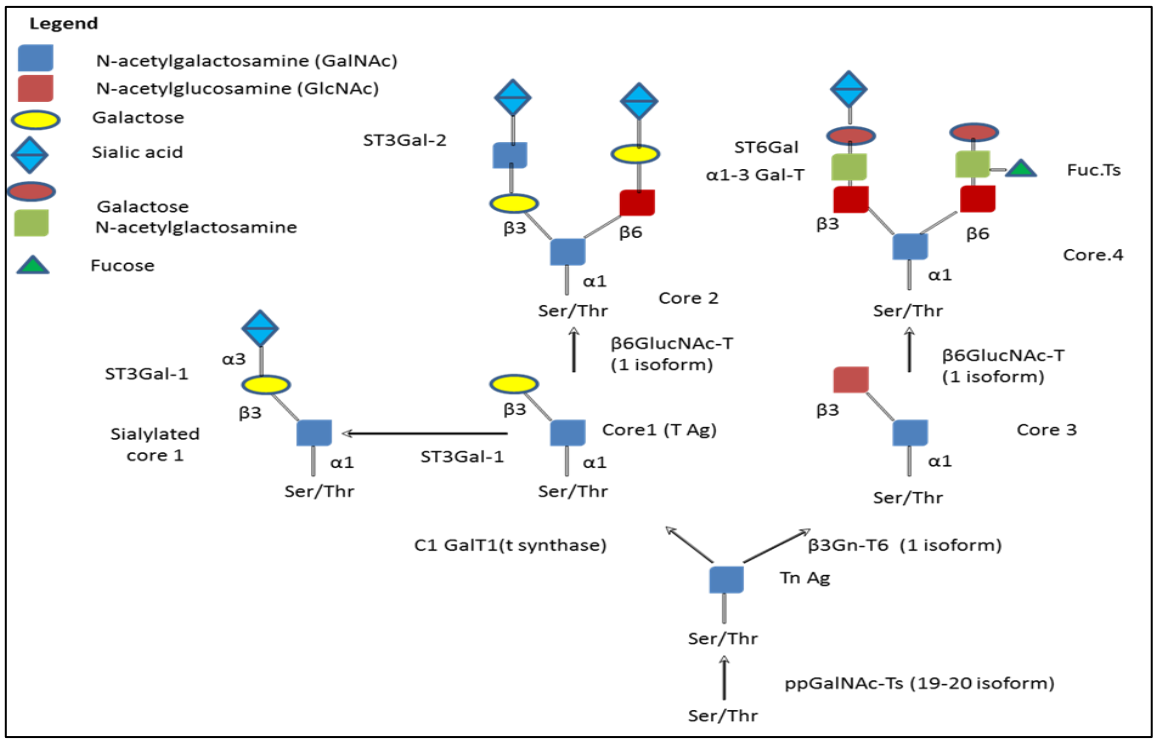


*Figure 1.3 A schematic structure of O-Linked glycosylation synthesis*

### 1.5.3 Sialylation

A change in sialylation is one of the most commonly reported alterations in glycosylation associated with cancer. The amount, type, and distribution of sialic acids on cell surface glycoproteins can be changed. Increased sialylation is often reported to be associated with the Thomsen-Friedenreich antigen (Gal/β1, 3GalNAcα-O-Ser/Thr) also known as T antigen Tn antigen (GalNAcα-O-Ser/Thr),

sTn or sialylated Lewis family antigens (Dall'Olio and Trere, 1993). The increase in sialylation may be as a result of the availability of target structures such as β1,6 branching glycans (Dall'Olio and Trere, 1993). The increase in sialylation has also been reported to be associated with O-linked glycosylation resulting in increased levels of N-glycolylneuraminic acid (a type of sialic acid) found in MCF-7, a breast cancer cell line (Devine *et al.*, 2014). It has also been reported that 'ST6 N-acetylgalactosaminide α2,6-sialyltransferase1 (ST6GALNAC1)' was more highly expressed in colorectal cancer stem cells, and that was associated with increased in sTn antigen in CD44 cancer stem cells (Ogawa *et al.*, 2017).

Sialic acid is usually involved in the immunogenicity, adhesion and cellular motility of cancer cells, due to the negative charge of sialic acid, which acts as an anti-adhesive factor allowing cancer cells to be dissociated from the primary tumour (Kitajima, Varki and Sato, 2015). *Sambucus nigra* agglutinin SNA is a lectin derived from the common elder plant and can be used to detect the change in sialylation of the glycoprotein. It binds to α -2,6 and α -2,3 linked sialic acid (Mehta *et al.*, 2016). dos-Santos *et al.* (2014) have used SNA to detect changes in the level of sialylation in ductal breast carcinoma, and they found that sialylation was increased in metastatic cancer compared to non-metastatic tumours.

### 1.5.4 Alteration in O-Linked glycosylation and metastasis

Aberration in O-Linked glycosylation represents a key factor in cell-cell interaction and invasion, which has an impact on cancer cell behaviour and metastasis (Itkonen and Mills, 2013). O-Linked glycans are usually shorter and more branched than N-linked glycans (Reviewed by Sears and Wong, 1998). However, in cancer metastasis, cells have less long and branched glycans than normal cells (Hauselmann and Borsig, 2014). Alterations in expression of several glycosyltransferases can result in aberrations in glycosylation. For example, ST6 transferases-1(ST6GalNAc-1) can modify O-linked glycosylation by adding the sialic acid to the Tn antigen and produce sTn antigen, consequently, inhibiting further elongation of the glycan (core 4), Figure 1.4. The presence of this structure has been associated with cancer cell adhesion and metastasis (Sewell *et al.*, 2006). Silencing of ST6GalNAc-1 can inhibit proliferation and invasion of gastric carcinoma (Tamura *et al.*, 2016). Moreover, decreased expression of Gal-

transferases leads to shortening in T antigen, and that was associated with an increase in the expression of ST3GalNAc 1(Tamura *et al.*, 2016).

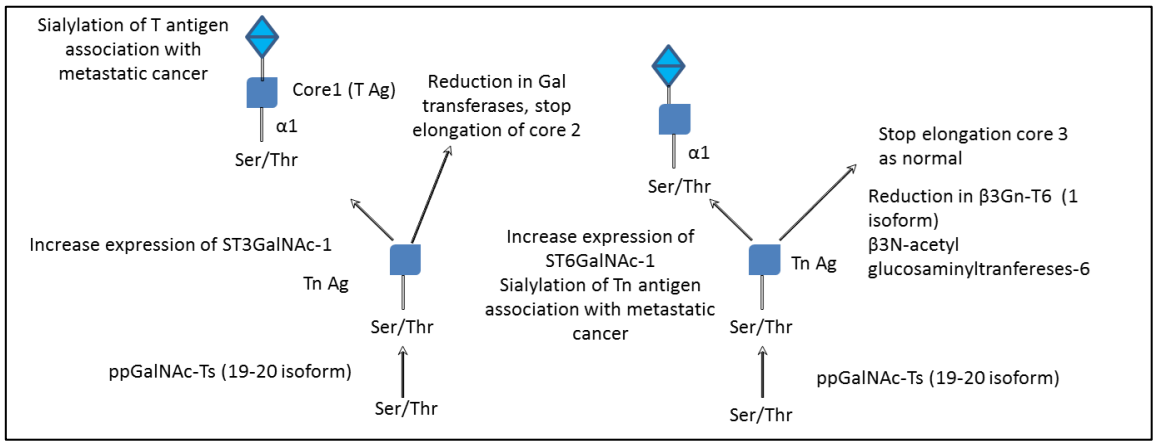


*Figure 1.4 A schematic diagram showed the aberration in O-linked glycosylation.*

In metastatic cancer, core 1 and 3 are often modified due to a reduction in the expression of β3N-acetyl glucosaminyl transferases-6 and Gal transferases and an increase in expression of ST6GalNAc1. These modifications frequently correlate with increased expression of β1,6-N-acetylglucosaminyltransferases (C2GnT1) resulting in elongation in O-glycans (reviewed by Hauselmann and Borsig, 2014). The latter is often associated with an increase in sialyl Lewis$^{a}$ (sLe$^{a}$) and sialyl Lewis$^{x}$ (sLe$^{x}$), which are tetrasaccharide carbohydrates commonly O-linked to proteins of the cell surface membrane. They can act as ligands for selectin-binding, enabling adhesion of cancer cells to the endothelium during metastasis (Pahlsson *et al.*, 1995; Thomas *et al.*, 2004; Chantarasrivong *et al.*, 2017).

### 1.5.5 Possible mechanisms contributing to alteration of glycosylation

Fundamentally, over-expression of glycosyltransferases in tumour cells leads to increased transfer of sugar moieties to protein and synthesis of cell surface glycan epitopes such as sLe$^{a}$ and sLe$^{x}$, (reviewed by Hauselmann and Borsig, 2014). Furthermore, hypoxia plays an important role in the up-regulation of glycosyltransferases related to aberrant glycosylation. For example, the synthesis of sLe$^{x/a}$ is facilitated by increasing the expression of several glycosyltransferases such as α1,3/4-fucosyltransferase-7 (FucT7) and α2,3-fucosyltransferases (Carvalho *et al.*, 2010). It has been reported that incubation of SW480 colon cancer cells under hypoxic conditions for 7 days can enhance the production of

sLe$^x$, E-selectin and sLe$^x$ promote adhesion of colon cancer (Koike *et al.*, 2004). An increase in sialylation of cancer cell glycoproteins has been reported to be associated with poor prognoses and cancer metastasis (Mi *et al.*, 2015; Kovacs *et al.*, 2016; Chen *et al.*, 2016). Moreover, an increase in 2,6 sialylation is usually regulated by up-regulation of ST6GalNAc and ST6Gal families in O-Linked and N-Linked glycosylation, respectively (reviewed by Pinho and Reis, 2015). Interestingly, down-regulation of the ST6GalNAc1is associated with shortening in the O-glycan structure of Tor Tn antigens and decrease in sTn epitopes (Springer, 1995).

### 1.5.6 Tn antigen

Tn antigen is a small O-glycan, which was first discovered by Dausset, Moullec and Bernard (1959) in a patient with haemolytic anaemia. Formation of Tn antigen can be catalysed by a family of glycosyltransferases called UDP-N-acetyl-α-D-galactosamine: polypeptide N-acetylgalactosaminyl-transferases (GalNAc-Ts) which catalyse the attachment of GalNAc to the polypeptide chain of a protein (Gill *et al.*, 2013) as shown in Figure 1.5. Tn antigen found at high levels in primary and cancer metastases (Gill *et al.*, 2013). On the other hand, a low level of Tn antigen has been found in normal tissues (Springer, 1984).

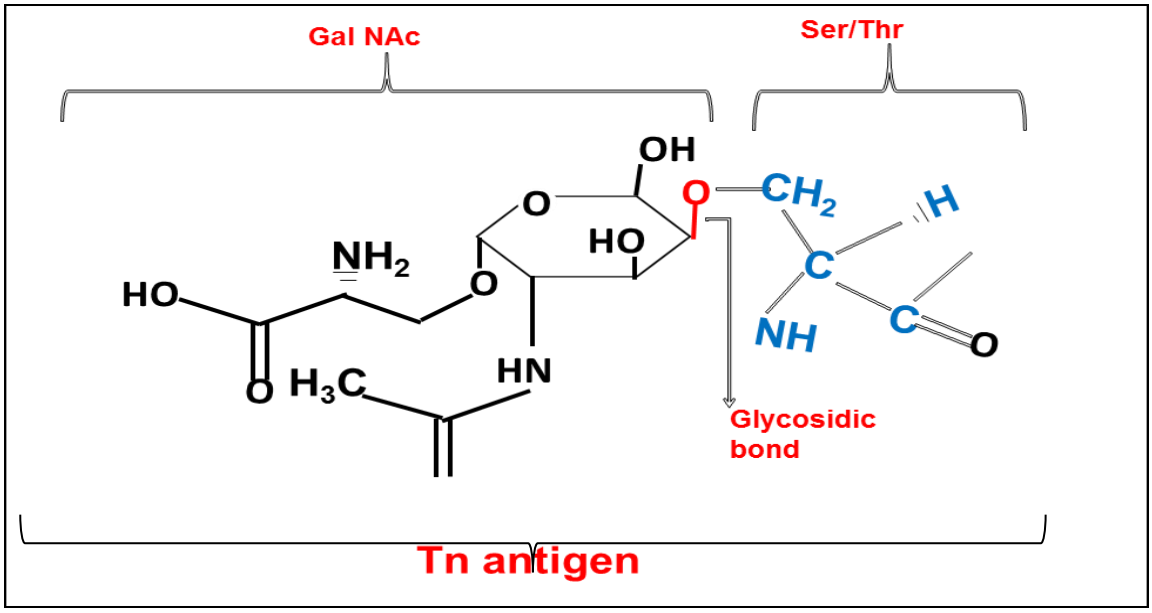


*Figure 1.5 A schematic diagram showed the structure of the Tn antigen.*

GalNAc glycan linked to the hydroxyl group of Ser/Thr by a glycosidic bond, forming the first structure in O-glycosylation.

Evidence showed the Tn antigen has a role in cell-cell adhesion and migration. Kishikawa *et al.* (1999) stated that T and Tn antigens have a specific role in the adhesion of breast cancer cell to the endothelial cells. They labelled ZR75-30 breast cancer cells with fluorescent 2′,7′-bis-carboxyethyl-carboxy-fluoresceintetraacetoxy-methyl ester (BCECF AM) and seeded them onto a monolayer of HLB100 normal endothelial cells. They showed that the adhesion of ZR75-30 breast cancer cells was specifically associated with T and Tn antigen.

Conversely, attachment of DU 4475c breast cancer cells to Kupffer cells was inhibited using T and Tn antigen in a dose-dependent manner (Springer, 1997). Moreover, an increase in the level of Tn antigen has been reported to be associated with localisation of laminin in the lamellipodia at the cell surface, resulting in a decrease in cell-cell adhesion and an increase in motility. Consequently, induce metastasis of HUH6 and Hs578t human breast cancer and 4T1 mouse mammary tumour cells in xenograft model' (Gill *et al.*, 2013). Tn antigen can be detected as the binding of *Helix pomatia* agglutinin (HPA) (Fukutomi *et al.*, 1989; Brooks *et al.*, 1993).

### 1.5.7. *Helix pomatia* agglutinin (HPA)

*Helix pomatia* agglutinin (HPA) is a lectin extracted from albumin gland of *Helix pomatia* (Roman snail) (Prokop, Uhlenbruck and Kohler, 1968; Dwek *et al.*, 2001). HPA has an antibacterial function in the Roman snail; it can protect fertile eggs from bacteria. It has also been reported that agglutinin such as HPA, plays an essential role in the immunity of invertebrate (Prokop, Uhlenbruck and Kohler, 1968). It is has been reported that binding reported being associated with poor prognosis and metastasis in breast, colon and other types of cancer (Dwek *et al.*, 2001). HPA detects glycans terminating an N-acetylgalactosamine (GalNAc), associated with poor prognosis breast cancer (Brooks and Leathem, 1991; Rambaruth, Greenwell and Dwek, 2012). HPA binding has also been reported in highly metastatic HT29 colon cancer cells (Lescar *et al.*, 2007). HPA can also tolerate exchange the position 3α GalNAc to βGal and binding to the T antigen (Sanchez *et al.*, 2006). However, the association between aberrant glycosylation in metastatic cancer cells detected by HPA and radiotherapy has never been studied.

### 1.5.8 Role of glycosylation in cancer metastasis

During metastasis, cells will acquire multiple alterations in exogenous and endogenous signals that can maintain dissemination and other subsequent cascades in cancer metastasis, which include EMT as described in section 1.3, (Banyard and Bielenberg, 2015; Lemieux *et al.*, 2009; Guarino, 2007). Aberration in the glycosylation of cell surface glycoprotein in cancer cells can activate cell membranes receptors, which increase cell mobility and enhance cell adhesion and invasiveness (Fortuna-Costa *et al.*, 2014).

### 1.5.9 The role of GalNAc T6 and ST6GalNAc I in cancer metastasis

It has been reported that ppGalNAc T6 is overexpressed in malignant breast tissues (Banford and Timson, 2017). Nevertheless, a high level of ppGalNAc T6 expression has also been observed in breast cancer specimens compared to the control, normal breast tissue (Patani, Jiang and Mokbel, 2008). A strong correlation between ppGalNAc T6 and human breast cancer initiation and development has also been observed, and it is considered an early event in the cancer-associated aberration of O-linked glycosylation (Berois *et al.*, 2006; Banford and Timson, 2017). ppGalNAcT6 has been reported to have an important role in the aberration of mucin-type-1 glycosylation in breast cancer (Park *et al.*, 2010). It is also observed to have a role in the localisation of adhesion molecules such as β-catenin and E-cadherin (Park *et al.*, 2010). Moreover, studies reported that there is an association between ppGalNAcT6 expression and EMT. For example, Park *et al.* (2011) stated that transfection of MCF-10 normal epithelial breast cells with ppGalNAcT6 induced EMT like changes in the cells. Trahan (2016) demonstrated that ppGalNAcT6 expression could disrupt the morphology of pancreatic acinar cells, in which the E-cadherin binding can be switched to P-cadherin binding (Tarhan *et al.*, 2016). Therefore, ppGalNAcT6 may have an important role in EMT, invasion and metastasis of cells.

The ST6GalNAc-1 is a sialyl 1 transferase enzyme, which plays a crucial role in mucin-type O-linked glycan chains where it transfers a sialic acid residue onto the glycan. ST6GalNAc-1 is frequently involved in the biosynthesis of the sialyl-Tn antigen sTn, and disialyl-T antigens sT (NeuAc-alpha2-3Gal-beta1-3[NeuAc-alpha2-6] GalNAc-alpha1-O-Ser/Thr)' (reviewed by Marcos *et al.*, 2004).

ST6GalNAc-I inhibits elongation of O-glycans in cancer cells by adding sialic acid to immature glycans. The former results from a reduction in the expression of β3Gal T6 and induction of ST3GalNAc and ST6GalNAc-I expression (Tamura *et al.*, 2016). It has been well reported that the low level of sTn antigen is present in foetal and normal adult tissues. Conversely, epithelial cancers clinical specimens displayed high levels of sTn (Hashiguchi *et al.*, 2016). Accordingly, sTn has been considered as a promising tumour marker, which can be targeted in a therapeutic study in the future.

## 1.6 Ionising irradiation

IR is high sufficient energy radiation that leads to the release of ions when passing through a medium, due to the transfer of the electron from a low level to the high level of energy. These types of radiation are either high linear energy transfer (LET) radiation, such as α particles (Helium atom nuclei), or low LET, including X-rays and γ-rays (electromagnetic radiation) (Hall *et al.*, 2006).

Human bodies are continuously exposed to IR from natural sources (cosmic radiation) or human activity such as medical sources. In the last decade, it has been reported that there has been an increase in the percentage of people exposed to ionising such as X-ray, gamma-ray and computed tomography scans (CT scan). Health institutions, airports and scientific centres, can also increase the risk of cancer formation as sources of IR (reviewed in Azzam *et al.*, 2016).

Several units are used to quantify radiation. Based on the international system of units (SI), radiation has been measured in the Gray (Gy), which is the unit of energy deposed in one Kg of mass, (1Gy = 1Jul/Kg). Whereas, Sievert (Sv) is the unit measuring the biological effect of absorbent radiation (1Sv = 1Gy) in low LET radiation. The biological effects of radiation are variable, according to the type of radiation. For example, the biological damage such as DNA damaged that results from exposure to 1 Gy α particle are three times more than the damage of being exposed to 1 Gy X-radiation, in which the dosage is multiplied by a quality factor (Q). Therefore, another unit, which is called the radiation absorbent dose (REM) (1 Sv = 100 rem) has been considered in order to quantify the biological effect of irradiation. It can be calculated by multiplying the dose of irradiation by the Q factor (Wakeford, 2004).

### 1.6.1 Biological effect of IR

For 100 years, radiation therapy has focussed on targeting DNA molecules to kill cancer cells. Single strand breaks (SSBs) and double-strand breaks (DSBs) have been recognised following IR (Vignard, Mirey and Salles, 2013). However, not only DNA can be affected by irradiation, but other components in the cell and tissue can also respond to IR, such as lipids, protein and cellular organelles such as mitochondria (Leach *et al.*, 2001), cell membranes (Haimovitz-Friedman *et al.*, 1994) and lysosomes (Persson *et al.*, 2005).

A massive change in the paradigm of radiation biology occurred in the 1990s, following the observation of biological changes in cells that had not been in the track of IR, or non-nuclear compartments that were hit by irradiation such as mitochondria (Kadhim *et al.*, 1992; Nagasawa and Little, 1992; Seymour and Mothersill, 1992; Wu *et al.*, 1999; Shao *et al.*, 2004).

The biological effects of radiation can be classified into two main categories: physical change and chemical reactions following irradiation. The initial effect can be viewed as a physical change in the cells following IR. Through this stage, radiation can interact with atoms and molecules in the cells, exiting or ionising them (Hall and Giaccia, 2012). The mechanism of how IR deposits energy and ionises matter is called Compton scattering, in which a photon is scattered by charged particles resulting in a reduction in energy and an increase in the wavelength of the photon (Hall and Giaccia, 2012). In this case, the photon deposits part of its energy in target electrons of atoms leading to an increase in the speed of the electron, which may cause extra ionising events. In the second mechanism, the photoelectric effect, a photon can deposit its entire energy into an electron in the atom, resulting in an exciting electron in the irradiated atom which travels from a low level to high level of energy and may be discharged and cause further ionising events (Hall and Giaccia, 2012). In the case of very high energy photons, such as ultra-gamma rays, these photons interact with atoms resulting in high-speed electron and positron; this excited electron can make further ionising atoms (Hall and Giaccia, 2012).

After the physical effect of IR, a chemical process takes place, where free radicals are generated and react with neighbouring organelles or substances in

the cells. These interactions can lead to biological changes in the irradiated or unirradiated cells or in the progeny cells (which will be described in detail in the following Sections).

*1.6.1. i Morphological effect*

Much evidence reported that cells exposed to IR could induce phenotypic characteristics like EMT (Zhou *et al.*, 2011). IR can contribute to the regulation of TGF-β expression, thus inducing EMT and cancer metastasis (Dancea, Shareef and Ahmed, 2009). Andarawewa *et al.* (2007) reported that the synergetic effect of IR and TGF-β promote EMT in non-malignant human mammary cells MCF-10, HMT3522 S1 and HMT3522 184v. Other evidence supporting the role of IR in the change of cell morphology was conducted by Zhou *et al.* (2011). They demonstrated that 2 Gy of gamma rays promote a change in the morphology of seven types of cancer cells, including MCF-7, MDA-MB-231 and PC14 cells. They also reported that this change was associated with an increase in TGF-β expression and invasiveness. Recent evidence showed that 2.3 Gy of IR promotes migration but not invasive of MDA-MB-231 breast cancer cells (Young and Bennewith, 2017). It has also been reported that IR and progesterone can induce cancer stem cells properties in MCF-10 human breast cells (Vares *et al.*, 2013).

*1.6.1.ii Cytoplasmic effect*

IR can also target large compartments in the cytoplasm such as mitochondria. Due to the large numbers of mitochondria and their role in oxidation-reduction mechanisms, mitochondria can play a crucial role in the biological effects of IR in irradiated cells (Yahyapour *et al.*, 2018). Mitochondria represent the main source of ROS in the cells due to Ox-redox reactions (Morgan and Liu, 2011; Francis-Oliveira *et al.*, 2018). ROS can be generated from exogenous and endogenous sources, as illustrated in Figure 1.6. The exogenous sources, such as IR, can hydrolyse water in the cells leading to the production of different types of ROS, such as hydrogen ion ($H^+$), hydroxyl ion (OH), hydrogen peroxide ($H_2O_2$) and hydronium ions ($H_3O^+$) (Tong *et al.*, 2015). ROS can interact and produce a lesion within neighbouring molecules, such as proteins lipids and DNA. These lesions could be unrepairable and produce lethal DNA damage, resulting in senescence, apoptosis and death of cells (Luo *et al.*, 2013). Conversely, cells

may be able to repair the damage in DNA; therefore, cells are returned to their normal function. In some cases the DNA damage is incompletely repaired; therefore, cells returned to life with a mutation in DNA, and that could induce genomic instability (GI), which can initiate tumours in the progeny (Azzam, Jay-Gerin and Pain, 2012).

ROS can target mitochondrial DNA (mtDNA) and disrupt mitochondrial function and thus cause an increase in endogenous ROS in the irradiated cells (Blasiak *et al.*, 2015). However, the level of ROS can return to normal levels by activation of the cell haemostasis pathway involving ROS scavengers such as peroxiredoxins (Graves *et al.*, 2009). An increase in levels of ROS in the irradiated cells can activate several pathways in the cell responses to IR. For example, an increase in ROS in irradiated cells can be associated with mtDNA damage and apoptosis (Zangar, Davydov and Verma, 2004; Blasiak *et al.*, 2015) through activation of the caspase system pathway (caspase 9 and caspase 3) (Circu and Aw, 2010).

Moreover, an increase in ROS in the cells can activate transcription factors that regulate the expression of genes that contribute to EMT. ROS can activate TGF-β, inducing EMT in MCF-10 human normal epithelial cells via activation of SNAIL, SMAD and ZEB transcription factors (Iizuka *et al.*, 2017).

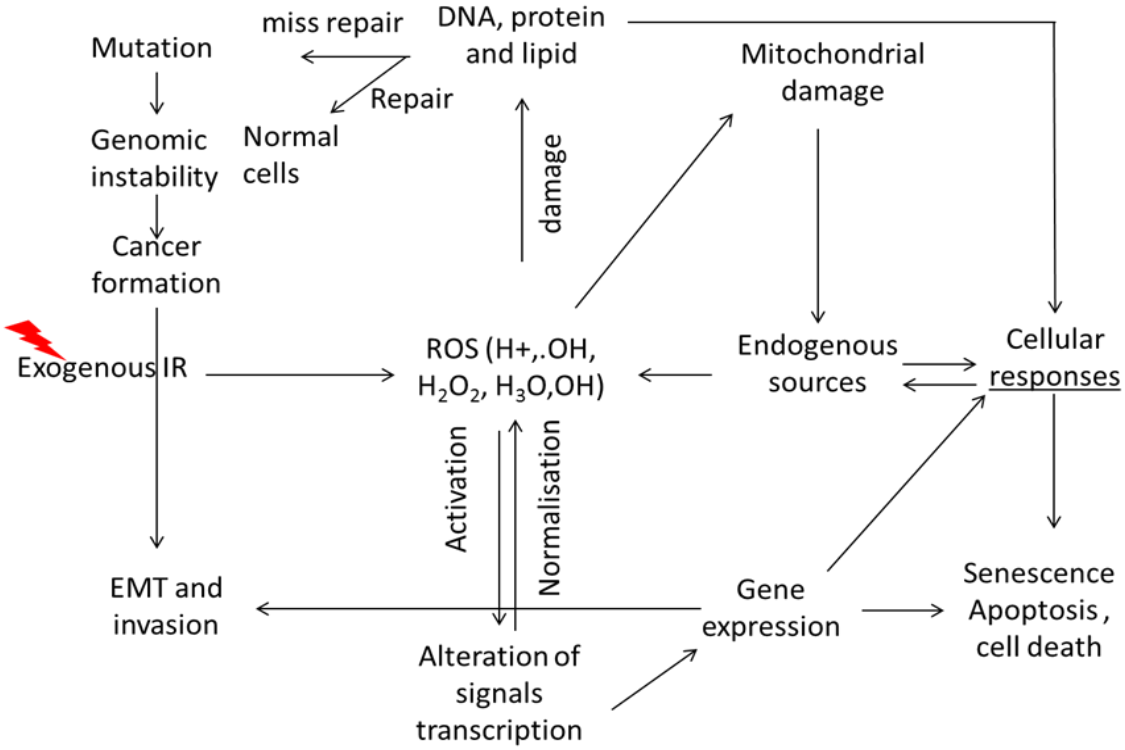


*Figure 1.6 A schematic diagram showed the possible mechanisms by which IR induces ROS and cellular responses.*

IR can hydrolyse a water molecule and produce ROS. Excessive amounts of ROS from exogenous and endogenous sources can induce DNA damage in the nucleus and the mtDNA. Induction of DNA damage could contribute to cellular responses, including apoptosis and cell death. Otherwise, cells will induce their DNA repair systems; DNA misrepair can induce changes in transcription factors, which frequently contribute to EMT and invasion. The progeny of cells surviving irradiation could have mutant DNA and possibly initiate tumours in the future.

### *1.6.1. iii Nuclear effects*

The speed and energy of IR photons have an influence on the biological and cellular responses of irradiated organisms (Nias, 1990). These effects, either as a result of the direct impact of irradiation on DNA or the release of ROS results in double-strand breaks (DSB) (Vignard, Mirey and Salles, 2013). This DSB consequently induce cellular responses such as apoptosis (Verbrugge *et al.*, 2008), necrosis (Hallahan *et al.*, 1989), DNA damage, chromosomal aberrations, mutation and GI, which can increase the risk of cancer formation (Lutze *et al.*, 1993; Kadhim, Marsden and Wright, 1998; Kadhim *et al.*, 1995).

IR has harmful effects on DNA. However, the other molecules within the cells such as water can be ionised, hence reacted with nearby DNA to produce an aberration (Hall and Giaccia, 2012). Due to the ability of radiation to deposit a

high quantity of energy in a small area, clusters of DNA damage and DSB appear. Clustered DNA damage is frequently associated with SSB and pair base lesions, and this results in lethal and unrepairable aberrations in DNA (Klungland and Bjelland, 2007).

### 1.6.2 Target effects of ionising irradiation

According to Marshall, Gibson and Holt (1970), cells should have at least one site to be targeted by IR to induce cell damage or cell death. The central molecule targeted in the cell is DNA. DNA damage can lead to chromosomal aberrations, genetic mutation and cell death (Biedermann *et al.*, 1991; Borrego-Soto, Ortiz-Lopez and Rojas-Martinez, 2015). However, literature reports that IR can also target cell membranes, causing cell death. Cells exposed to ionising radiation can generate ROS leading to oxidative damage to the membrane of the cells and its consequent role in the mechanism of apoptotic cell death (Mishra, 2004). Furthermore, radiotherapy can also induce cancer formation by increasing GI or affect the microenvironment of the irradiated zone, which can produce oncogenic factors such as cytokines (Kaup *et al.*, 2006).

### 1.6.3 Non-target effects of ionising radiation

It is accepted that the DNA molecules are the first target of IR in irradiated cells resulting in the production of DNA damage and free radicals such as ROS (Vilenchik and Knudson, 2006; Vignard, Mirey and Salles, 2013). In the last decades, the radiation biology paradigm was shifted from target to non-target effects (NTEs) of IR (Kadhim *et al.*, 1992; Azzam *et al.*, 1998; Morgan, 2003a; Little, 2006; Kadhim *et al.*, 2013; Pouget, Georgakilas and Ravanat, 2018). The phenomena of NTE has been extensively explored by researchers, to demonstrate the effects of IR in the cells and tissues that are not exposed to IR (Mothersill *et al.*, 2001). Kadhim *et al.* (1995) observed that IR induces genomic instability (GI) in the progeny of nearby unirradiated cells. Changes in cell function have also been observed due to non-targeted effects of IR (Lorimore, Coates and Wright, 2003; Hatzi *et al.*, 2015).

Much evidence suggests that the NTEs of IR can cause an irreversible change in the DNA structure, which can often pass to the progeny of cancer cells (Al-Mayah *et al.*, 2012). Chromosomal aberration and GI are also associated with an

increase in the inflammatory response and ROS production in the non-targeted cells (Lorimore and Wright, 2003; Iliopoulos, Hirsch and Struhl, 2009). Moreover, Mancuso *et al.* (2008) demonstrate that irradiated mice with shielded brains had increased incidence of a medulloblastoma tumour, and that was associated with DSBs and interstitial deletion in chromosome 13. Mothersill *et al.* (2001) have also reported that IR can induce biological changes in unirradiated cells such as GI and bystander effects (BE), described below in Sections 1.6.3.i and 1.6.3.ii.

*1.6.3. i Radiation-induced GI*

GI is a generic term that refers to a frequent mutation in the genome of cells, which can appear in the progeny. This alteration in the genome of the cells could include changes in the sequence of nucleic acids, chromosomal aberration and aneuploidy (Morgan, 2003b; Morgan, 2012; Kadhim *et al.*, 2013). Radiation-induced GI has also been defined as an increase in the rate of alteration within the genome of the progeny of irradiated cells (Morgan, 2003a). Kadhim *et al*. (1992) observed karyotype abnormalities in murine stem cells that were exposed to α-particles. GI can manifest as a chromosomal aberration, micronucleus formation, aneuploidy, gene amplification and microsatellite formation. The mutation can arise in the early period of exposure to radiation as well as in the progeny of the irradiated cells, leading to GI and cancer formation (reviewed by Kadhim *et al.*, 2013).

Several factors can influence GI in irradiated cells, including the type, dose, and dose rate of radiation, cell type and density in the culture (reviewed by Kadhim and Hill, 2015). The majority of studies concentrate on the effect of high and low LET such as α-particle and X-radiation, respectively. A cross-talk between GI and extracellular vesicles as signalling from the irradiated cell can stimulate chromosomal rearrangements in a non-target cell within the environmental radiation area or *vice versa* (Morgan, 2003a).

*1.6.3. ii Radiation-induced bystander effects*

Radiation-induced bystander effect (BE) is defined as the biological response of unirradiated recipient cells to IR via bystander signals from neighbouring irradiated cells (Najafi *et al.*, 2014). Nagasawa and Little (1992) were the first authors to observe BE in Chinese hamster ovary cells following irradiation. They

tracked 1% of Chinese hamster ovary cells using α-particle beam track. Cells were analysed for chromatid sister exchange. They observed that 30% of cells were affected by irradiation, manifesting as chromatid sister exchange. They stated that the unirradiated cells responded to signals secreted from the 1% of directly irradiated cells demonstrating ionising radiation-induced bystander effects.

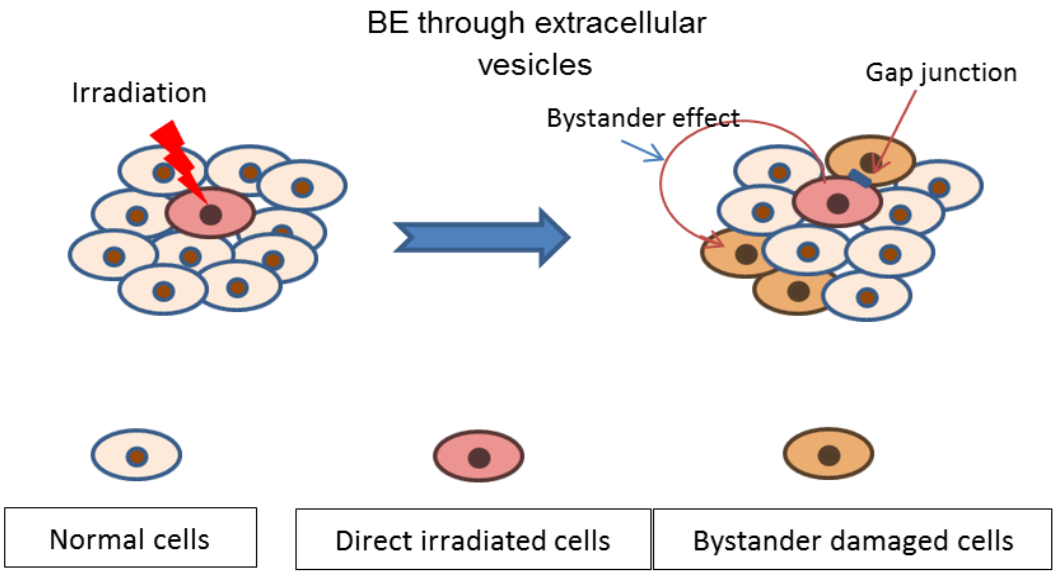


*Figure 1.7 A schematic diagram of BE of ionising irradiation.*

The irradiated cells produce soluble and insoluble factors that can induce damage in the unirradiated cells nearby, adapted from (Al-Mayah *et al.*, 2012).

The relationship between the IR and BE does not show a linear equation; which means that a low dose of radiation could induce maximum induction of BE (Ding *et al.*, 2005). For example, Schettino *et al.* (2005) demonstrated that the full BE effect of X-irradiation on V79-379A Chinese hamster cells was between 0.3-0.5 Gy X-ray when they exposed to dose rate between 0.01 and 0.5 X-ray in three-dimensional tissue cultures.

It has been well reported that signals from irradiated cells can cause damage in unirradiated cells. Mothersill and Seymour (1998) showed that considerable of DNA damage in the recipient cells was observed following transferring irradiated cell-conditioned media (ICCM) to unirradiated epithelial cells. This damage could be affected by the density and types of irradiated and unirradiated cells (Ballarini *et al.*, 2006). Moreover, Al-Mayah *et al.* (2012) demonstrated that ICCM could

induce DNA damage in recipient unirradiated MCF-7 cells. A recent study showed that an increase in ROS and glutathione levels following transfer ICCM of HaCaT human keratinocyte cells to unirradiated cells (Jella *et al.*, 2018).

### *1.6.3. iii Mechanisms of BE*

It has been well demonstrated that irradiated cells produce various factors which can be received by nearby unirradiated cells through media transfer or through gap junctions *in vitro*. Several mechanisms have been proposed to explain the BE; these include soluble factor transmission, oxidative metabolism and EV / exosomes transmission (Azzam *et al.*, 2002; Al-Mayah *et al.*, 2012; Azzam, Jay-Gerin and Pain, 2012; Al-Mayah *et al.*, 2015). However, mechanisms of bystander signalling related to the EMT are still incompletely clear.

Several experimental designs have been proposed to study the BE of IR. Using media transfer technique, Lyng *et al.* (2006) investigated the changes in the MAPK pathways, including P38, JNK and ERK; and calcium levels in human papillomavirus-immortalised keratinocytes cells (HPV-G) following ICCM media transfer. They found that the active form of JNK and ERK can be detected following exposure to ICCM. In addition, the ROS and calcium can also be elevated in the recipient cell, suggesting that ROS and calcium can act as important mediators in BE cells.

A microbeam technique has also been used to study the BE of IR. The Columbia microbeam has been used to deliver known numbers of charged α- particles for each cell. Using this technique allowed the examination of the responses of individual cells to IR and also an examination of the responses of irradiated and unirradiated cells to IR. Ponnaiya *et al.* (2007) used a microbeam technique to quantify the expression of cyclin-dependent kinase inhibitor (CDKN1a) following administration of 10 α particle's per cell for 50% of the cell population (Ponnaiya *et al.*, 2007). They found that CDKN1a expression in irradiated cells increased compared to the control cells. They have also found that the expression of CDKN1a in unirradiated cells in the same population as the irradiated cells increased compared to 0 α-particle control cells.

A grid shield method has also been used to investigate the BE of IR. Using this technique allows irradiating a part of the body or cell population and covering the

other parts to protect them from radiation. Lorimore *et al.* (1998) used this method to prove the BE of radiation. They observed that α-particles induce chromosomal aberration in mouse bone marrow progeny of unirradiated cells (Lorimore *et al.*, 1998). Another experiment supports this finding conducted by Hu *et al.* (2018); they irradiated Kunming mice with 4 Gy X-ray; either whole body, head or abdomen. They found that upregulation of mesenchymal markers (vimentin and N-cadherin) and downregulation in epithelial markers (E-cadherin) in tissue that had never been exposed to irradiation (Hu *et al.*, 2018).

The mechanism of BE is not fully understood; however, studies suggest that two possible mechanisms may be involved: either communication through gap junctions (GJ) (Azzam *et al.*, 1998) or transmissible soluble factors (Hickman *et al.*, 1994).

*1.6.3.iv The role of gap junction in intercellular communication*

Cells can communicate with each other using special structures called gap junctions (GJ), which consist of six transmembrane connexin proteins arranged in a cylindrical shape making a pore linking adjacent cells to each other (Czyz, 2008). GJ allow interaction of two hemi open channels of neighbouring cells by forming a small channel between the cells, in which molecules less than 1.5KD can pass through (Vinken, 2012; Zhou *et al.*, 2017).

It has been well reported that BE can be induced through gap junction intercellular communication (GJIC). Bishayee *et al.* (2001) demonstrate that free radicals can use the GJIC to induce BE in adjacent cells. They labelled Chinese hamster V79 cells with tritiated thymidine and mixed them with unlabelled cells. The labelled cells were hit by short-range β-particles. Dimethyl sulphide was used to treat the cells and block GJ. They found that unlabelled cells were protected from the effect of free radicals. The authors suggest that free radicals can produce BE through GJ. Azzam, de Toledo and Little (2003) had also reported that IR induced BE via GJIC.

Most recent evidence confirming the role of GJ in BE has been presented by Arora *et al*. (2018), They used NSCLC, H1299 lung cancer cells and H1355, H460 ovarian cancer cells and treated them with cisplatin. They found that cisplatin can regulate the induction of DNA damage through bystander GJIC in

high-density cell populations (Arora *et al.*, 2018). The study conducted by Wu *et al.* (2018) provides further evidence to support the role of GJIC in BE. They used a modified testicular cancer cell line, 1-10/DDP. They exposed mouse Leydig tumour cells to a series of the concentration of cisplatin DDP for 7 days to produce cisplatin-resistant cell line. They found that the capacity for migration and invasion of 1-10/DDP cells was elevated and was associated with an increase in the expression of the Cx43 protein and a decreased in the functional capability of GJ (Wu *et al.*, 2018). Furthermore, inhibition GJIC by retinoic acid can decrease the migration and invasion of 1-10/DDP cells.

*1.6.3. v The role of transmissible factors in intercellular communication*

As described above, cell-cell communication can be mediated via GJ. Other studies have demonstrated that BE can be induced in recipient cells using a media transfer approach. Media transfer BE has been well documented in the literature (Azzam *et al.*, 1998 ; Azzam, Jay-Gerin and Pain, 2012; Mothersill, Rusin and Seymour, 2017). Anzenberg, Chandiramani and Coderre (2008) stated that the media from irradiated DU-145 prostate cancer cells can increase the incidence of micronuclei in unirradiated DU-145 and AG01522 fibroblast recipient cells. Kanasugi *et al.* (2007) observed a chromosomal aberration in unirradiated fibroblast cells that were treated with media isolated from irradiated fibroblast cells. Moreover, Widel *et al.* (2012) proposed that irradiated human melanoma cells can induce BE in human fibroblast cells in a co-culture system. They suggest that irradiation induces ROS formation and that ROS could be transferred to unirradiated cells and induce BE.

*1.6.3. vi Extracellular vesicles and cell communication*

BE phenomena in cells that have not been exposed to radiation have been supported by a body of data from numerous publications. Irradiated and unirradiated cells can communicate using GJIC, or by soluble factors that are released into the surrounding medium. Microvesicles/exosomes are also known to be induced BE in recipient cells. Jella *et al.* (2014) observed an increase in the viability and intercellular calcium level in HaCaT keratinocytes cells that were treated with exosomes isolated from irradiated cell-conditioned media (ICCM). They also transferred exosome-depleted media to unirradiated cells and they

observed abrogation in the effect of ICCM media in term of viability and calcium induction.

Cell-cell communication via exosomes has also been seen in BHY and FaDu head and neck cancer cell lines following ionising irradiation (Mutschelknaus *et al.*, 2016). Exosomes that were isolated from ICCM and CCCM were transferred to unirradiated head and neck carcinoma cells. The authors showed that both exosomes from irradiated and unirradiated cells can increase the survival and proliferation of unirradiated cells. They have suggested that exosomes can transfer pro-survival factors that contribute to DNA repair in irradiated cells.

Moreover, exosome-induced BE has been reported to promote migration and invasion of cancer cells. Harris *et al.* (2015) demonstrated that exosomes isolated from invasive / metastatic MDA-MB-231 breast cancer cells induce the migratory effect of recipient MDA-MB-231 or MCF-7 cells compared to the cells treated with exosomes isolated from MCF-7 breast cancer cells. They also showed that MDA-MB-231 exosomes demonstrated 2 fold higher or lower proteins than MCF-7, they found 38 upregulated proteins and 30 of them had been reported to be involved in invasion and human breast cancer cells (Harris *et al.*, 2015).

## 1.7 Exosomes

As described above in Section1.6.3. vi, exosomes are small vesicles (40-150nm), which initially arise from endosomes (Suetsugu *et al.*, 2013). It has been reported that exosomes are secreted from both normal and cancer cells, and they contain DNA, mRNA, miRNA and protein molecules (Kumar *et al.*, 2015a; Kumar *et al.*, 2015b; Li *et al.*, 2015; Lai *et al.*, 2016; Languino *et al.*, 2016). According to Al-Mayah *et al.* (2012), exosomes secreted from irradiated cancer cells can stimulate DNA damage and chromosomal aberrations in bystander recipient cells. They also showed that inhibiting the RNA and protein molecules (using RNase A or heat, respectively) of exosomes derived from ICCM can abolish the induction of BE.

### 1.7.1 Exosomes cargo

Exosomes contain various types of molecules, including nucleic acids (DNA, mRNA, and miRNA), proteins (enzymes, cytokines, transmembrane proteins) and metabolites. The majority of exosomes contain transport and fusion proteins,

such as flotillin, annexins and Rab GTPase, Alix, and TSG101 (reviewed by Lindsey and Langhans, 2014; Brinton *et al.*, 2015), and exosomal metabolites include peroxidases, lipid kinases and pyruvate enzymes (Altadill *et al.*, 2016).

Moreover, there are several cytoplasmic proteins such as actin and tubulin that are found in exosomes. In addition to integrin and tetraspanin, heat shock proteins such as hsp70 and hsp90 have also been found in the exosome (Mathivanan, Ji and Simpson, 2010). Exosomes can also carry proteins that are involved in EMT, such as TGF-β (Li *et al.*, 2017e) and TNF-α (Hong *et al.*, 2016). One of the most important proteins that have been found in the exosomes is TGF-β, described in Section 1.3.3 which can play a critical role in physiological and pathological pathways in animal cells, including the developmental mechanistic pathway, (Perry, Anthony and Steiner, 1997), and cancer development and progression (Languino *et al.*, 2016; Yen *et al.*, 2017).

Studies state that exosomes can interact with the cell membranes via phosphatidylserine lipid (Keller et al., 2009) or ligand-receptor interactions (Thery et al., 2006). Exosomes can also fuse directly with the cell membrane to release contents to the cytoplasm. Otherwise, exosomes can enter the cells through ligand clathrin-mediated endocytosis (Morelli et al., 2004; Morelli et al., 2017). miRNA has also been found in the exosomes (Kruger *et al.*, 2014; Bernal *et al.*, 2014). For example, microarray analyses of MDA-MB-231 and MCF-7 exosomes showed a wide range of miRNA expression. In addition, they are found several oncogenic miRNA in both types of exosomes (Kruger *et al.*, 2014).

### 1.7.2 Exosome function

The function of exosomes varies from one type of cell to another, i.e. exosomes can either be activators or inhibitors. For example, exosomes released from dendritic cells can activate the immune system, directly or indirectly via cytokine production and T cell activation (Bianco *et al.*, 2009). Conversely, exosomes derived from cancer cells have an inhibitory effect on the immune system (Thery *et al.*, 2002; Clayton *et al.*, 2007).

As described previously in Section 1.2, the vast majority of cancer patient mortality results from the metastasis of cancer cells to distant sites away from the primary cancer source. Much effort has been put into understanding the role of

exosomes in the mechanisms of cancer cell metastasis. It has been reported that tumour-derived exosomes can influence tumour growth (Wang and Tang, 2010). Boelens *et al.* (2014) state that exosomes derived from H1299 and A549 highly invasive lung cancer cells could increase the migration of non-invasive H522 lung cancer cells. It has been stated that exosomes and their content carry essential factors for EMT, such as Ras and MMPs (Tauro *et al.*, 2013). The exosomes derived from the serum of patients with metastatic lung carcinoma promotes expression of vimentin and increased invasion and migration of human bronchial epithelial cell (HBECs) recipient cells (Rahman *et al.*, 2016).

The potential effect of exosomes on the behaviour of cells could result from the nature of exosome cargo (e.g. protein and RNA), which could be affected by several factors including ROS (Wang *et al.*, 2017). IR is one of the most critical factors that increase ROS and induce stress in human body cells resulting in increased exosome production (Szumiel, 2015).

Recent studies have concentrated on the effect of IR on exosome cargo, as well as its implications for human cells. Jelonek, Widlak and Pietrowska (2016) have documented that exposure to IR can lead to changes in the compositions of exosomes, which may reflect on cellular activity such as suppression of translation, transcription or induction of cell signalling. They examined proteins in the exosomes extracted from irradiated and unirradiated head and neck cancer cells. They showed great changes in the exosome contents post-irradiation compared to the control group. Three hundred eighty-four proteins were identified in exosomes post-irradiation, including 236 new proteins, which had not been detected in unirradiated exosomes. In addition, 69 proteins were found to be missing after exposure to 2 Gy X-ray; whilst only 217 proteins were detected in the exosomes from the control group.

Al-Mayah *et al.* (2015) stated that exosomes derived from irradiated MCF-7 cells have a long-lived effect on unirradiated cells due to both components of exosomes, protein and RNA molecules. Both exosome molecules (proteins and RNA) synergistically work to induce non-targeted effects of exosome cargo within the progeny of irradiated and unirradiated cancer cells.

However, the targeted and non-targeted effects of IR on cancer cell invasiveness and metastasis are not fully understood. Therefore, this study investigates the direct and bystander effects of IR on cancer cell invasion correlated with changes in glycosylation and EMT markers.

## 1.8 Aims

Radiation therapy is one of the most important methods for the treatment of cancer. However, most of the cases, cancer can be recurrent or distribution to other parts of the body following irradiation. This study aims to investigate the effect of X-radiation or exosomes derived from irradiated cells on the invasive capacity of luminal MCF-7 and basal MDA-MB-231 breast cancer cells. Cells were analysed 24 hours following 2 Gy X-irradiation or exosomes transfer to examine the change in the glycosylation and EMT markers as well as the number of invasive cells to the Matrigel. In addition, this study also aims to determine the expression of candidate genes and the level of proteins that could have a role in the invasion of breast cancer cells. This study will, therefore, investigate the expression of GalNAc-T6, vimentin, E-cadherin and TGF-β genes. Moreover, the study also will investigate the expression of transcription factors SLUG, SNAIL, ZEB, TWIST and MMP, which may be involved in the EMT and invasiveness. Candidate proteins (TGF- β, vimentin and E-cadherin) will also investigate. Moreover, candidate miRNA (Let7-a, miR-30a, miR-200a and miR-9a) will also be examined as they have a role in the expression of transcription factors associated with EMT and invasiveness.

Therefore, this study was established to:

1- Investigate whether a therapeutic dose of X-irradiation can change glycosylation and EMT markers and promote invasion of breast cancer cells.
2- Investigate the potential role of exosomes in the change of glycosylation and EMT markers and the invasion of breast cancer cells.
3- Investigate the role of direct irradiation and exosome transfer on the change of glycosylation EMT markers and the invasion of MDA-MB-231 breast cancer stem cells.
4- Achieve a better understanding of the mechanisms of breast cancer cell invasion regarding the change in the expression of candidate transcription factors, such as TGF-β, SLUG, SNAIL, ZEB, TWIST and MMP which may be

involved in breast cancer cells invasion following irradiation or exosome transfer.

# Chapter 2. Materials and Methods

## 2.1 Experiment design

The studies described in this thesis were conducted to investigate the role/effect of ionising radiation (IR) and cell-cell communication post-X-ray-irradiation on the invasive capacity of human breast cancer cells. To this end, various experiments were performed with the following aims, as illustrated in Figure 2.1:

1- Optimise the experimental conditions
2- Determine the effect of IR on glycosylation
3- Determine the impact of IR on markers of EMT
4- Investigate the effects of IR on the invasive capacity of breast cancer cells
5- Investigate the impact of cell communication post IR on the invasive ability of breast cancer cells
6- Investigate the impact of exosome cargo on the invasive ability of breast cancer cells
7- Investigate the role of IR on the invasiveness of breast cancer stem cells.

Four breast cancer cell lines have been chosen in this experiment, each of which has specific characteristics associated with invasiveness as will be described in Section 2.2. According to the responses of cells to the glycosylation and EMT markers, the study was optimised the best cell lines to be considered in the irradiation experiment. After which, the experiments in this study were divided into two categories (target/ direct and non-target/ bystander) effect of IR on invasiveness capacity of breast cancer cells. Eleven assays have been involved in the direct effect of IR on breast cancer cells which included cell count, cell viability, ROS, comet assay, apoptosis, invasion assay, biotinylated lectin, immunocytochemistry, flow cytometry, qPCR and western blot.

The other type of assays were set up to investigate the bystander effect of IR on the invasiveness of breast cancer cells, these assays involved classic bystander, were the media transferred to unirradiated cells and exosomes depleted media when exosomes free media were transferred to unirradiated cells, these two set of experiments involved two assays, invasion and cytochemistry assays. The second type of experiment involved in this category was exosomes bystander experiment. These experiments were set up to understand the effect of exosomes that were isolated from irradiated cells on invasiveness capacity of

unirradiated breast cancer cells. These experiments involved invasion assay, cytochemistry assay, flow cytometry qPCR and western blot assays. The final experiments underwent a bystander effect of IR was exosomes cargo inhibition to confirm the effect of exosomal protein and RNAs in the invasion of breast cancer cells, as demonstrated in Figure 2.1.

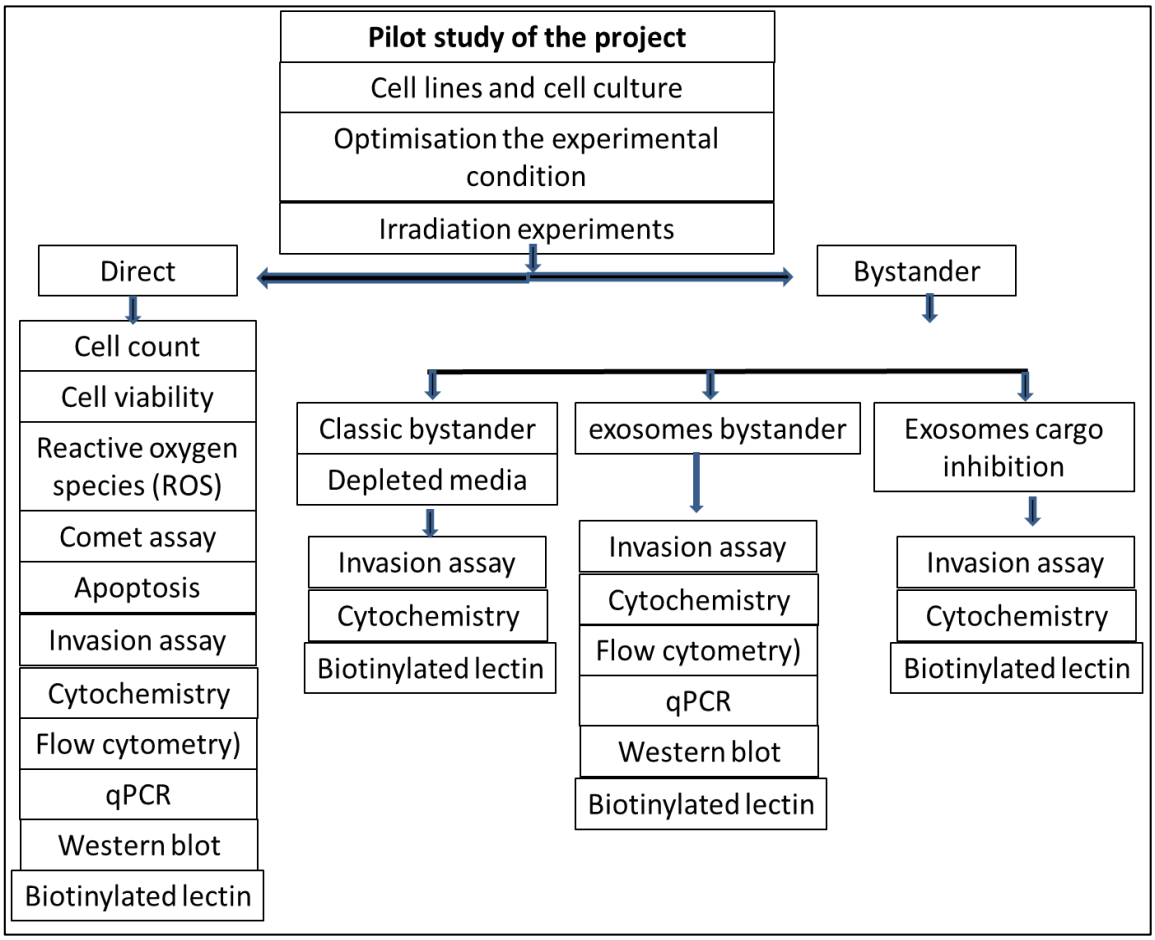


*Figure 2.1 A schematic diagram of the experimental design*

This diagram has illustrated the experiments and the assays that been done in this study. These assays have been utilised to investigate the effect of IR in the invasion of breast cancer cells. Before the irradiation experiments, this study has been used to optimise the best cell line of breast cancer. Following the optimisation of the experimental conditions, cells either exposed to direct X-irradiation or treated with exosomes isolated from irradiated and unirradiated cells. In the direct and bystander parts, cells were subjected to cell count, cell viability, ROS, comet, apoptosis, invasion, cytochemistry, flow cytometry, qPCR, and western blot.

## 2.2 Cell lines

Four human breast cancer cell lines (MDA-MB-231, MCF-7, ZR75-1, and BT474) were chosen to address these aims above, as each is known to display a range of phenotypes regarding glycosylation and EMT markers which can be considered as an indicator of aggressiveness. MDA-MB-231 is a basal triple-

negative (Oestrogen receptors negative (ER-), progesterone receptors negative (PR-) and human epidermal growth factor receptor 2 negative (HER2-)) and highly aggressive with aberrant glycosylation (Vazquez-Santillan *et al.*, 2016; Li *et al.*, 2017c). MCF-7 which is a luminal breast cancer cells and $HER2^{+}$, exhibit moderately aggressive and metastatic with aberrant glycosylation (Dai *et al.*, 2017); ZR75-1 low aggressive and metastatic with intermediate aberrant glycosylation and BT474 non-metastatic and with negligible aberrant glycosylation (Holliday and Speirs, 2011; Dai *et al.*, 2017). MCF-7, ZR75-1 and BT474 breast cancer cell lines (kindly provided by Dr Jostein Dahle (Oslo University, Norway) were retrieved from liquid nitrogen storage from our laboratory, while MDA-MB-231 cells were kindly donated by Professor John Harrison (Public Health England).

## 2.3 Cell culture

MCF-7 and MDA-MB-231 breast cancer cells were seeded in Dulbecco's Modified Eagle's Medium/Nutrient Mixture F-12 Ham (DMEM) (Sigma, RNBG2424). ZR75-1 and BT474 cells were cultivated in Iscove's Modified Dulbecco's Media (IMDM) (Gibco, 21980032). Both types of media were supplemented with 10% (v/v) foetal calf serum (FCF) (Sigma, F7524), 1% 2 mM L-Glutamine (Gibco, 25030), 1% penicillin / streptomycin solution (10,000 units of penicillin and 10 mg/mL streptomycin) (v/v) P/S, (Sigma, P0781) and 1% 250 ng/mL insulin (Sigma, 19278). All cell lines were grown in T75 or T175 tissue culture flasks at 37 $^{\circ}$C, 5% $CO_2$ at full humidity.

## 2. 4 Cell count using Erythrosin B viability stain

Haemocytometer method, with the aid of coverslip, was used to count the cells in the experimental samples. The haemocytometer has two counting areas; each side has composed of diverse size squares. The four large 1 mm X 1 mm corner squares (area of each is 1 $mm^2$) were used for counting cells. Each square subdivided into 16 small squares. The cover-slip was gently placed onto the haemocytometer. Accordingly, a 0.1 mm height is left between the cover-slip and the haemocytometer; thus, the volume of each large square is 1 mm X 1 mm X 0.1 mm = 0.1 $mm^3$ = 0.1 µl. Erythrosine B solution was prepared and mixed with the cell suspension, then the viable cells have been counted.

### 2.4.1 Erythrosin B solution preparation

Before counting the cells using erythrosin B viability stain and a Neubauer Haemocytometer (haemocytometer), first, a stock solution of erythrosin B was prepared: 0.4 g of erythrosin B powder (Sigma, E9259), 0.06 g of potassium phosphate monobasic (Sigma, 1551139) and 0.81 g of sodium chloride (Sigma, S7653) were added to 100 mL of Hanks solution (Sigma, H6648) on a magnetic stirrer hot plate. The solution was brought to a boiling point, and 1ml sodium hydroxide (Sigma, S8045) added to aid dissolution of all compounds; it was then left at the room temperature to cool. A working solution was made by adding one mL of stock solution to 4 mL of deionised water.

### 2.4.2 Cell count

To collect cells for counting, media was removed from the T75 tissue culture flasks using sterile pipette; then cells were washed with phosphate-buffered saline (PBS) (Gibco, 1786947). Cells were detached by the aid of a trypsin-EDTA solution (Sigma, T1426, E8008 respectively), 2 mL of a trypsin-EDTA solution was transferred into the T75 tissue culture flask, and rounded for one minute, then the trypsin-EDTA solution was discarded, and the cells were incubated at 37 °C for 3-7 minutes according to the type of cell line. After the incubation time, cells were detached and harvested using complete media, also according to the type of the cell line. Cells were collected in 15 mL Falcon tubes (ThermoFisher scientific, 227261). Cells were counted after diluting 1 in 2, i.e. 100 µL of each cell suspension was mixed with 100 µL of the erythrosin B working solution. 10 µL of the mixture was then transferred to each chamber of the haemocytometer. The cells were counted using a Nikon Eclipse TS 100 light microscope under 100 x magnifications. The average number of live cells was calculated and multiplied by the volume of the sample according to the following equation:

Number of cells / mL = (average number of cells in both sides of haemocytometer) x 2 x $10^{4.}$ ---- (1)

2 is the dilution factor, and $10^4$ represent 1 mL of cell suspension.

## 2.5 Irradiation

All irradiation experiments were conducted at the Gray institution, University of Oxford, using the MXR321 X-ray machine at 250 kV constant potential, 14 mA and a dose rate of 0.53 Gy/minute for 3.56 minutes.

Initial experiments focused on MCF-7 and the MDA-MB-231 cell lines. Cells were irradiated at 70% cell confluence with 2 Gy X-ray.

### 2.5.1 Cell viability

Quantitative determination of viable cells following irradiation was performed using the Muse Cell Analyser (Merck, 500-3115), which utilises small scale fluorescence detection and cytometry, enabling an analysis of individual cells. Laser-based fluorescence detection of each cell event evaluates up to 3 cellular parameters – cell size and 2 colours (detected in the red or yellow channels).. The Analyser detects stained cells at the optic-excitation of 650 nm, and emission of yellow fluorescence is detected at 576 nm with a ±28 nm band width, whilst red fluorescence is detected at 680 nm within a ±30 nm bandwidth.

Briefly, cells were stained by a specific dual DNA intercalating fluorescent dye. Cells that had lost their membrane integrity, thereby allowing the dye to enter and stain their nucleus were thus preliminarily characterised by the Analyser, as non-viable, i.e. dead or dying. Results were further validated by analysis of cellular size properties, which enabled the distinction of cells from debris.

MCF-7 and MDA-MB-231 cells were irradiated with 0 Gy (control / sham dose) and 2 Gy (final dose). At 4 hours post-irradiation, cells from each irradiation condition were harvested in phosphate-buffered saline (PBS), and 50 µL of each cell suspension (concentration $1x10^6$ cell/mL) was mixed and incubated with 450 µL of Muse count and viability reagent (Merck, MCH100102) which is composed of a mix of organic and inorganic compounds, including an alternative to trypan blue in 1.5 mL Eppendorf tubes, (VWR, 211-0015). Cells were incubated with the reagent for 5 minutes and then analysed for viability using the Muse Cell Analyser, as shown in Figure 2.2. The viability of MCF-7 and MDA-MB-231 cells were analysed according to the manufacturer's protocol. The viability of irradiated cells was calculated as a relative percentage to the living cells of the unirradiated control group.

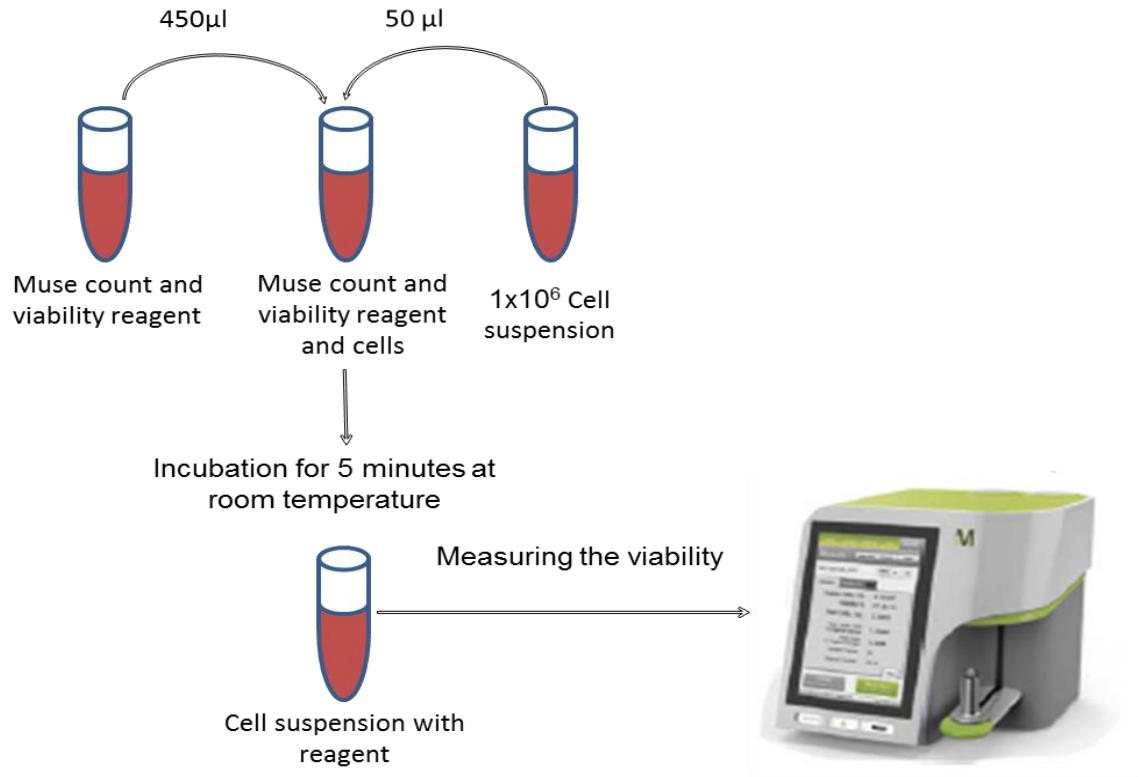


*Figure 2.2 A schematic diagram showed the summary of cell viability protocol using Muse cell analyser.*

Cells were mixed with count and viability reagent and left in the room temperature. The viability of cells was measured after 5 minutes of incubation with the reagent.

### 2.5.2 Reactive oxygen species (ROS)

*2.5.2. i Principles*

Quantitative measurements of reactive oxygen species (ROS) in MCF-7 and MDA-MB-231 cells undergoing oxidative stress after irradiation with 2 Gy X irradiation was performed using Muse oxidative stress kit (Merck, 4700-1665). The assay determines the relative percentage of cells that are ROS positive and ROS negative. After irradiation cells were harvested and incubated with dihydroethidium (Merck, 4700-1665) (DHE), a ROS reagent. They were then analysed according to the manufacturer's protocol. The principle of detection of ROS in the cells is comparable to the viability of the cells assay, Section 2.5.1, i.e. the Analyser detects stained cells at the optic-excitation of 650 nm, and emission of yellow fluorescence is detected at 576 nm with a ±28 nm band width, whilst red fluorescence is detected at 680 nm within a ±30 nm bandwidth.

The superoxide indicator dihydroethidium, also called hydroethidine, exhibits blue fluorescence in the cytosol until oxidised. Where it intercalates within the cell's

DNA, staining its nucleus a bright fluorescent red. DHE has been used for a long time to determine the level of ROS in the cells (Bindokas et al., 1996).

*2.5.2.ii Reagent preparation*

The Muse oxidative stress reagent (Merck, 4700-1665) and 1x assay buffer (Merck, 4700-1330) were warmed in the dark, to the room temperature. The oxidative stress reagent was diluted 1 in 100 in the 1x assay buffer. This solution (intermediate oxidative stress solution) was further diluted 1 in 80 in the 1x assay buffer (both dilutions were performed in the dark).

*2.5.2. iii ROS measuring*

Subsequent irradiation studies on MCF-7 and MDA-MB231 breast cancer cells increased. Fresh samples of each cell line were irradiated with 0 Gy and 2 Gy X-radiation. 30 minutes post-irradiation; cells were harvested in 1x assay buffer. 10 µL of each cell suspension was added to 190 µL of oxidative stress reagent working solution for each tube; extra tubes were made as a positive control (cells never been exposed to irradiation and mixed with ROS reagent and negative controls (cells never been exposed to irradiation and nor ROS reagent). Cells were incubated with oxidative stress reagent at 37°C for 30 minutes. $ROS^-$ and $ROS^+$ were measured using Muse cell analyser as shown in Figure 2.3.

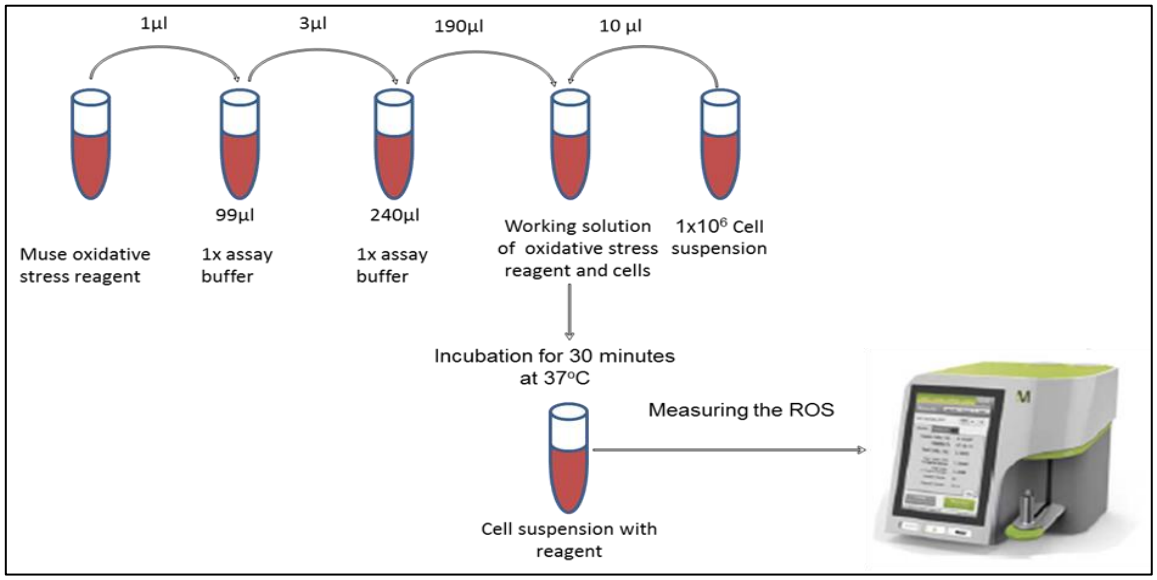


*Figure 2.3 A schematic diagram showed a summary of the ROS measuring protocol.*

Cells were mixed with ROS working solution for 30 minutes at 37 °C. ROS in the irradiated and unirradiated cells were measured.

The left panel shows the size of the cells. While the right panel shows the ROS, the left grey histogram showed $ROS^-$. Meanwhile, the red histogram showed the $ROS^+$ as shown in Figure 2.4.

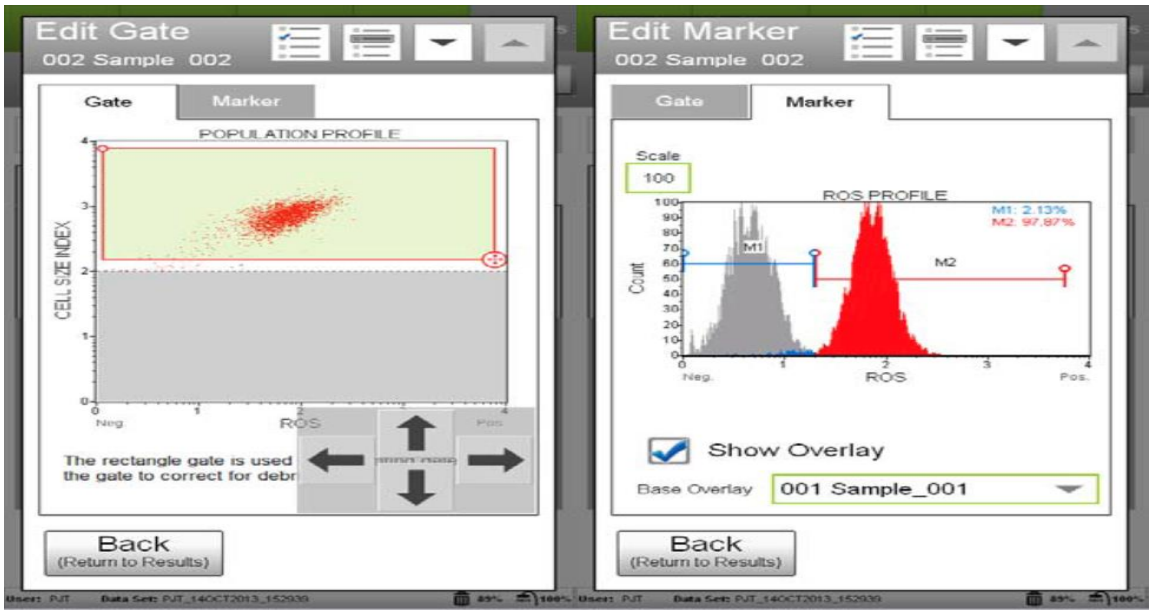


*Figure 2.4 A schematic diagram showed the principle of cell analyser (Muse) measuring ROS.*

The left panel of the graph shows the cell size (top Section). The right panel shows a diagram of ROS positive (red) and negative (grey) cells.

### 2.5.3 Comet assay

The alkaline single cell gel electrophoresis assay (comet assay) was utilised to determine the total DNA damage in comet tail following irradiation, as described in (Chandna, 2004; Al-Mayah *et al.*, 2012).

50 µL of media which contain approximately 2x $10^4$ of breast cancer cells in was mixed with 200 µL low melting point agar (LMPA), (Fisher Biotech, BP165-25) and placed on agarose-coated slides (Sigma, A9539-100). A homogenous/mono-layer of cells was created by placing a 22x50 mm coverslips on the drop of cell/agar suspension, and these were left flat in place for 10 minutes. The slides were then transferred to Coplin jars containing cold lysis buffer (2.5 M NaCl, 100mM EDTA (pH 8.0)), 10 mM Tris-HCl (pH 7.6) and 1% Triton X-100 (pH 10.0) and left overnight at 4°C. The slides were then transferred to an electrophoresis tank (Bio-Rad, UK) filled with electrophoresis buffer (0.3 M NaOH and one mM EDTA, pH13) and left at $4^0$C for 40 minutes. The electrophoresis tank was then run for 30 minutes, at 19V and 300 A. Slides were neutralised with neutralising buffer (0.4 M Tris-HCl, pH 7.5) for 5 minutes, and then washed with distilled water

for 10 minutes prior to immediate staining with diamond nucleic acid dye (Promega, H1181) working solution (1 µL diamond nucleic acid dye in 10,000 µL dilution of tris-base buffer). Cells were analysed using comet assay 5 software, and fluorescence microscopy (Nikon, Japan) and colour camera (Basler, Germany) cells were analysed under 20X magnification which can compare the DNA in comet tail (outside the nucleus) to the DNA in the nucleus.

### 2.5.4 Apoptosis assay

The apoptosis assay was used as the method to determine the presence of apoptotic cells related to the total number of the cells (Schwartz *et al.*, 1995). MCF-7 cells were irradiated with either 0 Gy or 2 Gy X-rays. 4 hours post-irradiation; cells were collected in 50 mL Universal tubes using PBS as described in Section 2.4.2 and centrifuged at 1200 rpm using Heraeus Megafuge 16 centrifuge (ThermoFisher, 75004230). Cells were fixed with 3:1 methanol: acetic acid fixative dropped onto clean slides using plastic Pasteur pipette, 1ml fine tip (Charlton scientific) and left to dry overnight. The dried slides were stained with 25 µL Prolong Gold anti-fade reagent with DAPI (Invitrogen, P36931) and viewed under a Zeiss Axioplan Pol Universal fluorescent microscope. The percentage of apoptotic cells (cells, where the nucleus is divided into several lobules a representative image, is shown in Figure 2.5to the total number of cells in 20 microscopic fields was counted. Five hundred cells at least were counted in total per each replicate. Cells were counted using Zeiss Axioplan 2 Upright Light/Fluorescence Microscope and ProgRes C3 camera under 40 x magnifications as shown in Figure 2.5, three replicates for each dose. Data were collected and statistically analysed using Fisher's exact test and Minitab 16 software.

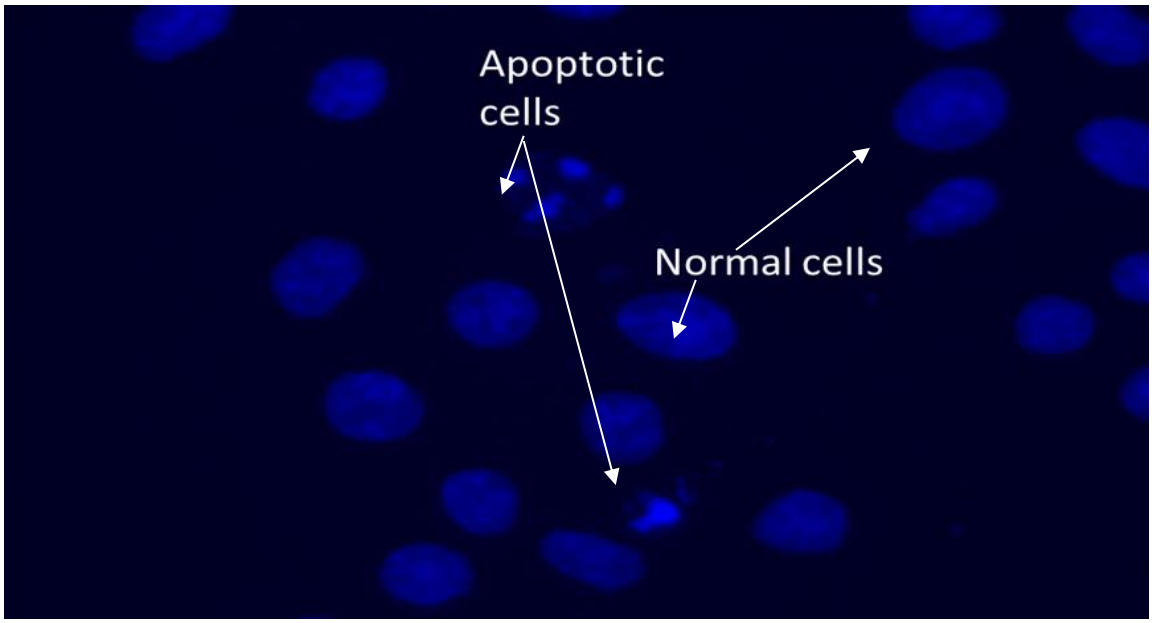


*Figure 2.5 Picture of apoptotic and normal cells.*

The number of apoptotic cells to the total number of cells in 20 microscopic fields was counted. The nucleus of apoptotic cells was divided into several lobes. Meanwhile, the nucleus of normal cells is one compact lobe.

## 2.6 Lectin- biotinylated cytochemistry – cell glycosylation

Four breast cancer cell lines (MDA-MB-231, MCF-7, ZR75-1 and BT474) were seeded on coverslips in 12 well plates and incubated for 24 hours to allow for cells to settled and grow. For each cell line, the media was removed from the wells; the cells were washed with growth media and then fixed with 4% formaldehyde in 1X PIPES buffer (piperazine-N, N′-bis (2-ethane sulfonic acid, Sigma, P1851) at 4$^{o}$C for 15 minutes. Cells were then washed with PIPES buffer and permeabilised with 0.1% v/v Triton X100 (Sigma, T9284) in 0.1 M PIPES buffer. They then underwent 3X washes with 0.1 M PIPES buffer before the addition of 3% v/v methanol/hydrogen peroxide. The endogenous peroxidase was then blocked with 9:1 methanol/hydrogen peroxide for 20 minutes at room temperature. The cells were washed 3X with Tris-base buffered saline TBS (1X) (Sigma, T5030-100TAB) which was prepared by dissolving 6.05 g Tris base and 8.76 g NaCl in 800 ml of dH2O. The pH was adjusted to 7.5 with 1 M HCl and make volume up to 1 L with dH2O. Cells were then blocked with 3% bovine serum albumin (BSA) in TBS (BSA / TBS) for 30 minutes. HPA was used to detect GalNAc glycans, (Fukutomi *et al.*, 1989; Brooks *et al.*, 1993) PHA-L to detect 1,6 N-linked glycans (Mitchell *et al.*, 1998) and SNA to detect sialic acid.

The concentration of HPA lectin was selected according to the method that was described in Lescar *et al.* (2007). Meanwhile, the concentration of PHAL and SNA was optimised in this study. To this end, cells were first labelled with 10µg/ml of PHA-L or SNA lectin for one hour and then labelled with 5 µg/ml avidin peroxidase for 30 minutes. Negative results were observed. Following this, samples of fresh unirradiated cells were labelled with 10 µg/ml of PHA-L or SNA lectin for 12 hours and then labelled with avidin-peroxidase. Once again, negative results were observed. The experiment was performed a third time, with 20 µg/ml of PHA-L and SNA lectin for 12 hours and prior to labelling with avidin-peroxidase for 30 minutes. Positive labelling was observed following this condition.

Therefore, for each cell line, cells in three wells were treated with either i) 10 µg/mL HPA (Sigma, L6512) in 1% BSA/TBS buffer for 3 minutes. ii) 20 µg/mL SNA (Sigma, L6890) for 12 hours or iii) 20 µg/mL PHA-L (Sigma, L2769) in 1% BSA/TBS buffer for 12 hours. All wells were then treated with five µg /mL avidin peroxidase (Sigma, A3151) in 1% BSA/TBS buffer for 30 minutes and then further treated with 3, 3'-diaminobenzidine (DAB) Peroxidase Substrate Kit (Vector, SK-4100) working solution for 3-5 minutes at room temperature. The working solution was made by added 2 drops of buffer stock solution PH 7.5, 4 drops of DAB stock solution and 2 drops of hydrogen peroxide to 5 ML of $dH_2O$. The DAB interacts with avidin-peroxidase to produce a brown colour; brown coloured cells, therefore, indicate a positive result (lectin binding), while unlabelled cells mean a negative result. Cells were then counterstained with Harris' haematoxylin (Sigma, HHS16) and dehydrated using a series of methanol washes (50%, 70%, 90%, 100%, and 100%). They were then dipped briefly into 100% xylene (Fisher, X/0250/17) and mounted on clean slides using a mixture of distyrene (polystyrene), tricresyl phosphate (a plasticiser) and xylene DPX (Sigma, 06522-100ML). Each sample has three replicates and positive and negative controls were applied. The positive control (cells labelled normally with lectin, avidin peroxidase and DAB, meanwhile, cells that not labelled with lectin, but just avidin peroxidase and DAB, represent a negative control, as shown in Figure 2.6. Five microscopically fields were chosen randomly and then a picture for each microscopical field has been taken using light microscopy (Axioplan, Germany) and colour camera (ProgRes, Germany). The positive and negative

cells were counted using ImageJ software, and the percentage of the brown cell to the total number of the cells in five microscopically field was calculated. Data were statistically analysed using Fisher's exact test and presented as a percentage of labelled cells to a total number of cells.

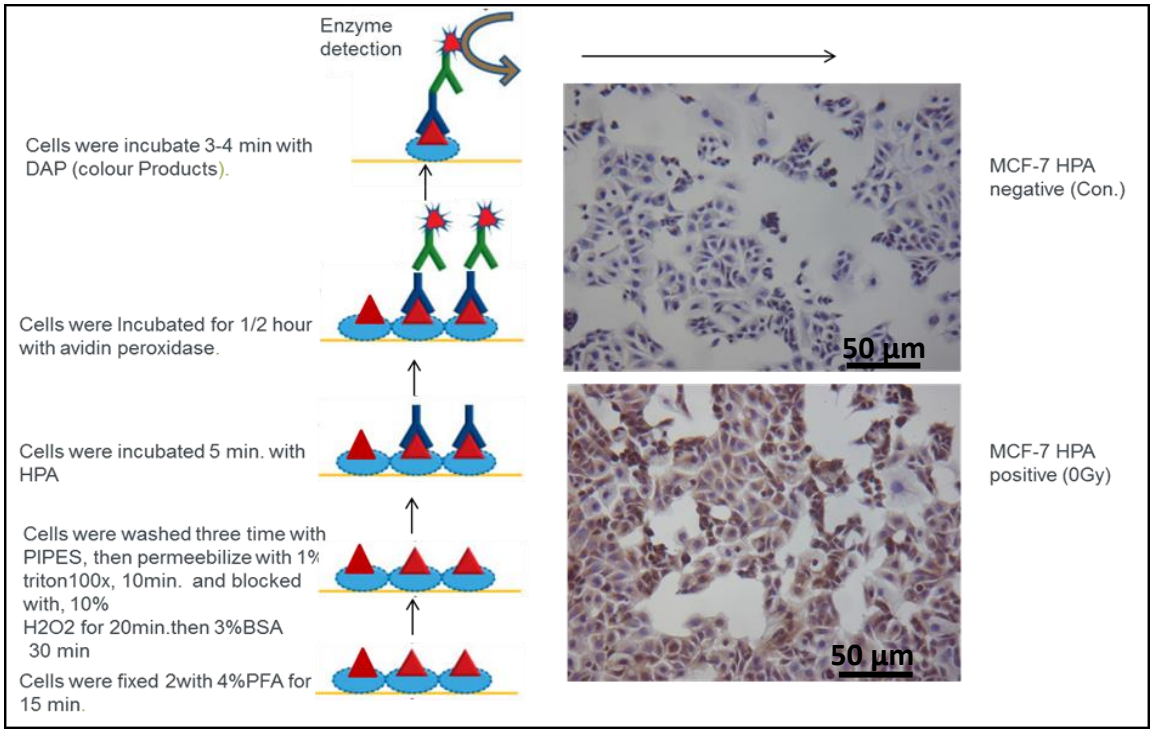


*Figure 2.6 A schematic diagram showed the principle of HPA biotinylated lectin positivity.*

## 2.7 Protein immunocytochemistry – EMT Marker assay

MDA-MB-231, MCF-7, ZR75-1 and BT474 breast cancer cells were seeded in 12 well plates and then treated with either 2 µg/mL of rabbit polyclonal anti-vimentin antibody (abcam, ab137321), 0.5 µg/mL of rabbit monoclonal anti-E-cadherin (phospho S838+S840) antibody [EP913(2)Y] (abcam, ab76319) or 4 µg/mL of rabbit polyclonal anti-N-cadherin antibody (abcam, ab12221). Cells were fixed and blocked similarly to the procedure used in the glycosylation detection as described in Section 2.6, and then labelled with primary antibodies. Cells were incubated with antibodies (anti-vimentin, anti-N-cadherin and anti-E-cadherin antibodies) overnight in the refrigerator at 4ºC. They were then washed 3X with PBS before treatment with four µg/mL donkey anti-rabbit IgG H&L horseradish peroxidase (abcam, ab6802) for 1 hour as a secondary antibody. DAB Peroxidase Substrate Kit (Vector, SK-4100) was added for 5 minutes to promote colour visualisation by interacting with secondary antibody. Cells were washed

three times with PBS counterstained with Harris' haematoxylin for 30 seconds and then washed with tap water. They then underwent a series of dehydration steps before mounting with DPX as described in Section 2.6. Immunopositive cells were visualised as brown when viewed using a light microscope. Positive and negative controls were applied. In the positive control, cells were labelled with a primary antibody, secondary antibody and DAB, whereas in the negative control, cells labelled with secondary antibody and DAB. The percentage of positive cells to the total number of the cells in the microscope field was counted and analysed as described in Section 2.6.

## 2.8 Flow cytometry

Flow cytometry is a technique that is used to investigate the physical and chemical characteristics of particles or cells in the fluidic system as it passes through a laser beam or beams. Cell components are labelled with a fluorescent dye and then excited by the laser to emit light in various wavelengths. The fluorescence can be measured to determine the properties of cells including number, size and fluorescent intensity of cells. The flow cytometry was set up to assess the data, three gates were opened (dot plot, histogram and statistical information). The standard sample was run first to determine the population of cells that need to be measured to set up the standard for other samples. A polygonal shape was chosen from the toolbar of the software and applied on the aggregation of dots in dot plot gate by which included and represented the main population of cells. From this population, the positive and negative cells were determined by laser channels of flow cytometry. The rest of the events, such as very large cells, dead cells and debris were excluded. Then the negative cells were determined from the gate of the histogram by moving the vertical line to the end of the histogram. Consequently, any cells on the left hand of the vertical line counted as negative cells and any cells on the right hand were counted as positive cells.

To identify the sub-population size and properties of the sample, sequential bivariate gating was used which are two-dimensional plots as a standard method. Based on the size of the event, threshold (of side scatter Y-axis) was set up beforehand to reduce the noise that comes from debris. So, any particle passes through the laser beams and has a size less than the threshold was excluded.

The other threshold was forward scattered (X-axis threshold), in which flow cytometry can count cells that have a minimum intensity of staining above the level of threshold. These events (cells) represent the positive event, the other events that reach the minimum size of the event and not reach the minimum quantity of emitting were counted as negative cells (Cossarizza *et al.*, 2017). Data from each cell are determined based on their fluorescent and light scattering. The data were presented as a single parameter histogram or plot for the correlated parameter. However, in this study, data were present as a histogram, because it showed the percentage of positive and negative cells and it can confirm the data of immunocytochemistry assay as it is presented as a histogram.

MCF-7 and MDA-MB-231 cancer cells were seed in T75 tissue culture flasks, three replicates for each cell line. Cells were cultivated in (DMEM) (Sigma, RNBG2424) for 48 hours. Media were discarded, and the cells were washed with PBS (Gibco, 1786947). Cells were then detached using 0.5% trypsin in EDTA solution (Sigma, T1426, E8008 respectively) and harvested in PBS by adding 10 mL of PBS to the T75. Cells were then collected in 15 mL Falcon tubes. Cells were counted using haemocytometer methods as described in Section 2.4.2 and washed three times with PBS and centrifuged at 300g for 7 minutes. They were then fixed with 80% methanol in distilled water for 5 minutes and further washed three times with PBS. The cells were then permeablised with 1% Triton x-100 in PBS for 10 minutes, centrifuged at 300g for 7 minutes and washed three times with PBS. They were then incubated with 2 µg/mL rabbit polyclonal anti-vimentin antibody (abcam, Ab137321) and rabbit monoclonal anti-E-cadherin (phospho S838+S840) antibody [EP913(2)Y] (abcam, ab76319) primary antibodies for 1 hour at room temperature. After which, they were washed three times with Tris base buffer solution Tween-twenty buffer (TBST buffer) which made of dissolving (2.4 g Tris HCl, 8 g NaCl, 1 mL of Tween 20 (Sigma, P1379-1L) in 1 L distilled water, pH 7.6). Cells then incubated with 2 µg/mL of Alexa Fluor® 488-conjugated goat anti-rabbit IgG polyclonal secondary antibody (abcam, ab150077) for 30 minutes at room temperature in the dark. The negative control was cells labelled with neither primary nor secondary antibody. Cells also labelled with secondary antibody only as a second negative control to be sure that is no

false results comes from the secondary antibody (background noise). Cell suspensions were analysed using Cytoflex 5 flow cytometry (Beckman Coulter Company) under the wavelength 480-495 nm (FITC). Cells that pass through the fluidic stream of Cytoflex 5 flow cytometry can be counted and separated to the positive fluorescent cells, which can emit fluorescent light and negative, not emit fluorescent light. The positive and negative cells were determined from the dot plot and histogram gates of a negative control sample. By using the toolbar of Cytoflex 5 flow cytometry programs, a polygonal shape was applied to the main population of cells on the dot plot gate of 0 Gy and 2 Gy cells. The other dots represent dead cells, large cells, debris, or other cells located outside the polygonal shape. Therefore, these events have been excluded from the percentage of positive and negative cells.

Accordingly, a histogram gate represents the cells determined by the polygonal shape. In addition, the vertical line was brought to the edge of the histogram from the right. From the negative control approximately, 99% of cells were negative and assessed on the left-hand side of the vertical line of the histogram gate, meanwhile the positive cell of the positive control was 76% (right-hand box of the histogram). Consequently, the system (flow cytometry) showed a high efficiency of analysis as shown in figure 2.7. The total events measured by the machine were at least 2000 cells per each run, and each sample was analysed in 3 biological replicates. Figure 2.7 represents the percentage of negative cells (left) and the percentage of positive cells (right).

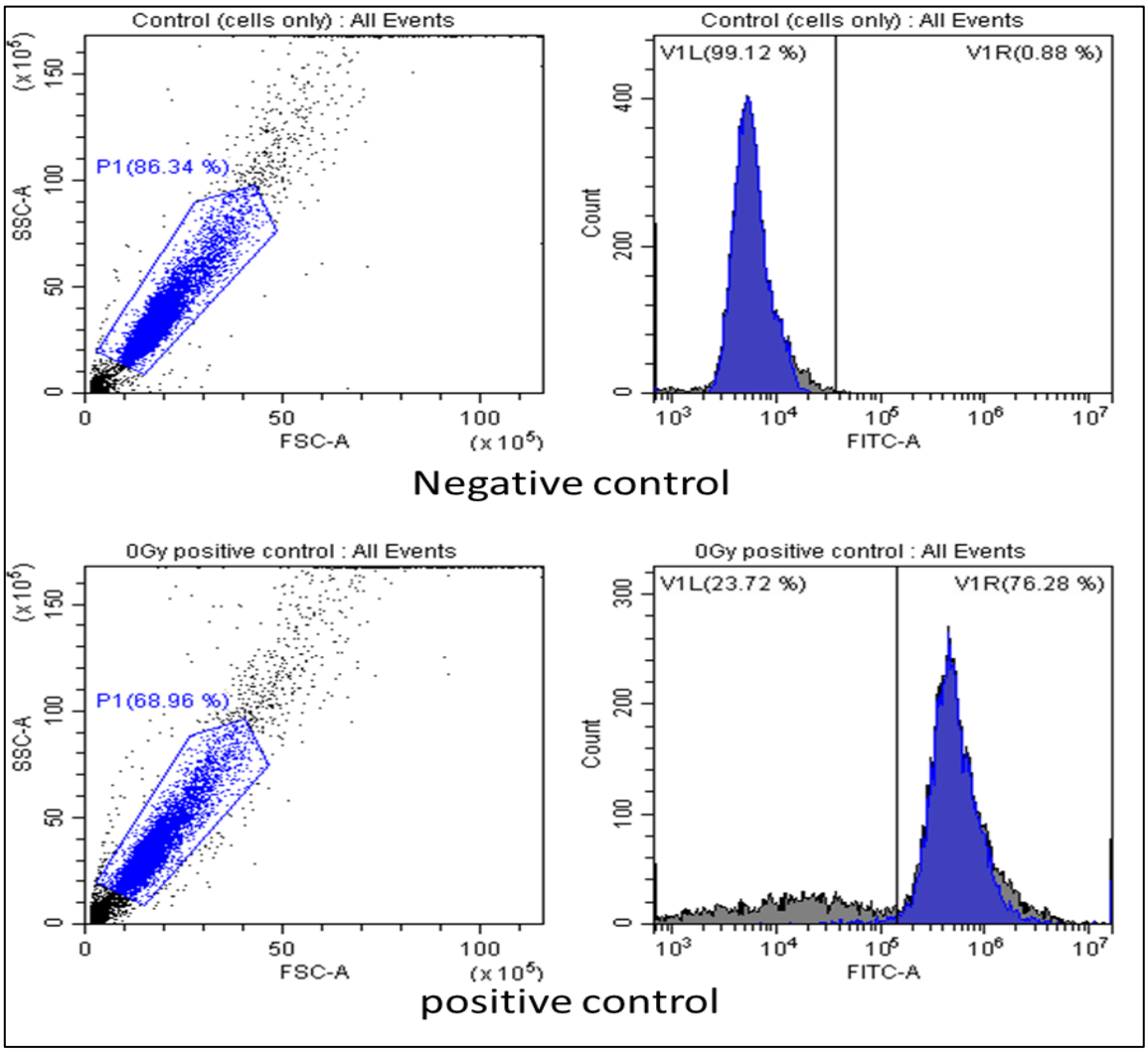


*Figure 2.7 Sample of flow cytometry.*

The blue colour in the histogram showed the main population of cells determined by the polygonal shape. While the grey colour represents the cells that have not included under the test. The negative cells appeared on the left hand of the histogram (V1L). While a positive cell labelled with primary antibody have found on the right hand of the histogram.

## 2.9 Breast cancer stem cell labelling

To investigate whether MDA-MB-231 cells exhibited stem cell properties, cells were seeded in T75 tissue culture flasks for 24 hours at optimum condition culture Section 2.3. At 70% cells confluence, media was discarded, and cells were washed with PBS and then detached by the aid of 2 ml of 0.05% trypsin in EDTA as described in 2.4.2. Cells were collected in 10 mL PBS. Cells were then washed, fixed and permeablised as described in Section 2.8. Cells were labelled with four µg/mL rabbit monoclonal [EPR1013Y] to CD44 (abcam, ab51037) and 4 µg/mL rabbit monoclonal anti-CD24 antibody [EPR3006(N)] (abcam, ab179821) at 4$^{o}$C for one hours. Cells were then washed three times with PBS and then

labelled with 2 µg/mL of Alexa Fluor® 488-conjugated goat anti-rabbit IgG polyclonal secondary antibody (abcam, ab150077) for 30 minutes at room temperature in the dark. Cells were washed three times with PBS. Three replicates for each sample were performed, the negative control was also measured by labelling MDA-MB-231 cells with 2 µg/mL Alexa Fluor® 488-conjugated goat anti-rabbit IgG polyclonal secondary antibody (abcam, ab150077) only. The CD44 and CD24 positive and negative cells were measuring using Cytoflex 5 flow cytometry (Beckman Coulter Company) under the wavelength 480-495 nm (FITC) as described in Section 2.8.

## 2.10 Optimisation of the Matrigel invasion assay

A transwell co-culture system was used to investigate the invasiveness capacity of the cancer cells. The co-culture system comprised of a 12 well plate, cover (Corning, 3336) and 12 transwells inserts (Corning, 353182) (Figure 2.8).

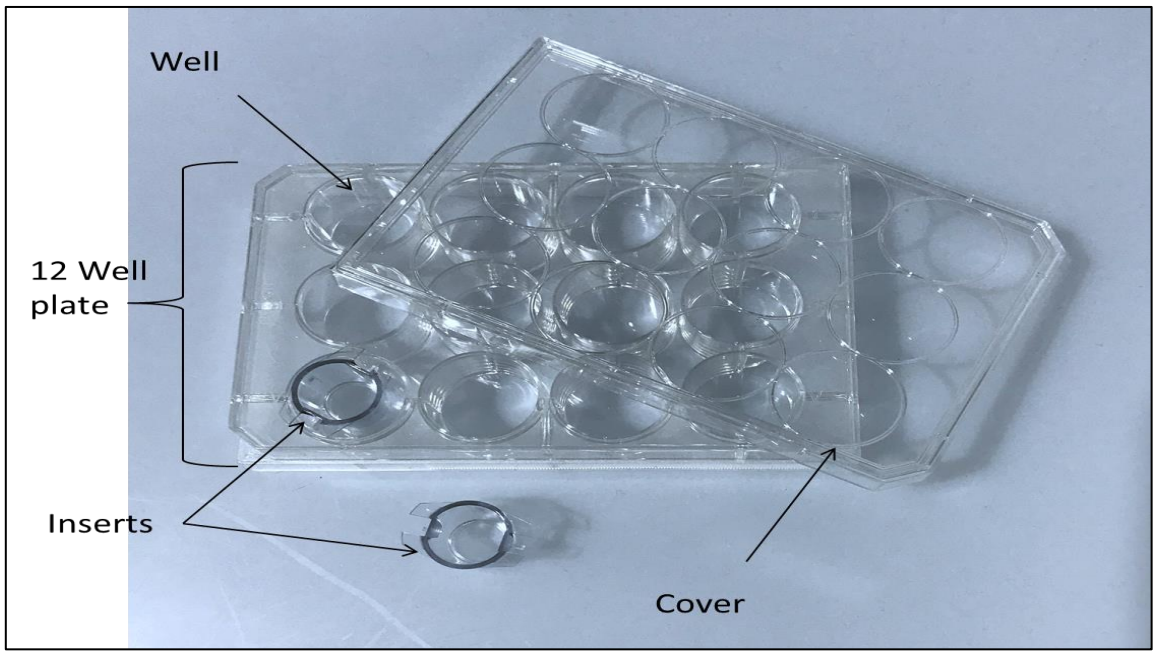


*Figure 2.8 A picture showing the co-culture system of the invasion assay.*

The inserts had a pore size of 8 µm and were coated with different concentrations of Matrigel, an extracellular matrix (ECM) gel (Sigma, E6909). Three different concentrations of Matrigel were prepared (0.5, 1.0 and 1.5 mg / mL) in serum-free media (enabling 3 insert replicates per Matrigel concentration). 9 inserts were aseptically added to 9 of the wells of the plate; 450 µL of each Matrigel concentration was then used to coat three inserts (150 µL/ well (i.e. nine inserts in total). The associated well plate cover was put on and the co-culture system

left at room temperature to enable the Matrigel to be dry overnight. The following morning, 1.5 mL of DMEM culture media (with serum) was added to 9 of the wells of a12 well plate.

One mL of unirradiated MCF-7 cells (1.25 x $10^5$ / mL in serum-free media) was carefully pipetted into each of the 9 Matrigel coated-inserts. The co-culture system was incubated for 24 hours at 37°C, 5% $CO_2$. Following incubation, the inserts were lifted from their wells and their media carefully removed. The inserts were then washed twice with PBS before undergoing a fixation with 3:1 methanol: acetic acid for 15 minutes, while the wells were discarded. The inserts were then washed three times with PBS.

The Matrigel layer and the cells that were growing on the Matrigel were removed using a swab of cotton; the inserts were left overnight to dry. Membranes were stained using eosin stain (Sigma, R03040) for 5 minutes and then washed in tap water and then stained with Harris' haematoxylin (Sigma, HHS16). Membranes were left to dry and then cut and loaded on the clean slide using DPX. All the cells that passed through the Matrigel coat, pores of the insert and subsequently attached to the underneath surface of the insert membrane were counted using a Zeiss microscope viewed using a 20 x objective lens (Axioplan, Germany).

Following optimisation of the invasion assay, further experiments were undertaken with MCF-7 and MDA-MB-231 cells to investigate the additional bystander effects of IR, cell-conditioned media and/or exosomes. To this end, MCF-7 and MDA-MB-231 cells were either directly X-irradiated with 0 Gy and 2 Gy or treated with cell-conditioned media (CCCM), irradiated cell-conditioned media (ICCM), exosomes that had previously been isolated from 0 Gy and 2 Gy media, exosome depleted media or exosomes cargo inhibition lysate as described below in Section 2.11 and 2.12.

As previously described, cells were harvested in serum-free media and seeded into the insert wells of a 12 well plate co-culture system (8 μm) coated with 0.5 mg/mL Matrigel, A schematic of the assay is shown in Figure 2.9. The data were calculated as this is the average of a total number of cells that invaded through

the membrane in 30 fields of view under 10x magnification in three replicates of three experiments.

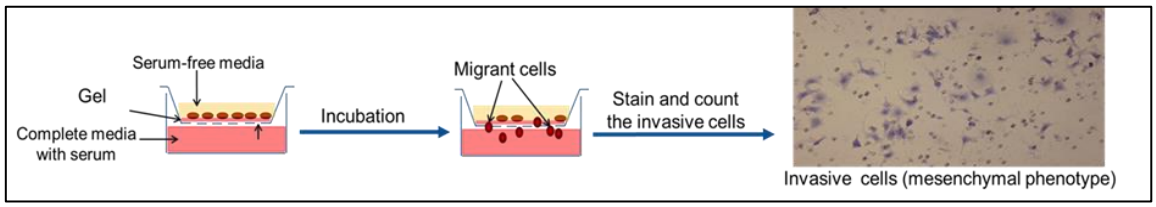


*Figure 2.9 A schematic diagram of the Matrigel invasion assay*

## 2.11 Bystander effect: Media transfer

MCF-7 and MDA-MB-231 breast cancer cells were subcultured in 75 $cm^2$ (T75) tissue culture flasks for four generations. Flasks were then irradiated at 70% cell confluence with either 0 Gy (sham-irradiation) or 2 Gy X-rays. 2 hours, 4 hours and 24 hours' time points following irradiation have been established as time points for the media transfer experiments. Irradiated cell condition media ICCM and unirradiated cells condition media CCCM were transferred to unirradiated cells, 24 hours following incubation with CCCM and ICCM cells were stained and counted as described above, data showed that four hours following irradiation presented more reliable data than 2 hours and 24 hours (data not shown).

It has been proposed that some are interfering between the effect of irradiation and the effect of extracellular vesicles and the number of cells in the flask. The irradiation can stop cells from dividing. Meanwhile, the control group continued to be divided, therefore the amount of the soluble factor in CCCM could be more than ICCM following 24 hours of irradiation, and that could give wrong results. 2 hours' time point following irradiation could be not enough for cells to produce more exosomes following irradiation. Therefore, four hours post-irradiation has been considered as the best time point for the rest of experiments, media transfer and exosomes bystander experiments. Four hours post-irradiation, the sham/irradiated media was filtered using a 0.2 µm membrane filter (Sartorius, 16534) before transfer onto samples of fresh unirradiated cells. Media from each flask was transferred to 1 container of unirradiated cells at 70% cell confluence (in each case, growth media had been removed from these unirradiated flasks before being replaced with the media from either the 0 Gy or 2 Gy X-irradiated flasks), three containers were set up for each dose. Cells were further incubated

at 37°C, 5% $CO_2$ for 24 hours and then seeded on to coverslips in 12 well plates for glycosylation and EMT markers assays. Three replicates per sample have been used and three independent experiments.

## 2.12 Exosomes isolation and purification

### 2.12.1 Exosomes isolation using ultracentrifugation method

CCCM and ICCM were collected in 50 mL Falcon tubes and centrifuged at 2,000 g for 15 minutes. The corresponding supernatant was then transferred into 50 mL sterile conical polypropylene centrifuge tubes (Alpha laboratories, CT1120) and further centrifuged for 30 minutes at 14,000g. The resultant supernatants were collected in 40 mL cellulose propionate tubes (Beckman Coulter, 344058) and further centrifuged at 120,000 g for 90 minutes. The supernatant from this was discarded, and the pellet containing the exosomes was collected in 500 µL of PBS.

### 2.12.2 Exosomes purification

qEV size exclusion columns include a resin with an approximate 75 nm pore size; therefore, small molecules and protein can enter these pores leading to refinement of EV from other particles. Size based liquid chromatography was used to purify exosomes. The procedure was performed following the manufacturer's instructions. The qEV columns were washed with 10 mL of filtered PBS. A further 5 mL of filtered PBS was added, and the time measured for its filtration (this should be less than 10 minutes). Following successful validation of the column, a sample was loaded into the column. The first three mL of filtrate was discarded, and after that 1.5 mL of filtrate aliquots, i.e. exosome fractions, were collected. These were then stored at $4^{o}C$ for future use.

### 2.12.3 Exosome characterisation.

The Classic Capture mode software for the qNano machine (Izon Company UK) was used to determine the size and concentration of exosomes, all manufacturer instructions were followed. In brief, the 'lower fluid cell' was wetted with 70 µL of the filtered qNano solution to help reduce surface tension, left for 2 minutes and then removed. A P200 qNano membrane, with the lot number facing up, was placed onto the holding stage and its stretch measured using callipers. The stretch reading value was uploaded into the computer software, and the tension

increased to 47 mm. The ‘lower fluid well' was carefully filled with 75 µL of the filtered qNano solution. The ‘upper fluid well’ was then carefully aligned onto the ‘lower fluid well’ and locked into position. Next, 35 µL of the filtered qNano solution was added to the ‘upper fluid well' and the voltage adjusted to obtain a current between 100 – 150 nA and a ‘noise’ of less than 10. The qNano was then calibrated using calibration solution 1/1000; this was run for 30 seconds or 500 particles as a minimum, whichever occurred first. Following calibration, the samples were run three replicates/sample. The results were analysed using the qNano software as shown in Figure 2.10.

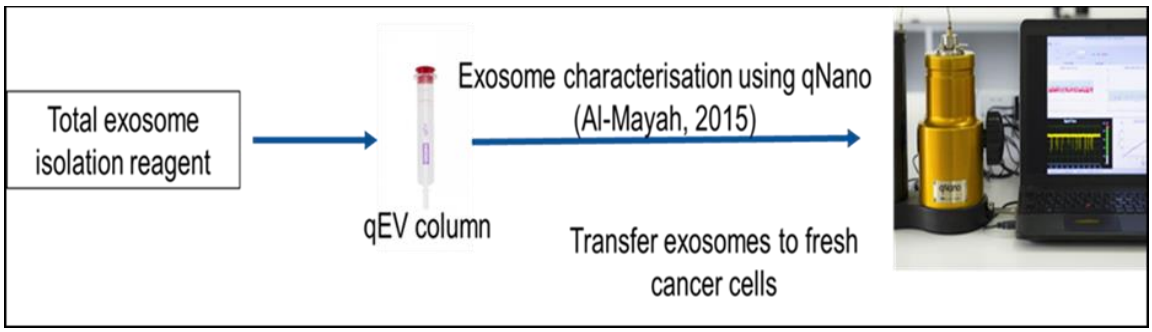


*Figure 2. 10 A schematic diagram showed exosome purification and characterisation*

### 2.12.4 Bystander effect: Exosome transfer

MCF-7 cells and MDA-MB-231 breast cancer cells were seeded in T175 tissue culture flask. Cells were irradiated with 0 Gy and 2 Gy X-irradiation, after 24 hours following irradiation exosomes were isolated using ultracentrifugation method Section 2.12.1. Exosomes were collected in 500 µL of PBS. Exosomes that were isolated from irradiated and unirradiated cells were transferred (50 µL for each well and 500 µL for each flask- according to the relative area) to MCF-7 cells and MDA-MB-231 fresh breast cancer cells were seeded on coverslips in 12 well plates, or in T175 tissue culture flasks respectively, three replicates per irradiation and control group. Cells were incubated under the normal culture condition for 24 hours post-treatment. Cells were then analysed for glycosylation, EMT markers and invasiveness, as described in Sections, 2.6, 2.7 and 2.10 respectively.

### 2.12.5 Bystander effect: Exosome depleted media transfer

MCF-7 and MDA-MB-231 cells were seeded in individual 175 $cm^3$ (T175) tissue culture flasks. Both cell lines were subcultured for 4 populations doubling (PD), before irradiation with 2 Gy X-rays. After 4 hours, exosomes were isolated as

described in Section 2.12.1.ii. The resultant supernatant was then transferred to unirradiated cells in T75 culture flasks and incubated for 24 hours cells. The cells were then analysed for glycosylation, EMT markers and invasiveness as described in Sections 2.6, 2.7, and 2.10 respectively.

### 2.12.6 Bystander effect: Exosomes cargo inhibition and transfer

MCF-7 and MDA-MB-231 cells were cultured in T175 tissue culture flasks and incubated until 70% confluent. The containers were then irradiated with either 0 Gy or 2 Gy X-rays and re-incubated at 37 °C. 4 hours post-irradiation, the unirradiated control condition media (CCCM) and irradiated cell condition media (ICCM) were collected from the flasks and processed for exosome isolation, using the ultracentrifugation method (described in Section 2.12.1.ii). Exosome pellets from CCCM and ICCM were each collected in 3 mL of distilled water and further divided into three fractions. For each irradiation treatment (0 Gy / 2 Gy), fraction no. 1 was treated with 30 µg/mL RNase-A (Sigma, 000000010109142001) and incubated in a 37 $^{o}$C water bath for 30 minutes. Fraction no. 2 was incubated in a 100 $^{o}$C water bath for 10 minutes. Fraction no. 3 was treated with RNase-A (30 µg/mL), incubated for 30 minutes in a 37 $^{o}$C water bath and then transferred to a 100 $^{o}$C water bath for 10 minutes.

All three fractions of exosomes were then added to corresponding flasks or 12 well plate of unirradiated MDA-MB-231 or MCF-7 cells, at 70% cell confluence. The flasks or 12 well plates were then incubated at 37 °C for 24 hours, and samples of each cell type were analysed for, glycosylation and EMT markers and invasiveness as described in Sections 2.6, 2.7 and 2.10 respectively.

## 2.13 Quantitative analysis of candidate genes associated with invasiveness

Quantitative polymerase chain reaction (qPCR) is an assay used to measure the change in the candidate genes expression as presented in Table 2.1 and 2.2, by using the linearity of DNA amplification to determine relative or absolute quantities of a known sequence in a sample by using a fluorescent reporter in the reaction. To determine the DNA expression in a known sample, firstly the total RNA was isolated and then complementary deoxyribonucleic acid (cDNA) was made as a template for qPCR.

*Table 2.1The primers used to determine genes expression pre and post-direct irradiation and pre and post-exosome transfer.*

| The primer | Orientation | Primer sequences (5'-3') |
|---|---|---|
| Vimentin | Forward | ATGGCTCGTCACCTTCG |
| | Reverse | AGTTTCGTTGATAACCTGTCC |
| E-cadherin | Forward | ACGCATTGCCACATACA |
| | Reverse | CGTTAGCCTCGTTCTCA |
| GalNAc-T6 | Forward | AGAGACAGGGCAGAGGGTAG |
| | Reverse | CCTTTGTCATGGCATCCCCT |
| TGFβ-1 | Forward | TAAAGGGTCTAGGATGCGCG |
| | Reverse | GACTTTTCCCCAGACCTCGG |
| Slug | Forward | AGCAGTTGCACTGTGATGCC |
| | Reverse | ACACAGCAGCCAGATTCCTC |
| Snail | Forward | AATCGGAAGCCTAACTACAGCG |
| | Reverse | GTCCCAGATGAGCATTGGCA |
| ZEB 1 | Forward | TCCCTGCCAAGAACAATGATCA |
| | Reverse | AGGTGATGGGGATGGTGTACTA |
| Twist | Forward | ACAGCCGCAGAGACCTAAAC |
| | Reverse | GGCCTGTCTCGCTTTCTCTT |
| MMP-9 | Forward | ACTCGGCTAACCCTCTTCCT |
| | Reverse | ACTCAGAATCTCACCGACGC |
| Act-β-1 | Forward | TGACCCAGATCATGTTTGAGA |
| | Reverse | TACGGCCAGAGGCGTACAGC |

*Table 2.2* The primers of candidate miRNAs.

| The primer | Orientation | Primer sequences (5'-3') |
|---|---|---|
| has-Let -7a | Forward | GGGGCTAATACTGCCTGGTAA |
| | Reverse | TTCACAATGCGTTATCGGATGT |
| has-miR200b | Forward | GTTAGAATTAGGGTTTTTGGGGAGG |
| | Reverse | ACCTATCAAACTTCTCAATATAAAC |
| has-miR-30a | Forward | GGGATTCTGAAGGTGGGTGG |
| | Reverse | AAGAGAGGCAGCTTTCACCC |
| has-miR-9a | Forward | CCAAGCTTATAAGTGAGCGCATTC |
| | Reverse | CGGAATTCGTGTTGGAGAACAGCA |

### 2.13.1 RNA isolation

MCF-7 and MDA-MB-231 cells were cultured in 75 $cm^2$ (T75) tissue culture flasks under optimum conditions of 37$^oC$, 5% $CO_2$ and 95% humidity. Cells were irradiated with 2 Gy X-ray at 70% confluence. Sham-irradiated cells (0 Gy X-irradiated) were established in parallel as a control group. RNeasy Mini kit (50) (QIAGEN, 74104) was then used to isolate total RNA as described below. Briefly, cells were collected after 4 hours of irradiation in 15 mL Universal tubes and centrifuged at 300 g for 5 minutes. The supernatant was discarded, and the cell pellet(s) flicked to create single cell suspensions. Ten mL of PBS was then added and the tubes were re-centrifuged at 300 g for 5 minutes. The supernatant was discarded, and the cells re-suspended in 350 µL of the RLT buffer (cell concentrations less than 5 x $10^6$). Each lysate was then homogenised by passing through individual 20-gauge needles five times. 1 volume of 70% ethanol was then added to the homogenised lysate and mixed by pipetting. 700 µL of each sample, including any precipitate, was transferred to an RNeasy spin column. The lids were gently closed, and the columns centrifuged for 15 seconds at 8,000 g. The supernatant was discarded, and 700 µL of RW1 buffer was added to each RNeasy spin column, the lids were closed, and the columns centrifuged at 8,000 g to wash the spin column membrane. The flow-through was discarded, and 500 µL of RPE buffer was added to the columns. The lids were again closed, and columns centrifuged for 15 seconds at 8,000 g. The flow-through was discarded, and 500 µL of RPE buffer was then added to the columns. Again, the lids were closed, and the columns centrifuged for 2 minutes at 8,000 g. The columns were then transferred into new 1.5 mL collection tubes, at which point, 30-50 µL of RNase-free water was added directly onto the spin columns membrane. The columns were centrifuged for 1 minute at 8,000 g, and the total collected RNA was measured using NanoDrop One (Thermos Scientific Company).

### 2.13.2 RNA treatment with DNase 1

Isolated RNA was treated with DNase 1 (Sigma, AMPD1-1KT) to remove any remaining DNA in the samples. To this end, eight µL of isolated RNA was gently mixed with one µL of 10 x reaction buffer and one µL of DNase 1 (amplification grade 1unit /µL) in 1.5 µL Eppendorf tubes. The tubes were incubated for 15

minutes at room temperature, and then one µL of stop solution was added. All samples were then the incubated at 70$^{o}$C for 10 minutes and then directly transferred to ice.

### 2.13.3 Formation of cDNA

The concentration of RNA in the samples post DNase-1 treatment was determined by iScript cDNA synthesis kit 170 (Bio-Rad, 8891) and NanoDrop One (Thermos Scientific Company). Briefly, 4 µL of 5x iScript Reaction Mix was mixed with 1 µL of iScript Reverse Transcript, 1 µL of RNA sample (500 ng / µL) and nuclease-free water in 0.5 mL Eppendorf tubes (total volume of specimen: 20 µL). The complete reaction mix was then incubated in a Thermal cycler set at the following parameters: 25$^{o}$C for 5 minutes, 46$^{o}$C for 20 minutes, 95$^{o}$C for 1 minute, held for 4 minutes.

### 2.13. 4 Master Mix

iTaq Universal SYBR Green Supermix (Bio-Rad, 1715122) was used to measure the expression of candidate genes. The associated qPCR kit protocol was followed. Briefly, 10 µL of iTaq Universal SYBR Green Supermix was mixed with 1 µL of cDNA 500 ng/µL, 2 µL of primers (forward and reverse) and 7 µL of nuclease-free water. Three replicates were performed for each sample. Plates were sealed and centrifuged at 1000 rpm for 2 minutes using Labnet MPS 1000 Mini Plate Spinner. Samples were then incubated in a Thermal cycler (qPCR Bio-Rad) set at the following parameters: 95$^{o}$C for 2 minutes, 95$^{o}$C for 10 seconds and 60$^{o}$C for 30 seconds x39 cycles. Finally, the collection was captured again for 5 seconds to measure the melting point for each primer. Cq data were displayed/analysed using the qPCR software. Further analysis was applied from a standard curve.

### 2.13.5 Relative Standard Curve

With each qPCR experiment, a series of known cDNA concentrations were made to generate the relative standard curve for the experiment. Cq values of standard samples were applied onto the Microsoft excel sheet according to the concentrations of cDNA. Microsoft excel displayed an equation in order to measure the unknown concentrations measuring by qPCR according to their Cq values. R-squared, which is the best fit of the regression line (the closer to 1, means the better fit line passes through all of the points) was also generated.

In Figure 2.11, Microsoft Excel software was used to generate the equation (y=2E-06x + 0.0276) according to the cDNA concentrations of standard samples and their inverted Cq values. The correlation between the Cq values and the cDNA concentrations was calculated according to equation 2 (R-squared 0.9893). The unknown sample concentrations of candidate gene expression were calculated as below:

y=2E-06x + 0.0276

As y is the inverted Cq value measuring by the qPCR; x is the gene expression concentration.

$Cq_{(sample)} = 2 \times 10^{-6} \times$ gene expression concentration + 0.0276

Gene expression concentration = $(Cq_{(sample)} - 0.0276) / 2 \times 10^{-6}$ ----------(2)

*Table 2.3 The standard concentration of the target gene loaded to the qPCR, Cq and their inverse Cq.*

The table showed the standard concentration of target gene expression, the quantitation cycle (Cq) of each concentration and the inverse of Cq. From the concentration of gene and the inverse Cq. The relative standard curve can be plotted and then the concentration of known gene expression can be calculated from equation 2.

| CON.(ng/µl) | 105.67 | 586.3 | 1172.6 | 1758.9 | 2287.9 |
|---|---|---|---|---|---|
| Cq | 36.11022 | 34.71023 | 33.10092 | 31.91232 | 31.21233 |
| inverse Cq | 0.027693 | 0.02881 | 0.030211 | 0.031336 | 0.032039 |

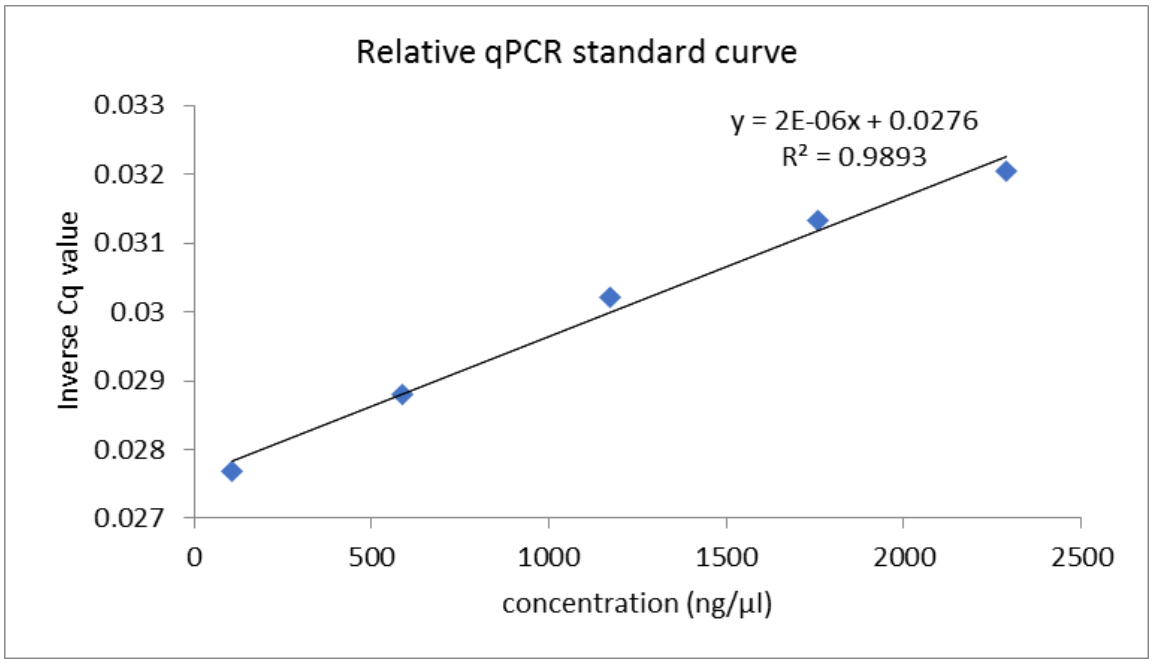


*Figure 2. 11 Standard Curve of control candidate gene*

Candidate genes expression were measured using the formula,

(Gene expression concentration = $(Cq_{(sample)} – 0.0276)/2 \times 10^{-6)}$)

## 2.14 Western blot assay

### 2.14.1 Cells lysate

MCF-7 and MDA-MB-231 cells were seeded in T75 culture flasks for 4 PD. Cells were irradiated with either 0 Gy or 2 Gy X-rays at 70% cell confluence. Cells were collected as described in Section 2.4.2. Irradiated and unirradiated cells pallet were lysed in proteinase inhibitor (Sigma, P8340-1ML) and RIPA lysis buffer (Sigma, 20-188) 1:10 dilution, 100 µL for each 1 x $10^6$ cells. Total protein concentration from irradiated and unirradiated cells was measured using BCA assay or Bradford method, as described in Sections 2.14.2 and 2.14.3 respectively.

### 2.14.2 Protein concentration using BCA assay

Complete protein isolation BCA kit (ThermoFisher Scientific, 23235) was used to measure the total protein in irradiated and unirradiated cell lysates. Master Mix was made of Reagent A (50 µL), Reagent B (48 µL) and Reagent C (2 µL) according to the kit procedure. 10 µL of each sample was mixed with 10 µL of working solution (master mix). In parallel, a 10 µL of various standards (2000, 1500, 1000, 750, 500, 250, 125 µg/mL) of bovine serum albumin kit

(ThermoFisher Scientific, 23235) also mixed with 10 µL of working solution. The tubes were incubated at 60$^{o}$C for 1 hour. The total protein concentration was detected using the NanoDrop One machine (ThermoFisher). Firstly, albumin standards were measured to enable a standard curve to be created, and the total protein from 0 Gy and 2 Gy irradiated cells were calculated from the curve in Microsoft Excel software (Figure 2.11).

### 2.14.3 Protein concentration using Bradford reagent method

Total protein concentration was measured using the Bradford method. Bovine serum albumin, BSA kit (ThermoFisher, 23208) was used to detect the total amount of protein in samples. Standard concentrations of BSA were made (2000, 1000, 500, 250, 125, 62.5, 31.25, 0 µg/mL). Five µL of each standard concentration and the samples (from 0 Gy and 2 Gy irradiated cells) were transferred to a 96 well plate in triplicate. 45µL of Bradford reagent (Sigma, 6916) was then added to each well. The concentration of protein was measured using the Spectra Max i3x plate reader (Molecular Devices Company) under 595nm wavelength, the unknown protein concentrations were calculated using Microsoft Excel software (Figure 2.12).

For example, the unknown sample concentrations of proteins were calculated as below:

y=0.0003x + 0.1006

As y is the absorbance of fluorescent light; x is the protein concentration.

Absorbance = 3 X$10^{-4}$ x protein concentration + 0.1006

Protein concentration = (Absorbance – 0.1006)/ 2 x 3x$10^{-4}$ ----------(3)

*Table 2.4 Standard proteins concentration and its absorbency under the 595nm.*

| Standard protein con. µg/ml | 0 | 31.25 | 62.5 | 125 | 250 | 500 | 1000 | 2000 |
|---|---|---|---|---|---|---|---|---|
| Absorbance | 0.341 | 0.379 | 0.409 | 0.448 | 0.516 | 0.628 | 0.861 | 1.247 |

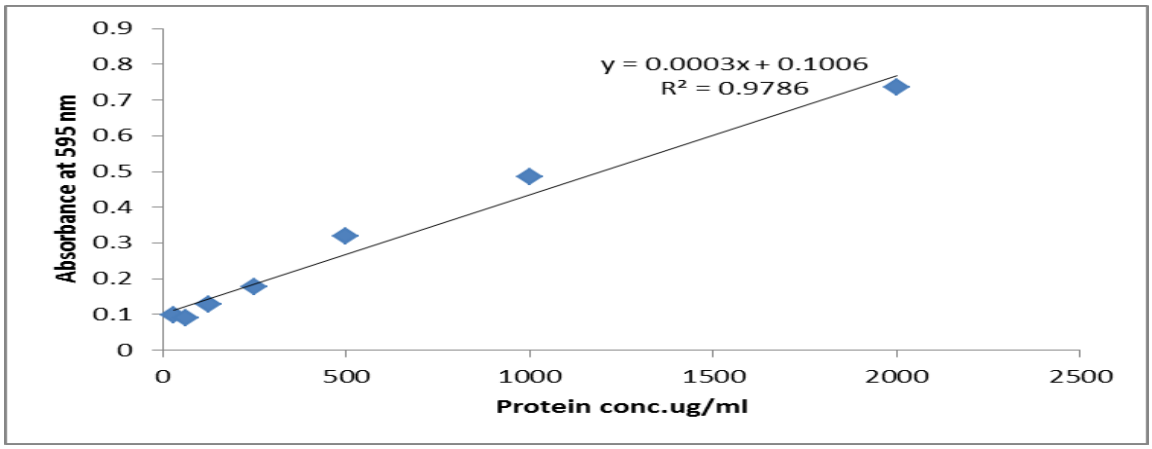


*Figure 2.12 Standard Curve of bovine albumin protein using the Bradford method*

The total proteins concentrations in the irradiated and unirradiated cells were measured. Exosomal proteins that were isolated from irradiated and unirradiated cells also were measured using the formula (Protein concentration = (Absorbance – 0.1006)/ 2 x 3x10-4).

Working from equation (3), 20 µg of each sample were transferred to each well of A mini-protean TGX stain-free gel (Bio-Rad, 456-8126) and then run in electrophoresis tank as described below in the Section 2.14.4.

### 2.14.4 Western blot procedure using the G2 Fast Blotter

Working running buffer was made by adding 100 mL of 10x Tris/ glycine/SDS buffer (Bio-Rad, 161-0732) to 900 mL of deionised water (final concentration of 1x solution: 25 mM Tris, 192 mM glycine and 0.1% (w/v) SDS, at pH 8.3).

2x loading buffer with DL-dithiothreitol (DTT) was then prepared. Briefly, 2mL of RunBlue LDS sample buffer (4x) (Expedeon, NXB31010) was mixed with 200 µL of 1 M of (DTT) solution (Sigma, A3816-50ML) and 1.8 mL of distilled water. 20 µg of each sample was then mixed with 15 µL of 2x loading buffer with DTT, and these were then heated at 70$^{o}$C for 5 minutes to denature the protein. A mini-protean TGX stain-free gel (Bio-Rad, 456-8126) was placed in electrophoresis tank facing inwards. The tank was then half filled with 1x running buffer. 5 µL of rainbow molecular weight marker (Amersham, GERPN800E) was loaded into one well of the gel. The denatured protein samples were then loaded into the other wells of the gel. The volumes of samples were loaded depending on the total protein concentration, a 20 µg of proteins were added to each well. A blank sample, loading buffer was considered as a negative control. Once all samples had been charged, the tank was then filled to the maximum mark with 1x running buffer. It was then run initially at 100 V for 10 minutes, and then increased to 160

V for 1 hour or until the sample had reached the end of the gel. A piece of polyvinylidene difluoride (PVDF) blotting membrane (Amersham, 10600090) was left to activate in methanol for 20 seconds and then rinsed in Transfer Buffer. Four sheets of western blotting filter papers (Thermo Scientific Pierce, 84783) were also pre-wet in transfer buffer. Two of them were then placed on the bottom plate of the G2 blotting cassette. They were then rolled to ensure that no air bubbles resided between them, which would otherwise result in a poor transfer of the gel. The pre-wet PVDF blotting membrane was then placed on top of these two filter papers.

The run gel was then removed from the electrophoresis tank and carefully removed from its plate. It was dipped into transfer buffer to remove the extra gel and then placed on the PVDF membrane and covered with the last two pre-wet filter papers. The lid of the G2 blotting cassette was then locked, and the blotter runs on Mixed Range MW program for 7 minutes using G2 Fast Blotter (Thermo-scientific) as shown in Figure 2.13.

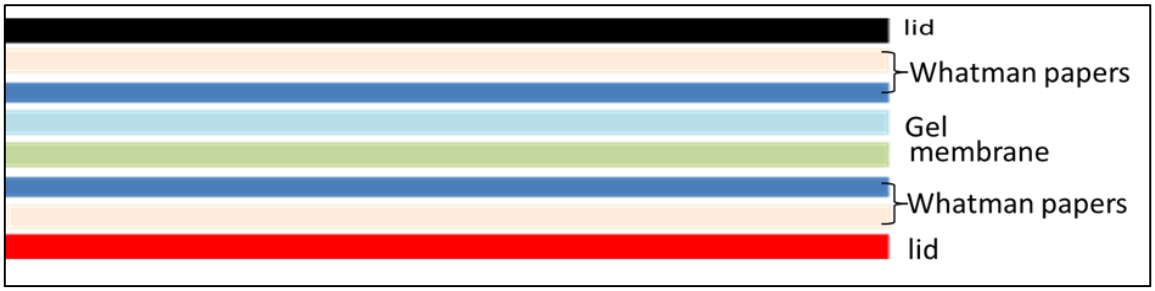


*Figure 2.13 Schematic diagram shows the principle of western blot*

The proteins in the gel transferred to the PVDF membrane using G2 Fast Blotter because the protein in the PVDF merman easily to plot and visualised as bands using (ChemiDoc$^{TM}$ MP imaging system Bio-Rad) with a 16-bit CCD camera.

Following the transfer of proteins from gel to the membranes were completed, the PVDF membrane was transferred directly for 1 hour to 5% BSA / TBST blocking buffer, which made by dissolving 5 g of BSA (Sigma, A2153-50G) in 100 mL TBST buffer. Following incubation with BSA / TBST blocking buffer, the membrane was incubated with a certain concentration of primary antibodies (0.5 µg/µL of TGF-β-1, 2 µg/µL anti-vimentin antibody and 0.5 µg/µL anti-E-cadherin antibody) (abcam, ab179695, ab137321 and ab76319) respectively overnight at 4$^{o}$C on a rolling mixer. The membrane was then washed three times with TBST buffer and then incubated with 2 µg/µL of secondary antibody (abcam, ab150077,

Alexa Fluor 488 goat anti-rabbit) for 1 hour in the dark at room temperature. It was then washed with TBST buffer. Protein bands were detected using (Bio-Rad ChemiDoc$^{TM}$ MP imaging system) with a 16-bit CCD camera.

### 2.14.5 Western blot quantification

Quantitative analysis of western blots was used to detect specific proteins and measure the relative change in their quantity following ionising irradiation compared to unirradiated samples. The results of western blot were analysed using Image lab software which enabled measurement of the optical density of the target band. The signal of the unirradiated band (0 Gy) for all endpoints were taken as standard and then a measurement of other bands was made in relation to this for each irradiation group / end-point. For example, the standard band of vimentin at 0 Gy gave a result of 1. Subsequent measurements of bands from each irradiated groups were thus determined by comparison to the relevant standard, i.e. higher, lower or equal to the standard. Histograms of all data were created, representing densitometry data drawn from blot images.

## 2.15 Statistical methodology

Apoptotic, glycosylation and EMT data including flow cytometry were presented as a percentage of apoptotic, glycosylation and EMT-positive cells (number of apoptotic, HPA, or EMT-positive cells to the total number of cells), these data represent nonparametric data. While comet assay data was demonstrated as a median. An average of the total number of invasive cells for 3 biological replicate experiments represented the invasion assay. qPCR and western blotting results were presented as mean ± SEM, as these data represent parametric data.

The raw data of the experiments above were subjected to the statistical analyses as following: Glycoprotein detection, immunocytochemistry, flow cytometry, viability, ROS and invasion assay results were subjected to Fisher's exact test using Minitab software; whereas comet assay data were analysed using the Mann-Whitney test (SPSS software). qPCR assay and western blot assay were subjected to the Student *t*-test.

# Chapter 3

**Effect of ionising radiation on glycosylation, EMT markers and invasive capacity of epithelial breast cancer cells**

## 3.1 Introduction

As described previously in Section 1.6, IR is high energy radiation that causes the release of ions via interaction of atoms in the medium, resulting in the DNA damage of irradiated cells (Hall and Giaccia, 2012; Azzam, Jay-Gerin and Pain, 2012).

DNA damage can lead to cell death, chromosomal aberrations and genetic mutation (Biedermann *et al.*, 1991; Bodnarchuk, 2003; Borrego-Soto, Ortiz-Lopez and Rojas-Martinez, 2015). Moreover, cells exposed to ionising radiation can generate ROS leading to oxidative damage to the membrane of the cells, and it has a consequent role in cell stress and apoptotic cell death (Mishra, 2004; Azzam, Jay-Gerin and Pain, 2012).

The effects of radiation on DNA molecules can induce irreversible changes in the DNA structure, which impact cancer treatment through inducing senescence and apoptosis (d'Adda di Fagagna *et al.*, 2003). However, cancer cells can repair DNA damage by inducing DNA repair machineries such as CHRK1, CHRK2, and p53 pathways (Bartek and Lukas, 2003; Reinhardt and Yaffe, 2009). These mechanisms could enhance cancer chemo-resistance and radio-resistance to therapy. It has also been reported that low dose of IR increases TGF-β expression in human keratinocyte U937 cells (Sekihara *et al.*, 2018). Therefore, change in the level of cytokines following IR may have a role in EMT and glycosylation of cell surface protein and invasion of cancer cells, and that needs to be addressed.

Glycosylation is a post-translational modification of the protein (Boscher, Dennis and Nabi, 2011; Varelas, Bouchie and Kukuruzinska, 2014) by addition of carbohydrate (glycan) to the amino acid residue in the polypeptide chain (Gill *et al.*, 2013). Glycosylation has an essential role in the physiological and developmental process of an organism (Ungar, 2009). For example, O-glycan thought to be mediated cell adhesion to a specific receptor in the endothelial cells such as leukocyte rolling and lymphocyte homing (Acheson, Sunshine and

Rutishauser, 1991). A study in Core 1 O-glycans showed an impact of glycosylation on cancer development and metastasis including epithelial-mesenchymal transition (Magalhaes, Duarte and Reis, 2017). The change in mucin-type O-glycosylation frequently associated with a change in the presence of Tn antigen in the cell surface mucin, as described in details in Section 1.5.6.

As described in section 1.5.4, an aberration in O-Linked glycosylation represents the key factor in the alteration in cell-cell communication, which has an impact on cancer cells behaviour and metastasis (Itkonen and Mills, 2013). O-linked glycosylation can be detected by HPA (Fukutomi *et al.*, 1989; Brooks *et al.*, 1993; Lescar *et al.*, 2007; Arab *et al.*, 2010).

Moreover, changes in sialylation are also associated with alteration in O-linked glycosylation as described in Section 1.5.3. SNA is a lectin, that is often used as a tool to detect α-2,6 and α-2,3 linked sialic acid (Mehta *et al.*, 2016).

N-glycosylation which is another type of protein glycosylation synthesis during the stage of translation by adding glycan to the amino group of asparagine residue of the peptide chain (Oliveira-Ferrer, Legler and Milde-Langosch, 2017). Aberrant in N-glycosylation frequently associated with cancer metastases. UDP-N-acetylglucosaminephosphotransferase which is an enzyme controlled N-glycosylation of E-cadherin and expressed by *DPAGT1* gene. An increase in the expression of *DPAGT1* usually associated with an increase in N-glycosylation of E-cadherin and decrease in the cell-cell interaction (Sengupta *et al.*, 2013), as results induce EMT, invasion and metastases of gastric cancer (Pinho *et al.*, 2013). PHA-L lectin can detect N-glycosylation in the protein. The changes in protein glycosylation notably associated with cancer metastasis and also altered the expression of several factors including E-cadherin and vimentin which contribute to EMT (Magalhaes, Duarte and Reis, 2017).

As described in section 1.3.1, E-cadherin is responsible for maintaining the normal structure of epithelial tissues by maintaining the polarity of the cells and increasing cell-cell adhesion (Tiwari *et al.*, 2012). Several genes and factors contribute to downregulation of E-cadherin, such as *TWIST*, *SNAIL*, and *SLUG* (Huber, Kraut and Beug, 2005; Zhao, Wu and Zhou, 2011). Over-expression of

*SNAIL1* gene can induce mesenchymal markers such as N-cadherin and vimentin which have important roles in the metastatic behaviour of cancer cells (Baum, Settleman and Quinlan, 2008; Warzecha and Carstens, 2012). N-cadherin which is cell membrane adhesion molecules can mediate cell adhesion and also could play an essential role in the invasive of cancer cell (Hazan *et al.*, 2000). They transferred N-cadherin to MCF-7 cells, resulting in the efficiently of adhesion and the number of invasive cells through Matrigel has been increased.

Vimentin has been recognised as an essential component in the cells which can regulate EMT, accordingly induces migration and invasion of cancer cells (Kokkinos *et al.*, 2007; Zhu *et al.*, 2011b). It has also been reported that IR can promote EMT markers (Hu *et al.*, 2018), by an increases the induction of ROS, as described in Section 1.6.1.i, which could have an impact on TGF-β-1 expression (Iizuka *et al.*, 2017). The latter is frequently involved in the regulation of *SLUG*, *SNAIL*, *ZEB*, *TWIST* and *MMP* gene expressions, resulting in changes in the morphology of cancer cells, i.e. a transition from epithelial to mesenchymal (Yu *et al.*, 2015).

The role of IR on the invasive capacity of breast cancer cells linked with changes in glycosylation and EMT markers have previously not been explored. Therefore, this study was set up to address these factors by focusing on two:

**Aim 1:**

1-Optimise experimental conditions, i.e. growth rate, labelling for glycosylation markers (HPA, SNA and PHA-L), EMT markers (vimentin, N-cadherin, E-cadherin) and Matrigel concentration in 3 different breast cancer epithelial cell lines (MCF-7, ZR75-1 and BT474).

**Aims 2:**

1- Study the effects of IR on DNA damage using the comet assay and apoptosis measurement.

2- Measure cell viability and ROS formation in the cells following irradiation.

3- Determine the correlation between HPA, vimentin, E-cadherin and invasive capacity of MCF-7 cells following IR.

4- Determine the candidate genes expression that is associated with the invasive capacity of MCF-7 cells.

5- Determine protein expression following IR and which is associated with the invasive ability of MCF-7 cells.

## 3.2 Results

### 3.2.1 Part (a): Optimisation of glycosylation, EMT markers and Matrigel condition and concentration.

*3.2.1.i Growth rate of cells*

To investigate the growth rate of breast cancer cells displaying differing metastatic phenotypes, MCF-7 (moderate metastatic cells), ZR75-1 (low metastatic cells) and BT474 (non-metastatic cells) were propagated for 20 populations doubling (PD). Prior to subculture, each cell line was routinely counted using haemocytometer method as described in section 2.4.2 and seeded at an identical cell density in individually labelled T75 tissue culture flasks until 20 PD. The cumulative PD for each cell line was then calculated according to the PD-equation "3."

$$\text{Doubling time} = \frac{\text{Duration} * \log(2)}{\log(\text{final concentration}) - \log(\text{initial concentration})} \quad \text{---(3)}$$

(Roth, 2006). The cumulative population doubling is the summation of previous cumulative PD + population doubling.

The cumulative PD results showed that the MCF-7 cells had higher growth rate and shorter population doubling compared to ZR75-1 and BT474 cells, as shown in Figure 3.1; MCF-7 was shown to have a PD of 24 hours; whilst ZR75-1 and BT474 cell lines had PDs of 26 and 28 hours, respectively.

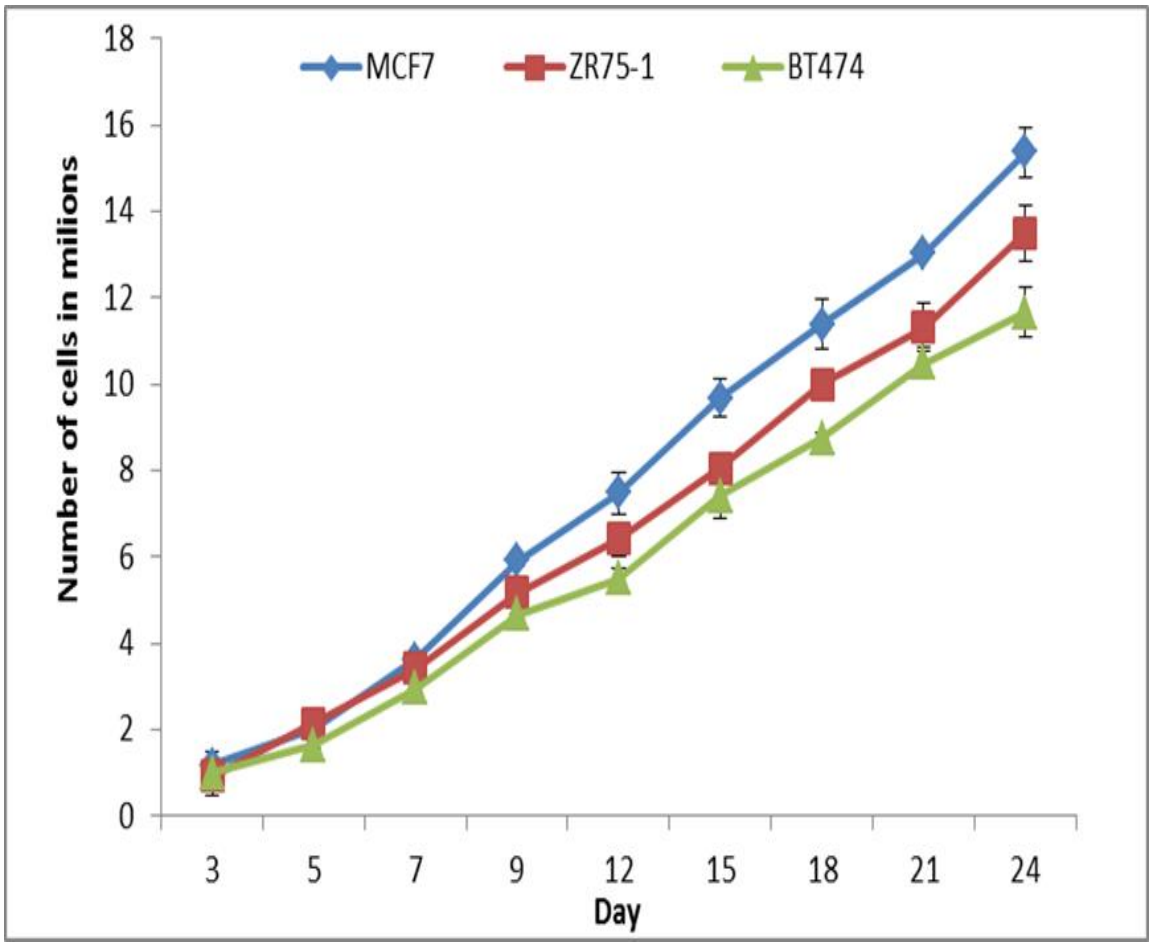


*Figure 3.1 The Growth rates of MCF-7, ZR75-1 and BT474 cell lines*

MCF-7 cells showed a higher growth rate compared to ZR75-1 and BT474 cells after 20 population doublings (PD). MCF-7 was shown to have a PD of 24 hours; whilst ZR75-1 and BT474 cell lines PD times were 26 and 28 hours respectively, resulting in an insignificant difference in the number of cells at 24 days in all 3 cell lines. The data presented as a total number of cells ± the SEM of three independent experiments. (*p≤0.05, ** p≤0.001, *** p≤0.0001).

### *3.2.1.ii HPA lectin labelling*

The lectin-biotinylated technique was used to detect HPA positive cells as described in Section 2.6. MCF-7 showed a significant (p≤0.0001) high percentage (78%) of HPA detecting (positive) cells compared to the ZR75-1 and BT474 cell lines (Figure 3.2). While ZR75-1 showed a significant (p≤0.0001) higher percentage (70%) of HPA positivity than BT474 detecting cells (64%). Data suggest that MCF-7 has greater HPA positivity than ZR75-1, which in turn is greater than BT474 cells.

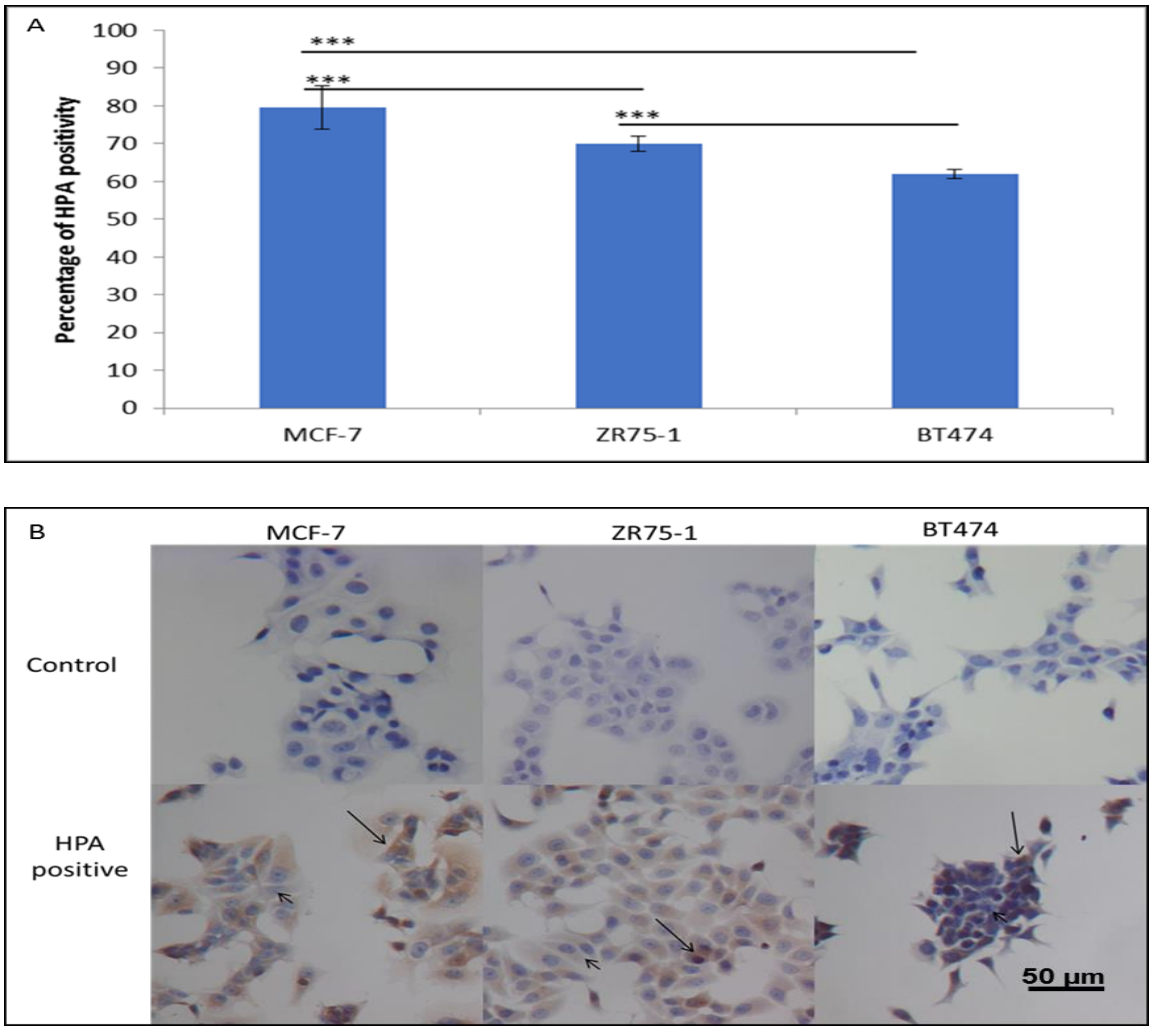


*Figure 3.2 Percentage of MCF-7, ZR75-1 and BT474 positive cells with HPA detecting GalNAc-glycans.*

The results showed a significant ($p \leq 0.0001$) increase in the percentage of MCF-7 cells labelled with HPA lectin compared to ZR75-1 and BT474 cells (Panel A). Panel B shows a representation of cells that are positive and negative to HPA. The large arrow pointed to a positive cell, i.e. cells appear brown, while the small arrow represents negative cells, i.e. cells appear blue. The negative control in these pictures, cells were not labelled with HPA lectin. The data presented as a percentage ± the SEM three independent experiments; (*$p \leq 0.05$, ** $p \leq 0.001$, *** $p \leq 0.0001$).

### *3.2.1.iii SNA lectin labelling*

Using the Lectin-biotinylated technique with SNA lectin to detect sialic acid as described in Section 2.6. MCF-7 cells were shown to have a significant ($p \leq 0.0001$) decrease (46.34%) in SNA positive cells compared to ZR75-1 (65.68%) and BT474 (59.63%) cells (Figure 3.3).

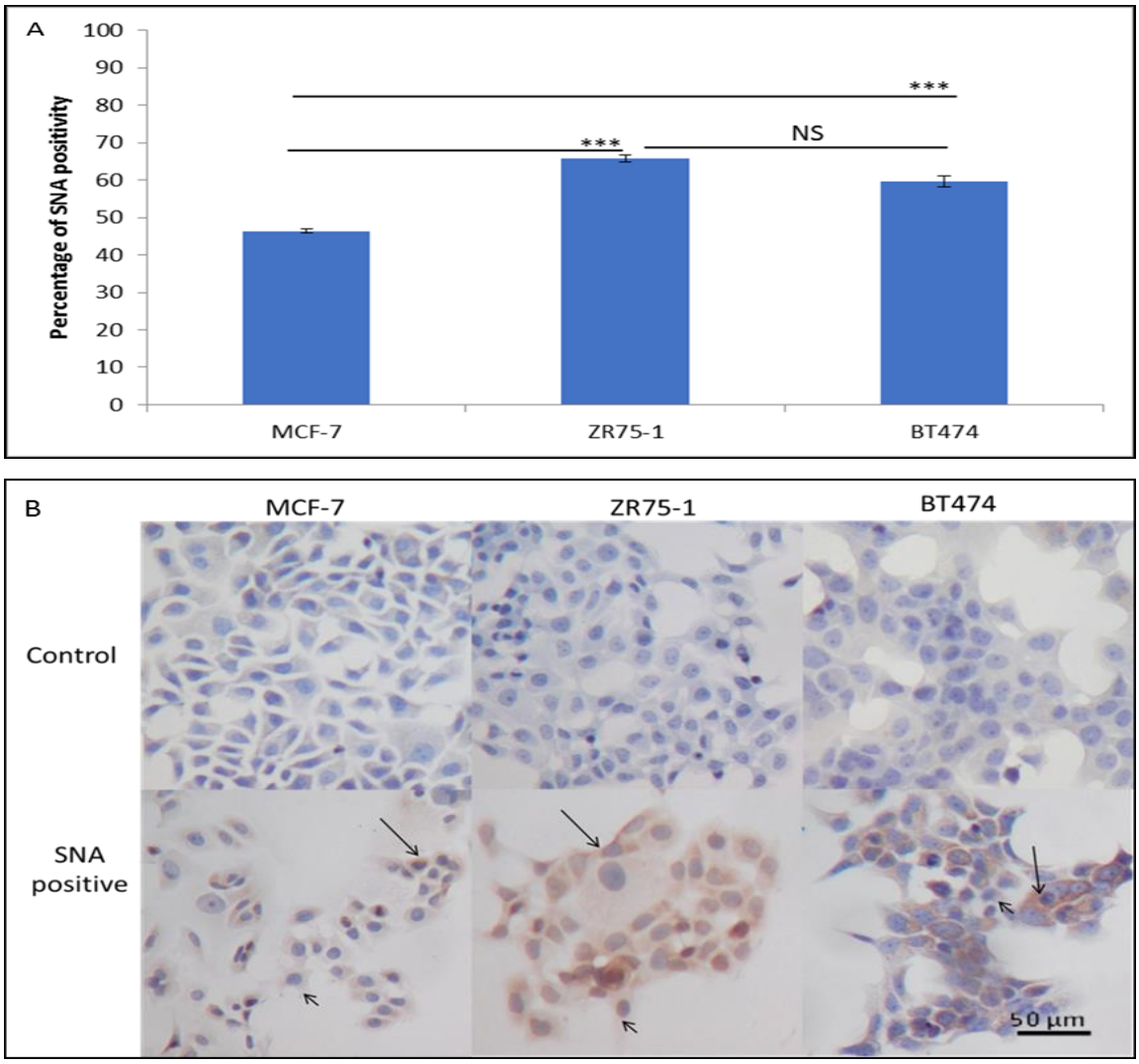


*Figure 3.3 Percentage of MCF-7, ZR75-1 and BT474 positive cells with SNA lectin to detect sialic acid.*

The results showed a significant ($p \leq 0.0001$) increase in the percentage of ZR75-1 and BT474 cells that were labelled for the binding of SNA compared to MCF-7 cells (Panel A). Panel B shows a representation of cells that are positive and negative for SNA labelling. Large arrows represent positive cells, i.e. cells appear brown; whilst small arrows represent negative cells, i.e. cells appear blue. The negative control in these pictures, cells were not labelled with SNA lectin. The data presented as a percentage ± the SEM of three independent experiments. (*$p \leq 0.05$, ** $p \leq 0.001$, *** $p \leq 0.0001$).

### *3.2.1.iv PHA-L lectin labelling*

The lectin-biotinylated technique was used to detect N-linked glycosylation in breast cancer cells, as described in Section 2.6. ZR75-1 and BT474 cell lines both showed a significant ($p \leq 0.0001$) increase (64.79%) and (60.98%) respectively in PHA-L positivity compared to MCF-7 cells (27.48%), as presented in Figure 3.4.

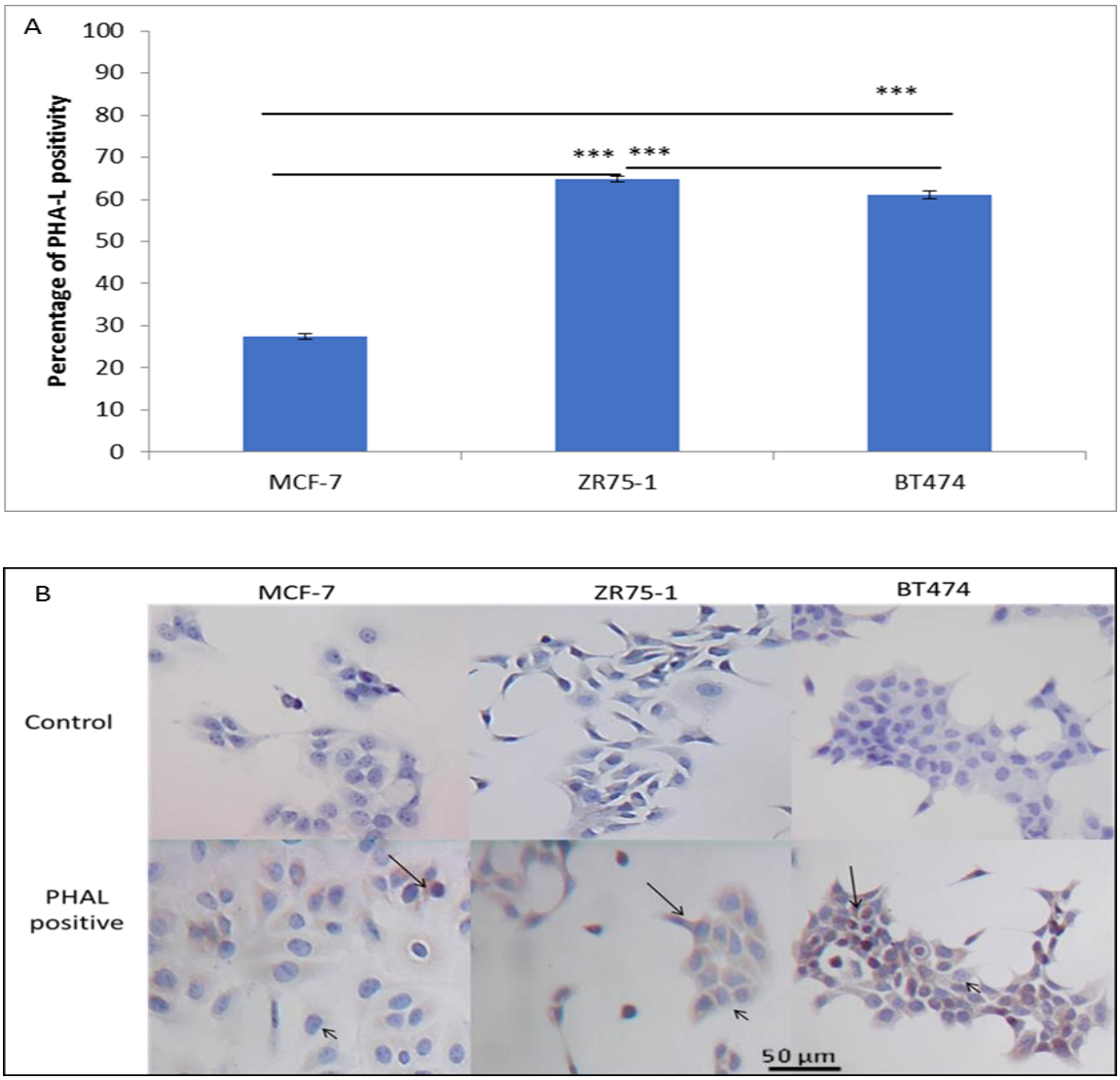


*Figure 3.4 Percentage of MCF-7, ZR75-1 and BT474 positive cells with PHA-L lectin detecting beta 1,6 branching N-glycans.*

The results showed a significant ($p \leq 0.0001$) increase in the percentage of ZR75-1 and BT 474 cells that were labelled for PHA-L lectin binding compared to MCF-7 cells (Panel A). Panel B shows a representation of cells that are positive and negative for PHA-L binding. The large arrows represent positive cells, i.e. cells appear brown; while small arrows represent negative cells, i.e. cells appear blue. The negative control in these pictures, cells were not labelled with PHA-L lectin. The data presented as a percentage ± the SEM of three independent experiments. (*$p \leq 0.05$, ** $p \leq 0.001$, *** $p \leq 0.0001$).

### *3.2.1.v EMT markers (vimentin, E-cadherin, N-cadherin) levels in the experimental cells*

Immunopositivity technique has been used to detect the vimentin, N-cadherin and E-cadherin positive cells as described in Section 2.7. Data showed both MCF-7 and BT474 cell lines showed a significant increase in vimentin immunopositivity ($p \leq 0.0001$) compared to the ZR75-1 cells. A higher number of vimentin positive

cells were observed in MCF-7 (68.6%) than that observed in BT474 (47.4%), although BT474 cells were shown to have a higher number of vimentin positive cells than ZR75-1 cells (59.4%) as shown in Figure 3.5.

N-cadherin immunopositivity was significantly greater in both MCF-7 cells and ZR75-1 cells ($p \leq 0.0001$ and $p \leq 0.05$ respectively) compared to BT474 cells, as shown in Figure 3.6.

Conversely, ZR75-1 and BT474 cells demonstrated a significantly higher level of E-cadherin immunopositivity ($p \leq 0.0001$) compared to MCF-7 cells. Both ZR75-1 and BT474 interestingly showed a similar percentage of E-cadherin immunopositivity (89% and 88% respectively), as shown in Figure 3.7.

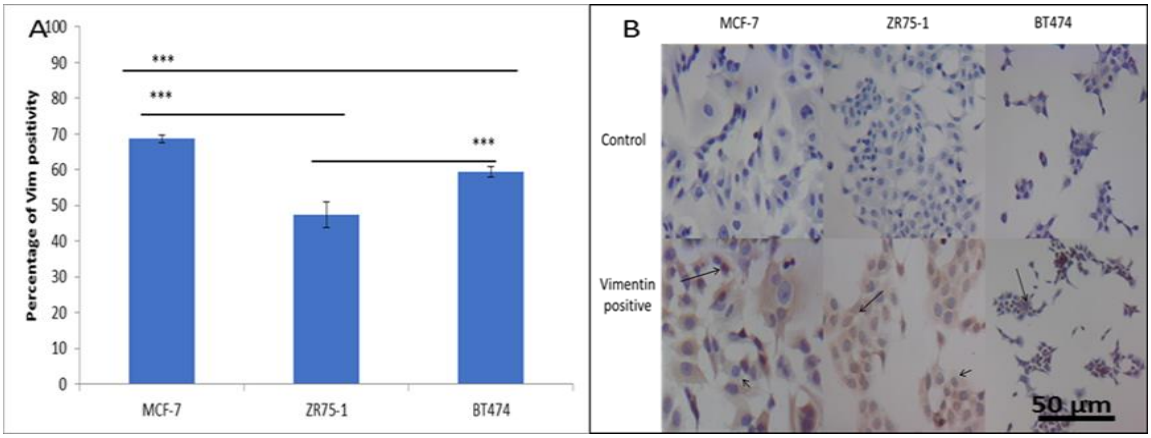


*Figure 3.5 Percentage of vimentin immunopositivity in MCF-7, ZR75-1 and BT474 cells.*

The results showed a significant increase in the percentage of vimentin immunopositive cells in both MCF-7 and BT474 ($p \leq 0.0001$) lines compared to ZR75-1 (Panel A). Panel B shows a representation of cells that are positive and negative for vimentin. The large arrow represents positive cells, i.e. cells appear brown, while the small arrows represent negative cells, i.e. cells appear blue. The negative control in these pictures, cells were not labelled with an anti-vimentin antibody. Data presented as a percentage ± the SEM of 3 independent experiments. (*$p \leq 0.05$, ** $p \leq 0.001$, *** $p \leq 0.0001$).

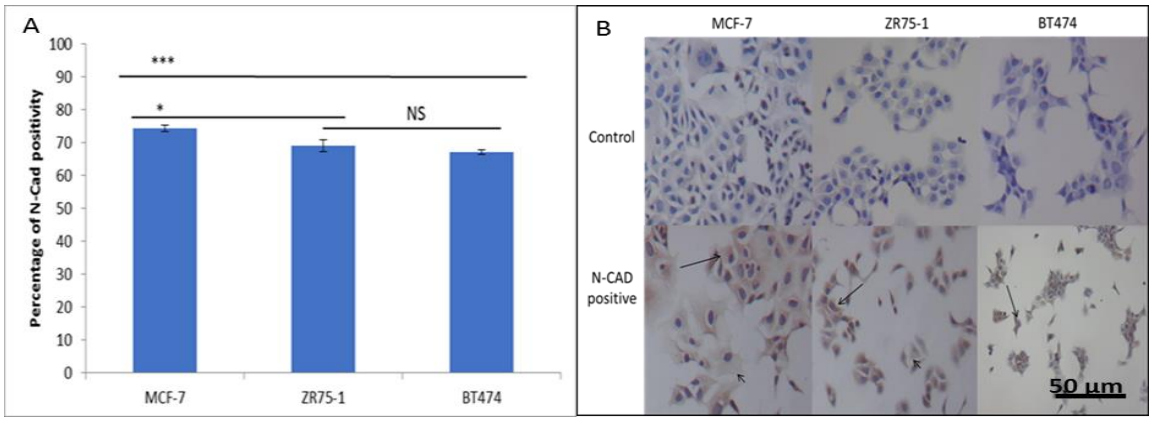


*Figure 3.6 Percentage of N-cadherin immunopositivity in MCF-7, ZR75-1 and BT474 cells.*

The results showed a significant increase in the percentage of N-cadherin positive cells in MCF-7 cells ($p \leq 0.0001$) compared to BT474. The results also show that MCF-7 cells demonstrated a significant ($p \leq 0.05$) increase in the percentage of N-cadherin positive cells compared to ZR75-1 (Panel A). Panel B shows a representation of cells positive and negative for N-cadherin. The large arrows represent positive cells, i.e. cells appear brown; while the small arrows represent negative cells, i.e. the cells appear blue. The negative control in these pictures, cells were not labelled with an anti-N-cadherin antibody. The data presented as a percentage ± the SEM of three independent experiments. (*$p \leq 0.05$, ** $p \leq 0.001$, *** $p \leq 0.0001$).

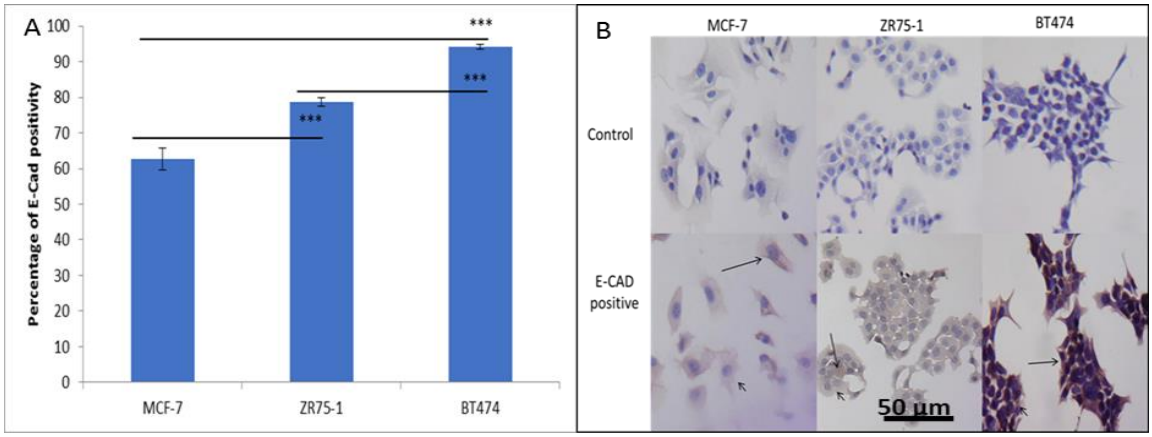


*Figure 3.7 Percentage of E-cadherin immunopositivity in MCF-7, ZR75-1 and BT474 cells.*

The results showed a significant ($P \leq 0.0001$) increase in the percentage of E-cadherin immunopositive cells in both the ZR 75-1 and BT 474 cells compared to MCF-7 cells (Panel A). Panel B shows a representation of cells that are positive and negative for E-cadherin. The large arrows represent positive cells, i.e. cells appear brown; whilst small arrows represent negative cells, i.e. cells appear blue. Data presented as a percentage ± the SEM of three independent experiments. (*$p \leq 0.05$, ** $p \leq 0.001$, *** $p \leq 0.0001$).

*3.2.1.vi Matrigel concentration*

The concentration of Matrigel has been optimised, as described in Section 2.10. Data showed that a concentration of 0.5 mg/ml of Matrigel showed significant (p≤ 0.0001) higher in the invasive cells compared to concentrations of 1 mg/ml and 1.5 mg/ml, as shown in Figure 3.8. The data, therefore, suggested that 0.5 mg/ml was the optimum concentration among three concentrations that were used in the stage of optimisation and was subsequently used in all the experiments.

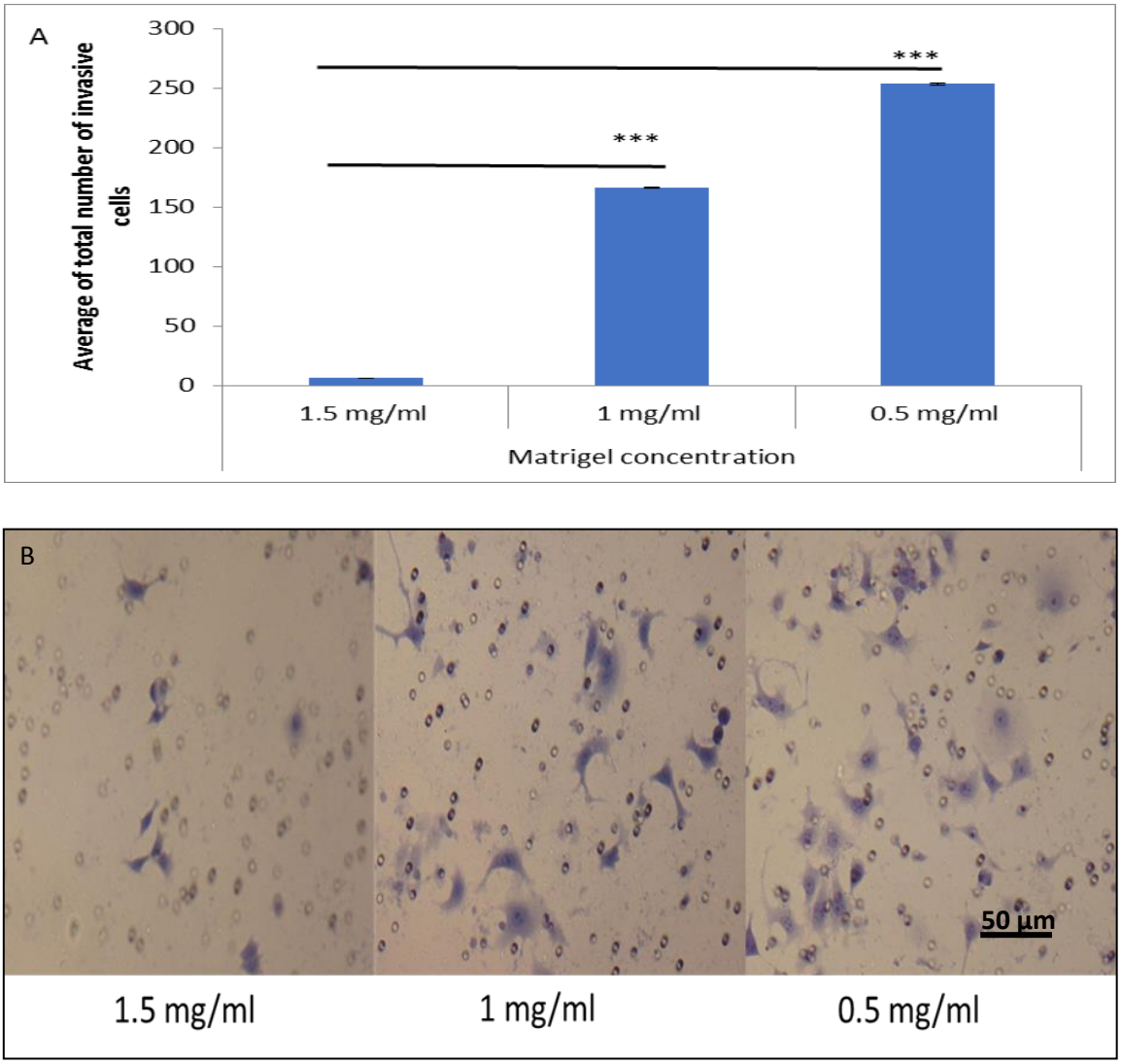


*Figure 3.8 Invasive cells at a different concentration of Matrigel.*

MCF-7 cells showed significant (p≤ 0.001) higher in the number of invasive cells (±2.8 standard deviation) when seeded onto Matrigel at a concentration of 0.5 mg/ml compared to 1 mg/ml and 1.5 mg/ml. The data presented as a mean ± the SEM of three independent experiments. (*p≤0.05, ** p≤0.001, *** p≤0.0001).

*3.2.1.vii HPA positivity/negativity measurement in the invasive MCF7 cells*

The result did not show a clear data of the HPA positivity/negativity in the upper and lower surfaces of insert membrane, due to the overlapped cells, which were unfeasible to be analysed and might give a false data as shown in Figure 3.9. Therefore, these experiments were repeated using MDA-MB-231 cells as described in chapter 5, Section 5.2.2.

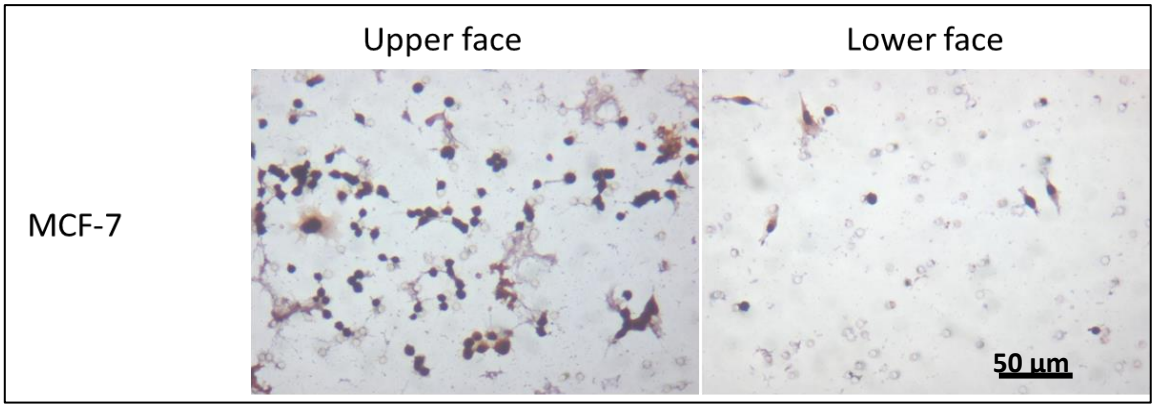


*Figure 3.9 HPA positivity/negativity of invasive and non-invasive MCF-7 cells in the upper and lower surface of the insert membrane of Matrigel co-culture system.*

Cells were overlapped, in particular, the upper surface of the insert. Therefore, the result of this experiment had not been considered in this study.

### 3.2.2 Part (b): irradiation experiments

In Section 3.2.1, the experiments concentrated on the optimisation of the experimental conditions prior to irradiation experiments. This part of the study was designed to investigate the effect of ionising irradiation (IR) on the viability, ROS, DNA damage, apoptosis, HPA positivity, EMT markers, invasive, genes and protein expression of MCF-7 cells.

*3.2.2.i Cell viability*

MCF-7 cells were exposed to either 0 Gy (Control) or 2 Gy X-rays. 4 hours following X-irradiation, the viability of the MCF-7 cells was measured using a Muse cell analyser described in Section 2.5.1. Cells showed a significant decrease ($p \leq 0.0001$) in the percentage of viable cells in the 2 Gy group compared to the 0 Gy / control group (48.6% and 81.8%, respectively). Likewise, the percentage of dead cells was correspondingly significantly increased ($p \leq$

0.0001) in the irradiated MCF-7 cells compared to 0 Gy irradiated cells (51.4% and 18.2%, respectively), as shown in Figure 3.10.

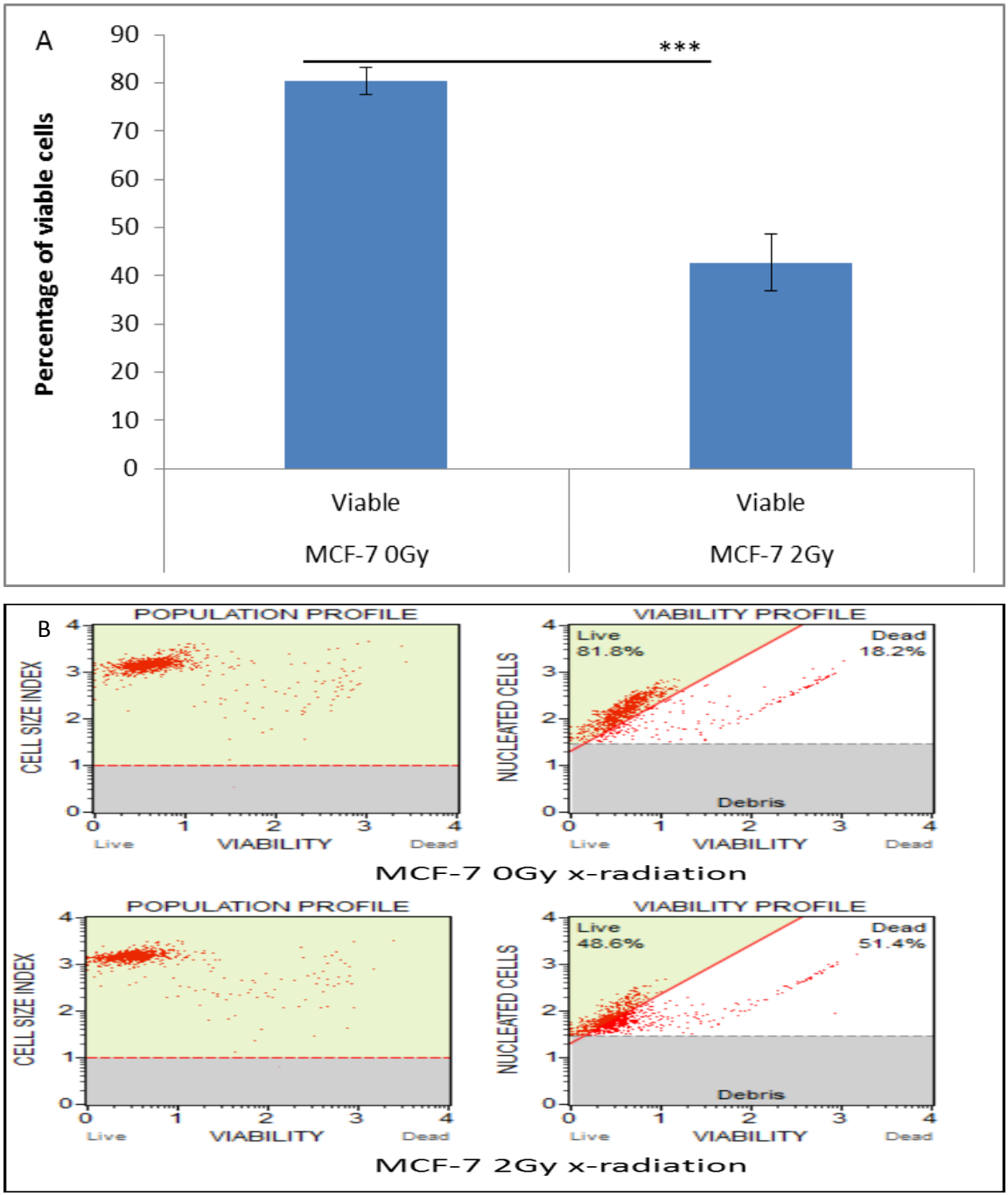


*Figure 3.10 Cell viability following 0 Gy / Control and 2 Gy X-irradiation*

MCF-7 cells showed significant (p≤ 0.0001) decrease in the percentage of viable cells following 2 Gy X-irradiation compared to 0 Gy X-irradiation. The data presented as a percentage ± the SEM of three independent experiments. (*p≤0.05, ** p≤0.001, *** p≤0.0001).

*3.2.2.ii Reactive oxygen species ($ROS^+$ / $ROS^-$)*

Muse cell analyser was used for measuring ROS in irradiated and unirradiated cells post 30 minutes of IR as described in Section 2.5.2. Data showed a significant ($p \leq 0.0001$) increase in the percentage of $ROS^+$ in MCF-7 2 Gy irradiated cells compared to that observed in the 0 Gy / control group (73% and 56%, respectively). In contrast, the percentage of $ROS^-$ cells was shown to have significantly decreased ($p \leq 0.0001$) following 2 Gy X-irradiation compared to 0 Gy (25.8% and 35.53%, respectively) as shown in Figure 3.11.

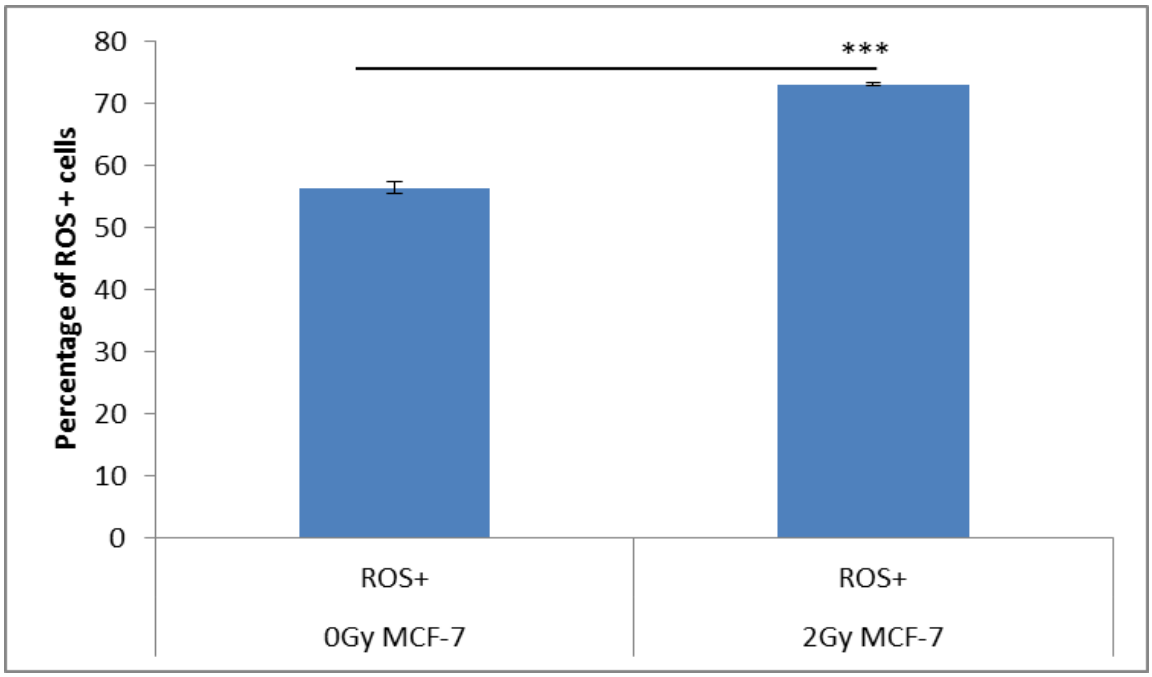


*Figure 3.11 Percentage of $ROS^-$ and $ROS^+$ in MCF-7 cells 30 minutes post irradiation.*

Cells showed a significant ($p \leq 0.0001$) increase in the percentage of $ROS^+$ in irradiated cells compare to control group (±0.5) SD. The data presented as a percentage ± the SEM of three independent experiments. (*$p \leq 0.05$, ** $p \leq 0.001$, *** $p \leq 0.0001$).

*3.2.2.iii DNA damage in MCF-7 breast cancer cells post ionising irradiation*

Total DNA damage was measured in the MCF-7 cells using Comet assay as described in Section 2.5.3. Cells showed a significant increase ($p \leq 0.001$) in the percentage of DNA in the comet tail indicating DNA damage, immediately following 2 Gy X-ray compared to the 0 Gy / control cells (11.38% and 8.68% respectively, as shown in Figure 3.13.

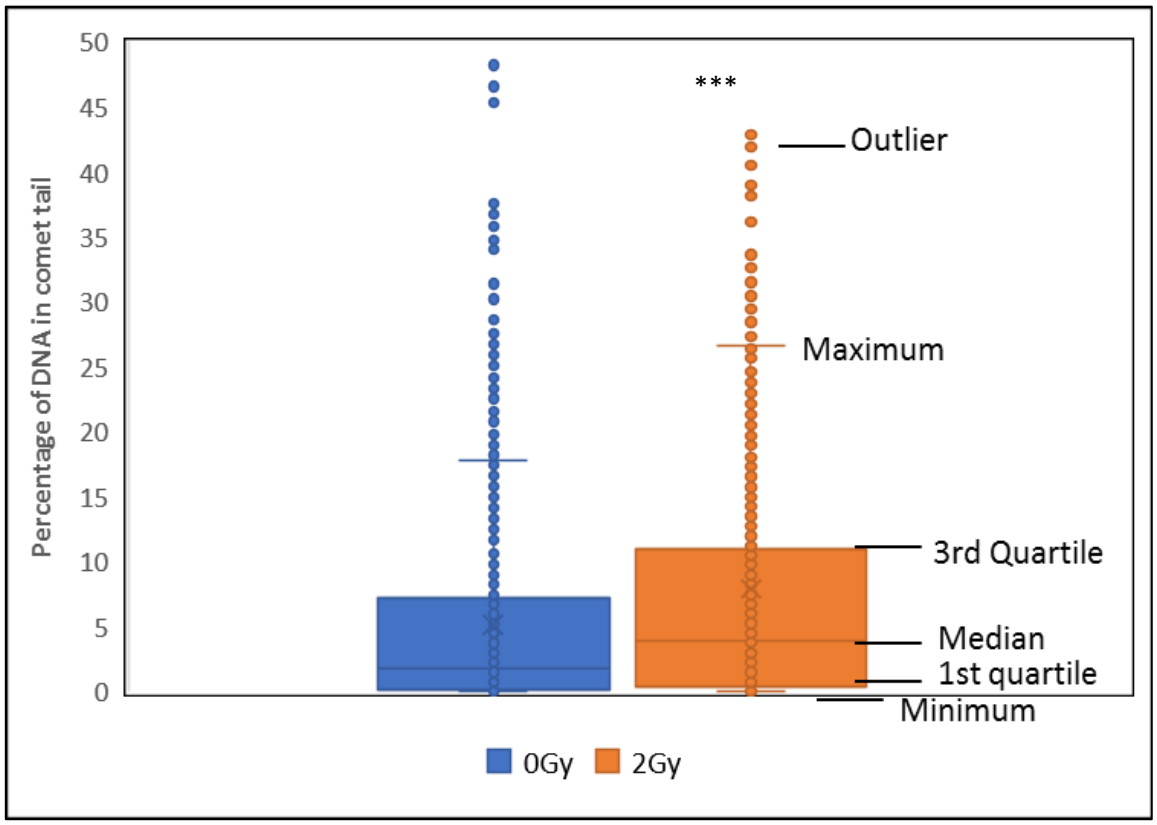


*Figure 3.12 Percentage of DNA in comet tail in MCF-7 cells at 4 hours following 0 Gy and 2 Gy X-irradiation.*

Cells showed a significant induction (p≤ 0.0001) of DNA damage in term of 1st quartile, median, 3rd quartile and maximum, following 2 Gy X-irradiation compared to the control cells (0 Gy). The data represented three independent experiments. (*p≤0.05, ** p≤0.001, *** p≤0.0001).

### *3.2.2.iv Apoptosis*

The percentage of apoptotic cells were measured as described in Section 2.5.4. MCF-7 cells that were exposed to IR showed a significant (p≤ 0.05) increase in the percentage of apoptotic cells as an initial response (4 hours) following 2 Gy X-irradiation compared to control 0 Gy cells, as shown in Figure 3.13.

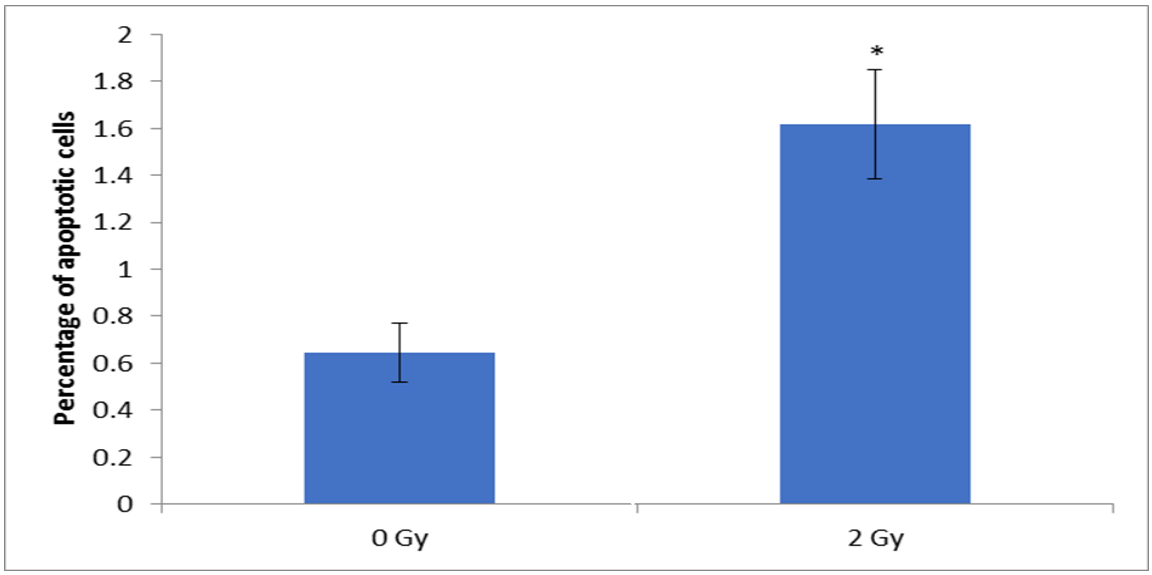


*Figure 3.13 Percentage of apoptotic cells at early time-point (4 hours) following irradiation.*

Cells showed a significant increase ($p \leq 0.05$) in the number of apoptotic cells 4 hours following exposure to 2 Gy X-irradiation compared to the 0 Gy (control cells). The data was presented as a percentage ± SEM of three independent experiments; (*$p \leq 0.05$, ** $p \leq 0.001$, *** $p \leq 0.0001$).

### *3.2.2.v The correlation between HPA, vimentin, E-cadherin and invasive capacity of MCF-7 cells following IR*

The HPA, EMT positivity and invasion of MCF-7 cells were measured following IR, as described in Sections 2.6, 2.7 and 2.10. In response to radiation, a significant ($p \leq 0.0001$) increase in the number of invasive cells was distinguished after 24 hours following 2 Gy X-irradiation in the MCF-7 cells, this was concurrent with a significant ($p \leq 0.0001$) increase in the level of vimentin immunopositivity and a significant ($p \leq 0.0001$) decrease in the level of E-cadherin immunopositivity after 24 hours following irradiation. Cells also demonstrated an increase in the level of the HPA positive cells at this time (Figure 3.14).

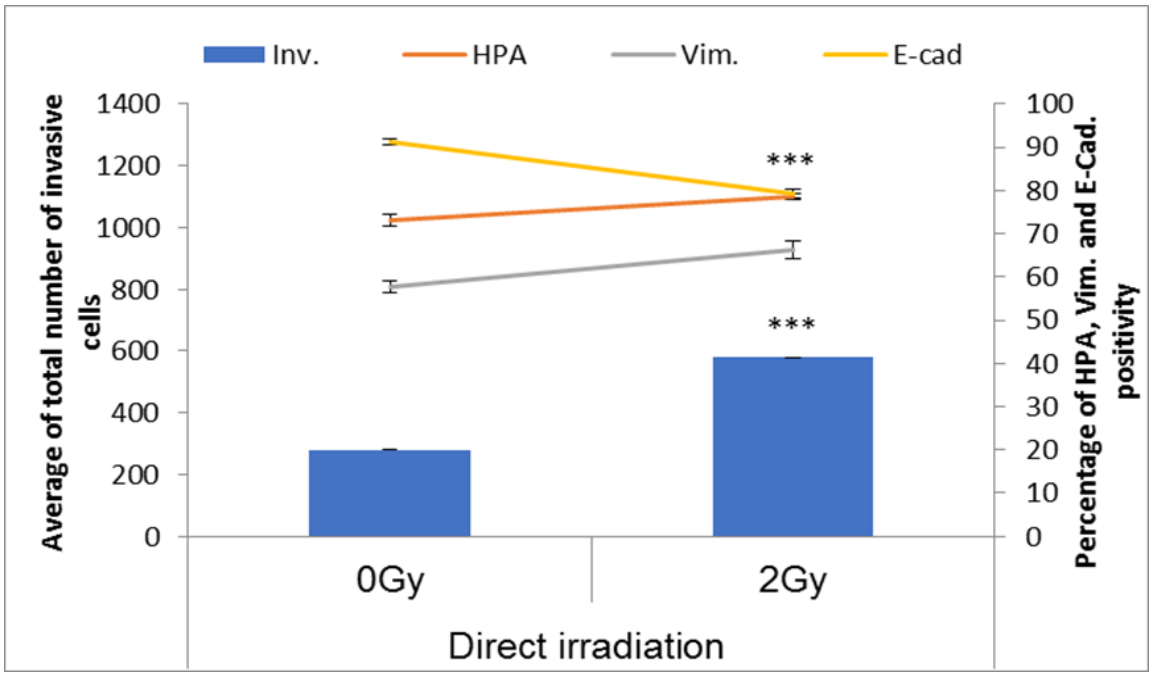


*Figure 3.14 Analysis of invasive capacity, EMT markers and HPA labelling in irradiated cells, (24-hour following irradiation)*

Cells showed a significant (p≤ 0.0001) increase in the number of invasive cells 24 hours following 2 Gy X-irradiation compared to control / 0 Gy. This finding was associated with a decrease in the epithelial marker, E-cadherin and an increase in the mesenchymal marker, vimentin. The data presented as a mean of a total number of invasive cells, and the percentage of HPA and EMT markers positive cells. The error bars represent SEM of invasive cells and the percentage of HPA and EMT markers of 3 independent experiments. (*p≤0.05, ** p≤0.001, *** p≤0.0001).

### *3.2.2.vi EMT markers following IR assessed using flow cytometry*

As described in Section 2. 8, cells were analysed for EMT markers post IR using a Beckman Coulter Flow cytometer. The results showed a significant increase (p≤ 0.0001) in vimentin immunopositivity in the 2 Gy X-irradiated cells compared to the 0 Gy cells (82.45% and 75.8%, respectively). Cells also showed a significant decrease (p≤ 0.0001) in E-cadherin immunopositive cells following 2 Gy IR compared to 0 Gy (85.9% and 90.6%, respectively), as shown in Figure 3.15.

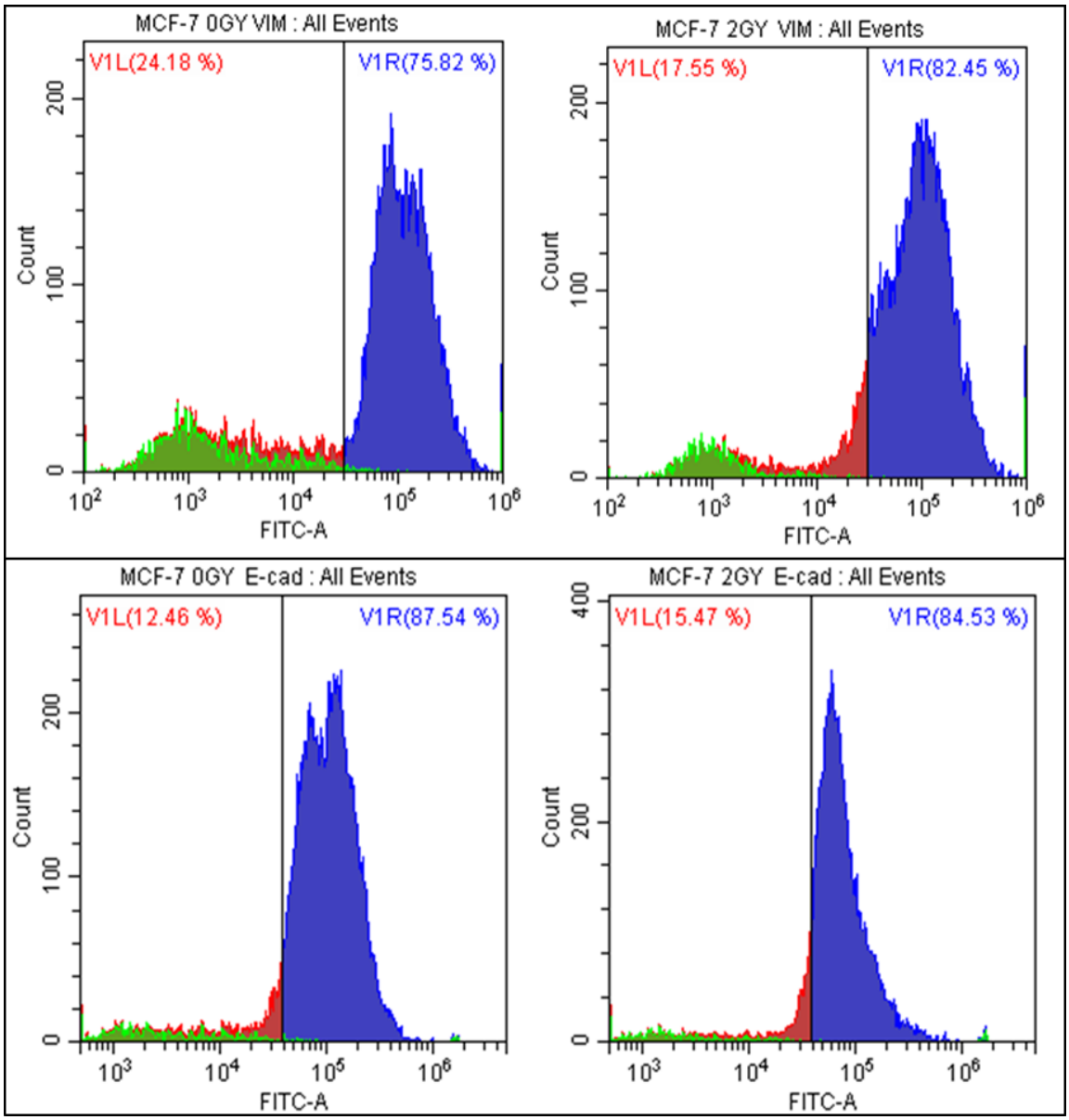


*Figure 3.15 Flow cytometry analysis for specific binding of EMT markers vimentin and E-cadherin 4 hours post-IR.*

MCF-7 cells showed a significant increase in the percentage of vimentin immunopositive cells blue colour and a significant decrease in E-cadherin immunopositive cells blue colour following 2 Gy IR using flow cytometer. The red colour represents cells that were not under the test. While the debris appeared in green colour. Data is representative of the distribution of results over 3 independent experiments.

### *3.2.2.vii Ratio of vimentin to E-cadherin and EMT*

The ratio of vimentin to E-cadherin could play an essential role in the invasion of breast cancer cells. This ratio was calculated as the percentage of vimentin positive cells to the total number of cells and the percentage of E-cadherin positive cells to the total number of cells that were counted. And then calculate the percentage of vimentin to the percentage of E-cadherin. As shown in Figure

3.16, the ratio of vimentin to E-cadherin was 39% in unirradiated cells whereas this ratio increases to 46% in MCF-7 irradiated cells. Data suggest that increasing the percentage of vimentin to E-cadherin in the irradiated cells enhance EMT and consequently invasion of cancer cells.

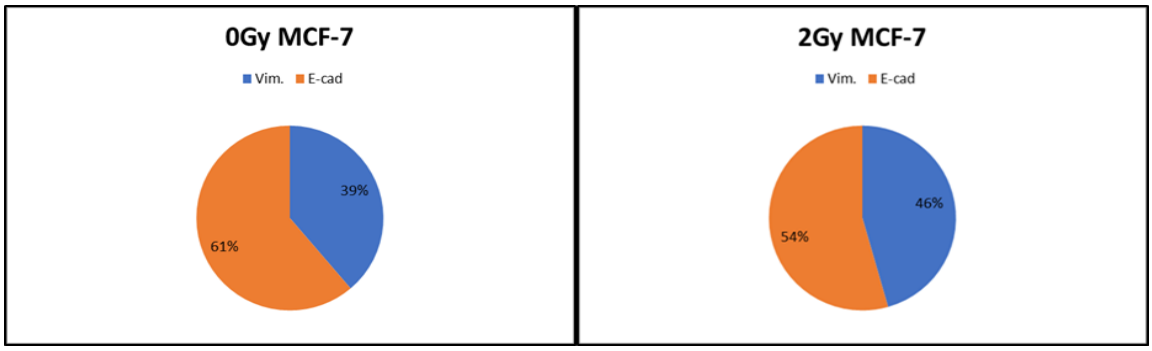


*Figure 3.16 Vimentin / E-cadherin ratio of positive cells in MCF-7 cell line 4 hours post-irradiation.*

Cells showed an increase in the ratio of vimentin to E-cadherin in 2 Gy X-irradiated MCF-7 cells compared to 0 Gy / control cells.

### *3.2.2.viii Vimentin and E-cadherin protein*

To confirm the findings of EMT markers, the level of vimentin and E-cadherin proteins pre-and following irradiation were quantified using western blot as described in Section 2.14. The subsequent data demonstrated a significant increase in the relative quantity (Panel A) of vimentin and a decrease in the relative quantity of E-cadherin following 2 Gy X-irradiation compared to that observed following 0 Gy (Figures 3.17). The 2 Gy-irradiated cells also showed a significant increase in the band intensity (Panel B) of vimentin and a decrease in E-cadherin protein, as shown in Figure 3.17. Actin- β protein has been used as a loading control.

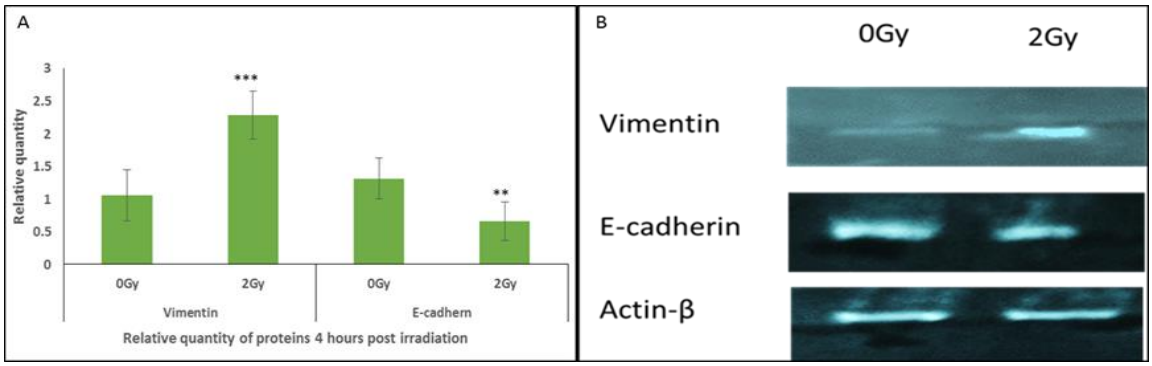


*Figure 3.17 Western blot showed the level of vimentin and E-cadherin in MCF-7 cell line 4 hours following X-irradiation.*

The relative quantity of vimentin has been increased following 2 Gy irradiation compared to that observed in the 0 Gy group (Panel A). In addition, the 2 Gy irradiated cells showed a significant increase in the band intensity of vimentin and proteins at 4 hours following irradiation compared to the 0 Gy cells (Panel B). Conversely, the 2 Gy cells also showed a significant decrease in the relative quantity of E-cadherin protein compared to that observed in the 0 Gy cells 4 hours following irradiation. Data presented as the mean ± SEM of 3 independent experiments (*p≤0.05, ** p≤0.001, *** p≤0.0001).

### *3.2.2.viii Vimentin, E-cadherin and GalNAc-T6 gene expression*

To determine whether 2 Gy X-irradiation exhibit change in gene expression that is associated with EMT and invasiveness; MCF-7 cells were irradiated with either 0 Gy or 2 Gy X-rays. 24 hours following irradiation candidate gene expression was measured as described in Section 2.13.

Cells showed significant (p≤ 0.0001) increase in vimentin and *GalNAc-T6* gene expression following 2 Gy X-irradiation compared to the 0 Gy / control cells. In contrast, the 2 Gy X-irradiated cells, showed significant (p≤ 0.0001) decrease in E-cadherin expression compared to their control counterpart cells, as shown in Figure 3.18.

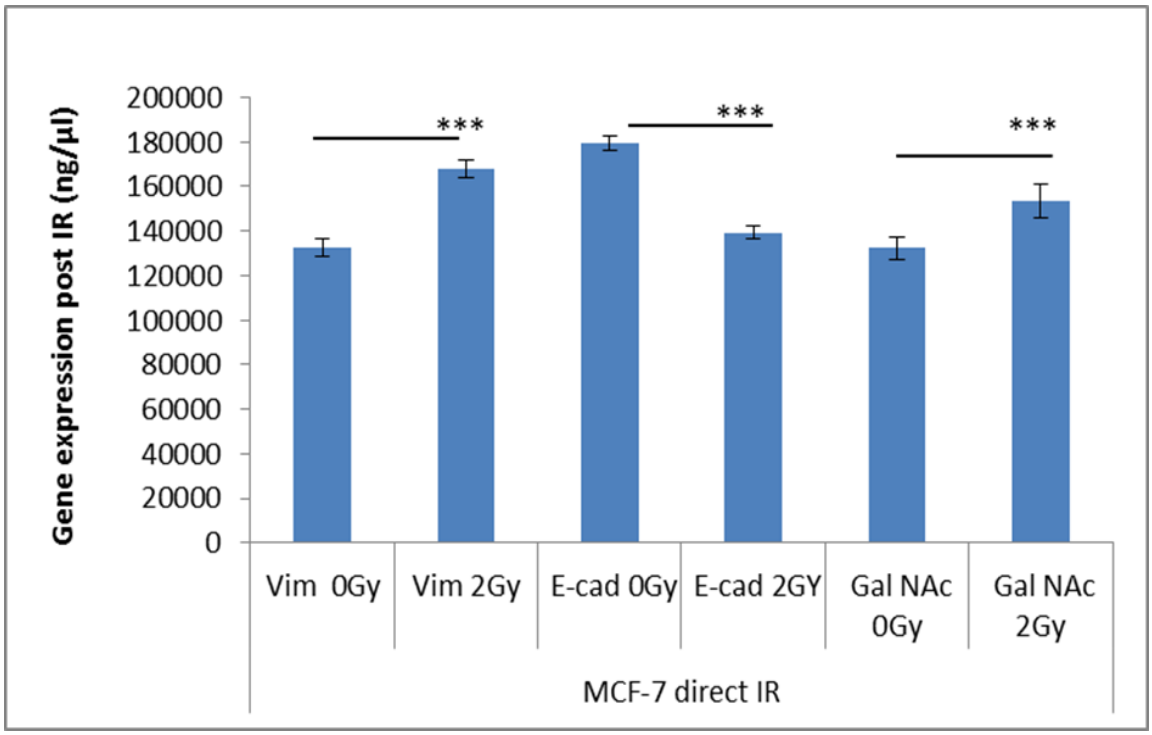


*Figure 3.18 Candidate gene expression following X-irradiation in MCF-7 cells.*

Cells showed a significant increase in vimentin, GalNAc-T6, 24-hours following 2 Gy irradiation compared to the control cells. In contrast, the former cells showed a significant decrease in E-cadherin expression. The error bars represent the SEM of the candidate gene expression, 3 replicate experiments were carried out. (*p≤0.05, ** p≤0.001, *** p≤0.0001).

### *3.2.2.ix TGF-β, SLUG, SNAIL, ZEB and TWIST genes expression*

MCF-7 cells were exposed to either 0 Gy or 2 Gy X-irradiation and then after 24 hours, candidate gene (*TGF-β1*, *SNAIL*, *SLUG*, *ZEB* and *TWIST*) expression was measured using qPCR, as described in Section 2.13. The 2 Gy X-irradiated cells were shown to have a significant (p≤ 0.001) increase in *TGF-β-1* gene expression compared to 0 Gy / control cells. The irradiated cells also demonstrated a significant (p≤ 0.05) increase in *SLUG*, *SNAIL* and *ZEB* genes expression compared to control cells. The irradiated cells also showed a significant (p≤ 0.0001) increase in *TWIST* gene expression compared to 0 Gy control cells, as shown in Figure 3.19. *MMP-9* gene demonstrates no expression in MCF-7 cells pre or post IR.

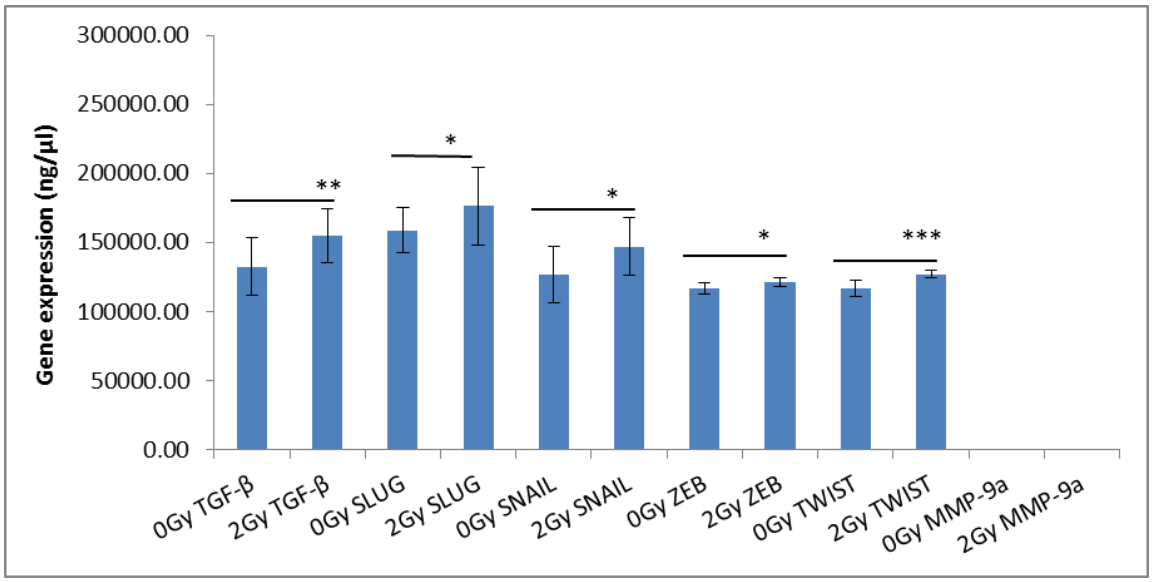


*Figure 3.19 Gene expression in MCF-7 cells following X-irradiation.*

Cells showed a significant increase in *TGF-β-1* gene expression following irradiation with 2 Gy X-rays compared to 0 Gy / control cells. The irradiated cells also showed a significant increase in the expression of *SLUG*, *SNAIL* and *ZEB* genes. Moreover, these cells showed a highly significant increase in the expression of *TWIST* genes compared to 0 Gy cells. The error bars represent the SEM of the candidate gene expression of 3 independent experiments. (*p≤0.05, ** p≤0.001, *** p≤0.0001).

### *3.2.2.x TGF-β protein using western blot assay*

It has been hypothesised that TGF-β could play a role in the invasive capacity of breast cancer cells following irradiation as a result of increased levels of ROS. Thus, to test this hypothesis, MCF-7 cells were seeded in T75 tissue culture flasks and subjected to either 0 Gy or 2 Gy X-irradiation. 24 hours following irradiation, the protein was then analysed with a Western blot assay as described in Section 2.14. The 2 Gy irradiated cells showed an increase in the relative quantity of TGF-β compared to the 0 Gy / control cells (Figure 3.20).

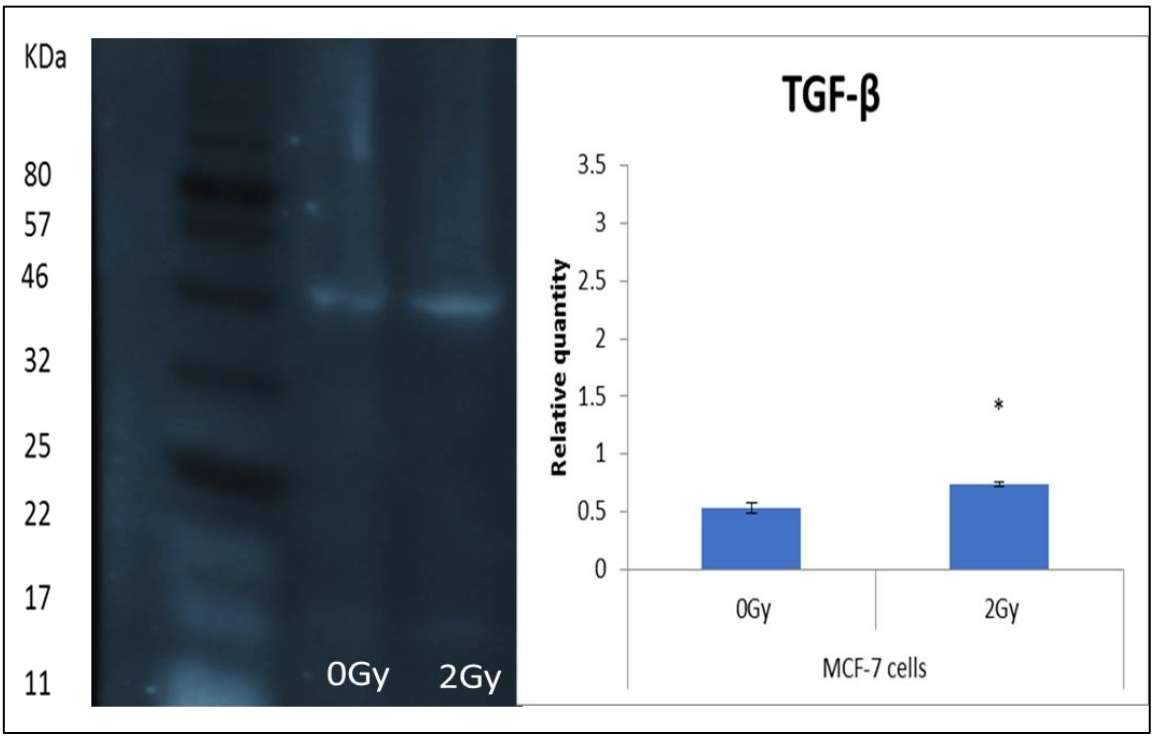


*Figure 3.20 TGF-β protein in MCF-7 using Western blot 24 hours following X-irradiation*

MCF-7 cells irradiated with 2 Gy demonstrated an increase in optical density of TGF-β after 24 hours of irradiation compared to control / 0 Gy cells at 46 kDa. The former also showed a significant increase in the relative quantity of TGF-β proteins at this time. The graph represents densitometry data drawn from blot images. The error bars represent SEM of the candidate protein of 3 independent experiments. (*p≤0.05, ** p≤0.001, *** p≤0.0001).

### *3.2.2.xi miRNA expression in MCF-7 following irradiation*

Candidate miRNA expressions of MCF-7 cells were measured following IR as described in Section 2.13. MCF-7 that were exposed to 2 Gy direct X-irradiation showed a non-significant change in the expression of Let-7a miRNA compared to 0 Gy unirradiated cells. Cells also demonstrated a significant (p≤ 0.001) increase in the miRNA 30a expression following 2 Gy X-irradiation compared to the unirradiated cell. Meanwhile, 2 Gy irradiated cells showed a significant (p≤ 0.0001) decrease in the miR-200b expression compared to unirradiated cells. Moreover, 2 Gy irradiated cell showed a highly (p≤ 0.0001) significant increase in the miR-9a compare to 0 Gy unirradiated cells as shown in Figure 3.21.

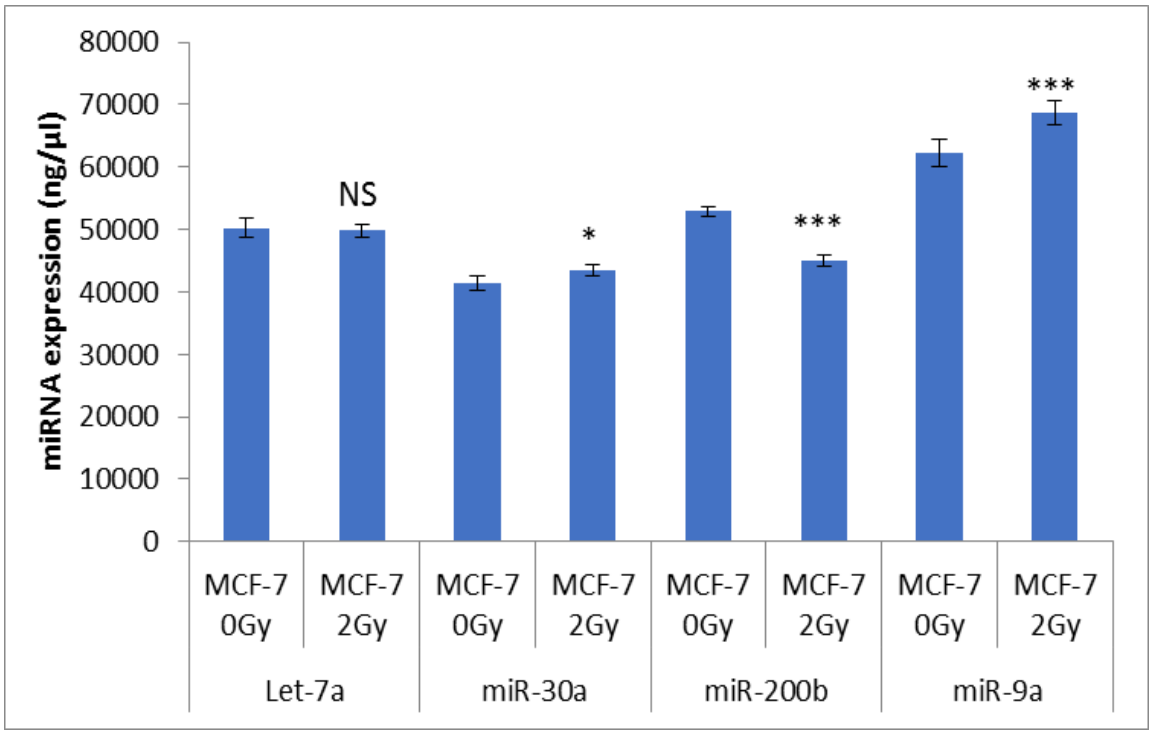


*Figure 3.21 The expression of candidate miRNA in MCF-7 Cells following direct irradiation.*

Cells were exposed to IR showed different responses in the candidate miRNA expression. On the time that cells showed a non-significant change in the let-7a expression, cells also showed a significant increase in the miR30a expression following irradiation. Meanwhile, the expression of miR-200b significantly decreased. Data also showed a highly significant increase in the expression of miR-9a following 2-Gy X-irradiation. The error bars represent the SEM of miRNA expression of 3 independent experiments (*p≤0.05, ** p≤0.001, *** p≤0.0001).

## 3.3 Discussion

IR deposits high energy in the molecules of a cell during interaction and can cause direct or indirect DNA damage (Bryant *et al.*, 2003). IR can also increase ROS in the irradiated cells (Azzam, de Toledo and Little, 2003; Guerci, Dulout and Seoane, 2004). Increased ROS in the irradiated cells could induce oncogenic factors such as TGF-β (Dizdaroglu *et al.*, 2002) which may be involved in cancer development (Iizuka *et al.*, 2017). Therefore, it suggested that IR can increase ROS production and TGF-β expression which may be involved in cancer cells dissociating, moving/migrating and invasion. To investigate the factors that could be involved in enhancing cancer cell metastasis following irradiation, the current study investigated the markers involved in glycosylation and EMT and consequently, the invasive capacity of MCF-7 following exposure to IR. The study also investigated the protein(s) and candidate gene expression that are associated with breast cancer invasiveness.

As described in results part 1, the optimisation of all experimental conditions, including a selection of the most appropriate breast cancer line to work with for our irradiation experiments, to this end, the investigations initially focused on three human breast cancer cell lines, each displaying a different phenotype, as described in Section 2.2. All cell lines were subcultured when they reached 70% confluence. For every subculture, cells were counted, and the cumulative population doubling level was calculated, as presented in Figure 3.1. All cells showed a logarithmic growth rate, and it was therefore concluded that the culture system for all three breast cancer cells was suitable. In addition, MCF-7 cells showed a higher growth rate than the ZR75-1 and BT474 cells.

Numerous publications have described the association between changes in glycosylation and metastasis (Gill *et al.*, 2013; Basu *et al.*, 2015; de Freitas Junior and Morgado-Diaz, 2016). Lectin biotinylated techniques have been used to detect aspects of cellular glycosylation reported in the literature to be of relevance to metastasis. Various Lectins including HPA, PHA-L and SNA have been successfully used to detect GalNAc glycans, 1, 6 N-linked glycans, and α-2,3 and α-2,6 linked sialic acid, respectively (Brooks and Hall, 2002). Other biomarkers have also been investigated, such as the EMT markers: vimentin, E-cadherin and N- cadherin (Mendes, Carvalho and van der Waal, 2010; Shankar and Nabi, 2015), which could have an impact on cancer metastasis. In the current study, cells demonstrated various degrees of EMT markers labelling which were dependant on the type of cell and markers (Figures 3.2, 3.3 and 3.4 respectively). MCF-7 cells were shown to be highly immunopositive for vimentin and N-cadherin and demonstrated low immunopositivity for E-cadherin compared to the ZR75-1 and BT474 cells (Figures 3.5, 3.6 and 3.7 respectively). It is known that cells with low E-cadherin and high vimentin expression will lose epithelial integrity and as a result, cells are more motile and invasive (Korsching *et al.*, 2005; Satelli *et al.*, 2016). Previous studies have also shown that HPA lectin is the best marker to detect aberration in the O-glycosylation due to its high affinity to the GalNAc amino sugar (Sanchez *et al.*, 2006; Peiris *et al.*, 2015).

Biotinylated lectin labelling, immunopositivity, aggressiveness and the quality of picture in term of discrete cells to be counted were the criteria to select

appropriate cell line for this study. Therefore, the current study selected MCF-7 cell line as a luminal epithelial breast cancer cells. This cell line moderate aggressiveness and metastases and have a high affinity to HPA lectin. Additionally, vimentin and E-cadherin were selected as markers of the mesenchymal and epithelial form of the cells respectively.

### 3.3.1 MCF-7 cells responses to radiation exposure.

MCF-7 cells were irradiated with either 0 Gy (Control) or 2 Gy X-irradiation. 4 hours following irradiation; the 2 Gy cells showed a significant decrease in their viability but an increase in ROS, as shown in Figures 3.10 and 3.11 respectively. Significant DNA damage was also observed in this group of cells, as shown in Figure 3.12. This finding could be due to the direct effect of IR on DNA or by the action of ROS, which is known to be activated during and after cell exposure to X-irradiation. Correspondingly, the observed induction of DNA damage in the 2 Gy irradiated cells was associated with an increase in the percentage of apoptotic cells and a subsequent increase in the percentage of dead cells (Figure 3.13). These findings were supported by other studies (Dizdaroglu *et al.*, 2002; Dizdaroglu and Jaruga, 2012) who stated that IR could target the DNA directly and cause single-strand or double-strand breaks (Dizdaroglu *et al.*, 2002).

Moreover, the current study found that the percentage of DNA damage observed in the 2 Gy irradiated cells was greater than the percentage of apoptotic cells. The differences in the significance between the DNA damage and the percentage of apoptotic cells could occur because not all the DNA damage caused lethal effects on the irradiated cells. It is well known that cells also can activate DNA repair machinery that may reduce the percentage of apoptotic cells in irradiated cells (Gerelchuluun *et al.*, 2015). On the other hand, an increase in the level of ROS may lead to an increase in the stress of the cells which could activate the *TGF-β –AKT1* pathway (discuss later), which could subsequently affect invasion capacity of breast cancer cells. It is well known that there is a link between the HPA positivity and invasiveness (Brooks, 2000). The findings in this study confirm the previous results; the finding shows a strong correlation between the percentage of HPA positive cells and the invasive capacity of MCF-7 cells (Figure 3.14). The association may be the result of an increase in the level of the Tn antigen, which could promote cells invasion and migration. Gill *et al.* (2013) have

demonstrated that the regulation of N-acetylgalactosamine-transferases (GalNAc-Ts) from the Golgi complex to endoplasmic reticulum can increase the level of Tn antigen, which promotes breast cancer invasiveness (Chia *et al.*, 2014). In addition, it is known, that the intensity of O-glycosylation and annexin 4 proteins is frequently associated with very poor patient lifespan (Peiris *et al.*, 2015). Furthermore, using proteomic and histochemistry analysis of HPA labelling, studies have revealed that annexin 4 appears to be a major carrier of O-linked glycosylation in lymph node-positive breast cancer (Peiris *et al.*, 2015). In addition, Park *et al.* (2011) state that GalNAc-T6 and GalNAc -T3 regularly correlate with tumour cell differentiation. However, only GalNAc-T6 is associated with cancer cell metastasis. Furthermore, silencing COSMIC chaperones can induce truncated O-glycosylation, particularly of core 1 (3-GalNAc-T) due to the epigenetic modification of chaperone protein rather than mutation, and this can increase the ability of cells to invade the Matrigel membrane (Radhakrishnan *et al.*, 2014a). Moreover, the current study demonstrated that X-irradiation induced invasive capacity of MCF-7 cells which was associated with an increase in immunopositivity of the mesenchymal marker vimentin and a decrease in the epithelial marker E-cadherin (Figure 3.14). Flow cytometry results confirm that IR increases vimentin immunopositive cells and decreases E- cadherin immunopositivity (Figure 3:15).

The results of this study support the findings in other studies. Tsukamoto *et al.* (2007) state that X-irradiation induces a change in the phenotype of HEC1A cells from epithelial to mesenchymal, loss of cell polarity with a reduction in cell-cell interaction and an increase in cell motility by the formation of pseudopodia.

As mentioned earlier in Sections 1.3.1, 1.3.2 and 1.3.3, there is a correlation between TGF-β and EMT. An increase in the quantity of TGF-β in irradiated cells was associated with downregulation of E-cadherin and increase in the expression of vimentin and other transcription factors SLUG, SNAIL, ZEB and TWIST as shown in Figures 3.19. It has been reported that TGF-β can regulate downstream Wnt/beta-catenin pathway that inhibits E-cadherin protein and increases the invasiveness of breast cancer cells (Ma *et al.*, 2017). Moreover, TGF-β could target *SLUG* gene resulting in downregulation of E-cadherin protein which

promotes breast cancer cell dissociation and invasion (Takano *et al.*, 2007; Dhasarathy *et al.*, 2011; Sritananuwat *et al.*, 2017). In addition, other mechanisms could contribute to the invasiveness of cancer cells following X-irradiation. Data in this study have shown that irradiated cells can produce a significant increase in the level of TGF-β, (Figure 3.20). Then TGF-β protein may target TGF-β receptors, which can activate the protein kinase B, also known as AKT1, pathway (Lee *et al.*, 2007) leading to phosphorylation of vimentin and activation the vimentin-scrib protein complex (a membranous protein found in human cells, which is involved in the proliferation, polarity and migration of cancer cells) (Zhu *et al.*, 2011b). The latter can promote migration and invasion of cancer cells (Phua, Humbert and Hunziker, 2009), as shown in Figure 3.22.

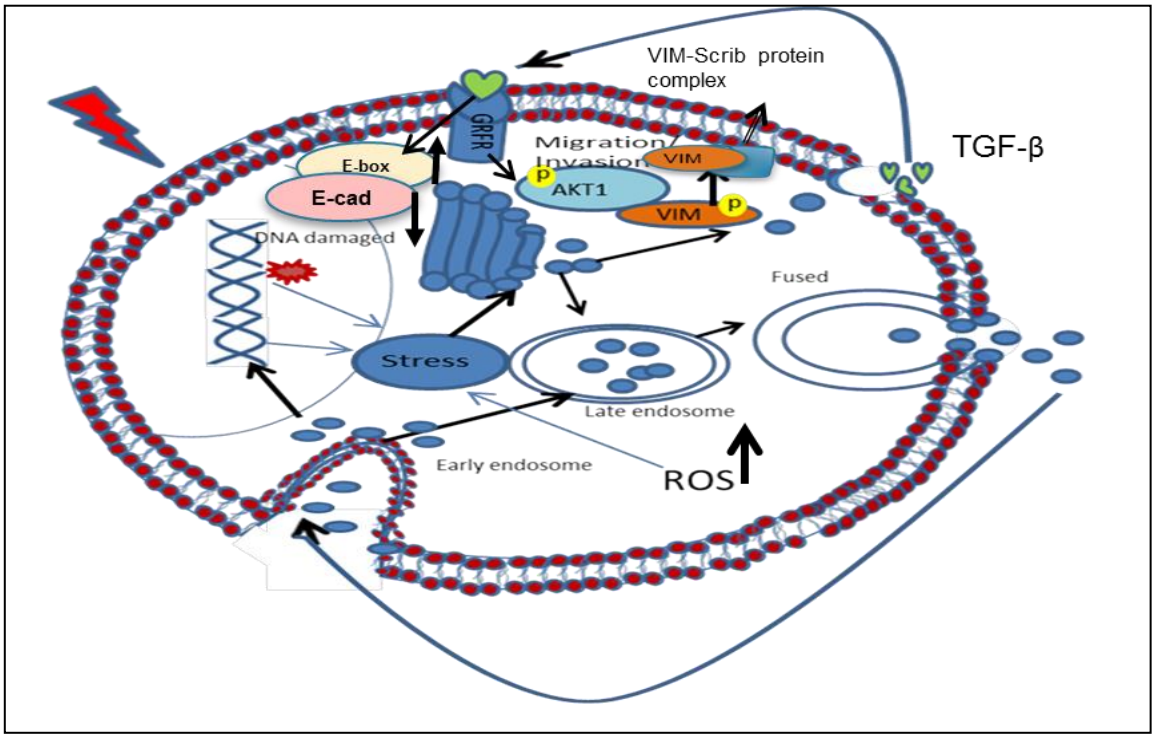


*Figure 3.22 A schematic diagram to illustrate the possible mechanisms that may contribute to the migration and invasion of MCF-7 luminal breast cancer cells post-irradiation.*

IR can induce DNA damage and activate the apoptotic pathway and increase the stress in the irradiated cells. IR can also increase ROS formation and increase the stress of irradiated cells. The stressful cell produces a high number of EVs/ Exosomes. These EVs can traffic to the endosomes and release into the outside of the cells. These exosomes carry miRNA and protein such as TGF-β, the later can interact with the TGF-β receptor and activate several pathways including AKT1. Consequently, inhibit E-cadherin and active vimentin phosphorylation and induce EMT and invasion of cancer cells.

The qualitative data on vimentin and E-cadherin immunopositivity and western blot analysis were confirmed using qPCR assay. The data showed a significant increase in vimentin expression and decreased in E-cadherin following irradiation encouraging EMT in breast cancer cells, and promoting migration and invasion in irradiated cells (Figure 3.17, 3.18).

The possible mechanisms involved in cell migration and invasion can be described, as the ionising irradiation can increase $ROS^{+}$ (Figure 3: 11) leading to an increase in the stress of cancer cells. Stressed cells can produce a high abundance of vimentin, which subsequently activates several downstream mechanisms involving the *AKT1* gene, which in turn, activates the serine/threonine-protein kinase. Thus, the phosphorylation of vimentin protein leads to protecting it from the action of proteolytic enzymes. Accumulation of phosphorylated vimentin induces the formation of a vimentin-scrib protein complex can cause acceleration in cell motility, leading to an increase in the ability of cancer cells to invade other tissues (Zhu *et al.*, 2011b). The latter, vimentin-scrib protein complex can protect scrib protein from degradation by the proteasome system. Thereby, vimentin can provide a stabilising effect on scrib protein during EMT, promoting cell motility and migration (Satelli and Li, 2011; Hascoet *et al.*, 2015).

Conversely, reduction in E-cadherin expression enhances cell mobility which enables cells to dissociate from each other and move. The decrease in the expression of E-cadherin as a consequence of increased expression of helix-loop-helix transcription factors such as *TWIST* and zinc finger factors such as *SLUG, SNAIL* and *ZEB1* genes which downregulate E-cadherin expression, thus promote the breast cancer cell migration (Figure 3:16). Declined expression of E-cadherin reduces cell-cell communication and enhances EMT by blocking the E-cadherin-catenin pathway (Zhu, Leber and Andrews, 2001; Kilic *et al.*, 2016).

In summary, this study for the first time showed the possible integrated process that IR can increase the HPA positive cells and invasive capacity of irradiated cells. IR promotes changing the mesenchymal/epithelial ratio of MCF-7 breast cancer cells which could be as a result of an increase in production of cytokine

TGF-β, decrease in the expression E-cadherin protein and increase in vimentin expression. IR can increase the ROS production and that could lead to an increase in the stress of irradiated cells. Consequently, increase secretion of extracellular vesicles/ exosomes which could have an impact on cancer invasion, and that will be described in chapter 4.

# Chapter 4

## The role of microvesicle/exosomes in the invasion of luminal breast cancer cells

### 4.1 Introduction

Exosomes which are double-membrane nanoparticles (40-150 nm) contain various types of molecules including nucleic acids (DNA, mRNA, and miRNA), proteins (enzymes, cytokines, transmembrane proteins) and metabolites (peroxidases, lipid kinases and pyruvate enzymes) (Mao *et al.*, 2016; Lv *et al.*, 2017). The majority of exosomes contain transport and fusion proteins, such as flotillin, annexins and Rab GTPase, Alix, and TSG101 (reviewed by Kahlert and Kalluri, 2013; Kahlert *et al.*, 2014; Lindsey and Langhans, 2014; Brinton *et al.*, 2015). Much evidence has stated that exosomes can carry proteins that are involved in EMT, such as TGF-β (Yang *et al.*, 2011; Syn *et al.*, 2016).

The function of exosomes varies from one type of cell to another, i.e. exosomes can either be activators or inhibitors. For example, exosomes released from dendritic cells can activate the immune system directly or indirectly via cytokine production and T cell activation (Bianco *et al.*, 2007; Bianco *et al.*, 2009). On the other hand, cancer cells produce exosomes, which have an inhibitory effect on the immune system (Thery *et al.*, 2002; Clayton *et al.*, 2007; Clayton *et al.*, 2011). Exosomes also play a critical role in cancer development, progression and invasion (Greening et al., 2015; Soung et al., 2016) as described in detail in Section 1.7

The potential effect of exosomes on the behaviour of breast cancer cells normally results from the nature of exosome cargo, which can be affected by several factors including cell stress (Chen *et al.*, 2011; Vulpis *et al.*, 2017). IR is one of the most important factors that increase the stress of human cells. It has been reported that cells under the stress of IR can produce greater amounts of exosomes than unirradiated cells (Jelonek *et al.*, 2015).

Recent studies have concentrated on the effect of exosome derived from irradiated cells and its cargo on the invasion of MCF-7 breast cancer cell. Jelonek, Widlak and Pietrowska (2016) have documented that exposure to IR

can lead to changes in the cargo of exosomes, which may have effects on the cellular activity of cancer cells such as suppression of translation, transcription or induction of cell signalling. They examined proteins in the exosomes extracted from irradiated and unirradiated head and neck cancer cells. Abundant changes were observed in the exosome contents post-irradiation compared to the control groups. For example, Jelonek et al. (2015) found a change in the exosome proteins post 2 Gy irradiation, 384 proteins were identified in the exosomes that were isolated from head and neck carcinoma cells compared to 217 proteins in 0 Gy control cells. They also identified that 69 types of proteins were missing in irradiated exosomes group and 236 types of proteins were identified only following irradiation (Jelonek *et al.*, 2015).

Al-Mayah *et al.* (2015) have shown that exosomes derived from irradiated MCF-7 cells have long-lasting effects on the DNA and telomerase activity of unirradiated cells, resulting from the components of exosomes, including protein and RNA molecules. Exosome cargo molecules (proteins and RNA) can act synergistically to induce non-targeted effects in the progeny of irradiated and unirradiated cancer cells. Wang *et al.* (2017) demonstrate that IR can induce ROS and subsequently increase the number of exosomes in irradiated cells.

As described in chapter 3, the data showed the direct effect (targeted effect) of IR can promote the invasive capacity of MCF-7 cells. However, the non-targeted effects of IR on cancer cell invasiveness and metastatic potential are not fully understood yet. Therefore, the objective is to analyse the non-targeted effect of IR (the classic bystander effect, exosome bystander and exosomes cargo inhibition) on MCF-7 breast cancer cells. In order to achieve this, the following were carried out:

1- Characterisation of the exosomes derived from CCCM and ICCM regarding their size and concentration.

2- Determination of the change in immunopositivity of EMT markers (vimentin and E–cadherin) in MCF-7 cells following media transfer.

3- Determination of the change in the HPA labelling in MCF-7 cells following exosomes transfer.

4- Determination of the change in the invasive capacity of MCF-7 cells following treatment with exosome-depleted media.

5- Investigation of the effect of exosome cargo inhibition on the invasive capacity, EMT (vimentin and E-cadherin) and glycosylation HPA markers of MCF-7 cell.

6- Determination of the expression of candidate genes such as the GalNAcT6, as well as detection of changes in vimentin and E-cadherin expression and another candidate gene that listed in Tables 2.1 and 2.2.

7- Determination of the expression of TGF-β protein in the exosomes and in the cells treated with exosomes, which may have an impact on cancer cell invasion.

8- Determination of the change in the expression of specific exosomal miRNA, which may be associated with the invasive capacity of MCF-7 cells.

## 4.2 Results

### 4.2.1 Invasive capacity of MCF-7 cells post media transfer

Fresh unirradiated MCF-7 cells were treated with CCCM and ICCM four hours following irradiation. Following 24 hours of incubation, cells were analysed for glycosylation EMT and invasion as described in Section 2.11. Highly significant induction of invasive cells was observed ($p \leq 0.0001$) after 24 hours post 2 Gy ICCM transfer. The average of total number of cells invaded through the membrane was 734 cells (in total); compared to the total number of cells invaded through the membrane in the cells that were treated with CCCM was 375 (in total); this was concurrent with an increase ($p \leq 0.0001$) in the level of vimentin immunopositivity (68.93%) compared to 0 Gy BE which is only (54.77%). MCF-7 cells also demonstrate a significant ($p \leq 0.0001$) decrease in the level of E-cadherin immunopositivity (After 24 hours post 2 Gy media transferred (79.2%) compared to the E-cadherin positive cells (87.8%) post 0 Gy BE. Cells also demonstrated an increase ($p \leq 0.0001$) in the level of the HPA positive cells (83.8%), 24 hours post 2 Gy ICCM transfer compared to the level of HPA positivity post 0 Gy media transfer (74.4%) (Figure 4.1).

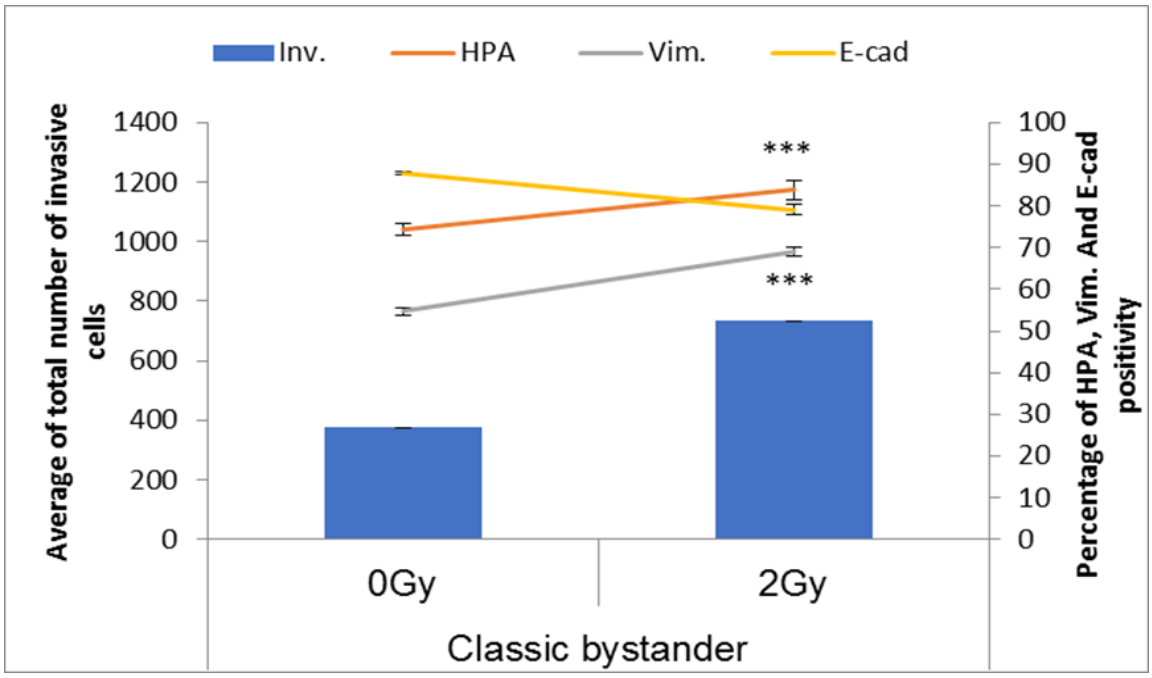


*Figure 4.1 Invasive capacity, EMT markers and HPA labelling in bystander effect MCF-7 cells after 24 hours post-media transfer.*

Cells showed a significant (p≤0.0001) increase in the number of invasive cells post ICCM transfer compared to CCCM, and this associated with a decrease in E-cadherin and an increase in vimentin positivity. Cells also showed an increase in the percentage of HPA positive cells at 2 Gy BE cells compare to 0 Gy BE cells. The data presented as a mean of a total number of invasive cells, and the percentage of HPA and EMT markers positive cells. The error bars represent the SEM of invasive cells and the percentage of HPA and EMT markers of 3 independent experiments. (*p≤0.05, ** p≤0.001, *** p≤0.0001).

### 4.2.2 Exosomes characterisation

The size and concentration of exosomes were measured as described in Section 2.12.3. Data demonstrated a significant (p≤0.05) change in the size of exosomes (104nm in diameter) at 4 hours post 2 Gy irradiation, compared to 0 Gy exosomes (95nm in diameter). Data also showed a significant (p≤0.0001) increase in the exosome concentration ($5.4X10^{10}$ exosome/ml) produced by 2 Gy irradiated cells compared to the exosomes that were isolated from unirradiated cells ($4.20X10^{10}$ exosome/ml) as shown in Figure 4.2A. Data also showed that the exosomes isolated from irradiated and unirradiated cells exhibited bands of TSG-101 57 kDa higher than expected 46 kDa and CD63 30-60 kDa as it expected (Figure 4.2A). Bands it looked quit expanded, however it is consistant with brevious studies (Van Deun *et al.*, 2014; Kowal *et al.*, 2016). However, western blot showed clear bands at 12 kDa and faint band at 25 kDa.

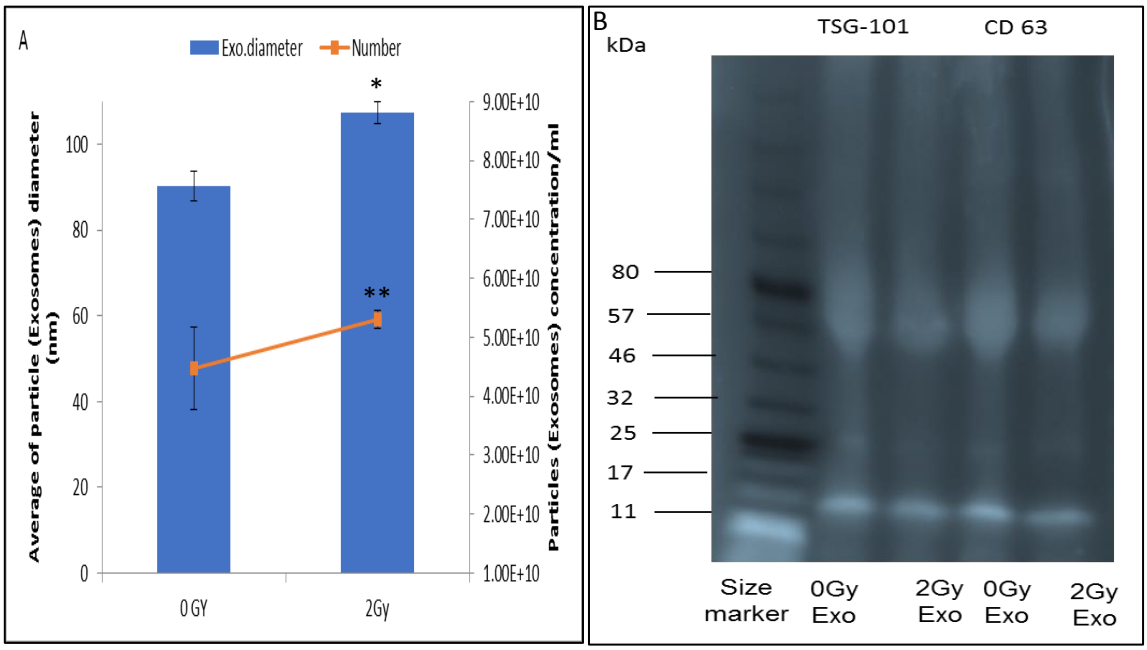


*Figure 4.2 Mean exosome size and concentration and exosome markers (TSG101 and CD63) in MCF-7 cells 4 hours following 2 Gy X-irradiation.*

A) Cells showed a significant difference in exosome size at 4 hours post-irradiation compared to exosomes that were isolated from unirradiated cells; whereas, an increase in exosome concentration/ml was observed in the irradiated cells following 2 Gy X-irradiation. B) Western blot data also showed TSG101 57 kDa higher than expected 46kDa and CD63 bands 30-60 kDa confirmed the presence of exosomes in the collection. The data presented as a mean ± SEM of 3 independent experiments. (*p≤0.05, ** p≤0.001, *** p≤0.0001).

### 4.2.3. EMT markers following exosome transfer, assessed using Flow cytometry

MCF-7 cells were treated with exosomes derived from 0 Gy CCCM and 2 Gy ICCM. After 24 hours post-incubation, cells were labelled with anti-vimentin and anti-E-cadherin primary antibodies were measured, as described in Section 2.8. A significant increase (p≤0.001) in vimentin immunopositivity (77.50%) in 2 Gy exosome-treated cells compared to 0 Gy-exosome-treated cells (53.21%). Cells also displayed a significant decrease (p≤0.001) in E-cadherin immunopositivity (76.28%) following 2 Gy exosome transfer compared to 0 Gy exosome-treated cells (86.75%), as shown in Figure 4.3.

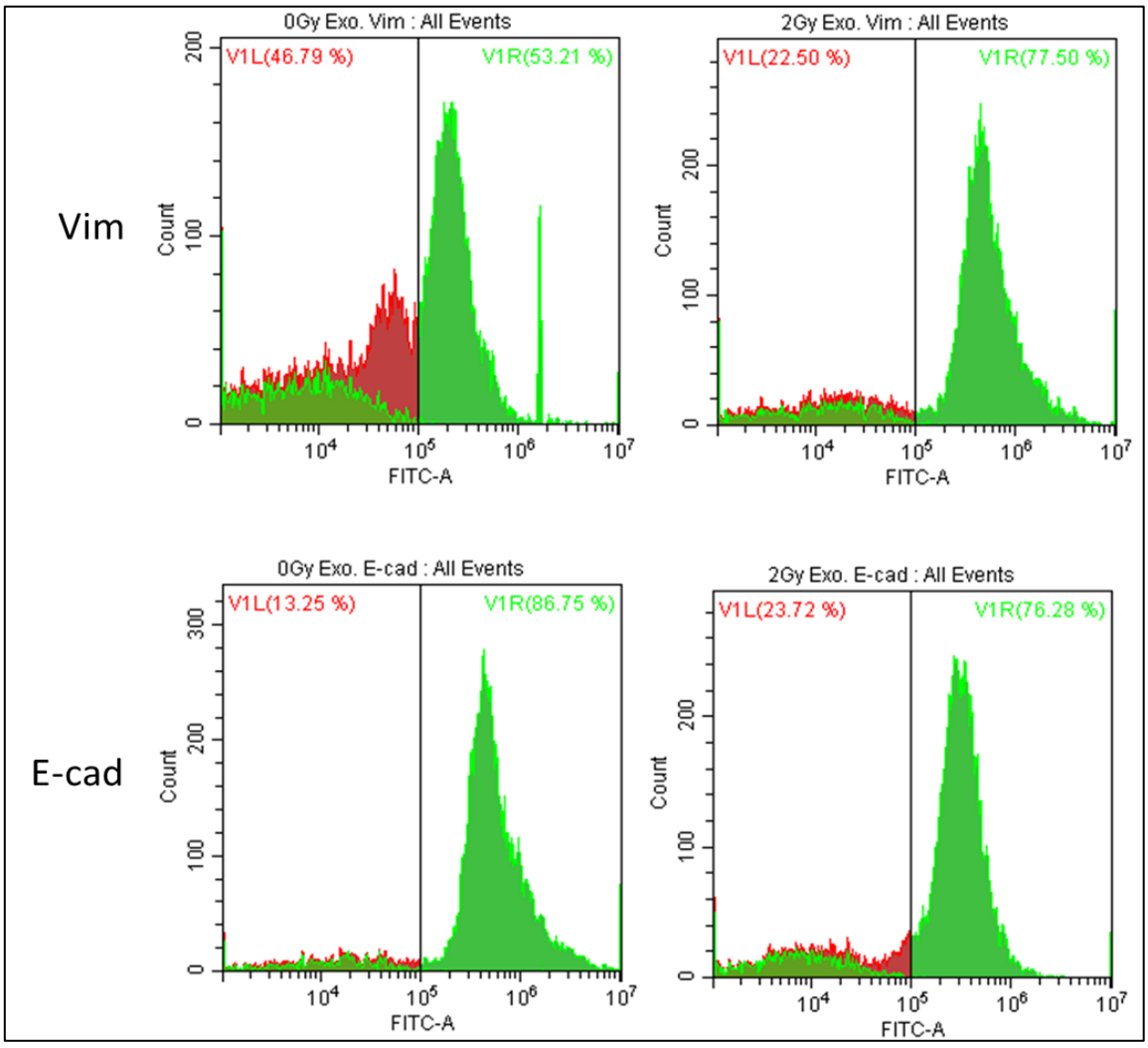


*Figure 4.3 Flow cytometry analysis for specific labelling of EMT markers (vimentin and E-cadherin) in the cells post-exosomes transfer.*

MCF-7 cells showed a significant increase in the percentage of vimentin immunopositivity (green colour) in the right hand of the histogram by 2 Gy ICCM exosome-treated cells compared to CCCM exosome-treated cells. Data also showed a significant decrease in E-cadherin immunopositivity (green colour) by 2 Gy ICCM exosomes treated cells compared to the cells treated with exosomes isolated from CCCM. The red colour represents a population of cells outside the main population that determined by polygonal shape. While green colour in the left hand of histogram represents the debris. The plot is representative of the distribution of data from 3 experiments.

### 4.2.4 The level of Vimentin and E-cadherin proteins following exosomes transfer

Western blot analyses of vimentin and E-cadherin as described in Section 2,14 support this result. Western blot analyses of proteins derived from cells that were treated with CCCM and ICCM exosomes (Figure 4.4), which confirm an increase in the level of vimentin proteins and decrease in E-cadherin protein in ICCM

exosomes recipient cells compared to CCCM exosomes recipient cells. Actin- β has been used as a positive control.

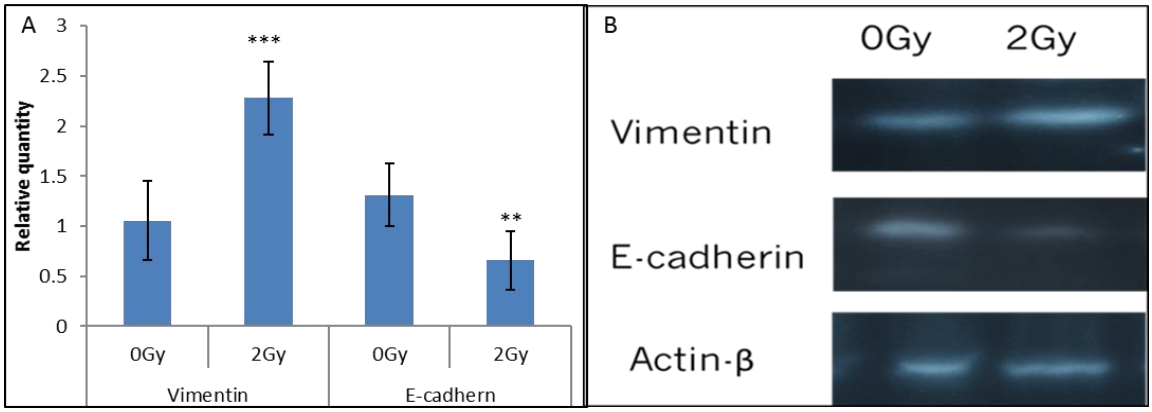


*Figure 4.4 Western blot of Vimentin and E-cadherin proteins in MCF-7 exosome treated cells following 24 hours of exosome transfer.*

Cells showed a significant increase in the relative quantity of vimentin and decreased in the E-cadherin protein (Panel A) following exosomes transfer. Cells also exhibited an increase in the intensity of vimentin bands samples derived from 2 Gy exosome treated cells compared with 0 Gy exosome-treated cells. Cells also demonstrate a significant decrease in the intensity of E-cadherin protein after treated with 2 Gy exosomes compared with 0 Gy exosomes treated cell (Panel B). The graph represents densitometry data drawn from blot images. The data presented as a mean ± the SEM of three independent experiments (*p≤0.05, ** p≤0.001, *** p≤0.0001).

### 4.2.5 Bystander effect: exosome transfer

MCF-7 cells were treated with CCCM and ICCM exosomes as described in Section 2.12.4. Data showed a significant (p≤0.0001) increased in the number of invasive cells after 24 hours post-incubation 2 Gy ICCM. The total number of cells that invaded through the membrane in ICCM exosome treated cells was 1239 cell, compared to the total number of cells invaded through the membrane in the cells that were treated with exosomes isolated from CCCM was 611 cells under the same condition (Figure 4.5).

Cells treated with ICCM exosomes showed a significant (p≤0.0001) increase in the level of vimentin. The percentage of cells that were immunopositive for vimentin was 75.36% in three replicates of each dose of treatment and in three experiments compared to the percentage of cells that were immunopositive for vimentin 67.58% in CCCM exosome-treated cells.

The current data also showed a significant (p≤0.0001) decrease in the E-cadherin markers. The percentage of cells that were immunopositive for E-cadherin was 71.48% that were also observed in the cells treated with exosomes from ICCM following 2 Gy X-irradiation compared to the percentage of cells that were immunopositive for E-cadherin (80.54%) in CCCM exosome-treated cells.

Cells also demonstrated a significant (p≤ 0.0001) increase in the level of the HPA positive cells after 24 hours of incubation with exosomes from ICCM 2 Gy X-irradiation. The percentage of cells that were immunopositive for HPA was (83.8%), exosomes treated cells compared to the percentage of cells that were immunopositive of HPA 74.4% following 0 Gy CCCM exosome-treated cells as shown in Figure 4.5

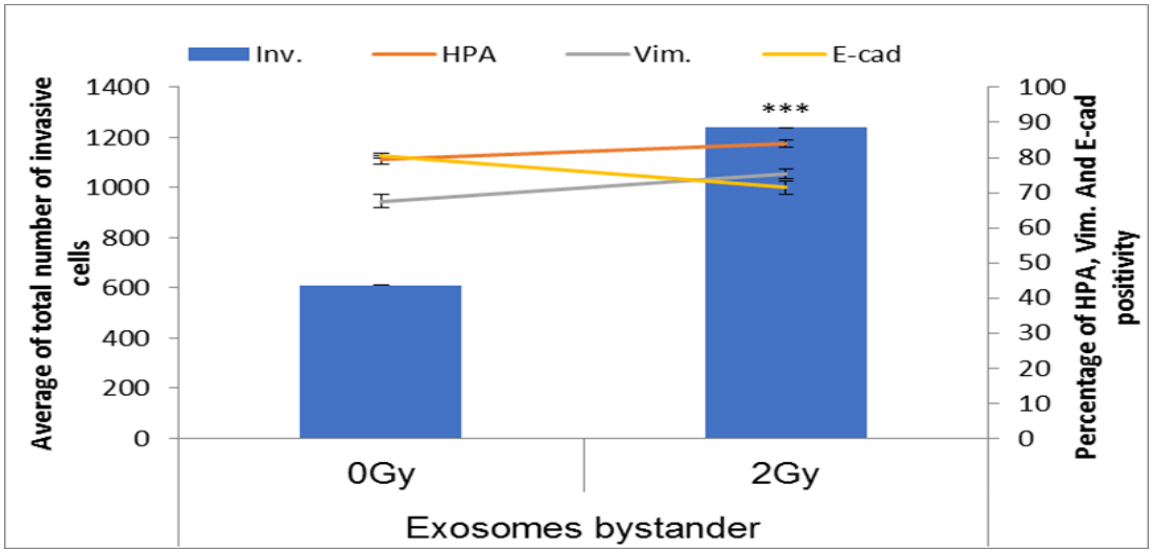


*Figure 4.5 Effects of exosomes on the invasiveness of MCF-7 cells.*

Exosomes were isolated from CCCM (0 Gy) and ICCM 2 Gy X-ray and then transferred to healthy, unirradiated cells. Cells showed a highly significant increase in the number of cells that invaded the Matrigel membrane associated with an increase in the HPA labelling cells and vimentin immunopositivity and a decrease in the E-cadherin immunopositivity. The data presented as a mean of a total number of invasive cells, and the percentage of HPA and EMT markers positive cells ± the SEM of 3 independent experiments. (*p≤0.05, ** p≤0.001, *** p≤0.0001).

### 5.2.6. Exosome-depleted media transfer

The previous experiments (assessing classic bystander and exosome bystander effects) showed that the media and exosomes derived from ICCM have an impact on invasiveness capacity of MCF-7. To confirm the role of exosomes in invasive of the breast cancer cell. MCF-7 cells were treated with 0 Gy CCCM and 2 Gy ICCM exosome-depleted media. Cells were then analysed for invasion,

EMT markers and HPA positivity as described in section 2.12.5. Under this condition, cells did not show a significant change in the number of invasive cells after treatment with 2 Gy ICCM exosome-depleted media compared with CCCM exosome depleted media. Cells also did not show a significant difference in the levels of vimentin and E-cadherin and HPA immunopositivity (Figure 4:6).

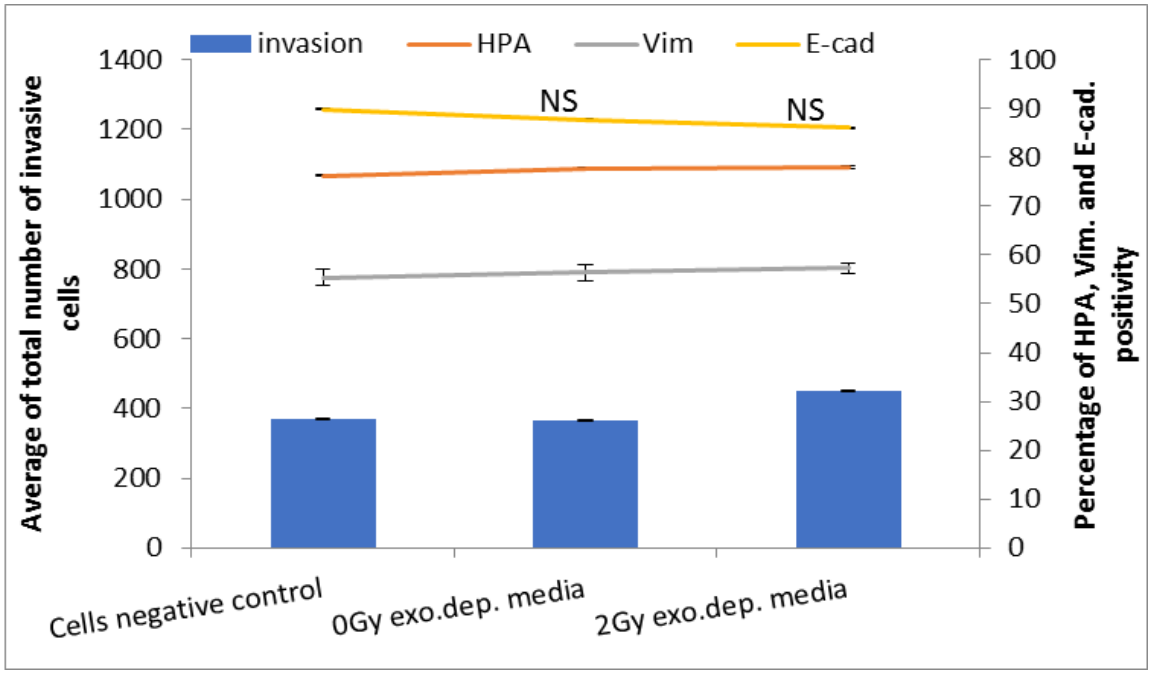


*Figure 4.6 Effect of exosome-depleted media on the invasive capacity of MCF-7 cells.*

MCF-7 cells were treated with 0 Gy, and 2 Gy exosome-depleted media, cells showed a non-significant increase in the percentage of invasive cells when exposed to 2 Gy exosome-depleted media compared to cells treated with 0 Gy exosome-depleted media. Cells also did not show a significant increase in the percentage of HPA, vimentin and E-cadherin positivity when exposed to 2 Gy exosome-depleted media compared 0 Gy exosome-depleted media). The data presented as a mean of a total number of invasive cells, and the percentage of HPA and EMT markers positive cells. The error bars represent the SEM of invasive cells and the percentage of HPA and EMT markers. (*p≤0.05, ** p≤0.001, *** p≤0.0001).

### 4.2.7 Expression of genes following exosomes transfer in MCF-7 cells

To quantify whether the MCF-7 cells that were treated with an exosome isolated from ICCM, exhibit differences in gene expression in unirradiated cells. CCCM and ICCM treated cells were analysed for gene expression as described in Section 2.13.

Analysis of qPCR results showed a significant (P≤0.0001) increase in the vimentin gene expression in 2 Gy exosome-treated cells compared to the 0 Gy control group. Cells also showed a significant (p≤0.001) increase in *GalNAc-T6*

expressions in 2 Gy exosome-treated cells compare to 0 Gy exosome-treated cells. Meanwhile, the level of E-cadherin expression was significantly (p≤0.001) decrease in the cells that were received exosomes isolated from 2 Gy irradiated cells compared with 0 Gy exosome-treated cells as shown in Figure 4.7.

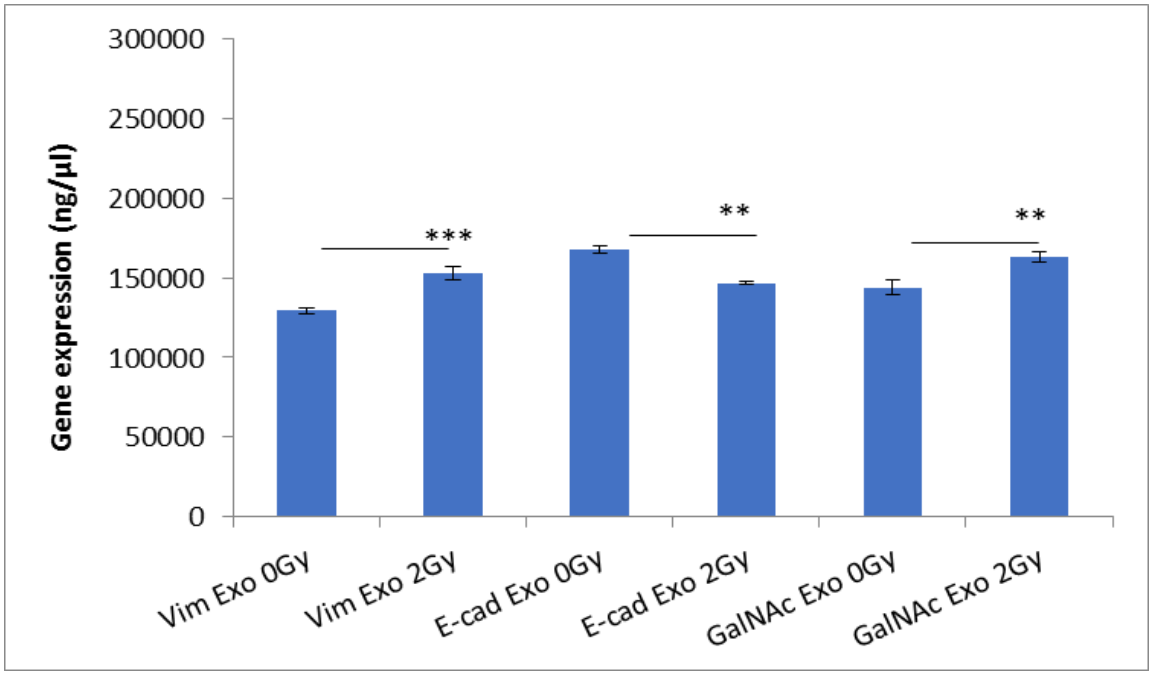


*Figure 4.7 Gene expression in MCF-7 recipient cells following exosome transfer.*

MCF-7 cells treated with exosomes that were isolated from 0 Gy and 2 Gy-irradiated cells. 24 hours post-exosome-transfer, cells showed an increase in vimentin and a decrease in E-cadherin expression. Cells also showed a higher level of *GalNAc-T6* expression post ICCM exosomes transfer. The error bars represent SEM of the candidate gene expression, 3 replicate experiments were carried out. (*p≤0.05, ** p≤0.001, *** p≤0.0001).

### 4.2.8 E-box genes expression and TWIST

CCCM and ICCM treated cells were analysed for gene expression as described in Section 2.13. Data showed a significant (P≤0.001) increase in the E-box (*SNAIL*, *SLUG*) gene expression post 2 Gy exosome transfer compared with 0 Gy exosome transfer. Meanwhile, ZEB gene expression was not significantly increased in 2 Gy exosome-treated cells compared with control. Moreover, 2 Gy exosome-treated cells showed a significant (P≤0.001) increase in *TWIST* expression compared with 0 Gy exosome-treated cells as shown in Figure 4.8. Meanwhile, *MMP-9a* gene showed no expression in CCCM and ICCM exosomes treated MCF-7 cells.

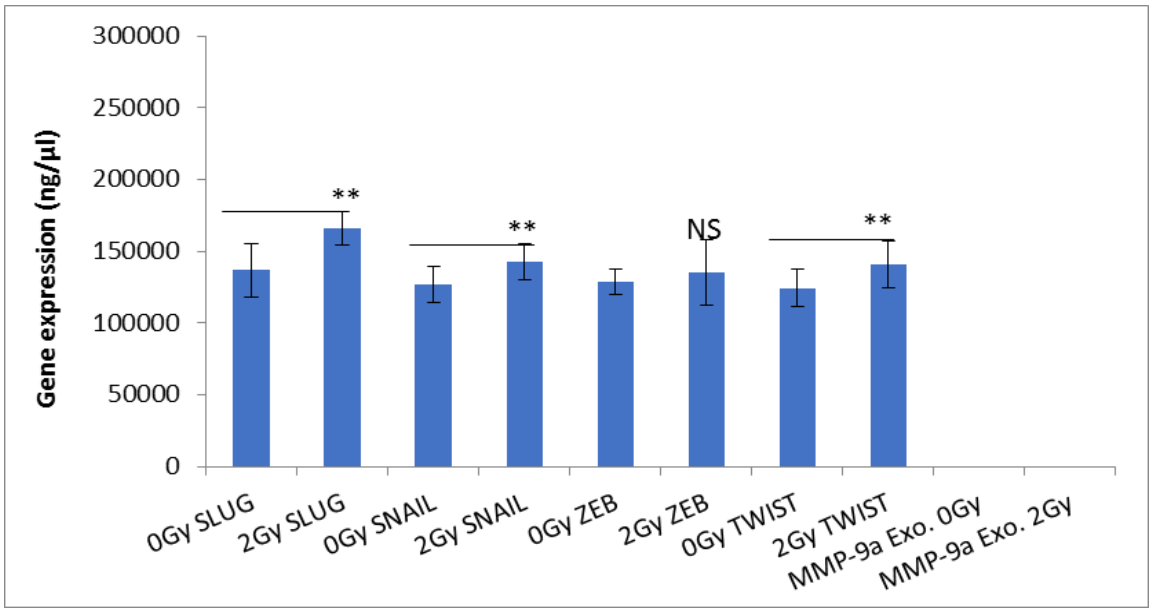


*Figure 4.8 Expression of E-box gene and TWIST in exosome recipient cells.*

2 Gy exosome-recipient cells showed a significant increase in *SLUG*, *SNAIL and TWIST* genes expression compared to 0 Gy control. An insignificant increase in *ZEB* gene expression was observed in 2 Gy exosome-recipient cells compared with 0 Gy exosome-recipient cells. The error bars represent SEM of the candidate gene expression, 3 replicate experiments were carried out. (*p≤0.05, ** p≤0.001, *** p≤0.0001).

### 4.2.9 TGF-β in exosome recipient cells

In order to investigate the TGF-β expression in the exosome-treated cells, qPCR and western blot techniques were utilised as described in Sections 2.13 and 2.14. Cells showed a significant (P≤0.001) increase in TGF-β expression in 2 Gy exosome-treated cells, compared to those treated with exosomes derived from unirradiated cells, as shown in Figure 4.9 A. The western blot data confirm the results of qPCR, where a higher TGF-β (46 kDa) protein concentration (P≤0.05) was observed in cells treated with exosomes extracted from 2 Gy -irradiated cells compared to the 0 Gy control as shown in Figure 4.9 B.

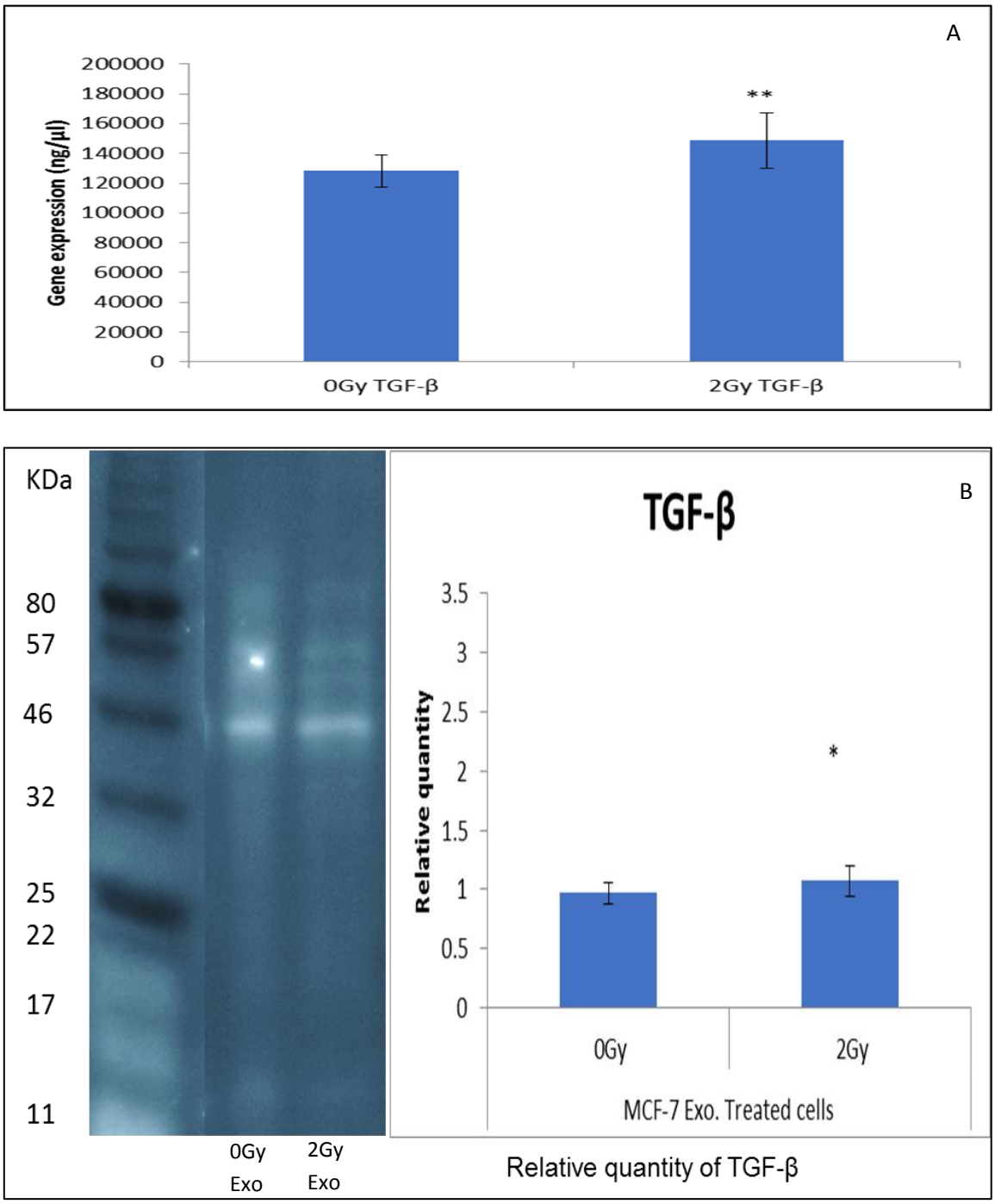


*Figure 4.9 qPCR and western blot of TGF-β in MCF-7 cells 24 hours post exosomes transfer.*

Panel A qPCR data showed a significant increase in the TGF-β expression 46 kDa in 2 Gy exosome recipient cells compared to the control (panel A). Western blot data also showed a significant increase in the level of TGF-β proteins 46 kDs in exosome treated cells compared the control 0Gy (panel B). The graph represents densitometry data drawn from blot images. Data presented as a mean of the relative quantity of protein in the cells ± SEM of 3 independent experiments. (*p≤0.05, ** p≤0.001, *** p≤0.0001).

### 4.2.10 Exosomal miRNA

Candidate miRNAs of 0 Gy and 2 Gy exosomes were analysed using qPCR as described in Section 2.13. Data showed non- significant differences in Let-7a expression between CCCM and ICCM exosomes. However, a significant (P≤0.0001) reduction in miR-200b was observed in exosomes derived from ICCM compared to CCCM exosome. Conversely, high levels of miR-9a (P≤0.0001) and miR-30a (P≤0.05) was detected in the ICCM exosomes compared to those extracted from CCCM (Figure 4.10).

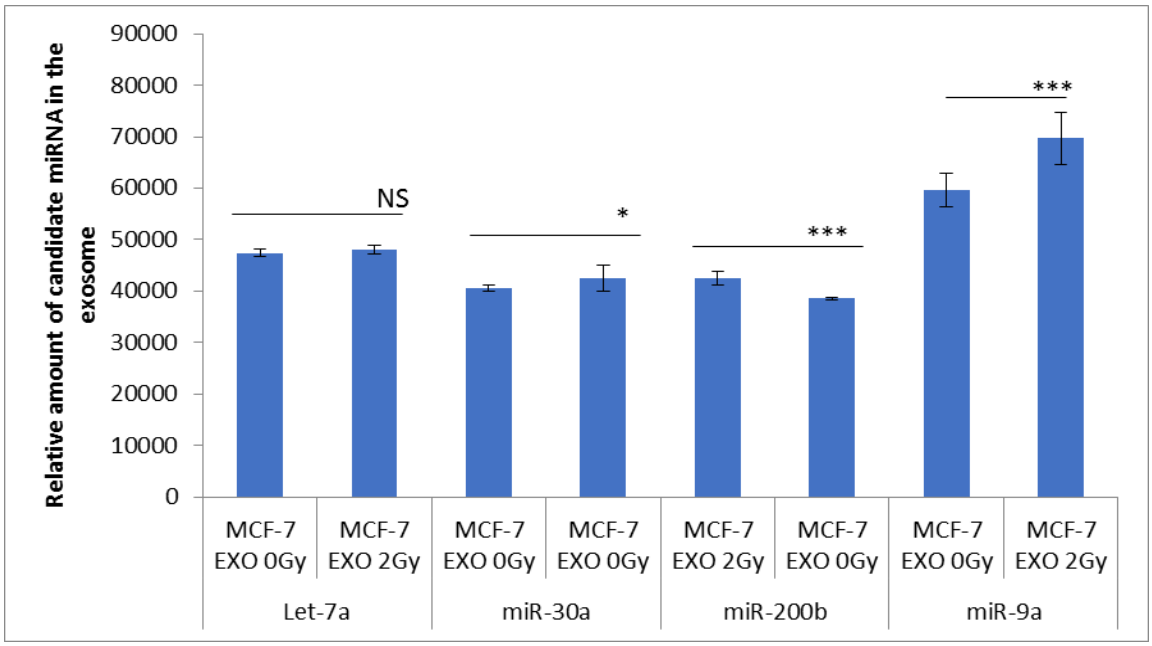


*Figure 4.10 miRNA profile of CCCM and ICCM MCF-7 exosomes.*

Not significant changes in the expression of Let-7a was observed in the CCCM and ICCM exosomes. However, ICCM exosomes showed a significant (p≤0.0001) decrease in the expression of miR-200b and increased in miR-9a compared to CCCM exosomes. Data also showed a significant (p≤0.05) increase in the miR-30a expression in the ICCM MCF-7 exosomes compare to CCCM MCF-7 exosomes. The data presented as a mean ± SEM of 3 independent experiments. (*p≤0.05, ** p≤0.001, *** p≤0.0001).

### 4.2.11 TGF-β in MCF-7 exosomes

To investigate whether TGF-β can be carried and transferred by exosomes, TGF-β was detected/measured in the exosomes derived from CCCM and ICCM using Western blot as described in Section 2.14. The results demonstrated that exosomes extracted from both CCCM and ICCM carry TGF-β. Interestingly, exosomes derived from ICCM demonstrated a higher level of TGF-β protein (p≤0.05) than CCCM exosomes. Interestingly exosomes seem to carry high

amount of active TGF-β, 12 kDa than latent TGF-β 46kDa as shown in Figure 4.11.

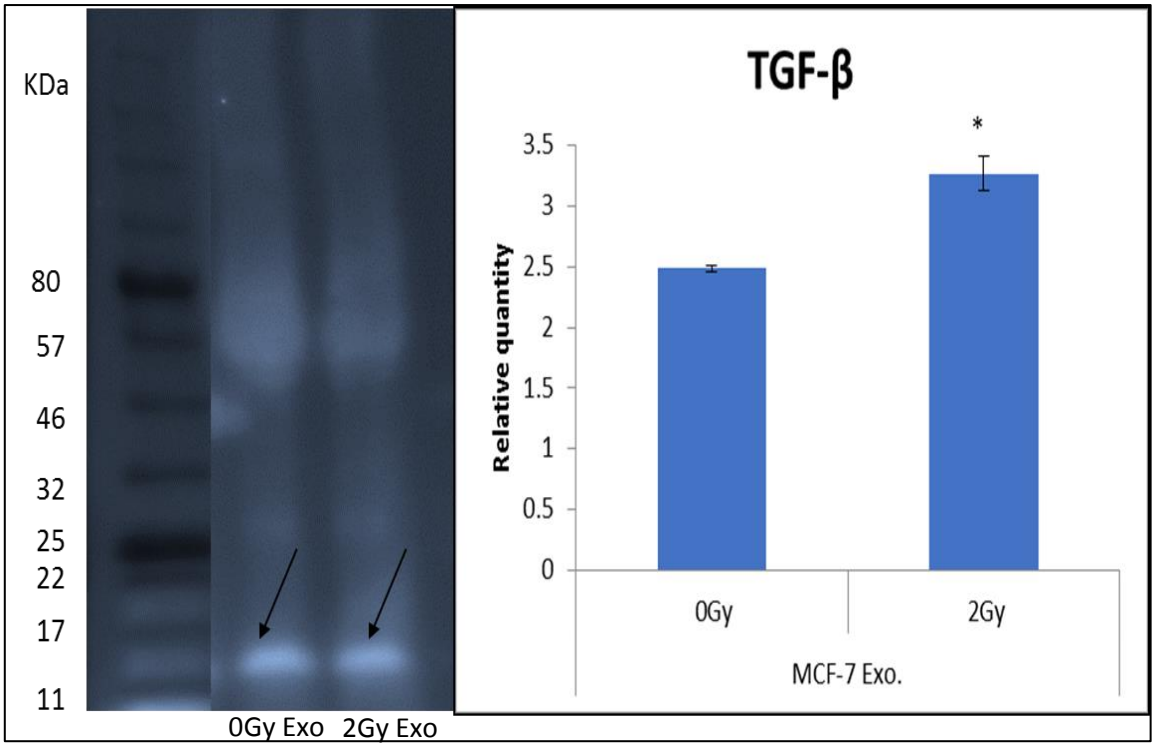


*Figure 4.11 TGF-β of CCCM and ICCM exosomes.*

ICCM exosomes showed a significant increase in the level of active TGF-β 12 kDa (black arrows bands) compared to CCCM exosomes. The graph represents densitometry data drawn from blot images. The data presented as mean ± SEM of 3 independent experiments. (*p≤0.05, ** p≤0.001, *** p≤0.0001).

### 4.2.12 Inhibition of exosomal RNA

Exosome RNAs from CCCM and ICCM were inhibited/digested with RNase-A prior to adding to naïve bystander cells as described in Section 2.12.6. Interestingly, a significant reduction in the number of invasive cells (p≤0.0001) was observed in both CCCM and ICCM RNase-exosome treated cells compared to cells that received untreated exosomes from CCCM and ICCM, and that was associated with a decrease in the percentage of HPA and vimentin immunopositive cells and an increase in the percentage of E-cadherin immunopositive cells, as presented in Figure 4.12. Cells treated with CCCM and ICCM exosomes showed a significant (p≤0.0001) increase in the number of invasive cells, and this was also associated with an increase in HPA positivity. Cells also demonstrated a high level of vimentin positivity and a decrease in the percentage of E-cadherin positive cells compared to untreated cells. The 'cells'

and ‘cells treated with heated RNase’ groups-A represent the negative and positive control respectively, as shown in Figure 4.12.

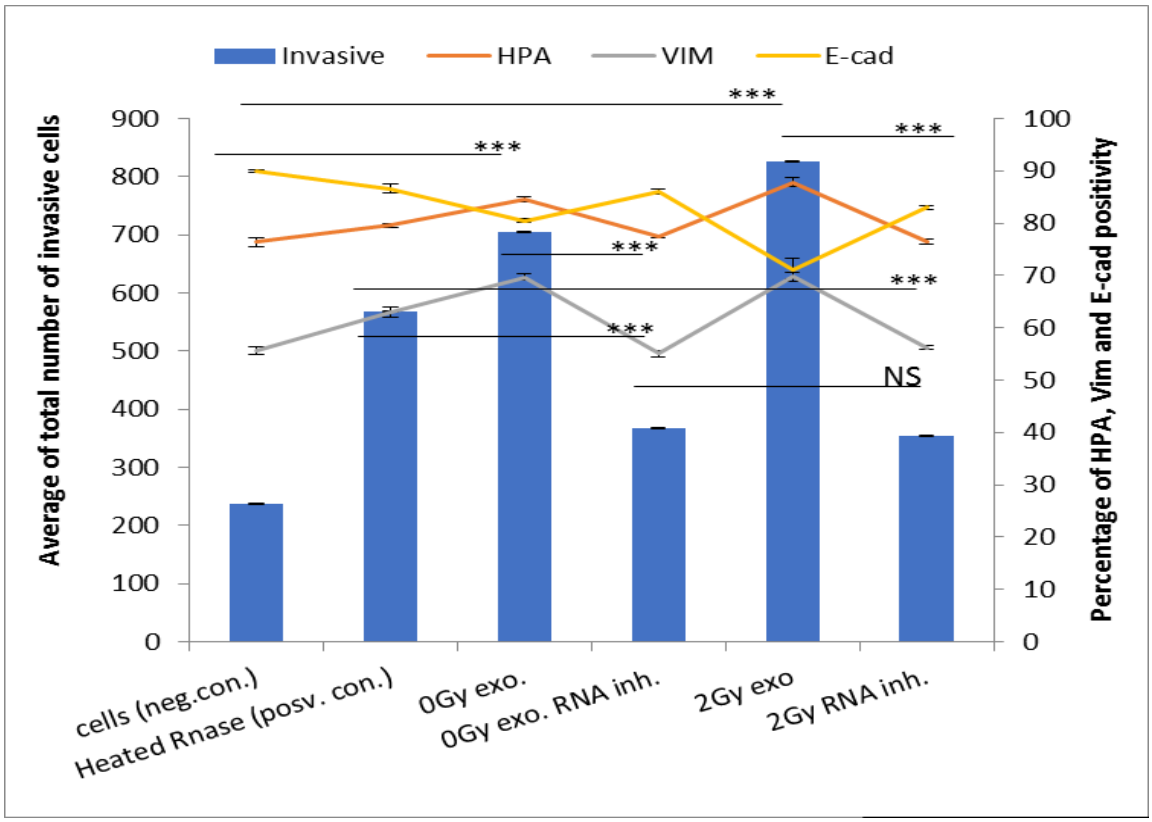


*Figure 4.12 Effect of exosome treatment and exosomal RNA inhibition on MCF-7 cells.*

The number of invasive cells significantly increased in ICCM exosome-treated cells compared to CCCM exosome-treated cells, and this was associated with an increase in the percentage of HPA and vimentin positivity and a decrease in the percentage of E-cadherin immunopositive cells. Cells also showed a significant decrease in the number of the invasive cells of the Matrigel membrane in the groups of cells that treated with 0 Gy or 2 Gy exosomes- RNA inhibited and that was associated with a reduction in the percentage of HPA and vimentin immunopositive cells, and an increase in E-cadherin immunopositive cells compared to exosome-treated cells. The negative control was fresh cells, never been exposed to irradiation or exosomes transfer), the positive control consisted of cells which were treated with heated RNase). The data presented as a mean of a total number of invasive cells, and the percentage of HPA and EMT markers positive cells. The error bars represent the SEM of 3 independent experiments. (*p≤0.05, ** p≤0.001, *** p≤0.0001).

### 4. 2.13 Inhibition of exosome proteins

Heat-treated exosomes were transferred to naïve fresh cells, which were subjected to invasiveness assays and assessed for EMT markers and HPA positivity as described in Section 2.12.6.

A significant reduction in the capacity of invasiveness was observed in the cells that received heated exosomes derived from CCCM and ICCM compared to

those that received unheated exosomes, as shown in Figure 4.13. Furthermore, there was a non-significant difference in the invasiveness of cells that were received 2 Gy ICCM heated exosome compare to the cells that were received 0 Gy CCCM heated exosomes.

Cells treated with heated exosomes also showed a significant decrease in vimentin and HPA labelling in comparison with those treated with unheated exosomes. Moreover, E-cadherin increased in the heated-exosomes treated cells compared to unheated-exosomes treated cells. Fresh untreated cells also were applied as a negative control (Figure 4.13).

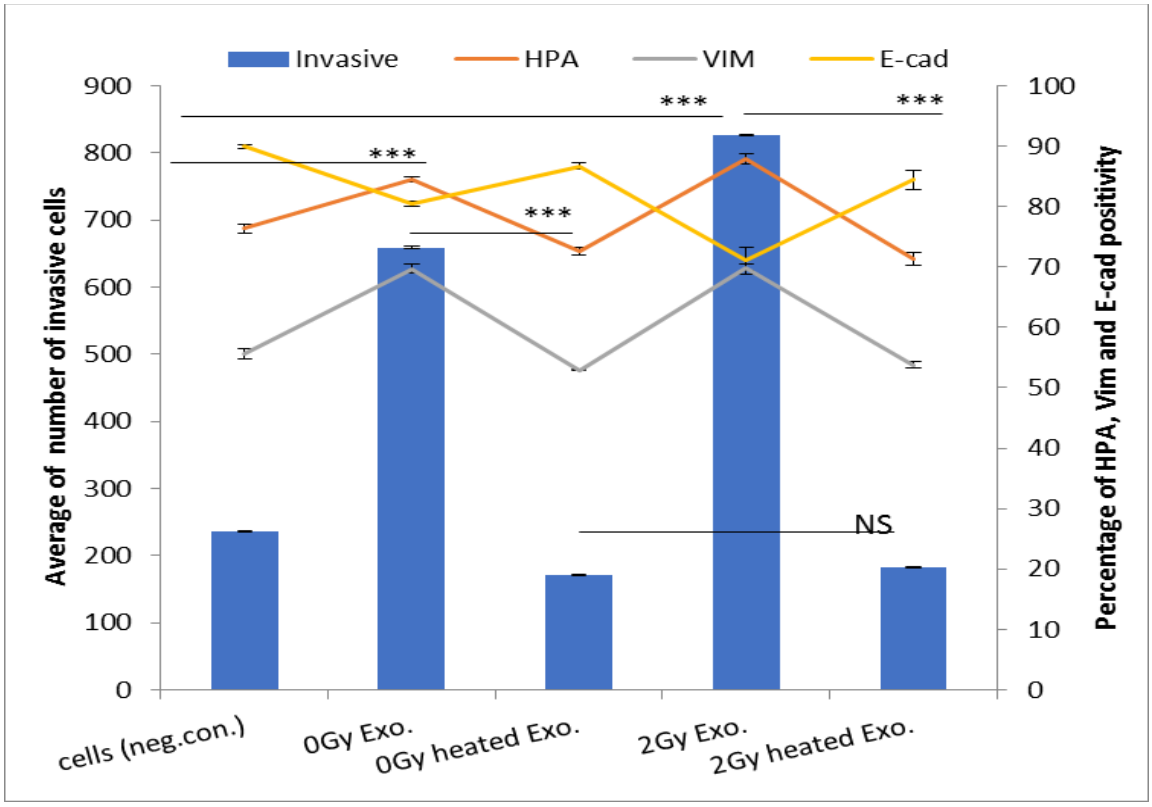


*Figure 4.13 Effect of exosome treatment and exosomal protein inhibition on the invasiveness of MCF-7 cells.*

A significant decrease in the invasiveness of MCF-7 cells at 0 Gy and 2 Gy heated-exosomes treated cells compared to 0 Gy and 2 Gy exosomes treated respectively. Cells also showed a significant increase in the number of invasive at 2 Gy exosomes treated cells compared to 0 Gy exosomes treated cells. Meanwhile, 0 Gy and 2 Gy exosome protein-treated groups did not show significant differences in the number of invasive cells compared to control (unirradiated cells) group. The negative control (fresh cells, never been exposed to radiation or exosomes transfer) was applied. The data presented as a mean of a total number of invasive cells, and the percentage of HPA and EMT markers positive cells. The error bars represent the SEM of 3 independent experiments. (*$p \leq 0.05$, ** $p \leq 0.001$, *** $p \leq 0.0001$).

### 4.2.14 Inhibition of exosomal RNAs and proteins

Both RNA and protein molecules in exosome were inhibited as described in Section 2.12.6 then transferred to naïve fresh cells. The latter were analysed for invasiveness, EMT markers and HPA positivity.

Cells that were treated with exosome-inhibited-cargo showed a highly significant ($p \leq 0.0001$) decrease in the number of invasive cells compared to the cells that were treated with 0 Gy and 2 Gy exosomes. Moreover, EMT markers returned to the background levels in the cells treated with exosome-inhibited-cargo, and that also associated with a decline in the HPA and vimentin and an increase in E-cadherin positivity to the normal level. The negative control was also applied were the fresh cells never been exposed to exosome transfer, where is the positive control group, were the cells treated with heated RNase showed an increase in the number of invasive cells and HPA and vimentin positivity compared to the negative control (cells group), as shown in Figure 4.14.

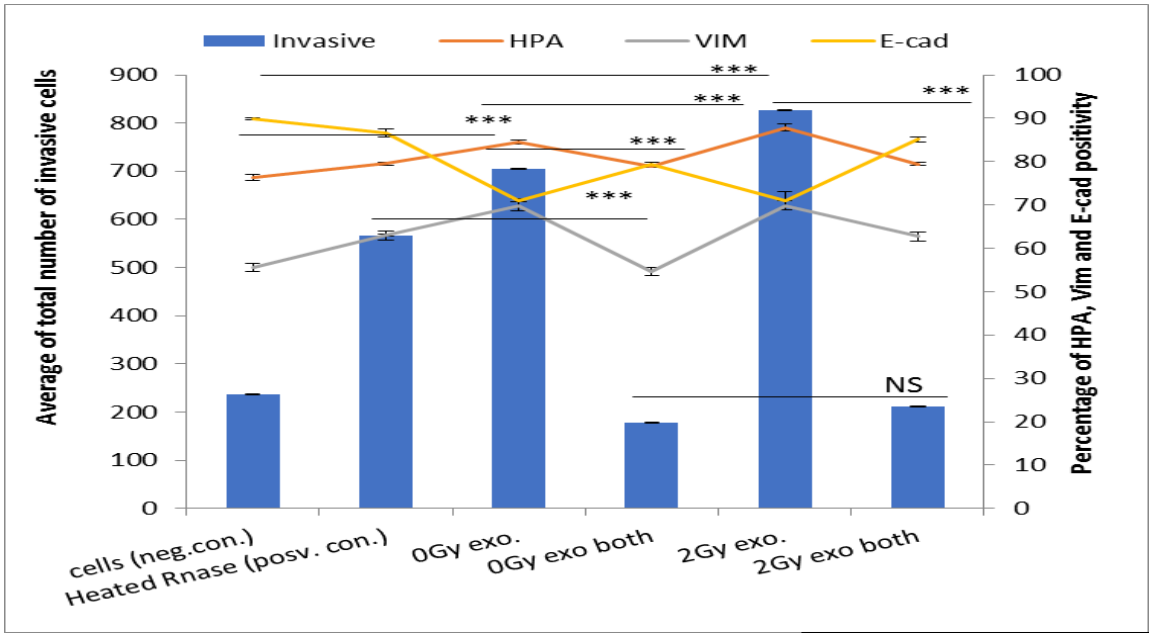


*Figure 4.14 Effect of exosome-treated cells and exosomal cargo (RNA and protein) inhibition on the invasiveness of MCF-7 cells.*

Cells showed an increase in the invasive capacity of MCF-7 cells at 0 Gy, and 2 Gy exosomes treated cells compared to treated cells. The number of invasive cells at 0 Gy and 2 Gy exosomes inhibited cargo treated cells was returned to the same level of control ± standard error. The level of HPA, vimentin and E-cadherin were returned to the same background of control untreated cells. The negative control (fresh cells, never been exposed to irradiation or exosomes transfer), a positive control (cells were treated with heated RNase) were played. The data presented as a mean of a total number of invasive cells, and the percentage of HPA and EMT markers positive cells. The error bars represent the SEM of 3 independent experiments. (*$p \leq 0.05$, ** $p \leq 0.001$, *** $p \leq 0.0001$).

## 4.3 Discussion

The study described in this chapter focuses on the role of exosomes extracted from irradiated MCF-7 cells on invasiveness capacity of unirradiated MCF-7 cells. To investigate the bystander effect of ionising irradiation on unirradiated cells, CCCM and ICCM were transferred to fresh unirradiated MCF-7 cells. Cells were analysed for change in HPA positive cells as an O-glycosylation marker, and vimentin and E-cadherin positivity as EMT markers. Cells showed a significant increase in the number of invasive cells in 2 Gy ICCM recipient cells compared to CCCM recipient cells 24 hours post-media transfer, and that was associated with an increase in the mesenchymal marker, vimentin, and a decrease in the epithelial marker, E-cadherin. Data also showed an increase in the HPA positive cells following media transfer (Figure 4.1).

It has been well established that the transfer of ICCM media has bystander effect on unirradiated cells (Lyng, Seymour and Mothersill, 2000; Mothersill *et al.*, 2001). Therefore, media transfer is a very established technique to be utilised in order to induce BE, in which signalling within ICCM can be transferred to fresh cells and induced BE in naïve unirradiated cells such as an increase in the percentage of cells in G2/M phase (Jella *et al.*, 2013). There are also studies showed that exosomes have a role in the IR induced bystander effect (Jella *et al.*, 2014; Al-Mayah *et al.*, 2015; Jelonek, Widlak and Pietrowska, 2016). To ascertain whether the signal transferred to the recipient cells is as soluble factors, or is passed through exosome formation and transfusion, irradiated and unirradiated exosomes were isolated, characterised and fresh unirradiated MCF-7 cells were treated with them.

In order to investigate the role of exosomes in the process of cancer cell invasion, exosomes characteristic and function have were explored. Data showed that IR increased exosome secretion/concentration. The number of exosomes significantly increased in 2 Gy irradiated groups compared to the 0 Gy/control group. Moreover, the size of exosomes was significantly changed (104nm in diameter) at 4 hours post-irradiation compare to (95 nm in diameter) control 0 Gy. It has been shown that cells under stress produce more exosomes than unstressed cells (Azzam, de Toledo and Little, 2003; Azzam, Jay-Gerin and Pain, 2012; Arscott *et al.*, 2013; Mutschelknaus *et al.*, 2016). However, the

mechanisms behind the increase in the number of exosomes are still poorly understood and need further investigation.

In order to investigate the invasion of breast cancer MCF-7 cells post exosome treatment, exosomes were isolated from CCCM and ICCM, 4 hours following X-irradiation and transferred to unirradiated MCF-7 cells. (Figure 4.5) Cells showed a significant increase in the number of invasive cells after treatment with 2 Gy ICCM exosomes in comparison to 0 Gy CCCM exosome treated cells 24 hours post exosome transfer. These data suggest that exosomes extracted from irradiated cells caused an increase in the invasiveness of unirradiated cells. The findings also showed that a high level of HPA positivity was associated with high levels of vimentin, and low levels of E-cadherin, in 2 Gy exosome-treated cells. Western blot data showed an increase in the level of vimentin and decrease in E-cadherin proteins in 2 Gy exosome treated cells. These results show a clear correlation between BE of IR, HPA-binding, EMT markers and the invasive capacity of MCF-7 breast cancer cells.

The reason behind the increase in the percentage of cells that invade the Matrigel membrane after irradiation is not fully understood. The data suggest that irradiated cells release more exosomes than unirradiated cells (Figure 4.2) and that exosome cargo differs between irradiated and unirradiated cells, which have been observed previously (Jelonek *et al.*, 2015; Mutschelknaus *et al.*, 2017).

The current study suggested that it possible that both differences in number and cargo of exosomes may have an impact on the characteristics and behaviour of the cancer cells, such as the EMT and ability of cancer cells to dissociate and move. Consequently, increasing the invasiveness of ICCM exosome-treated cells (unirradiated cells treated with exosome extracted from irradiated cells). As described above that an increase in the invasion of MCF-7 breast cancer cells was associated with an increase in the vimentin immunopositive cells, and that could have an impact on the EMT of cells treated with exosomes. The study supports this finding directed by Rahman *et al.* (2016). They investigated the effect of exosomes that were isolated from highly metastatic and non-metastatic lung cancer serum patient on human bronchial cells (HBECs). They found an increase in the vimentin expression in the HBECs that received exosome isolated

from highly metastatic lung cancer serum. Changes in the level of vimentin was associated with a change in the shape of HBECs from epithelial to mesenchymal. They also found that exosomes that were isolated from the serum of patients in the last stage of lung cancer promote migration and invasion of HBECs. The authors propose that exosomes promote vimentin levels which might have a crucial role in the EMT in recipient HBECs (Rahman *et al.*, 2016). Al-Mayah *et al.* (2015) and Yu *et al.* (2017) stated that both protein and RNA molecules contained within exosomes, synergistically work together to induce genomic instability and bystander effects in exosome recipient cells. Shi *et al.* (2016) reported that exosomes derived from mesenchymal stem cells (MSC) of nasopharyngeal cells could induce proliferation, migration and EMT, due to the change in morphology of the cells and increase in vimentin level and a decrease in E-cadherin expression.

To confirm the role of exosomes in the invasive capacity of MCF-7 cells or whether the ICCM contain soluble factors which can influence MCF-7 cell invasiveness, fresh MCF-7 cells were treated with exosome-depleted media from irradiated and unirradiated cells. Cells showed a non-significant increase in the number of invasive cells after treatment with 2 Gy exosome-depleted media compared to control 0 Gy exosome-depleted media, as shown in Figure 4.6. This result suggests that specific molecules in irradiated media can contribute to the invasive capacity of MCF-7 cells despite an insignificant increase in the number of invasive cells at 2 Gy depleted media. Therefore, exosomes seem to be the main reason in MCF-7 invasiveness post IR.

Flow cytometry and western blot data also confirmed the suggestion above, in which the levels of vimentin and E-cadherin proteins in cells treated with ICCM exosomes (Figures 4.3 and 4.4) were significantly higher compared to CCCM exosomes recipient cells. Consequently, this can increase the invasive capacity of cells (Yu *et al.*, 2017).

Furthermore, qPCR data showed that exosomes derived from irradiated cells increased the expression of vimentin and *GalNAc-T6* genes and decreased E-cadherin gene expression as shown in Figure 4.7. The possible mechanisms can be involved in migration and invasion of MCF-7 breast cancer cells are clarified

as shown in Figure 4.15. Exosomes isolated from irradiated cells could contain specific factors such as miRNA that result in the activation of the growth factor TGF-β-1. The active form of TGF-β-1 can activate the cell membrane growth factor receptors TGFR, which in turn activate phosphoinositide 3kinase (PI3K), leading to phosphorylation of protein kinase B (also known as, AKT1) (Rao *et al.*, 2017). Phosphorylated AKT1 turns on phosphorylation of vimentin (Zhu and Zhou, 2011; Zhu *et al.*, 2011b) Phosphorylated vimentin can resist proteolysis of the proteolytic enzymes and reduce apoptosis. An increase in the level of phosphorylated vimentin in the recipient cells promotes the activity of the *AXL* gene and increases migration and invasion of cancer cells (Vouri *et al.*, 2016). Moreover, increases in the level of phosphorylated vimentin can lead to an increase in the formation of the vimentin-scrib protein complex. The latter resists the proteolysis, which can lead to increased migration and invasion of cancer cells (Phua, Humbert and Hunziker, 2009). Alternatively, an increase in TGF-β could activate another pathway involving the zinc finger protein box, *SNAIL* and *SLUG* gene expression, which inhibits expression of E-cadherin leading to a reduction in the abundance of E-cadherin protein in the cell membrane. Consequently, this can increase cell dissociation and motility.

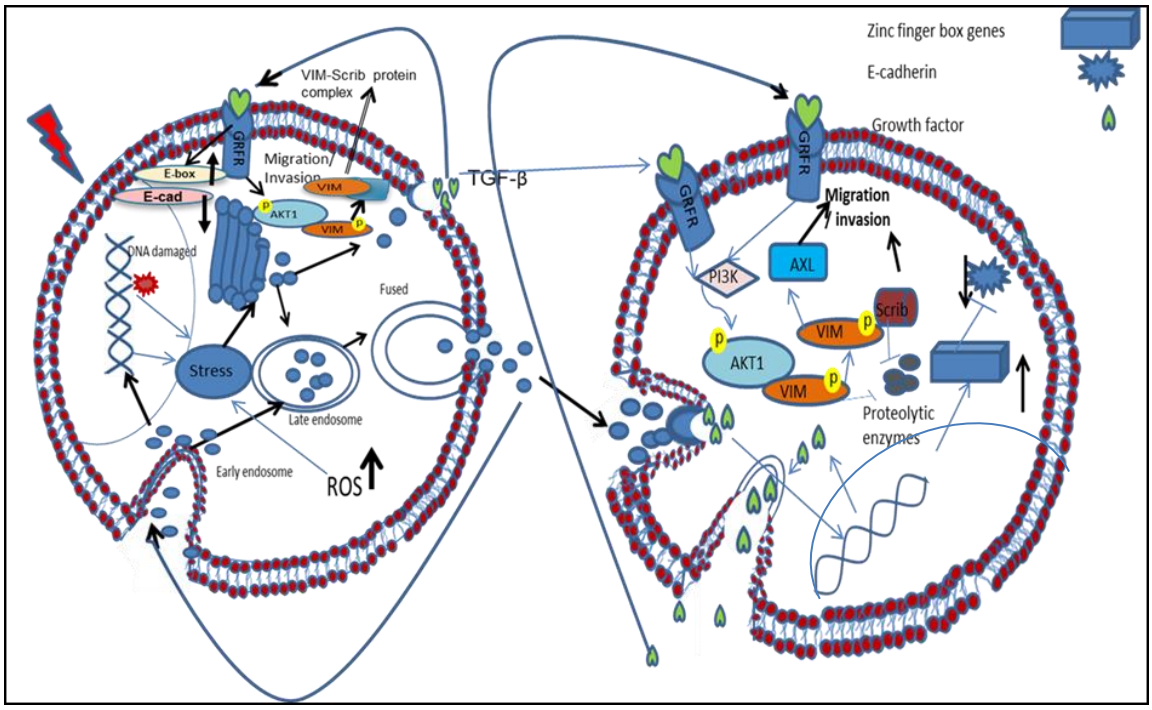


*Figure 4.15 Schematic diagram illustrates the possible mechanisms of exosomes bystander induce migration and invasion of cancer cells.*

Cells exposed to IR showed an increase in the level of ROS and DNA damage that leading to increasing the stress in the irradiated cells. Cell under stress can produce high quantities of cytokines, which can traffic to the endosomes as EVs / exosomes and release outside the cells. EVs/ exosomes cytokines such as TGF-β can interact with the receptors on the cell surface and activate pathways associated with activation of E-box genes; as a result, inhibition of E-cadherin. Conversely, activation of the TGF-β receptor can activate AKT1 genes leading to overexpression of vimentin. On the other hand, exosomes that were released from irradiated cells can internalise to the recipient cells and release its cargo (protein and RNA) in the cytoplasm of recipient cells. These cytokines can activate E-box genes and inhibit the expression of E-cadherin. Similarly, cytokines can activate AKT1-vimentin pathway leading to phosphorylation of scribe protein and activate AXIL protein and increase migration and invasion of recipient cells.

The data presented here is also supported by Arscott *et al.* (2013) who studied the potential effects of exosomes derived from irradiated cells on the invasive capacity of unirradiated glioblastoma cells. They found that exosomes derived from irradiated cells can induce a migratory effect on unirradiated cells. Radiation can also alter the cargo of exosomes. For instance, Jelonek *et al.,* found that 236 new types of protein in the exosomes that were isolated from irradiated head and neck squamous carcinoma cells (HNSCC) (Jelonek *et al.*, 2015). Moreover, exosomes that were isolated from HNSCC following exposed to IR and transfer to unirradiated cells enhance migration of HNSCC recipient cell (Mutschelknaus *et al.*, 2017). They irradiated BHY and FaDu HNSCC cells with gamma rays and then isolated the exosomes and transferred them to unirradiated cells. Using

proteomic analyses of protein, they showed a change in the exosomal protein component, 39 proteins were upregulated for example, (PDAP1, FGFR1, RPSA, PDAI4, ANP32A, SSB, HMGB3), and 36 proteins down-regulated including (PABPC1, RAB11B, HSPA8,ACTG1, RAB1P, PHGDH) in the exosomes isolated from irradiated cells compared to exosomes that were isolated from unirradiated cells (Mutschelknaus *et al.*, 2017).

It has been reported that over-expression of vimentin has an essential role in EMT in breast carcinoma (Gilles *et al.*, 2003). The researchers have used eight types of breast cancer cell lines '(BT474, BT20, T47D, MCF-7, MDA-MB-231, BT549, Hs578T, and MDA-MB-435)'. They study the relation between vimentin and localisation of the β-catenin in these cell lines. They found MCF-7, BT474, T47D and BT20 are epithelial, not invasive cells with high expression of E-cadherin and low level of vimentin. Meanwhile, MDA-MB-435, Hs578T, BT549, and MDA-MB-231 are fibroblastic shape, invasive cells, with a high level of vimentin and low level of E-cadherin. The study also showed that localisation of β-catenin in the nucleus and the cytoplasm of vimentin positive cells. Vimentin expression can also be down-regulated by inhibiting expression of AXL receptor tyrosine kinase genes (Asiedu *et al.*, 2014), plasminogen activator, urokinase *PLAU*, and integrin subunit beta 4 (ITG-β*4* ) (Kawakami *et al.*, 2015; Stewart *et al.*, 2016).

Moreover, exosomal cargo (miRNA and protein) could have a potential role in breast cancer invasiveness. Data presented here showed that inhibition of exosomal miRNA, exosomal proteins, or both, led to a decrease in the invasion of MCF-7 as presented in Figure 4.12, 4.13 and 4.14. Further investigations including TGF-β and candidate exosomal miRNA expression confirmed these results. Data found that exosomes were isolated from irradiated cells exhibited a high expression of TGF-β. Findings suggested that ICCM exosomes can transfer a larger amount of TGF-β to the recipient cells than CCCM exosomes. Data also suggest that exosomal RNA and proteins could play a critical role in the invasive of MCF-7 cells in *vitro*. Previous studies have also confirmed the role of TGF-β in cancer invasive and metastasis. David *et al.* (2016) reported that TGF-β can

inhibit the invasion of breast cancer cells by activating Sox4 and inducing apoptosis.

In contrast, TGF-β can induce angiogenesis and promote invasiveness of lung cancer (Yu *et al.*, 2015). The current study showed that an increase in the expression of TGF-β was associated with an increase in the expression of vimentin and a decrease in the expression of E-cadherin. The data in this study concomitant with previous studies, confirm the role of TGF-β in the EMT and invasive of cancer cells. TGF-β has been found elevated in the samples of gastric cancer, that is associated with lymph node metastasis (Yen *et al.*, 2017). The researchers also found there is no correlation between the level of TGF-β and the age, gender and location of cancer. Moreover, they found a strong correlation between the TGF-β expression and the stage of cancer, high level of TGF-β was associated with late-stage of gastric carcinoma. Other evidence in the role of TGF-β used rat mesangial cells. The researchers irradiated cells with gamma rays. They found an increase in the level of TGF-β-1(O'Malley *et al.*, 1999).

The novel findings in this study conclude that the IR can promote EVs/exosomes formation in irradiated cells and these vesicles can transfer oncogenic factors such as TGF-β which can regulate expression of E-box gene transcription factors. Consequently, the reduction of E-cadherin level and increase the expression of vimentin. The data also showed an increase in the HPA positivity following exosomes transfer, and that was associated with a change in the EMT markers. Therefore, the invasive capacity of MCF-7 cells was increased. However, the relationship between IR, TGF-β, glycosylation and cancer invasion need to be addressed, and that will discuss in the last chapter.

# Chapter 5

## Ionising radiation promotes invasiveness capacity of breast cancer stem cells

## 5.1 Introduction

Breast cancer cells have different origins and showed diverse in their ability to metastasise as described in Sections 1.1 and 2.2. MCF-7 cells as moderate metastasis cells, showed high responses to IR and media factors, as demonstrated in the previous chapters. In comparison, breast cancer stem cell (BCSCs) responses to IR need to be addressed; this could reveal different responses to IR and media factors. Certain types of breast cancer cells can metastasise and initiate cancer in distant. This group of cells was termed triple-negative breast cancer cells. These types of cancer cells can also exhibit cancer stem cell phenotypes such as $CD44^{+high}$/ $CD24^{-low}$ and aldehyde dehydrogenase - 1 ($ALHD1^{+}$) (Phillips, McBride and Pajonk, 2006; Jin *et al.*, 2016; Li *et al.*, 2017c). Much evidence has been shown that MDA-MB-231 breast cancer cells exhibited cancer stem cells properties (Phillips, McBride and Pajonk, 2006; Holliday and Speirs, 2011; Li *et al.*, 2017c; Yamamoto *et al.*, 2017; Konge *et al.*, 2018). For these reasons, MDA-MB-231 cells might be better candidates for looking at 'stemness'.

Cancer stem cells (CSCs) were first recognised in human blood cancer, acute myeloid leukaemia (Gibbs *et al.*, 2011). In breast cancer, CSCs have also been identified and termed BCSCs. They are identified by the presence or absence of cell surface markers, CD44 and CD24. Al-Hajj *et al.* (2003) demonstrate that human BCSC displays $CD44^{+high}$ and $CD24^{-low}$.

CSC has been described as a unique tumourigenic factor in cancer studies. It is thought to be responsible for tumour initiation (Tysnes and Bjerkvig, 2007). In the paradigms of cancer development, it was hypothesised that CSC could play an essential role in the initiation and progression of cancer. It has been reported that cancer arises from a subset of cells which have the ability of self-renewal and also to differentiate to different types of cells which contribute to the formation of a cancer mass (Dhawan *et al.*, 2014). CSC seems to undergo asymmetrical division, results of this division one cells as a daughter who has the same

characteristic of original cells and can divide and initiate other cancer cells. The second cells have a high potential capacity for proliferation and differentiation. As a result, the tumour has a heterogeneous proportion of cells including CSC, CSC progenitor-like cells, and mature cancer cells (Wicha, Liu and Dontu, 2006; Kaur, Singh and Kaur, 2014). Evidence showed that knockdown of CD44 causes differentiation of breast CSCs to adult cancer cells. Pham *et al.* (2011) isolated the $CD44^{+}/CD24^{-}$ cells from primary tumours of 10 patients and maintained cells in primary tissue culture; they knocked down the CD44 using hairpin RNA lentivirus. The results showed a decrease in the tumourigenicity of cells in the immune inhibited mice and also altered in cell cycle and the expression profile of some genes linked with stemness.

Furthermore, the metastasis of CSC can be regulated by transcription factors such as TGF-β, SNAIL, SLUG, and TWIST. TGF-β is known to be an important regulatory factor during embryonic and cancer development, involving of growth, differentiation and migration of cells (Jia *et al.*, 2014; Li, Wei and Ding, 2016; An *et al.*, 2018).

Interestingly, BCSCs that were generated using TGF-β exhibit EMT morphology and radio-resistance characterisation (Konge *et al.*, 2018). They have treated human mammary epithelial cells (HMLE) with TGF-β-1 for 5-10 days with the replacement of media every 48 hours, after a period of incubation; they found a significant increase in the percentage of $CD44^{+}$, $CD24^{-}$ cells in the population of treated cells compared to the control non treated cells. Using phase-contrast microscope, they also found that TGF-β-1 treated cells exhibited morphological changes from cuboidal epithelial cells to fibroblast-like cells and mesenchymal cells. These results suggest that TGF-β involved in the regulation of EMT in HMLE treated cells. They also measured the viability of cells following exposure to IR; they found that cells that were treated with TGF-β-1 exhibited a high percentage of live cells compared to untreated cells. However, the mechanisms involved in TGF-β and glycosylation in the invasiveness of BCSCs following IR remains incompletely understood.

Furthermore, extensive evidence suggests that cancer stem cells are more resistant to radiotherapy than other primary cancer cells (Phillips, McBride and

Pajonk, 2006; Wang *et al.*, 2014a) via regulation the intrinsic factors, such as cyclin-dependent kinases (CDKs) and DNA repair and survival pathways (Ronchini and Capobianco, 2001). These factors can transfer to unirradiated cells via EVs and induce the non-targeted effect of IR. Moreover, proteomic analyses of EVs/exosomes cargo showed that protein in exosomes that were isolated from MDA-MB-231 showed different hierarchy than MCF-7 exosomes (Kruger *et al.*, 2014).

IR is routinely used for treating cancer. With the improvement and development of the technique, radiotherapy has become an effective tool to treat more than 50% of cancer cases (Delaney *et al.*, 2005). However, there remains high mortality from cancer due to recurrence and metastasis of cancer cells following irradiation (Li *et al.*, 2016b). Studies have demonstrated that CSCs are claimed to be responsible for radiotherapy resistance and recurrence in various type of cancer (Li *et al.*, 2016b). For example, Phillips, McBride and Pajonk (2006) stated that MDA-MB-231 breast cancer cells display cancer stem cell characteristics, such as being $CD44^+$ and $CD24^-$ and showed resistance to IR. de Jong *et al.* (2010) reported that $CD44^+$ larynx cancer showed greater resistance to radiotherapy in comparison to $CD44^-$ cases, as described in detail in Section 1.4. Moreover, Du *et al.* (2011) stated that pancreatic cancer cells that exhibit cancer stem cell markers CD133 and are undergoing EMT are more resistant to the chemo-radiotherapy.

The relationship between radiation and EMT has attracted growing attention during the last decade. As described in section 1.6.1, a considerable number of studies have demonstrated that IR can induce phenotypic characteristic similar to EMT in irradiated cells (Zhou *et al.*, 2011; Vares *et al.*, 2013; Young and Bennewith, 2017). For example, KYSE-150R radio-resistant oesophageal cancer cells showed morphological changes similar to EMT, and this was associated with an increase in the mesenchymal markers, snail and twist and a decrease in the epithelial marker E-cadherin (Su *et al.*, 2015).

Moreover, various studies have reported the involvement of IR in inducing EMT and induce cancer stem cells properties. Wang *et al.* (2013b) state that the ratio of CSC in PC-3, LNCaP, and DU145, prostate cancer cell culture was increased

following exposure to IR. Lagadec *et al.* (2012) revealed that IR could induce cancer stem cell properties in non-cancer stem cell-like breast cancer cells, the authors exposed (SUM159PT) breast cancer cell, isolated from breast cancer specimens, T47D and MCF-7 breast cancer cells to various doses of irradiation for five days. They found an increase in the percentage of $CD44^{+}$/ $CD24^{-}$ and ALDH1 positive. The authors suggest that the population of CSC was significantly increased following irradiation in a dose-dependent manner.

Glycosylation of CD44 and CD24 could play a crucial role in the invasion of CSCs as described in Section 1.4.1. Briefly, CD44 has been identified as a universal marker for CSCs in many types of cancer as alone or with other markers such as CD24 (Yan, Zuo and Wei, 2015). Altered glycosylation of CD44 has been shown to be associated with metastases of human cancer (Hakomori, 1996). Thus, it has been proposed that BCSCs may express different signalling than MCF-7, that could contribute to IR induce invasion of cancer cells.

The role of IR and exosomes derived from irradiated cells on the invasive capacity of BCSCs linked with changes in glycosylation and EMT markers have previously not been explored. Therefore, this study was set up to investigate the targeted and non-targeted effect of IR (the classic bystander effect, exosome bystander and exosomes cargo inhibition) on MDA-MB-231 BCSs. To achieve these objectives, the following was carried out:

1- Investigate CSC markers in the MDA-MB-231 cells.

2. Determine the role of the positivity and negativity of HPA in the invasive MDA-MB-231 cells

3- Measure the cell viability and ROS formation.

4- Determine the invasive capacity of MDA-MB-231 BCSs directly following IR

5- Determine the candidate genes that are associated with the invasive capacity of MDA-MB-231 BCSs.

6-Determine protein expression following IR and which is associated with the invasive ability of MDA-MB-231 BCSs.

7- Characterisation of the exosomes derived from irradiated and unirradiated cells regarding their size and concentration.

8- Determination of the change in immunopositivity of EMT markers (vimentin and E–cadherin) in MDA-MB-231 BCSs following media transfer.

9- Determination of the change in immunopositivity of the glycosylation marker HPA in MDA-MB-231 BCSs following exosomes transfer.

10- Determination of the change in the invasive capacity of MDA-MB-231 BCSs following treatment with exosome-depleted media.

11- Investigation of the effect of exosome cargo inhibition on MDA-MB-231 BCSs invasive capacity, EMT (vimentin and E- cadherin) and glycosylation HPA markers.

12- Determination of the expression of candidate genes such as the GalNAc-T6, as well as detection of changes in vimentin and E- cadherin and other candidate genes expression that listed in Table 2.1.

13- Determination of the expression of TGF-β protein in the exosomes and in the cells treated with exosomes, which may have an impact on cancer cell invasion.

14- Determination of the change in the abundance of exosomal miRNA, which may be associated with the invasive capacity of MDA-MB-231 BCSs.

## 5.2 Results

### 5.2.1 Cancer stem cell labelling

MDA-MB-231 cells were labelled for the presence of CD44 and CD24. Flow cytometry was used to detect the CD44 and CD24 negative and positive cells, as described in section 2.9. Data demonstrated that 91.61% of MDA-MB-231 cells showed positive labelling to the CD44 antibody. Meanwhile, 1.26% of the cells were CD24 positivity, and the rest of the cells showed negative responses to the CD24 antibody, as shown in Figure 5.1.

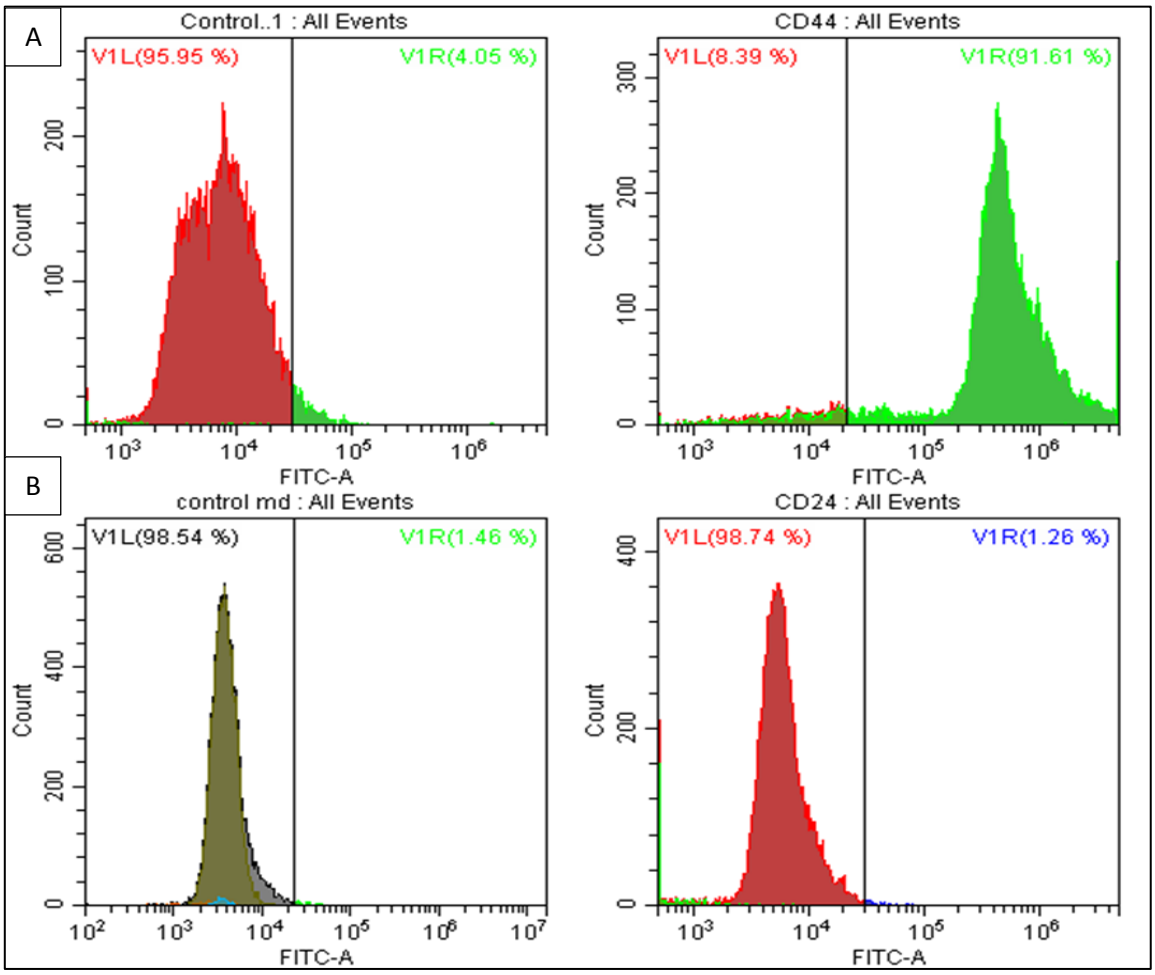


*Figure 5.1 Cancer stem cell labelling.*

MDA-MD-231 breast cancer cells were labelled with anti CD44 and anti CD24 antibodies; cells showed CD44 positive and CD24 negative responses. The red colour represents the negative cells to CD44. While green colour represents positive cells to CD44, panel (A). The greenish colour in the left hand represents the negative cells to the CD24. Cells also did not exhibit positive responses to CD24; Therefore, the histogram did not move to the right hand of the gate, panel (B) The experiment was carried out in triplicate. The plot is representative of the distribution of data from 3 experiments.

### 5.2.2 The role of HPA positivity/negativity in the invasive of MDA-MB-231 cells

MDA-MB-231 cells for both the upper and lower surfaces of the insert membrane appeared singular and discrete and hence easier to analyse for positive and negative cells as shown in Figure 5.2 panel A. Therefore, MDA-MB- 231 were considered the best candidate to describe the role of HPA positivity in the invasiveness of the breast cancer cells compared to MCF-7 cells.

Cells showed a high level of HPA positivity (90%) in the upper surface of the insert compared to the negative HPA cells after 4 hours. Cells continued to

maintain the level of HPA positivity (90%) after 8, 16 and 24 hours; in other words, cells did not show any change in the HPA negativity/positivity in the upper surface cells. In contrast, after 4 hours, HPA negative cells (80%) were observed higher in the lower surface of the insert (Cells passed through the membrane) compared to the HPA positive cells (20%). However, over time, the percentage of HPA negative cells decreased in preference to a gradual rise in positive labelled cells, which increased from 20% to approximately 40% after 8 hours incubation and this level was further increased at subsequent time-points reaching ~ 55% HPA positivity after 16 and 24 hours as shown in Figure 5.2.

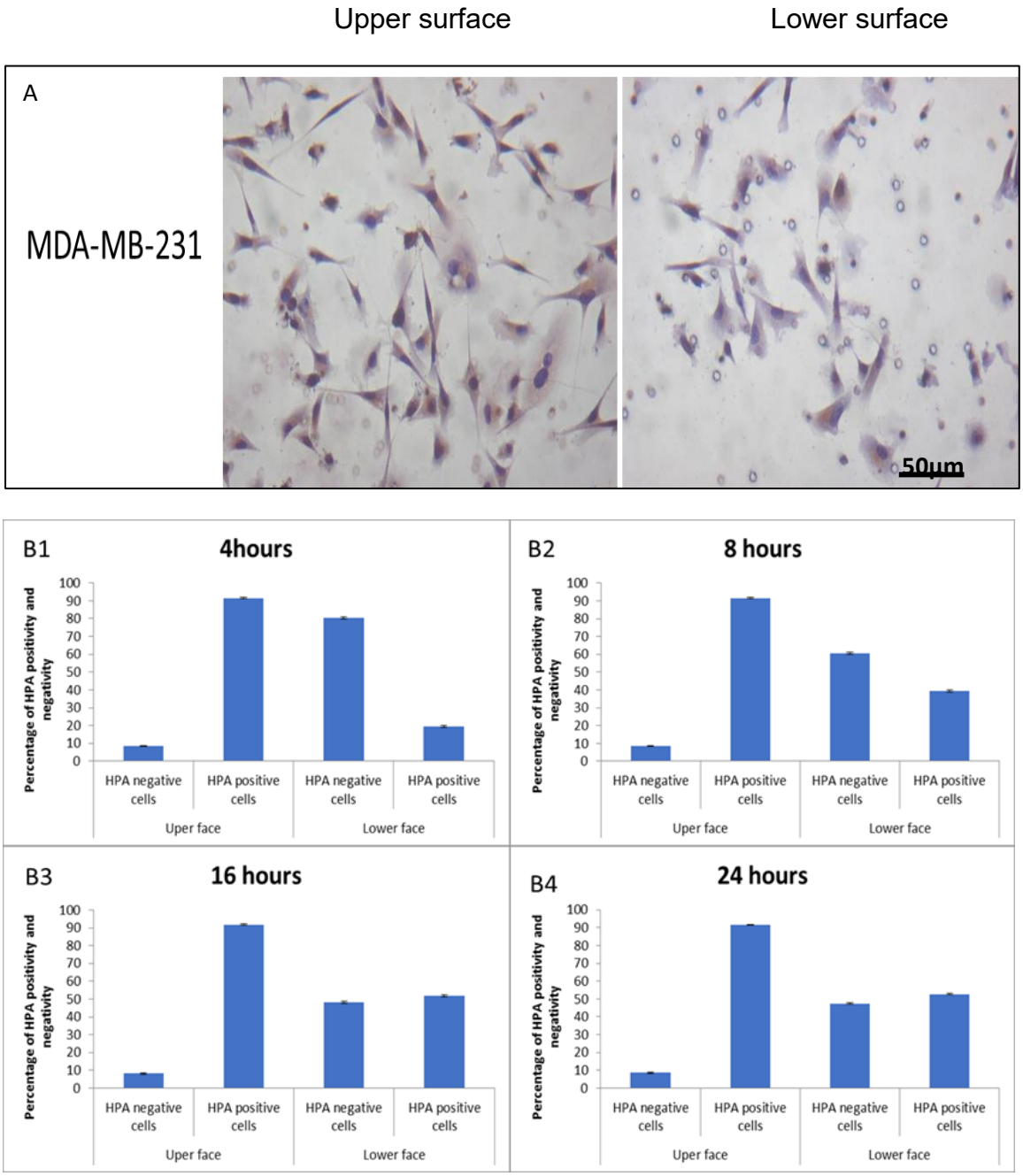


*Figure 5.2 Percentage of HPA positivity and negativity in MDA-MB-132 cancer cells in the upper and lower surfaces of inserts in the transwell co-culture system.*

MDA-MB-231 is shown to be discrete in both upper and lower side of the inserts membrane. A clear characteristic future of the negative and the positive cells were observed, panel A. A high percentage of MDA-MB-231 cells that had passed through the insert membrane were HPA negative after 4 hours (Panel B1), while the percentage of HPA negative cells were shown to have decreased over time (B2, B3, and B4). The data presented as a percentage ± the SEM of three independent experiments. (*$p \leq 0.05$, ** $p \leq 0.001$, *** $p \leq 0.0001$).

### 5.2.3 Cell viability

Cell viability was measured as described in Section 2.5.1. Irradiated MDA-MB-231 cells showed a significant ($p \leq 0.0001$) decrease (72.3%) in the percentage of viable cells after 2 Gy X-irradiation compared to 0 Gy irradiated cells (83.6%). 2 Gy irradiated cells also showed a significant ($p \leq 0.0001$) increase in the percentage of dead cells (27.7%) compared to 0 Gy cells (16.4%) as shown in Figure 5.3.

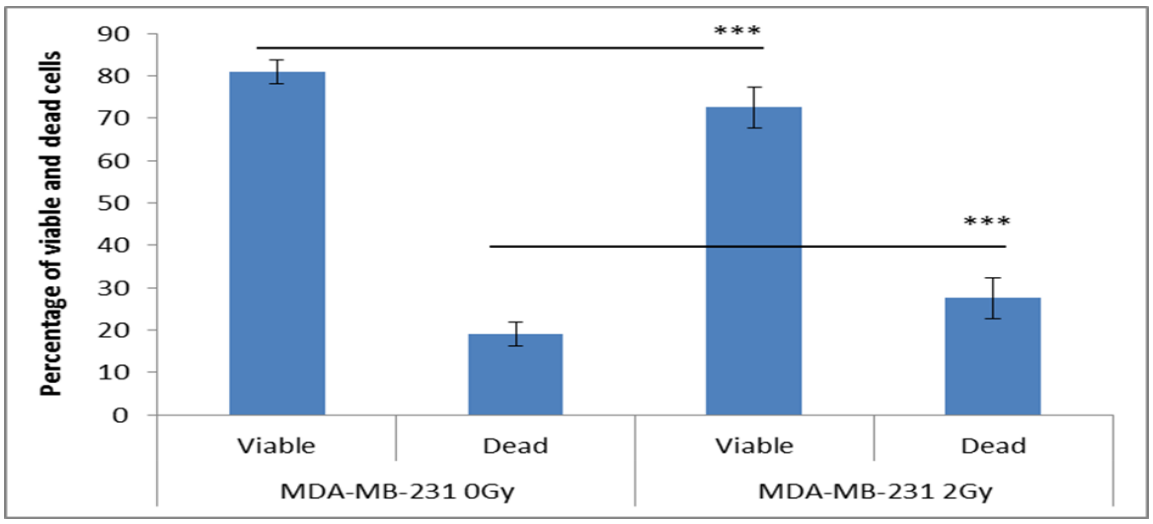


*Figure 5.3 Viability of MDA-MB-231 cells post IR.*

Cells showed a significant decrease in the viability of irradiated cells compared to unirradiated cells (±5.8) standard deviation. The data presented as a percentage ± the SEM of three independent experiments. (*$p \leq 0.05$, ** $p \leq 0.001$, *** $p \leq 0.0001$).

### 5.2.4. Reactive oxygen species

ROS was measured in the cells after 30 minutes following irradiation using Muse cell analyser as described in Section 2.5.2. MDA-MB-234 showed a non-significant change in the percentage of $ROS^+$ cells (11%) following 2 Gy x-irradiation compare to 0 Gy unirradiated cells (13%) as shown in Figure 5.4. A non-significant change in the total number of $ROS^+$ cells was also observed between 2 Gy irradiated and 0 Gy unirradiated cells Figure 5.4. B.

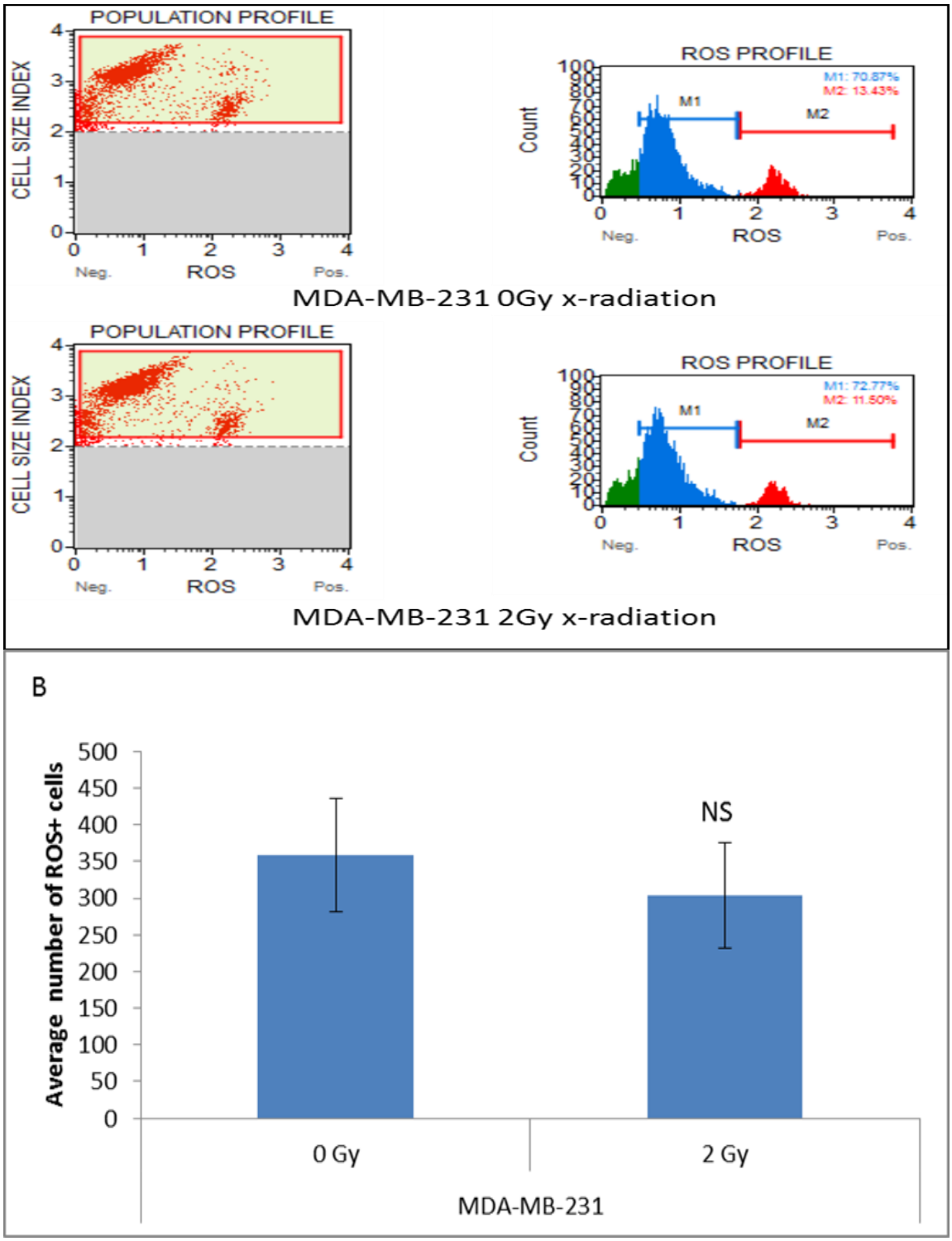


*Figure 5.4 ROS$^+$ in MDA-MB-231 cells post IR.*

Cells showed a non-significant decrease in the number of ROS$^+$ cells at 2 Gy irradiated cell compare to 0 Gy cells. The data presented as a percentage ± the SEM of three independent experiments. (*p≤0.05, ** p≤0.001, *** p≤0.0001).

### 5.2.5 Invasiveness capacity of MDA-MB-231 cells following IR

HPA, EMT markers and invasion of MDA-MB-231 cells were analysed as described in Sections 2.6, 2.7 and 2.10. The irradiated cells showed a significant ($p \leq 0.0001$) increase in the number of invasive cells (1712 cells) out of 75000 cells at 2 Gy IR compared to 0 Gy irradiation (1232 cells) out of 75000 cells. Cells also demonstrated a significant ($p \leq 0.0001$) induction in the level of vimentin immunopositivity (76%) compared to 0 Gy cells (67%). Moreover, a significant decrease in E-cadherin immunopositive percentage (77%) was observed in comparison with 0 Gy cells (82%)., MDA-MB-231 cells also showed a significant ($p \leq 0.0001$) increase in the HPA positive cells (72%) post 2 Gy irradiation compared to 0 Gy control (62%), as presented in Figure 5.5.

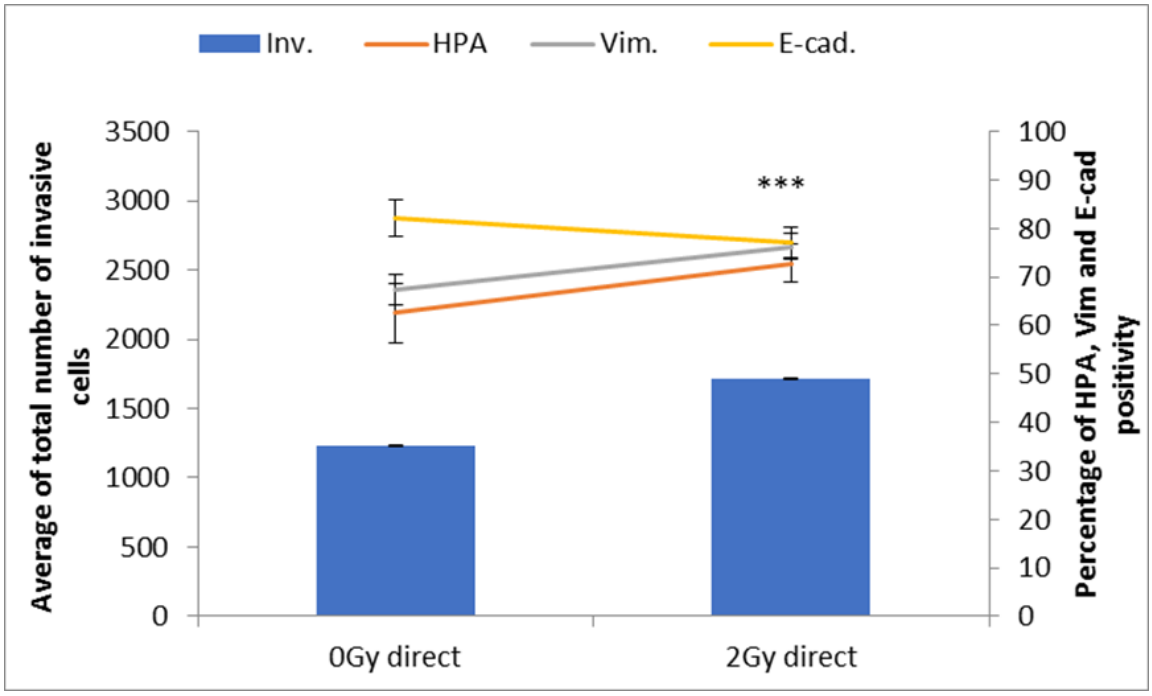


*Figure 5.5 Analysis of invasive capacity, EMT markers and HPA labelling in irradiated MDA-MB-231 cells*

After 2 Gy irradiation, there was a significant increase in the percentage of invasive cells. There was also a significant increase in the vimentin immunopositive cells and a decrease in E-cadherin positivity, and this was associated with an increase ($p \leq 0.0001$) in the percentage of HPA positive cells compared to 0 Gy control. The data presented as a mean of a total number of invasive cells, and the percentage of HPA and EMT markers positive cells. The error bars represent the SEM of invasive cells and the percentage of HPA and EMT markers. The experiment was carried out in triplicate; (*$p \leq 0.05$, ** $p \leq 0.001$, *** $p \leq 0.0001$).

### 5.2.6 The ratio of vimentin/ E-cadherin following direct IR

The ratio of vimentin to E-cadherin in the MDA-MB-231 cells was 45% before irradiation. This ratio was increased to 50% following 2 Gy X-irradiation as shown in Figure 5.6.

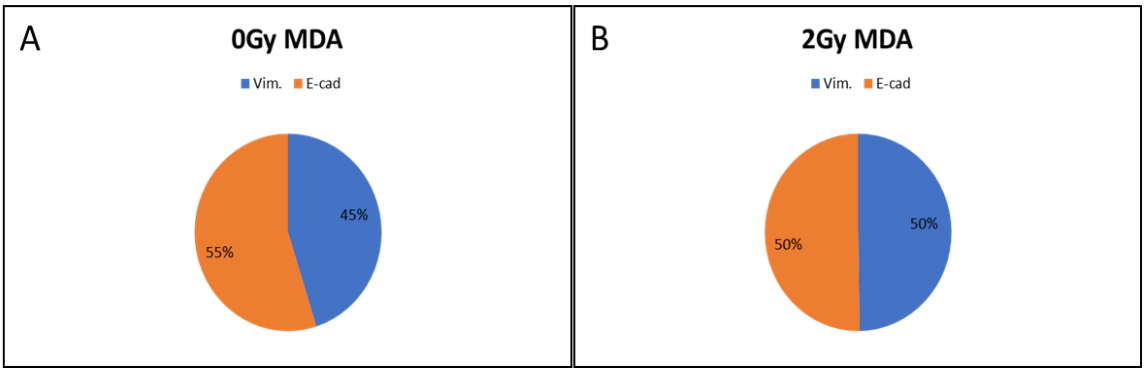


*Figure 5.6 The ratio of vimentin to E-cadherin in MDA-MB-231 breast cancer cells following 2 Gy X-irradiation.*

The ratio of vimentin to E-cadherin increased to 50% following 2 Gy in MDA-MB-231 breast cancer cells compared to 45% in control irradiated cells. The data presented as a percentage of 3 independent experiments.

### 5.2.7. EMT markers following IR using Flow cytometry

To confirm previous data of EMT markers (vimentin and E-cadherin) that were presented in Section 5.2.5, MDA-MB-231 were exposed to IR. After 24 hours post-irradiation, vimentin and E-cadherin immunopositivity were analysed in the cells using flow cytometry as described in section 2.8. Cells showed a significant ($p \leq 0.0001$) increase in the percentage of vimentin positive cells (88.6%) post 2 Gy irradiation compared to 0 Gy cells (82%). Irradiated cells also presented a significant ($p \leq 0.0001$) decrease in the percentage of E-cadherin immunopositivity (73.89%) compared to 0 Gy cells (control) (79.63%) as shown in Figure 5.7

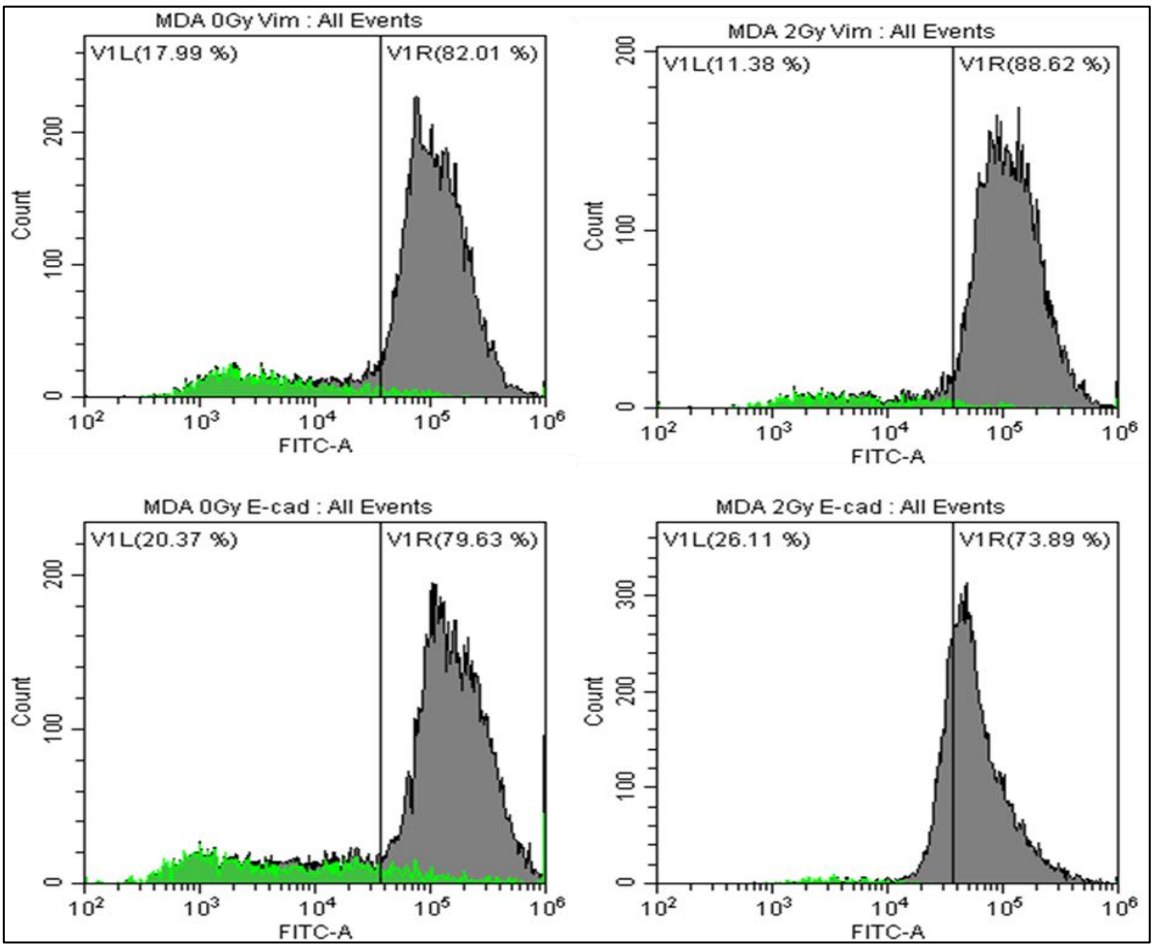


*Figure 5.7 Flow cytometry analyses for specific binding of EMT markers vimentin and E-cadherin post-IR.*

MDA-MB-231 cells showed a significant (p≤ 0.0001) increase in the percentage of vimentin immunopositivity and significant (p≤ 0.0001) decrease in E-cadherin immunopositivity post 2 Gy IR compared to 0 Gy cells. Grey colour represents the main population of cells under the test. While a green colour represents the cells outside the polygonal shape. The plot is representative of the distribution of data from 3 experiments

### 5.2.8. Vimentin, E-cadherin and GalNAc-T6 gene expression post-IR

In order to confirm the relevant genes associated with vimentin, E-cadherin and GalNAc-T6, qPCR was used to detect the candidate genes that were described in Table 2.1 and Section 2.13. MDA-MB-231 cells showed a significant (p≤ 0.0001) increase in the expression of vimentin following 2 Gy X-ray compared to the 0 Gy unirradiated cells. Cells also demonstrate a higher level of GalNAc-T6 expression (p≤ 0.0001) in the 2 Gy irradiated cells compared to the 0 Gy cells. Nevertheless, cells showed a significant (p≤ 0.0001) decrease in the level of E-cadherin expression in the 2 Gy irradiated cells compared to the control as shown in Figure 5.8.

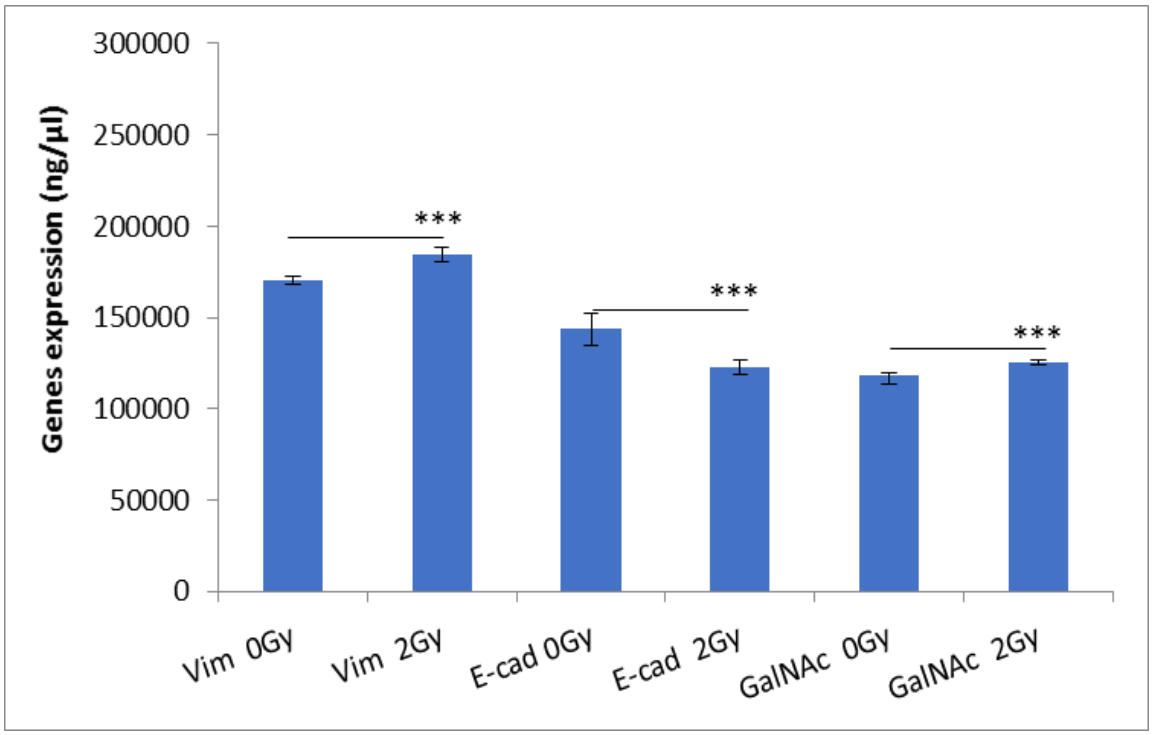


*Figure 5.8 Candidate genes expression following IR in MDA-MB-231 cells.*

Cells showed a significant increase in vimentin and GalNAc-T6 expression 4-hour post-irradiation. Also, cells showed a decrease in E-cadherin expression. The error bars represent the standard error of the candidate gene expression. The data presented as a mean ± the SEM of three independent experiments. (*p≤0.05, ** p≤0.001, *** p≤0.0001).

### 5.2.9 E-box genes, *TWIST* and *MMP* gene expression

In order to target the molecular mechanisms that may be involved in EMT following X-irradiation. After 24 hours following irradiation, E-box genes (*SLUG*, *SNAIL*, *ZEB*), *TWIST* and *MMP* gene expressions were measured using qPCR as described in Section 2.13. Cells showed a significant (p≤ 0.001) increase in *SLUG* and *ZEB* gene expression following 2 Gy X-irradiation compared to sham irradiated 0 Gy cells. Cells also showed a significant (p≤ 0.05) increase in *SNAIL* gene expression following irradiation compared with 0 Gy irradiated cells. A highly significant (p≤ 0.0001) increase in *TWIST* and *MMP* gene expression was also observed in 2 Gy irradiated cells compared to 0 Gy sham unirradiated cells as shown in Figure 5.9.

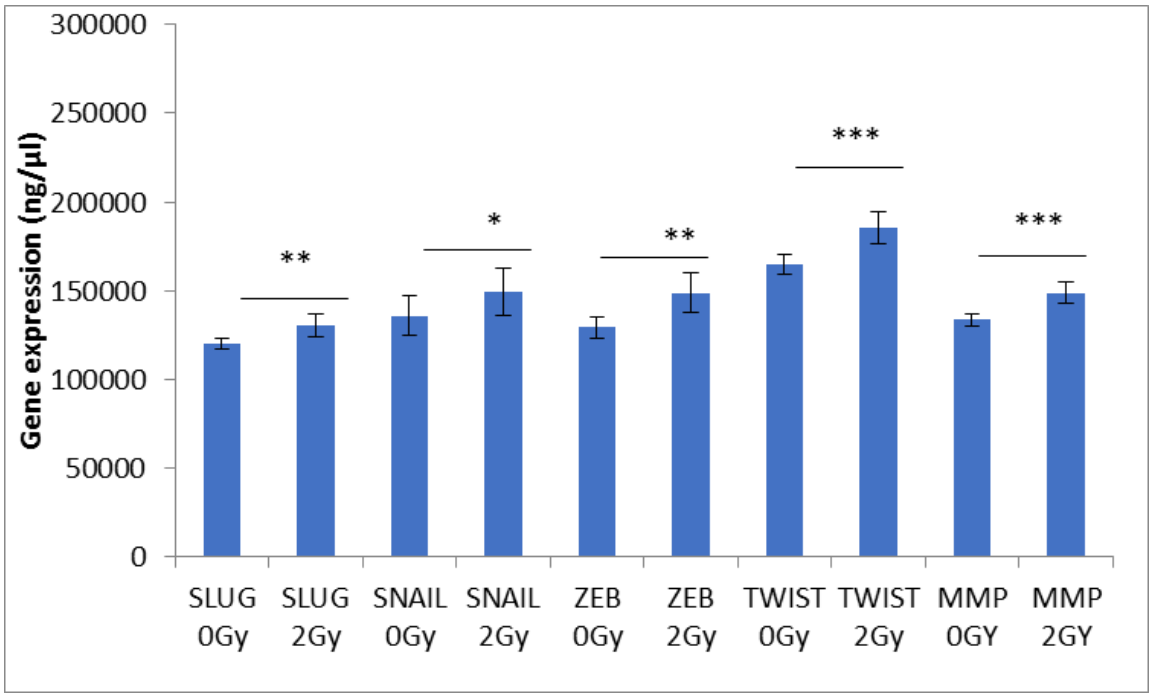


*Figure 5.9 E-box (SLUG, SNAIL and ZEB), TWIST and MMP genes expression following X-irradiation.*

*SLUG* and *ZEB* gene expression were significantly increased in MDA-MB-231 cells following X-irradiation compared to 0 Gy sham irradiated cells. There was a significant change in *SNAIL* gene expression following 2 Gy IR compared to 0 Gy sham cells. *TWIST* and *MMP* gene expression were also significantly increased in 2 Gy X-irradiated cells compared to 0 Gy sham unirradiated cells. The data presented as a mean ± the SEM of three independent experiments. (*p≤0.05, ** p≤0.001, *** p≤0.0001).

### 5.2.10 TG-F β in MDA-MB-231 cells following X-radiation

To confirm whether the level of TGF-β protein and gene expression were increased in MDA-MB-231 cells post-IR, cells were exposed to 0 Gy and 2 Gy X-irradiation. TGF-β gene and protein expression were measured using qPCR and western blot as described in Sections 2.13 and 2.14. Cells showed a significant (p≤ 0.001) increase in the TGF-β gene expression following 2 Gy X-irradiation compared to the unirradiated 0 Gy cells (Figure 5.10 A). Western blot assay was used to determine the levels of TGF-β protein following X-irradiation. Cells showed a significant (p≤ 0.001) increase in the quantity of TGF-β protein after 2 Gy irradiation compared to the 0 Gy cells. Cells also demonstrated an increase in the relative quantity of irradiated cells compared to the control cells as shown in Figure 5.10.B.

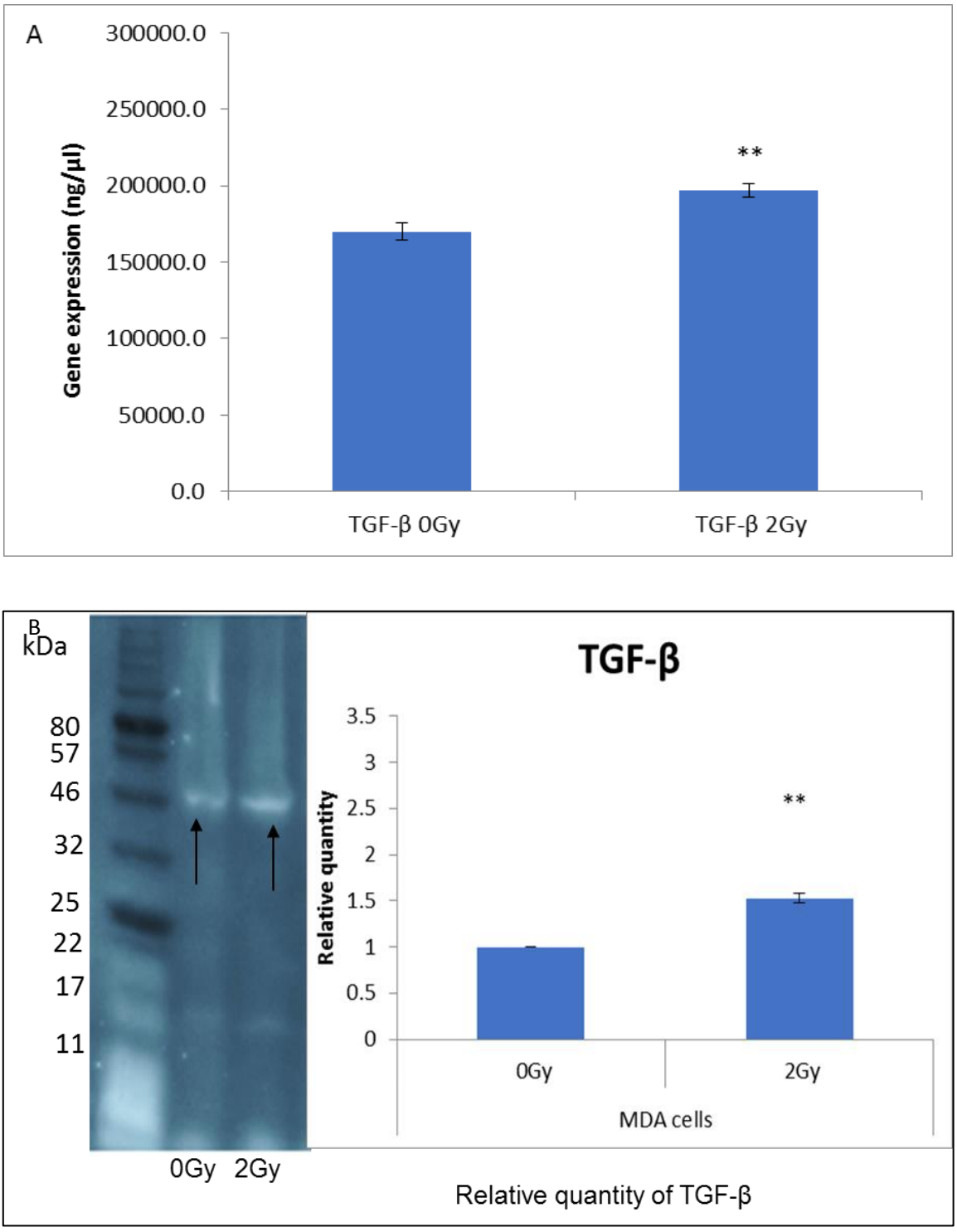


*Figure 5.10 qPCR and western blot of TGF-β in MDA-MB-231 cells following irradiation.*

There is a significant increase in the gene expression and the level of TGF-β at 2 Gy compared to 0 Gy direct irradiation. Cells also showed a significant increase in the relative quantity of TGF-β protein 46 kDa at 2 Gy irradiation compared to 0 Gy irradiated cells (black arrows) after 24 hours post-irradiation. The graph represents densitometry data drawn from blot images. The data presented as a mean ± SEM of three independent experiments. (*p≤0.05, ** p≤0.001, *** p≤0.0001).

### 5.2.11 Bystander effect: Media transfer

In order to investigate whether the IR induces cell communication associated with invasiveness, CCCM and ICCM media were transferred to unirradiated cells as described in Section 2.11.

Cells showed a significant ($p \leq 0.0001$) increase in the number of invasive cells following ICCM transfer compared to the cells treated with CCCM or the control, cells group. Cells also demonstrated a significant ($p \leq 0.0001$) increase in the percentage of vimentin and HPA positive cells following ICCM transfer compared to CCCM treated cells or control cells group. Meanwhile, ICCM treated cells showed a significant ($p \leq 0.0001$) decrease in the E-cadherin immunopositive cells compared to the cells treated with CCCM or control cells group. Moreover, a non-significant increase in the number of invasive cells was observed in CCCM (0 Gy media treated cells) compared to cells group control as shown in Figure 5.11.

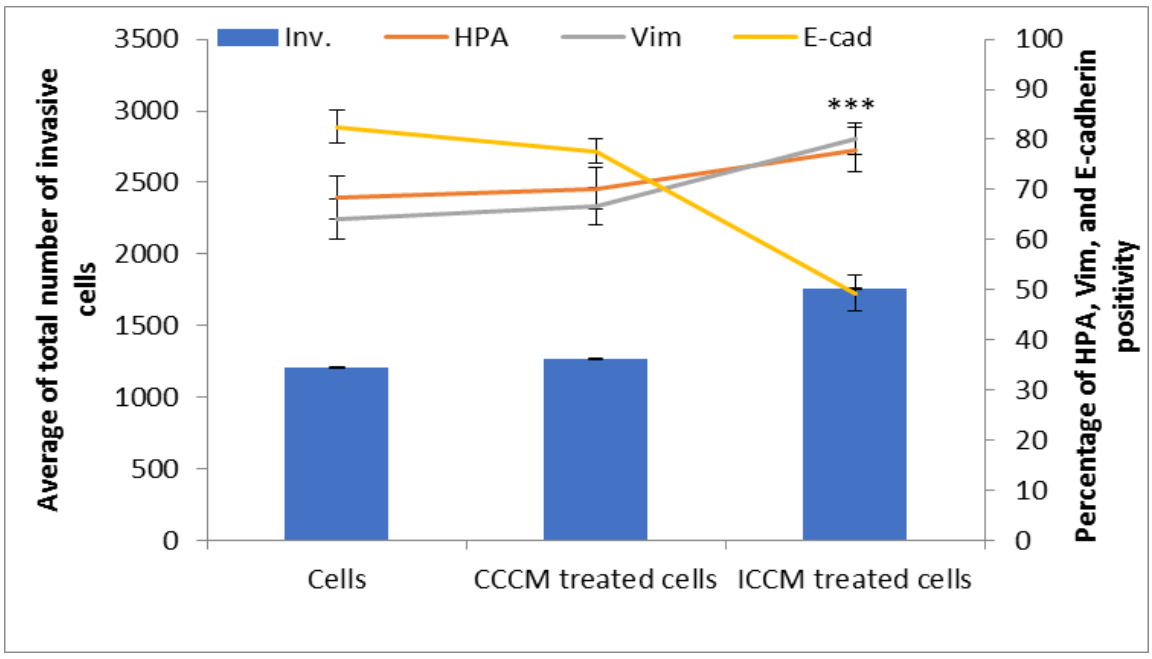


*Figure 5.11 Analyses of invasive capacity, EMT markers and HPA labelling in bystander effect cells, 24 post-media transferred.*

Cells showed a significant increase in the number of invasive cells at 2 Gy BE cells compared to control and 0 Gy BE cells, and this was associated with a decrease in epithelial marker E-cadherin and an increase in the mesenchymal marker vimentin. Cells also showed an increase in the percentage of HPA positive cells following 2 Gy BE cells compared to 2 Gy BE cells or the control cells group. The error bars represent the standard error of the mean of invasive cells and the percentage of HPA and EMT markers. The experiment was carried out in triplicate. (*$p \leq 0.05$, ** $p \leq 0.001$, *** $p \leq 0.0001$).

### 5.2.12 Size and concentration of exosomes in MDA-M-231 post IR

Size and concentration of exosomes were characterised as described in Section 2.12.3. Cells showed significant ($p \leq 0.0001$) increase in the concentration of ICCM exosomes ($1.2X10^{11}$ exosomes/ml) at 2 Gy X-irradiation compared to exosomes derived from 0 Gy irradiated cells; however, a non-significant increase in the size of exosomes was observed in ICCM exosomes compared to exosomes isolated from CCCM after 4 hours post-irradiation as presented in Figure 5.12.

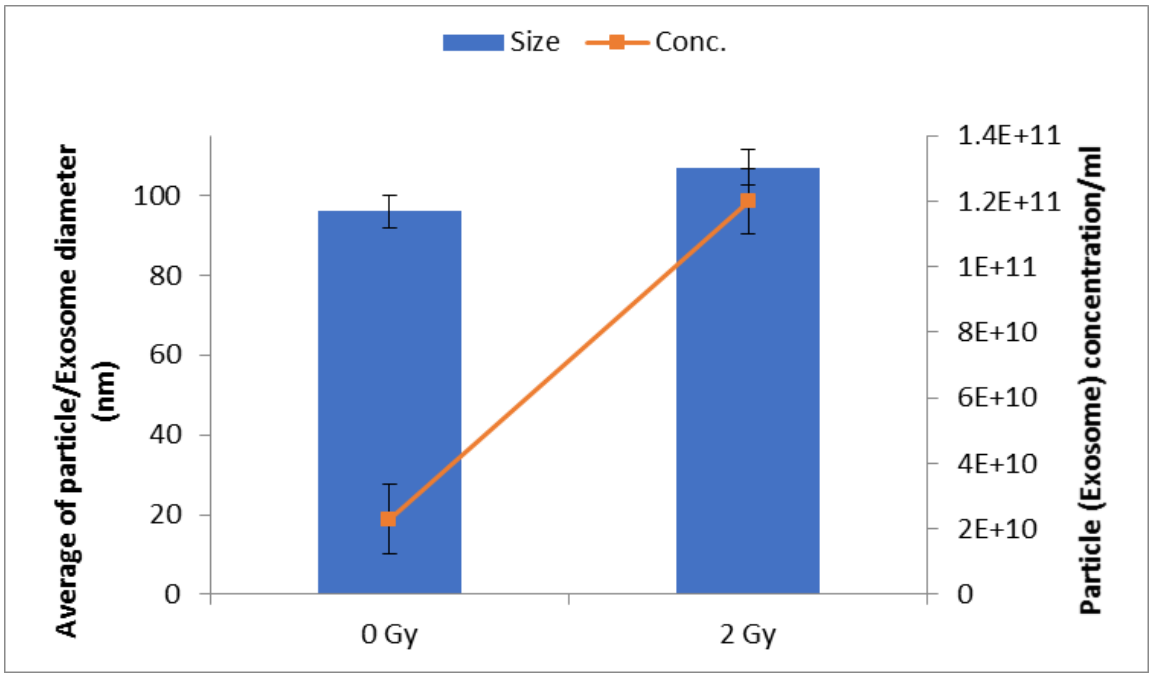


*Figure 5.12 Mean exosome size and concentration in irradiated MDA-MB-231 cells 4 hours following 2 Gy X-irradiation.*

Cells showed a non-significant difference in exosome size at 4 hours post-irradiation; whereas, a significant increase in the exosome's concentration/ml was observed that were isolated from irradiated cells following 2 Gy X-irradiation. The error bars represent the standard error of exosomes size and concentration. The experiment was carried out in triplicate; (*$p \leq 0.05$, ** $p \leq 0.001$, *** $p \leq 0.0001$).

### 5.2.13 Invasive capacity of MDA-MB-231 post exosome transfer

HPA, EMT markers and invasion of MDA-MB-231 cells were measured following exosomes transfer as described in Section 2,12,4. A significant ($p \leq 0.0001$) increase in the number of invasive cells was observed post-ICCM exosome transfer compared to the cells treated with CCCM exosomes. Cells also showed a significant ($p \leq 0.0001$) increased in the vimentin positive cells and a decrease ($p \leq 0.0001$) in E-cadherin positive cells. Moreover, cells showed a significant ($p \leq$

0.0001) increase in the HPA positive cells post 2 Gy ICCCM transfer compared to the 0 Gy CCCM transfer as presented in Figure 5.13.

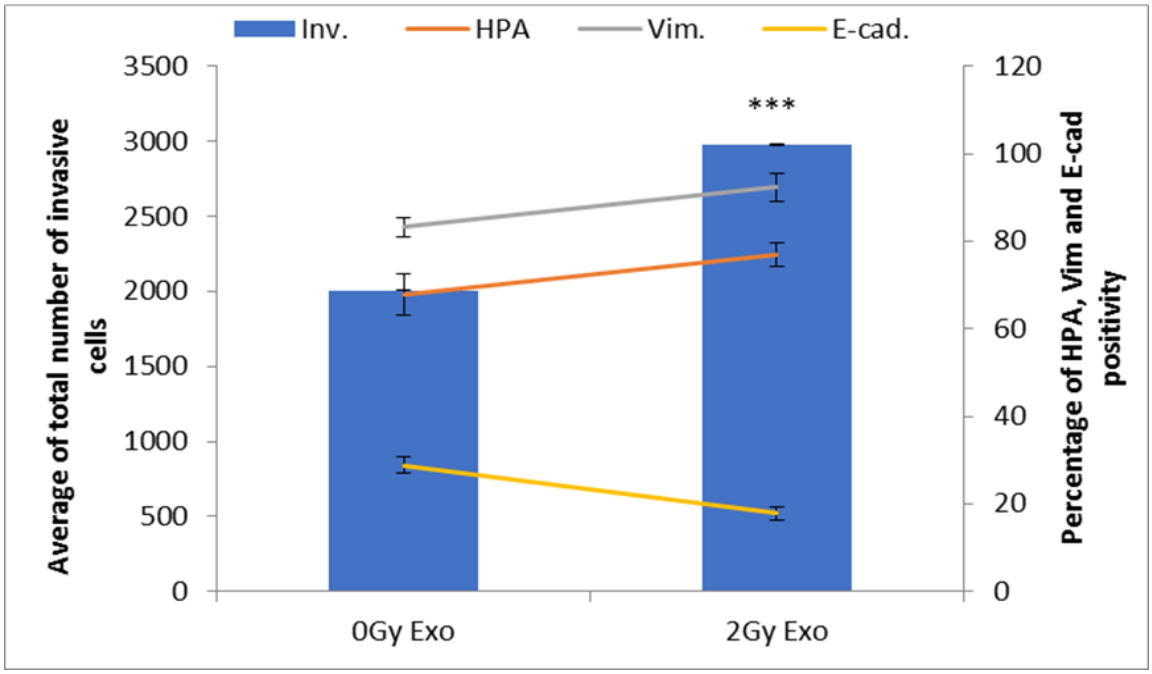


*Figure 5.13 Effects of exosomes on the invasiveness of MDA-MB-231 cells.*

Exosomes were isolated from CCCM (0 Gy) and ICCM of 2 Gy irradiated cells and then transferred to healthy unirradiated cells. Cells showed a significant increase in the percentage of cells that invaded the Matrigel membrane associated with an increase in the HPA labelling of cells and vimentin immunopositivity, and a decrease in the E- cadherin immunopositivity. The error bars represent the SEM of invasive cells and the percentage of HPA and EMT markers. The experiment was carried out in triplicate; (*p≤0.05, ** p≤0.001, *** p≤0.0001).

### 5.2.14 EMT markers following exosome transfer assessed using flow cytometry

MDA-MD-231 unirradiated cells were exposed to CCCM and ICCM exosomes, the percentage of vimentin and E-cadherin positive cells were analysed using flow cytometry as described in Section 2.8. Data showed a significant increase in the percentage of vimentin immunopositive cells after 2 Gy ICCM exosomes transfer compared to the CCCM exosomes treated cells. A significant decrease in the percentage of E-cadherin positive cells was observed post ICCM exosomes treatment compared to the cells that received CCCM exosomes as shown in Figure 5.14.

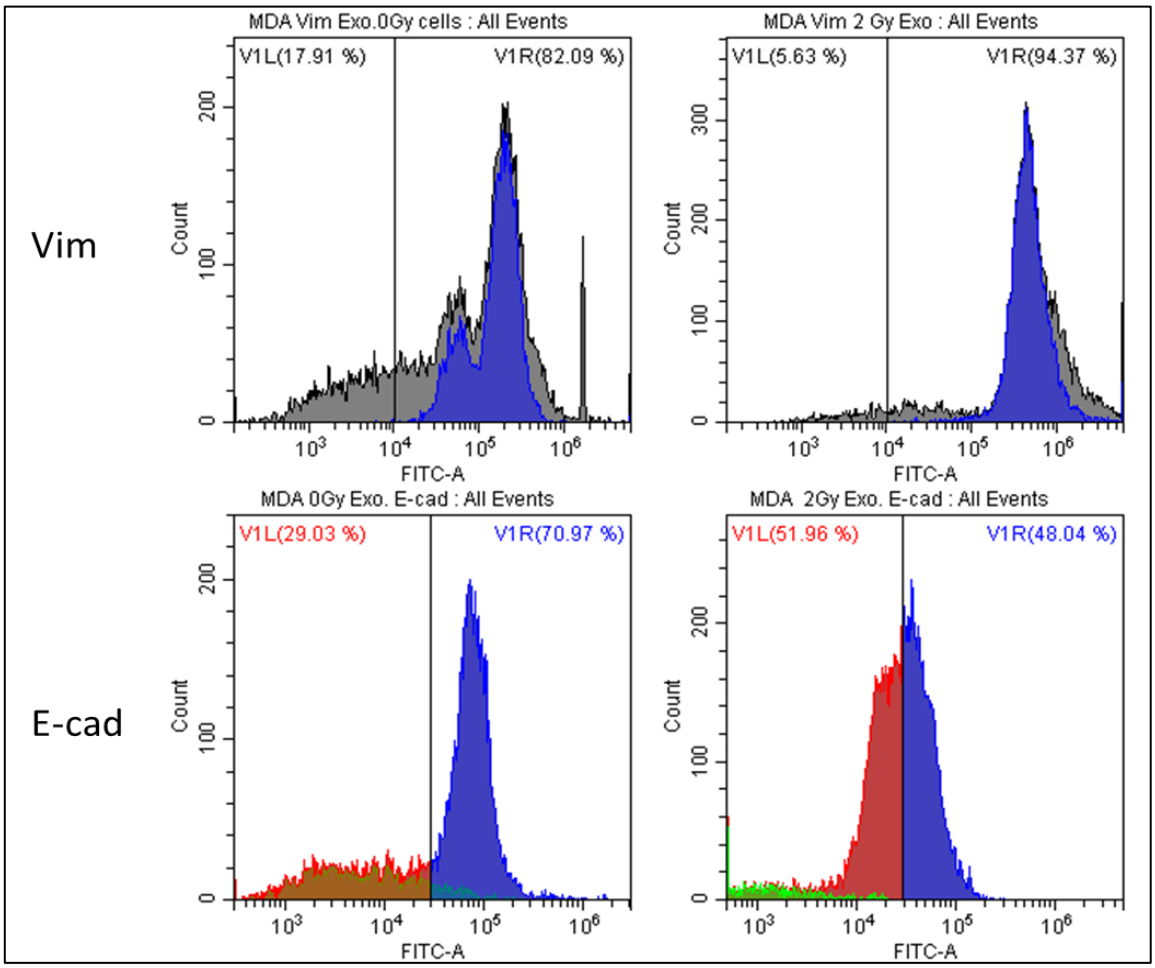


*Figure 5.14 Flow cytometry analysis of EMT markers vimentin and E-cadherin post-exosomes transfer.*

There was a significant (p≤ 0.0001) increase in the number of vimentin immunopositive cells 2 Gy exosomes treated cells compared to 0 Gy exosomes treated cells, right hand of the histogram. There was also a significant (p≤ 0.0001) decrease in E-cadherin immunopositivity in post 2 Gy exosomes transfer cells compared to cells treated with exosomes isolated from CCCM, right hand of the histogram. The blue colour represents the cells positively react with E-cadherin. Meanwhile the red colour represents cells negatively react with E-cadherin. The green colour represents the cells outside the polygonal shape and not involved in test. The plot is representative of the distribution of data from 3 experiments.

### 5.2.15 Gene expression post exosome transfer

In order to confirm the data for vimentin, E-cadherin and HPA positivity, qPCR was utilised to measure candidate genes expression following exosome transfer as described Section 2.13. Cells showed a significant increase in vimentin gene expression post ICCM exosomes transfer compared to the CCCM exosomes treated cells. Cells also showed a significant decrease in E-cadherin gene expression in 2 Gy ICCM exosomes recipient cells compared to the cells that treated with CCCM exosomes. Moreover, cells showed a significant increase in

the GalNAc-T6 gene expression post 2 Gy ICCM exosomes transfer compared to CCCM exosomes treated cells as presented in Figure 5.15.

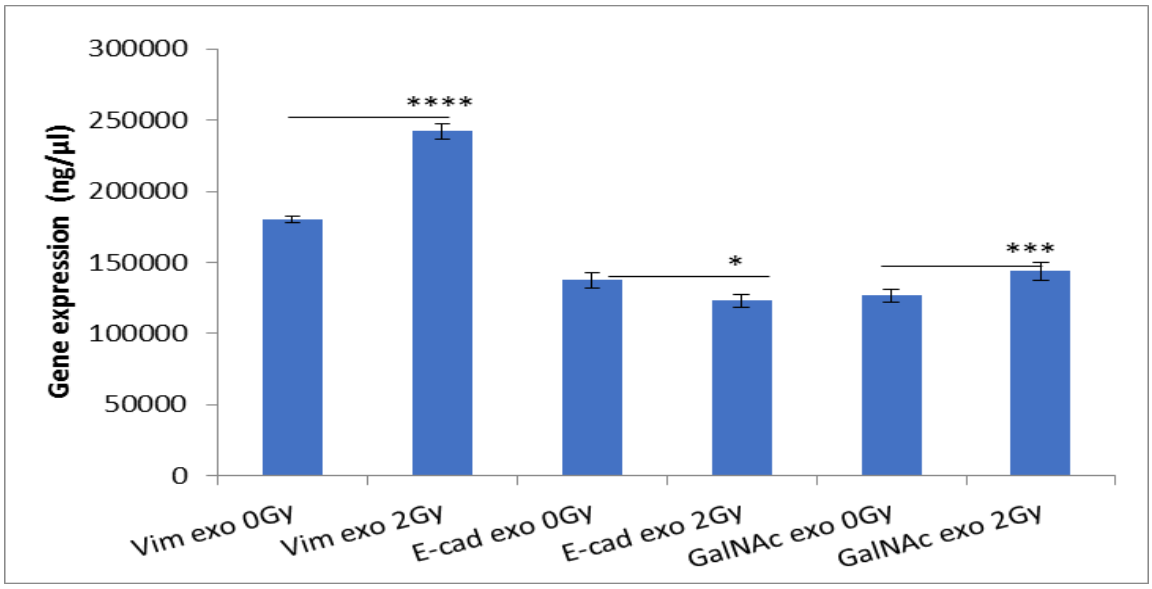


*Figure 5.15 Genes expression in MDA-MB-231 recipient cells following exosomes transfer.*

MDA-MB-231 cells treated with 2 Gy ICCM exosomes and 0 Gy CCCM exosomes. 24 hours following exosome treatment, cells showed an increase in vimentin gene expression and a decrease in E-cadherin gene expression in 2 Gy ICCM exosomes treated cells. Cells also showed a high level of *GalNAc-T6* expression flowing 2 Gy exosomes transfer. The error bars represent the SEM of the candidate gene expression, 3 replicate experiments were carried out. (*p≤0.05, ** p≤0.001, *** p≤0.0001).

### 5.2.16 E-box genes expression and TWIST in the exosome recipient cells

As described in Section 4.3.7 and the literature, E-box genes (*SLUG*, *SNAIL* and *ZEB*) control the expression of E-cadherin (Giroldi *et al.*, 1997; Yamashita *et al.*, 2004; Kilic *et al.*, 2016) and the EMT can be regulated by *TWIST* and *MMP* gene expression via TGF-β (Pozharskaya *et al.*, 2009; Smit *et al.*, 2009; Fan *et al.*, 2015; Wang *et al.*, 2016). To address whether the exosomes can carry substances such as protein and RNA that could induce EMT in MDA-MB-231 recipient cells, qPCR was used to investigate the mechanism behind inhibition of E-cadherin gene expression post-2 Gy-exosome transfer, as described in Section 2.13. MDA-MB-231 cells were treated with 0 Gy exosomes and 2 Gy exosomes. After 24 hours post exosome transfer, cells were lysed, and candidate genes expression were analysed using qPCR as described in Section 2.13.

Data showed a significant (p≤0.05) increase in the E-box (*SNAIL*, *SLUG*) gene expression post 2 Gy exosome transfer compared with 0 Gy exosome transfer.

Moreover, highly significant (p≤0.0001) increase in *ZEB* gene expression was observed in 2 Gy exosome-treated cells compared with control. Moreover, 2 Gy exosome- treated cells also showed a significant (p≤0.05) increase in *TWIST* and highly significant (p≤0.0001) increase in *MMP gene* expression compared with 0 Gy exosome-treated cells as presented in Figure 5.16.

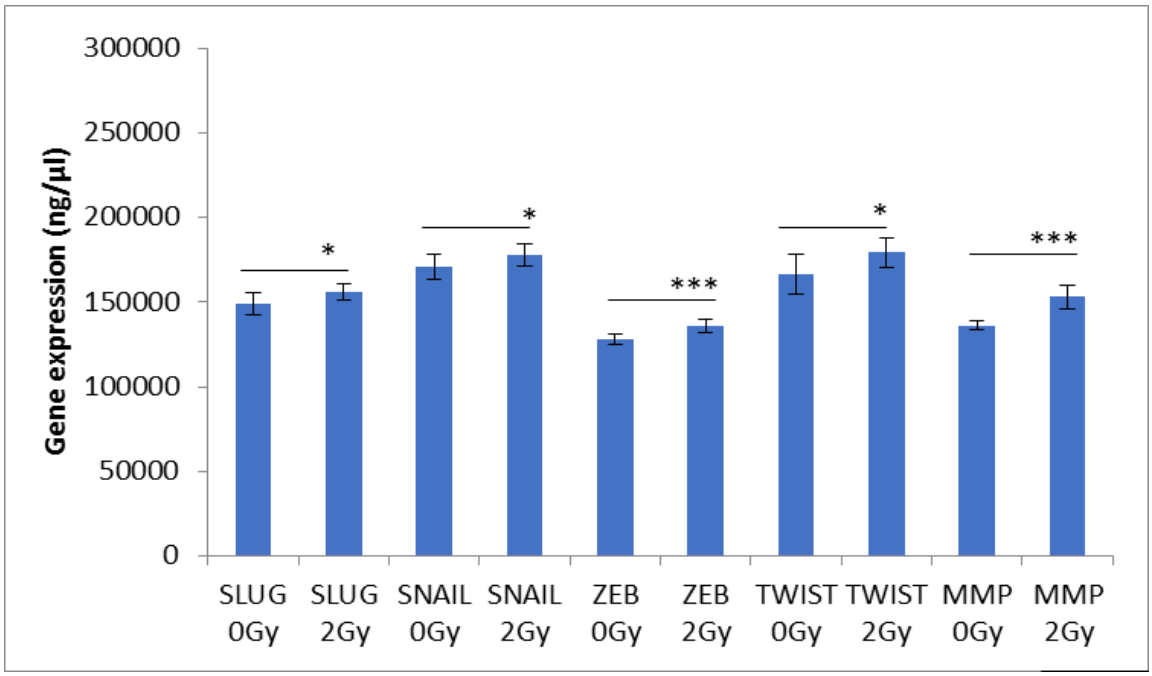


*Figure 5.16 Expression of E-box gene, TWIST and MMP in exosome recipient cells.*

2 Gy exosome-recipient cells showed a significant increase in *SLUG* and *SNAIL* gene expression compared to 0 Gy control. A highly significant increase in *ZEB* and *MMP* genes expression was also observed in 2 Gy exosome-recipient cells compared with 0 Gy exosome-recipient cells. 2 Gy exosome-treated cells also showed a significant increase in *TWIST* gene expression compared with 0 Gy exosome-treated cells. The error bars represent the SEM of the candidate gene expression of 3 independent experiments. (*p≤0.05, ** p≤0.001, *** p≤0.0001).

### 5.2.17. TGF-β gene and protein expression post exosome transfer

To investigate whether the TGF-β has a role in the invasive capacity of MDA-MB-231 breast cancer cells, qPCR and western blot were performed to measure the amount of TGF-β in the experimental groups as described in Sections 2.13 and 2.14. The 2 Gy ICCM exosome treated cells showed a significant increase in TGF-β gene expression compared to the 0 Gy exosome treated cells. A significant (p≤0.05) increase in the quantity of TGF-β protein was observed in the ICCM exosome recipient cells compared to the CCCM exosomes treated cells.

Cells that received ICCM exosomes showed a significant (p≤0.05) increase in the intensity of latent TGF-β band 46 kDa compared to the CCCM exosomes treated cells. However, the active TGF-β showed a faint band in 12 kDa, as shown in Figure 5.17.

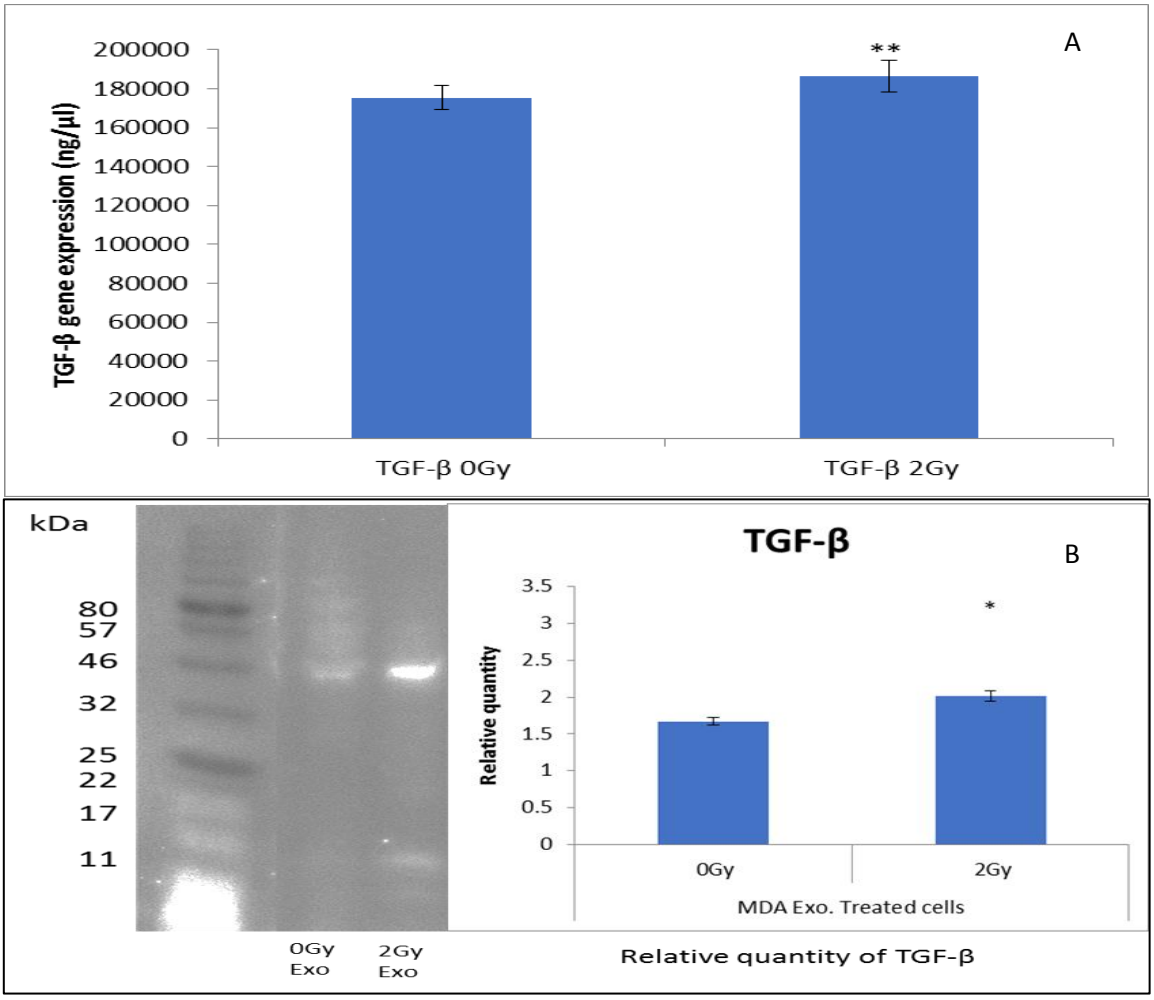


*Figure 5.17 TGF-β gene and protein expression post exosome transfer in MDA-MB-231 recipient cells.*

The expression of TGF-β gene using qPCR was a significant (p≤0.001) increase following exosomes transfer (panel A) and that was associated with a significant (p≤0.05) increase in the level of TGF-β proteins 46 kDa in 2 Gy exosomes recipient cells compared to 0 Gy exosomes treated cells 4 hours post-treatment. There was no clear band showed at 12KDa. Western blot also showed an increase in intensity and volume of TGF-β bands in 2 Gy exosome treated cells (Panel B). The graph represents densitometry data drawn from blot images. Data presented as a mean ± SEM of 3 independent experiments. (*p≤0.05, ** p≤0.001, *** p≤0.0001).

### 5.2.18. Exosome-depleted media transfer

In order to confirm the influence of exosomes on the invasiveness of MDA-MB-231 cells, CCCM and ICCM exosome depleted media were transferred to unirradiated fresh cells. After 24 hours following ICCM exosome depleted media

transfer, HPA, EMT markers and invasion of MDA-MB-231 cells were measured as described in section 2.12.5. There was a very low significant increase in the number of invasive cells compared to the cells received CCCM depleted media. However, both recipient cell populations did not demonstrate a significant change in vimentin and E-cadherin immunopositivity. Moreover, cells did not show a significant difference in the HPA positivity following depleted media transfer as shown in Figure 5.18.

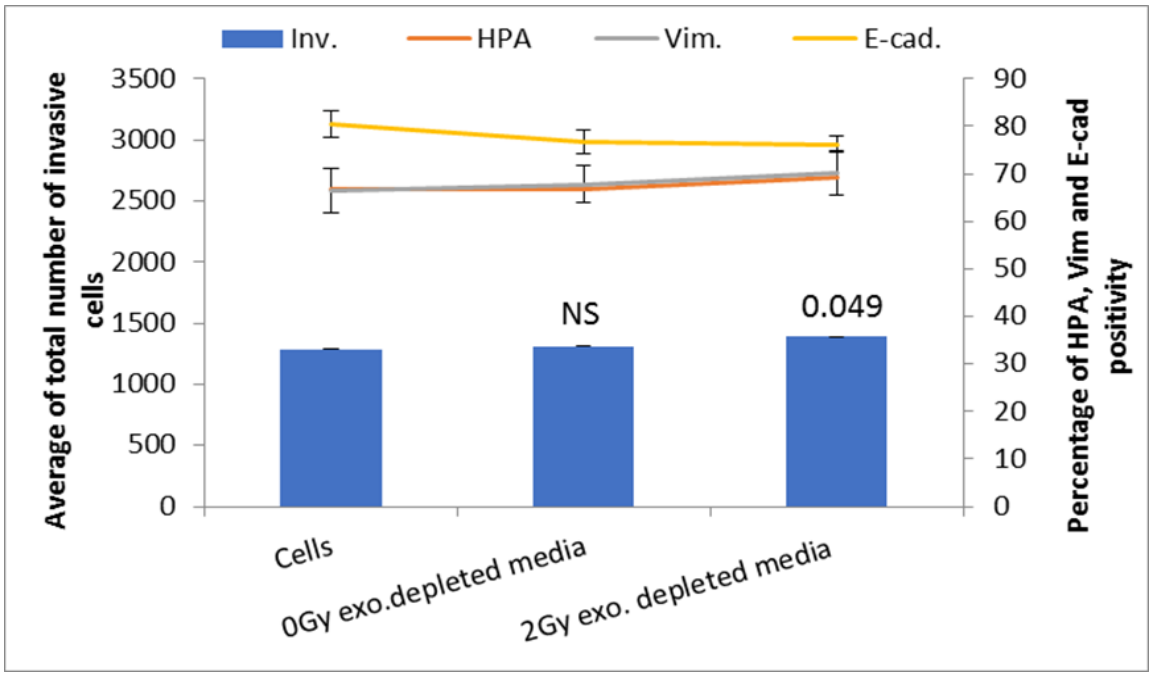


*Figure 5.18 Effect of exosome depleted media on invasiveness capacity of MDA-MB-231 cells*

MDA-MB-231 cells were treated with 0 Gy CCCM, and 2 Gy ICCM exosome depleted media. Cells showed a significant ($p \leq 0.05$) increase in the percentage of invasive cells after 2 Gy ICCM exosome depleted media compared to cells treated with 0 Gy CCCM exosome depleted media. There was not a significant difference between the number of invasive cells after treatment with 0 Gy media depleted exosome compared to control group cells. In addition, a non-significant change in the percentage of vimentin, E-cadherin and HPA positive cells was observed after treatment with 2 Gy exosome depleted media compared to 0 Gy exosome depleted media. The data presented as a mean of a total number of invasive cells, and the percentage of HPA and EMT markers positive cells. The error bars represent the SEM of 3 independent experiments. (*$p \leq 0.05$, ** $p \leq 0.001$, *** $p \leq 0.0001$).

### 5.2.19 Relevant exosomal miRNAs in MDA-MB-231 cells

To identify candidate miRNAs in the exosomes that could have a role in cancer cell invasion, 0 Gy and 2 Gy exosomes were lysed, and total RNA was measured. Candidate exosomal miRNA (Let-7a, miR-30a, miR-200b and miR-9a) expressions were explored using qPCR, as described in Section 2.13. These

miRNAs have been chosen in this study because they have an important role in EMT and invasion of cancer cells (Kim *et al.*, 2012; Chan and Wang, 2015; Chang *et al.*, 2015; Cheng *et al.*, 2012; Ma *et al.*, 2010). Data showed a significant increase in the expression of miR-9a in the exosomes isolated from ICCM compared to the 0 Gy CCCM isolated exosomes. 2 Gy ICCM isolated exosomes showed a significant decrease in the expression of miR-30a compared to the 0 Gy CCCM isolated exosomes. ICCM isolated exosomes did not show a significant change in the expression of Let-7a and miR-200b compared to CCCM isolated exosomes, as shown in Figure 5.19.

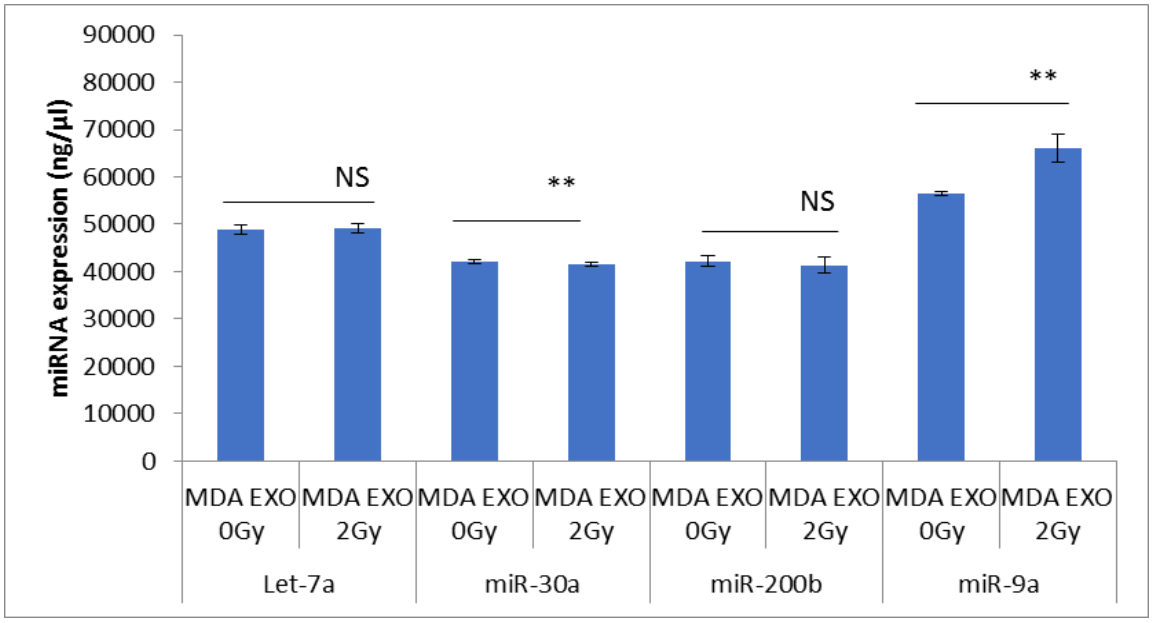


*Figure 5.19 miRNA profile of CCCM and ICCM MDA-MB-231 exosomes.*

ICCM exosomes display a significant (p≤0.001) increase in the abundance of miR-9a compared to CCCM exosomes. However, ICCM exosomes showed significant (p≤0.001) decrease in the amount of miR-30a compared to CCCM exosomes. Non-significant change in the level of Let-7a and miR-200b was observed in the exosomes isolated from ICCM compared to CCCM exosomes. The error bars represent the SEM of the relative quantity of miRNA in the exosomes of 3 independent experiments. (*p≤0.05, ** p≤0.001, *** p≤0.0001).

### 5.2.20 TGF-β in MDA-MB-231 exosome

CCCM and ICCM exosomes protein were analysed using western blot assay as described in Section 2.14, confirm the presence of TGF-β in the exosome that was isolated from ICCM and CCCM. However, exosomes that were isolated from ICCM showed an increase in the relative quantity of TGF-β 46 kDa compared to 0 Gy CCCM exosomes as shown in Figure 5.20.

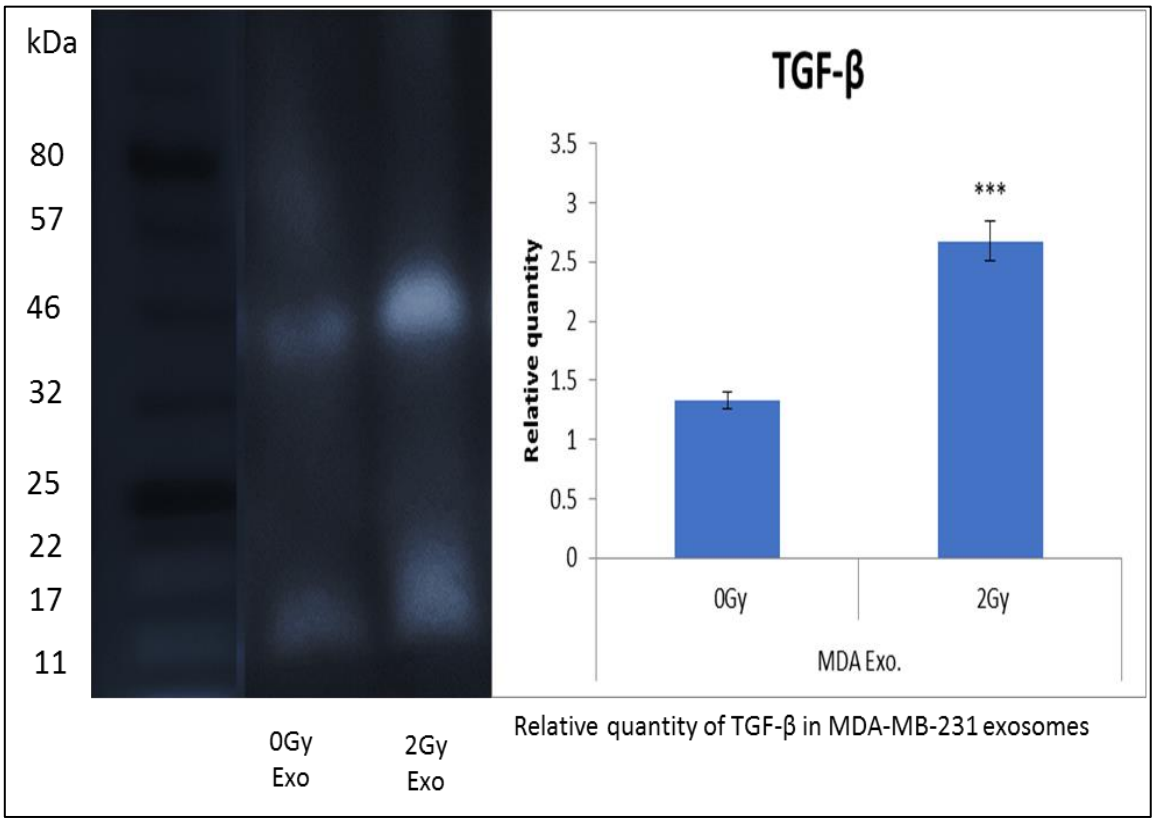


*Figure 5.20 TGF-β in MDA-MB-231 exosomes.*

Exosomes that were isolated from irradiated cells showed a significant increase in the relative quantity of TGF-β protein, latent 46 kDa at 2 Gy exosomes compared to the control 0 Gy exosomes. The graph represents densitometry data drawn from blot images of 46 kDa band. The data also showed an increase in the density of TGF-β 12 kDa at 2Gy exosome compared to 0 Gy exosome. The data presented as mean ± SEM of 3 independent experiments. (*p≤0.05, ** p≤0.001, *** p≤0.0001).

### 5.2.21. Inhibition of exosomal cargo

To investigate the effect of exosome cargo molecules (RNAs and proteins) on invasiveness capacity of MDA-MB-231 cells, exosomes were lysed and divided into three fractions. The first fraction was treated with RNase-A to digest RNA molecules of exosomes. The second fraction was heated at 100$^{o}$C to inhibit the exosome proteins. The third fraction was treated with RNase-A and then heated to inhibit both RNA and protein molecules of exosomes. Then the exosome fractions were transferred to fresh unirradiated cells as described in Section 2.12.6.

#### *5.2.21. i Inhibition of exosomal RNAs*

Data showed that cells were received RNase-A treated exosomes (exosomal RNA inhibition at both doses of irradiation- CCCM exosomes RNA inhibited group

and ICCM exosomes RNA inhibited group) showed a significant decrease in the number of invasive cells compared to cells treated with CCCM 0 Gy exosomes or ICCM 2 Gy exosomes respectively. There was also a significant decrease in the number of HPA and vimentin positive cells and an increase in E-cadherin positive cells in the same groups. Moreover, a non-significant change in the number of invasive cells was observed in cells that received CCCM exosomes treated RNase-A compared to cells received ICCM exosomes treated RNase-A, and also in comparison with the positive control (heated RNase-treated cells) and negative control cells group. Interestingly, the number of invasive cells and levels of HPA and EMT marker-positive cells in the exosome-RNA inhibition recipient cells returned to the same level as that of unirradiated cells (negative control) as shown in Figure 5.21.

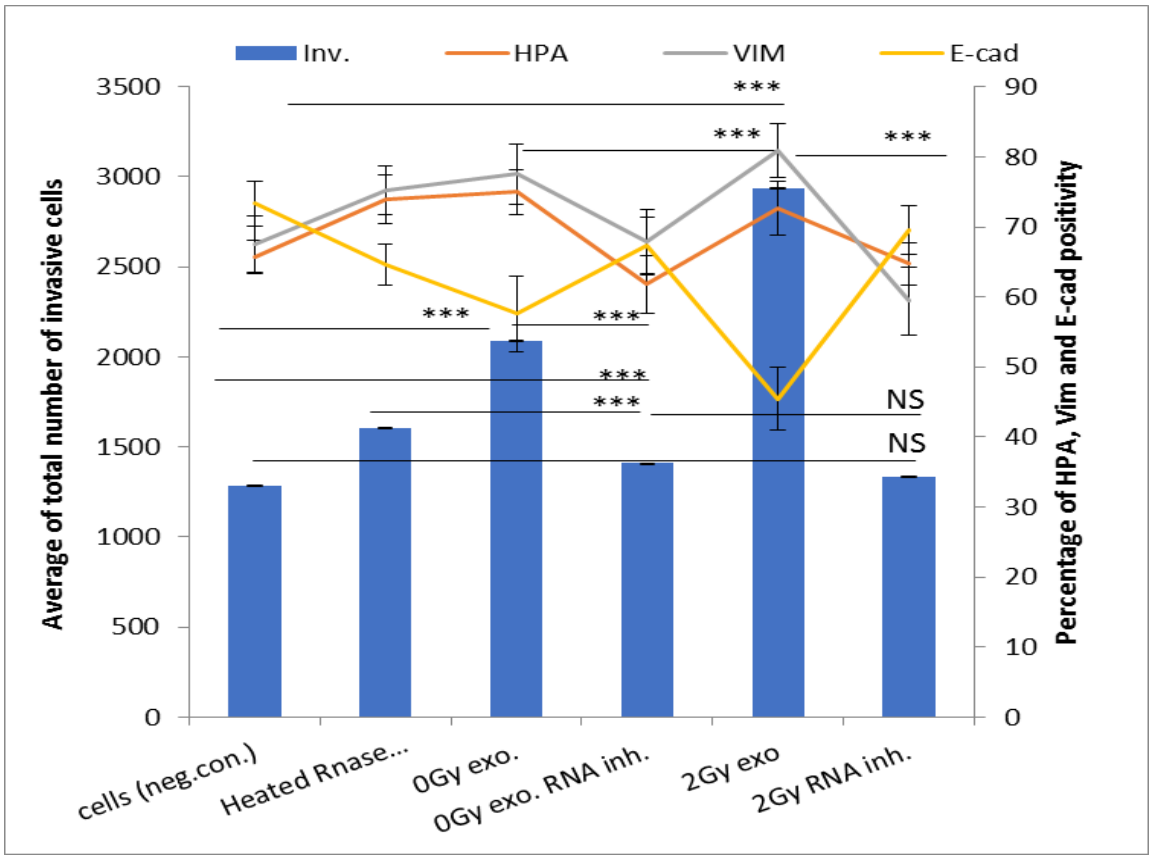


*Figure 5.21 Effect of exosome treatment and exosomal RNA inhibition on MDA-MB-231 cells.*

The number of invasive cells significantly (p≤0.0001) increased in 2 Gy exosome treated cells compared to 0 Gy exosome treated cells. Both groups 0 Gy exosomes treated cells and 2 Gy exosomes treated cells showed a significant increase in the number of invasive cells compared to the negative control (cells group), and that also was associated with an increase in the HPA and vimentin positivity and a decrease in E-cadherin positive cells. There was also a significantly (p≤0.0001) reduced in the number of invasive cells at 0 Gy and 2 Gy exosomal RNA inhibition compared to exosomes treated cells. The number of invasive cells, HPA and EMT markers in RNA inhibited groups returned to the same level of the negative control (cell group). Heated Rnase group is a positive control. The data presented as a mean of a total number of invasive cells, and the percentage of HPA and EMT markers positive cells ± the SEM of 3 independent experiments (*p≤0.05, ** p≤0.001, *** p≤0.0001).

### *5.2.21. ii Inhibition of exosomal protein*

Cells treated with the heated exosomes showed a significant decrease in the number of invasive cells compared to those treated with unheated exosomes that were isolated from CCCM (0 Gy exosomes) and ICCM exosomes (2 Gy exosomes). These cells also demonstrated a significant decrease in the number of vimentin-immunopositive cells compared to the cells that received unheated exosomes following. Conversely, the percentage of E-cadherin immunopositive cells increased in the heated exosome recipient cells compared to those that

received unheated exosomes. A significant decrease in the percentage of HPA positive cells was also observed in the cells that were treated with. CCCM or ICCM heated exosomes. The number of invasive cells, HPA and EMT positivity, returned to the same level of the negative control ('cells' group) as shown in Figure 5.22.

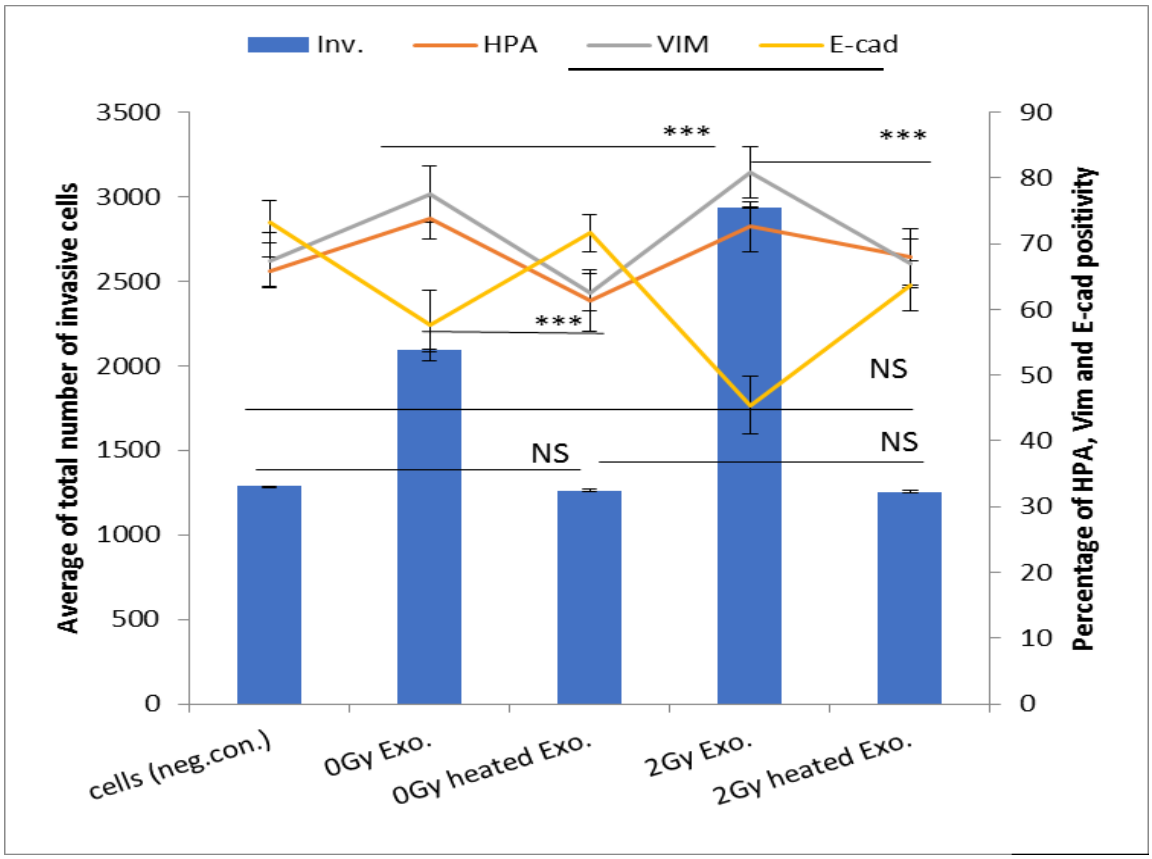


*Figure 5.22 The initial effect of exosome treatment and exosomal protein inhibition on the invasive capacity of MDA-MB-231breast cancer cells.*

A significant increase in the invasive capacity of 0 Gy and 2 Gy exosome treated MDA-MB-231 cells compared to the control group (cells). 2 Gy exosome treated cells also showed a significant increase in the number of invasive cells compared to 0 Gy exosome treated cells. Meanwhile, 0 Gy and 2 Gy exosomal protein inhibition groups showed a significant reduction in the number of invasive cells, HPA vimentin positivity and an increase in E-cadherin positive cells compared to 0 Gy exosomes treated cells, and 2 Gy exosomes treated cells respectively. However, 0 Gy and 2 Gy heated exosomes tread cells groups did not show significant differences in the number of invasive cells or HPA, vimentin and E-cadherin positive cells compared to the negative control (cells group). The data presented as a mean of a total number of invasive cells, and the percentage of HPA and EMT markers positive cells ± the SEM of 3 independent experiments (*p≤0.05, ** p≤0.001, *** p≤0.0001).

### *5.2.21 iii Inhibition of exosomes protein and RNA*

MDA-MB-231 cells that were treated with exosome cargo inhibition (protein and RNA) showed a significant decrease in the number of invasive cells compared to the 0 Gy, and 2 Gy exosome treated cells, respectively. Interestingly, the number

of invasive cells in both groups (0 Gy exosomes cargo inhibition and 2 Gy exosomes cargo inhibition) returned to the same level of invasive cells of the negative control (cells group). The reduction in the number of invasive cells in the cells treated with exosomes inhibited cargo showed a decrease in HPA and vimentin positivity and an increase in E-cadherin positive cells compared to 0 Gy and 2 Gy exosomes treated cells respectively. Interestingly, the level of HPA, vimentin and E-cadherin positive cells returned to the same level of negative control (cells group) an The number of immunopositive cells for vimentin was significantly decreased, and immunopositive for E-cadherin significantly increase after treatment with RNase treated/heated (heated Rnase positive control) in comparison to the cells that received CCCM and ICCM exosomes. A significant decrease in the HPA positivity was also observed in these cells compared to the 0 Gy, and 2 Gy exosome treated cells, as shown in Figure 5.23. A negative control (fresh cell) and positive control (Heated RNase treated cells) have been utilised in this experiment for comparisons purpose, as the other groups of exosomes treated with RNase to inhibit the exosomal RNA and then inhibit the activity of RNase by heat. Therefore, the other group was treated with heated RNase.

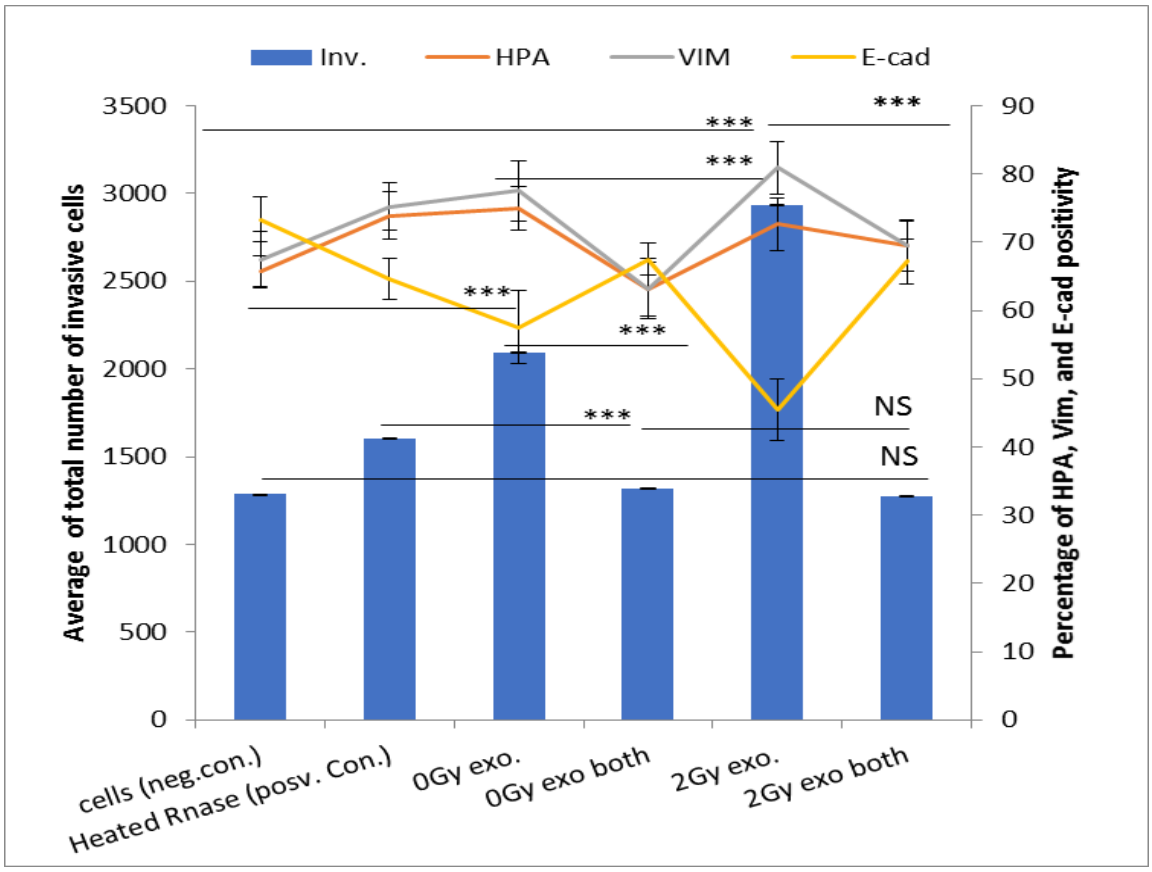


*Figure 5.23 Effect of exosomes treated cells and both exosomal cargo (RNA and protein) inhibition on the invasive capacity of MDA-MB-231 cells.*

A greater number of MDA-MB-231 cells were invasive after treatment with 0 Gy, and 2 Gy exosomes treated cells compared to the negative control (cells group). The number of invasive cells at 0 Gy and 2 Gy exosomes inhibited cargo was returned to the same level of unirradiated cells control. The reduction in the number of invasive cells was associated with a decrease in HPA and vimentin positive cells and a decrease in E-cadherin positive cells comparison to positive control or negative control. Interestingly the number of invasive cells and the level of HPA vimentin and E-cadherin following exosomes cargo inhibition returned to the same level of the negative control (cells group). The data presented as a mean of a total number of invasive cells, and the percentage of HPA and EMT markers positive cells. The data presented as a mean of a total number of invasive cells, and the percentage of HPA and EMT markers positive cells ± the SEM of 3 independent experiments (*p≤0.05, ** p≤0.001, *** p≤0.0001).

## 5.3 Discussion

As described in Section 2.2., MDA-MB-231 cells are a basal and triple-negative breast cancer cells which reveal cancer stem cell characteristic (Phillips, McBride and Pajonk, 2006; Holliday and Speirs, 2011; Li *et al.*, 2017c; Yamamoto *et al.*, 2017; Konge *et al.*, 2018). The current data confirm the previous studies as described in Section 5.1. Therefore, MDA-MB -231 cells were tested for stem cells characteristics using flow cytometry; cells exhibited high levels of $CD44^{+}$ and low levels of $CD24^{-}$ as shown in Figure 5.1. This result was consistent with

previous studies which reported that MDA-MB-231 display CSC properties, such as $CD44^+$ and $CD24^-$. It has been stated that MDA-MB-231 cells demonstrate cancer stem cells characteristics when labelled with CD44, CD24 and ALDH. MDA-MB-231 also showed an increase in a number of mammosphere formation when cultured in a very low FBS media (Phillips, McBride and Pajonk, 2006; Jin *et al.*, 2016; Vazquez-Santillan *et al.*, 2016; Li *et al.*, 2017c).

It was hypothesised that IR could induce BCSCs migration and invasion. The data in the current study confirm this hypothesis; the study showed that MDA-MB-231 cells displayed cancer stem cells property. Secondly, to investigate factors that could involve in BCSCs invasion and metastases following IR, or following exosomes transfer. The current study investigates glycosylation, EMT markers and invasion of MDA-MB-231 basal BCSCs to the Matrigel. The study also investigates the candidate genes, proteins and miRNA that could involve in the invasiveness of breast cancer stem cells following IR or exosome transfer.

In order to address whether the physiological activity of cancer cells has an impact on HPA negativity/positivity, HPA was measured in the MDA-MB-231 cells seeded onto the insert membrane of a Matrigel co-culture system after 4, 8, 16 and 24 hours. Data showed that cells in the upper surface demonstrated a higher level of HPA positivity compared to the HPA negative cells (No change in the percentage of HPA negativity/positivity throughout the biological time points) as shown in Figure 5.2. Data suggested that MDA-MB-231 can show a high percentage of HPA when the cells seeded on the Matrigel and low level of HPA binding when cells moved and pass-through the matrigel. The decrease in the HPA positive cell could be as a result of the physiological activity of cells such as a change from epithelial to mesenchymal type. It has been reported that the presence of T/Tn antigen in cell surface proteins was reduced in the cells that underwent EMT (Li *et al.*, 2013). In this study, they treated Huh7 hepatocellular cancer cells with hepatocellular growth factor (HGF), and they have shown a change in the shape of Huh7 cells from epithelial to mesenchymal and reduced in the affinity of glycoproteins to the lectin.

Cells that passed through the membrane showed a high percentage of HPA negativity; however, the HPA positive cells increased ~ 20% to ~ 40% after 8

hours, reaching the settled status of HPA positivity (~ 55%) after 16 hours. This percentage of HPA positivity was maintained by MDA-MB-231 cells that passed through the membrane after 24 hours as shown in Figure 5.2. Data suggested that MDA-MB-231 cells may need to be negative HPA to pass through the membrane. Then HPA positivity will increase in these cells to reach the settled level attached to the lower surface of the membrane.

This experiment may be considered as the first attempt of investigating the impact the physiological status of the cell on the HPA negativity/positivity in the invasive cells.

In order to investigate the responses of MDA-MB-231 to IR, cells were irradiated with 2 Gy X-irradiation. A half an hour later, a significant decrease in the viability of irradiated cells was observed following IR compared to unirradiated control cells as shown in Figure 5.3. However, the MDA-MB-231 cells showed a non-significant decrease in the level of ROS following irradiation (Figure 5.4). Surprisingly, the level of ROS in MDA-MB-231 cells was very low in irradiated and unirradiated cells. The reduction in the percentage of $ROS^{+}$ cells was associated with an increase in the level of *TWIST* and *SNAIL* gene expression, Figure 5.9. TWISTs have also been reported to increase ROS scavengers and reduce the level of ROS in human diploid fibroblast cells (HDF) (Floc'h et al., 2013). Therefore, it can be suggested that increase the level of TWIST expression following IR can activate ROS scavengers such as glutathione (Rosi et al., 2007), consequently reducing cell death and increasing radio-resistance and metastasis. Data suggest that there was a correlation between the ROS and the expression of *TWIST* and *SNAIL* and *MMP* genes expression. Increased expression of *TWIST, MMP* and *SNAIL,* may contribute to reducing ROS by controlling ROS scavengers such as 24-dehydrocholesterol reductase (Dhcr24) (Konge *et al.*, 2018) via inhibiting the activity of caspase three during apoptosis (Lu *et al.*, 2008). SLUG and ZEB genes expression also have shown a correlation between these genes expression and ROS reduction, and this association need further study in the future.

It is well established that IR increases the stress of irradiated cells and consequently mediated ROS, DNA damaged apoptosis and cells death (Azzam,

Jay-Gerin and Pain, 2012). However, the experimental data in the current study showed that MDA-MB-231 cells displayed a low level of ROS and this is consistent with previous studies. Phillips, McBride and Pajonk (2006) and Diehn *et al.* (2009) demonstrated that BCSCs exhibit a radioresistant character and low level of ROS. Konge *et al.* (2018) observed a decrease in the level of ROS in CD44+/ CD24- HMLE cells treated TGF-β compared to the CD44-/CD24+ untreated cells.

MDA-MB-231 cells showed a significant increase in the number of invasive cells following IR or following exosomes transfer, and that was associated with an increase in the vimentin positive cells and a decrease in E-cadherin positive cells, in Figures 5.5 and 5.13, respectively. Flow cytometry results confirm that IR and exosome transfer promotes the expression of mesenchymal markers and decreased expression of epithelial markers in the irradiated and exosome recipients cells (Figure 5.7 and 5.14). Data suggest that IR and exosomes that were isolated from irradiated cells can induce invasion of MDA-MB-231 cells, and this is associated with induction of the mesenchymal marker (vimentin) and a decrease in the epithelial marker E-cadherin.

Data also showed that an increase in the invasion of MDA-MB-231 cells was associated with an increase in the level TGF-β following IR or exosome transfer as shown in Figures 5.10 and 5.17. These data supported the previous findings with MCF-7 cells. However, the factors contributing to an increase in the level of TGF-β in irradiated MDA-MB-231 cells could be different in term of ROS level or genes activity than irradiated MCF-7 cells as discussed in the previous chapter.

A possible mechanism that could explain the role of IR and exosomes derived from irradiated cells in the invasiveness of MDA-MB-231 cells is illustrated in Figure 5.24. IR is directly targeting the cells and inducing DNA damage or stimulates cells to produce substances which can traffic to the extracellular vesicles/exosome which induce a bystander effect on unirradiated cells (Ref). At the initial time, 30 minutes following irradiation. IR induces ROS and activates DNA damage, apoptosis, and the cell death pathway. However, IR can also induce the TWIST transcription factor (Figure 5.9) which is strongly associated with a change in the ratio of vimentin / E-cadherin (Figure 5.6) and

overexpressed in $CD44^{+}/CD24^{-}$ cells (Figure 5.1). Vesuna *et al.* (2009) reported that MDA-MB-231 cells and MCF-7 modified cells (transfer twist gene to MCF-7 cells) express a high level of the TWIST transcription factor, associated with an increase in the population of $CD44^{+}/CD24^{-}$ Cells in MCF-7/$_{TWIST}$ cells.

Moreover, IR can also induce matrix metallopeptidase 9 (*MMP9*) expressions, Figure 5.9. The latter can activate the latent TGF-β in the extracellular matrix (Kobayashi *et al.*, 2014). Activation of TGF-β1 turns on activation of TGF- β receptor 1 (TGFBR1) and then TGFBR2 and the SLUG-EMT pathway (Annes, Munger and Rifkin, 2003) resulting in an induction of invasiveness of MDA-MB-231 cells.

Data from western blot, invasion assay and qPCR suggest that Initial experiments conducted here indicate that TGF-β could play a role in invasion.' of MDA-MB-231 cells. In addition, the qPCR data showed a significant change in the expression of *MMP* gene and that could play a role in the invasion of cancer cells which need to confirm by a farther study in the future.

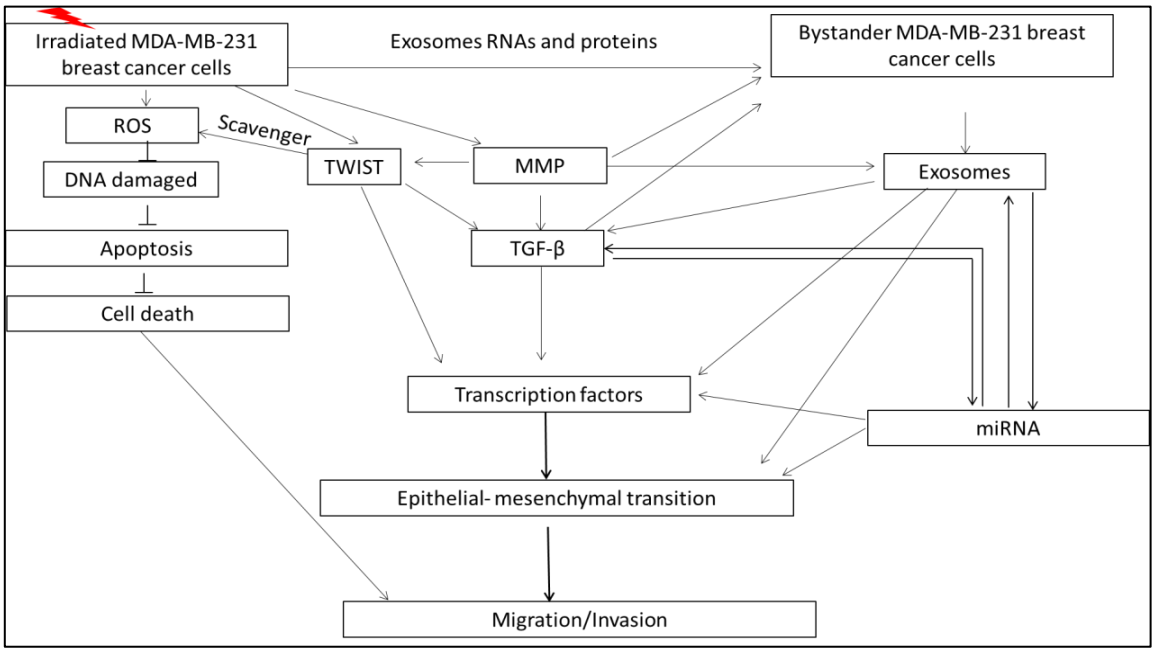


*Figure 5. 24 The schematic diagram showed the possible mechanisms of IR induced invasion of MDA-MB-231 cells.*

IR induces ROS in irradiated cells. IR can also increase *TWIST* gene expression, which promotes cells to produce ROS scavengers, leading to neutralised ROS production. The low level of ROS decreases DNA damaged and consequently apoptosis and cell death. IR also induces *MMP* gene expression, and the later can induce TGF-β, which can activate several pathways involved with transcription factors and miRNA leading to EMT and increase invasion.

These results are supported by other studies. Phillips et al. (2006) stated that MDA-MB-231 breast cancer cells are resistant to convention therapy such as IR. Moreover, Konge *et al.* (2018) demonstrated that the TGF-β induces changes in the morphology of HMLE epithelial cells to mesenchymal form with radioresistant and stem cell characteristics.

Moreover, proteins and RNAs from the irradiated cells can traffic to the outside of cells as extracellular vesicles/exosomes and effect unirradiated cells (Munich *et al.*, 2012). Data showed that exosomes derived from 2 Gy irradiated MDA-MB-231 cells showed a significant decrease in miRNA 30a expression as shown in Figure 5.19, and also a significant increase in the level of TGF-β, (Figure 5.20). Therefore, inhibition of miRNA 30a may lead to an increase in TGF-β protein; consequently, increase the invasive capacity of cancer cells. Yang *et al.* (2018b) reported that miRNA 30a could downregulation of TGF-β in laryngopharyngeal carcinoma. Much evidence also showed that miR-30a is responsible for inhibition the vimentin (Cheng *et al.*, 2012), and *SNAIL* (Wang *et al.*, 2014b; Chan and

Wang, 2015) gene activity and prevents cell metastasis. miR-30a can target the messenger RNA of vimentin and *SNAIL* preventing them from being translated into an active form of the proteins. In other words, X-irradiation reduces the abundance of miR-30a in irradiated cells and increased expression of *SNAIL* and vimentin, causing an increase in the invasiveness of irradiated MDA-MB-231cells. miR-9a was significantly increased in the exosomes isolated from irradiated cells compared to unirradiated exosomes derived cells as illustrated in Figure 5.19. miR-9a was observed to be associated with an increase in the level of TGF-β and invasion of MDA-MB-231 cells. It has been reported that miR-9a directly targets the 3′ untranslated region (UTR) of mRNA of E-cadherin preventing it from being translated into effective protein (Ma *et al.*, 2010), which allows cancer cells to dissociate from the original mass and metastasise to different organs.

The mechanisms of cancer cell invasion including EMT and glycosylation are complicated. Changes in the glycosylation of cell surface proteins could play a role in cancer invasion and metastasis. Data showed an increase in the percentage of HPA positive cells, and that was associated with an increase in the number of invasive cells following direct IR or following exosome transfer as illustrated in Figures 5.5 and 5.13.

Moreover, data showed an increase in the expression of *GalNAc-T6*, which is a gene responsible for the production of polypeptide N-acetylgalactosaminyltransferase-6, essential for adding the first monosaccharide GalNAc to the Ser or Thr in the Golgi apparatus to initiate the O-liked glycosylation (Bennett *et al.*, 1999b). Increased expression of GalNAc-T6 is associated with an increase in HPA positivity that might result from an increase in the unconjugated Tn antigen in the cell surface protein. Consequently, it might increase ST6GalNAc-1 expression in the irradiated cells or exosomes recipient cells. ST6GalNAc-1, as described in Section 1.5.9, which is an enzyme responsible for adding sialic acid to the Tn antigen and produce sTn antigen (Haugstad *et al.*, 2016) which is essential for aberration in the elongation of O-glycosylation. Changes in glycosylation of EMT proteins by the aid of glycosyltransferases, such as ST6GalNAC-1 may have an impact on cancer adhesion and invasion. Increase in sTn antigen assists in adhesion of cells. For

example; change in sialylation of E-cadherin influences adhesion and invasion of pancreatic cancer cells (Bassaganas *et al.*, 2014).

As discussed above, proteins and RNAs can be transported from irradiated cells and influence unirradiated cells with the aid of exosomes. This mechanism could play an important role in the invasion of breast cancer cells. To confirm the role of exosomes in bystander effect IR on the invasion of cancer cells, exosome-RNA, exosome-proteins or both (exosome-RNA and exosome-proteins) were inhibited. The decline in the invasion of MDA-MB-231 breast cancer cells and the level of vimentin and E-cadherin were returned to the normal levels in the unirradiated cells following treated the cells with exosomes-cargo-inhibited, as shown in Figures 5.21, 5.22 and 5.23. Data suggest that exosome-cargo has a role in the invasion of breast cancer cells by transporting protein and RNA to unirradiated cells as a bystander effect of IR.

The other factor could play a role in cancer invasion following exosomes transfer is the exosomal miRNA,. Data in Figure 5.19 showed a significant reduction in miR-30a expression in the ICCM exosomes compared to CCCM exosomes. Data also showed a significant increase in miR-9a in exosomes isolated from ICCM compared to exosomes isolated from CCCM. The reduction in the expression of miR-30a and an increase in the expression of miR-9a could have a role in cancer invasion and metastasis. It has been reported that miR-30a can inhibit vimentin expression by binding to the UTR of the vimentin gene, resulting in inhibition of vimentin transcription and translation. Consequently, reduce in the EMT and cancer cells migration and invasion (Yan, Ma and Gao, 2017).

It could be suggested that the reduction in the expression of miR-30a following ICCM exosome transfer led to the activation of vimentin gene expression and an increase in vimentin protein. Accordingly, an increase in the invasion of MDA-MB-231 breast cancer cells (Wei *et al.*, 2008).

On the other hand, an increase in miR-9a in ICCM exosomes can lead to downregulation of E-cadherin by activation of EGFR and consequently activate TWIST and TGF-β gene expression (Gwak *et al.*, 2014; D'Ippolito *et al.*, 2016). An increase in TWIST and TGF-β expression were reported associated with an

increase in the EMT and cancer invasion and metastasis (Yang *et al.*, 2016; Shao *et al.*, 2018)

In conclusion, the unique results of the current study showed that physiological activity of MDA-MB-231 breast cancer stem cell plays a crucial role in the change of glycosylation of cancer cells which could have an impact on the invasive capacity of these cells. Moreover, exposed MDA-MB-231 cells to IR can activate transcription factors, which influence the regulation of protein and miRNAs relevant to EMT and glycosylation positivity, and as a result, promote migration and invasion of MDA-MB-231 breast cancer cells. IR can cause irradiated cells to produce a high quantity of exosomes and increase the invasion of BCSCs.

# Chapter 6: Discussion

Breast cancer is one of the most common cancers worldwide, and in spite of advances in early diagnosis and treatment, mortality from this disease is still high. Most of the associated deaths are as a result of secondary cancer, i.e. cancer cells that have dissociated from the original/primary cancer mass and, as a result of metastasis, formed new distant foci (Krakhmal *et al.*, 2015; Cancer Research, 2018).

Treatment by radiation is still one of the most common conventional therapies for cancer. It has been reported that up to 40% of cancer cures can be attributed to radiotherapy (Baskar *et al.*, 2012). X-radiation is a type of low energy radiotherapy, which can directly target DNA molecules of cancer cells and induce an irreversible change in the DNA of the irradiated cells, leading to apoptosis and cell death (Guerci, Dulout and Seoane, 2004).

However, exposure to ionising radiation (IR), can lead to excitation of ions in the irradiated medium and subsequent release of reactive oxygen species (ROS) around the irradiation track, which target nearby cell organelles such as mitochondria (Azzam *et al.*, 2002), which can induce non-targeted effects of IR. For example, X-radiation can ionise $H_2O$ molecules in the irradiated cells and release ROS which targets the DNA and the membranes of irradiated cells. Consequently, irradiated cells can communicate with other cells through the release of several communication molecules including cytokine-mediated ROS (Yang *et al.*, 2007; Yoshino and Kashiwakura, 2017), Ca++ (Lyng *et al.*, 2006) and extracellular vesicles (EVs) / exosomes (Jelonek *et al.*, 2015). EVs can target unirradiated cells and produce oncogenic factors such as RNA and protein which can induce bystander effect in cells that never been exposed to irradiation (Al-Mayah *et al.*, 2015). However, not all cells exposed to a single dose of irradiation exhibit the same responses to irradiation. Several factors play a critical role in how the cell reacts to irradiation, such as the dose and dose rate of radiation, the type of radiation and the type and the physiological activity of cancer cells including migration and invasion of cancer cells (Cancer Research, 2018).

Studies have shown that IR can promote the migration and invasion of cancer cells (Young and Bennewith, 2017). However, the mechanisms behind this are not fully understood. Therefore, this study aimed to:

1- Investigate whether a therapeutic dose of X-irradiation can promote invasion of breast cancer cells and study the potential role of the exosomes in this process.
2- Achieve a better understanding of the mechanisms involved in breast cancer cells invasion following irradiation regarding the change in Epithelial-Mesenchymal Transition (EMT) and glycosylation markers.

## 6.1: The initial response of a breast cancer cell to IR

In the current study it has been shown that 1) X-irradiation increases the induction of DNA damage, apoptosis and ROS (chapter 3) and an increase in DNA damage and apoptosis leads to a decrease in cell viability (Figure 3.10). However, results show that a decrease in the viability of breast cancer cells was associated with an increase in the production of ROS in MCF-7 cells. These findings support previous studies by Leach *et al.* (2001) who demonstrated that oxidising events generated in cells exposed to IR induce ROS production and thereby increase the stress on irradiated cells. The stressed cells subsequently release substances to their neighbouring unirradiated cells, i.e. inducing a non-targeted effect of IR in the neighbour unirradiated cells.

Moreover, in the current study, an increase in ROS in irradiated cells was associated with an increase in the level of TGF-β protein which, in turn, was associated with an increase in vimentin (a mesenchymal marker) and a decrease in E-cadherin (an epithelial marker) leading to EMT and enhanced invasion of breast cancer cells. Studies have shown that ROS can regulate the biogenesis and expression of miRNA. For example, several enzymes can control the biogenesis of miRNA, including the ribonuclease Dicer which plays a central role in the maturation of miRNA (Suarez *et al.*, 2007; Ha and Kim, 2014). Downregulation of Dicer has been associated with ageing-related oxidative stress in cerebromicrovascular endothelial cells (Ungvari *et al.*, 2013). In contrast, Dicer can affect ROS production because of negative feedback, thereby controlling cellular homeostasis (Liu *et al.*, 2015). Knockout of Dicer is notably associated with a decrease in ROS production in human microvascular endothelial cells

(Shilo *et al.*, 2008). Data suggest that IR can induce ROS in irradiated cells which can control miRNA production and the latter regulates ROS production through negative feedback (Cheng *et al.*, 2012).

Conversely, in the current study, MDA-MB-231 cells showed a non-significant change in the level of ROS following IR that may be due to an increase in production of ROS scavengers (Konge *et al.*, 2018), as discussed that in Section 5.3.

## 6.2: Direct effect of IR in the invasion of breast cancer cells

Here, X-irradiation studies showed a strong correlation between vimentin and E-cadherin gene expression and invasiveness in both luminal (MCF-7) and basal (MDA-MB-231) breast cancer cells. An increase in vimentin expression and a decrease in E-cadherin expression was observed, suggesting that this inverse relationship promoted EMT and invasiveness of breast cancer cells, as shown in Figures 3.15 and 5.7. Interestingly, the MDA-MB-231 basal breast cancer cells showed a highly significant increase in the proportion of invasive cells compared to MCF-7 cells following X-irradiation, and that was also associated with an increase in vimentin and decrease in E-cadherin immunopositivity.

Data described in Section 3.2.2. ii showed that X-irradiation can promote ROS production in MCF-7 cells and that was associated with an increase in TGF-β expression in irradiated cells which could promote EMT and accordingly an increased invasion of breast cancer cells. Conversely, in spite of the reduction in the level of ROS in the MDA-MB-231 cells following IR, TGF-β expression was higher, and that may be a result of an increase in the expression of TWIST and MMP transcriptions factors, as discussed in Section 5.3.

Increase in the level of TGF-β in both cell lines could indicate that this mechanism may play a crucial role in breast cancer invasion and metastasis (Wendt *et al.*, 2013). TGF-β could activate several pathways related to the invasion of cancer cells including canonical (genes alteration) Slug pathway (Xue *et al.*, 2014; He *et al.*, 2018) and non-canonical (cytokines and growth factors) Slug pathway, such as phosphorylation of vimentin and activation of *AKT1* (Hamidi *et al.*, 2017).

The current study also showed that an increase in the number of HPA positive cells following X-irradiation or exosomes transfer was associated with an increase in the number of invasive cells in both breast cancer cell lines, as shown in Figures 3.14 and 5.5. Interestingly, both the MCF-7 and MDA-MB-231 cells showed an increase in the percentage of HPA positive cells following 2 Gy X-irradiation. However, the MCF-7 breast cancer cells showed a higher percentage of HPA positivity compared to MDA-MB-231 breast cancer cells (Figures 3.14 and 5.5); this will be discussed in more detail in Section 6.5.

Data also showed that vimentin and E-cadherin seemed to be the main players in the invasiveness of breast cancer cells. The ratio of vimentin to E-cadherin could play a critical role in the invasive capacity of cancer cells. Data in Figure 3.15 and 5.7showed that the ratio of vimentin to E-cadherin (Vim/E-cad) in both cell lines was increased following 2 Gy X-irradiation. However, the ratio of Vim/E-cad in MDA-MB-231 cells was higher than that observed in the MCF-7 cells; 50% and 46% respectively. Current data suggest that an increase in the ratio of vimentin to E-cadherin can be associated with an increase in the invasiveness of breast cancer cells, i.e. MDA-MB-231 basal breast cancer cells have a greater invasive capacity compared to MCF-7 luminal breast cancer cells.

## 6.3: Non-targeted effect of IR / exosomes on the invasion of breast cancer cells

The results as described in Sections 4.2.2 and 5.2.12 showed an increase in the exosome concentration in ICCM following X-irradiation. Much published evidence showed that cells under stress release more exosomes than non-stressed cells (Atienzar-Aroca *et al.*, 2016). Al-Mayah *et al.* (2015) demonstrated that the concentration of exosomes that were isolated from MCF-7 ICCM was higher compared to CCCM exosomes. In parallel, the current data also showed an increase in the number of invasive cells following exosome transfer (Figure 4,5 and 5.13). These results suggest that exosomes from irradiated and unirradiated cells have a significant role in the invasion of breast cancer cells.

Data in this study also showed that an increase in TGF-β expression was associated with a decrease or increase in miRNA expression in the exosome as described in Sections 4.2.10, 4.2.11 and 5.2.19, 5.2.20. TGF-β and miRNA can

traffic to the exosomes and be transported to the neighbouring cells or other cells in distant sites and induce EMT and promote invasiveness of cancer cells (Hazawa *et al.*, 2014). Data in Sections 5.2.19 and 5.2.20 showed the presence of candidate miRNAs (Let-7a, miR-30a, miR-200b and miR-9a) and TGF-β, respectively, in the exosomes of irradiated and unirradiated breast cancer cells. In addition, the level of TGF-β in exosomes isolated from irradiated cells was higher than the level of TGF-β in exosomes isolated from unirradiated cells in both MCF-7 and MDA-MB-231 cells. Much evidence supports this finding. For example, Jella *et al.* (2014) reported that the concentration of exosome increased following exposure of human keratinocyte HaCaT cells to different doses of γ rays. They also showed an increase in the concentration of exosomes in a dose-dependent manner. Al-Mayah *et al.* (2015) stated that X-irradiation induces MCF-7 cells to produce a higher number of exosomes compared to unirradiated cells. They also proved that the cargo of exosomes (RNA and protein) mediated a bystander effect on unirradiated cells. Here, exosomes release their cargo (protein and RNA) to the recipient cells as described previously in Section 1.7.1. Hence, the recipient cells are activated and change from an epithelial to a mesenchymal form, and as a result, the invasive capacity of breast cancer cells is increased. It has been reported that exosomes can carry TGF-β proteins which can promote EMT (Li *et al.*, 2017e). This study showed the association between an increase in the level of TGF-β derived from exosomes isolated from X-ray irradiated cells and the invasion of breast cancer cells.

## 6.4 Possible mechanisms involved in the invasion of breast cancer cells following IR or exosomes transfer.

The possible molecular mechanistic pathways that could explain the behaviour of cancer cells following IR or following exosome transfer is illustrated in Figure 6.1. Ionising radiation can target DNA and induce apoptosis and cell death. However, IR can increase ROS formation, leading to TGF-β upregulation. TGF-β can target the SLUG and SNAIL pathway and increase the invasion of cancer cells. Activation of *SLUG*, *SNAIL* and *ZEB* genes leads to inhibition/repression of E-cadherin, consequently inducing an EMT.

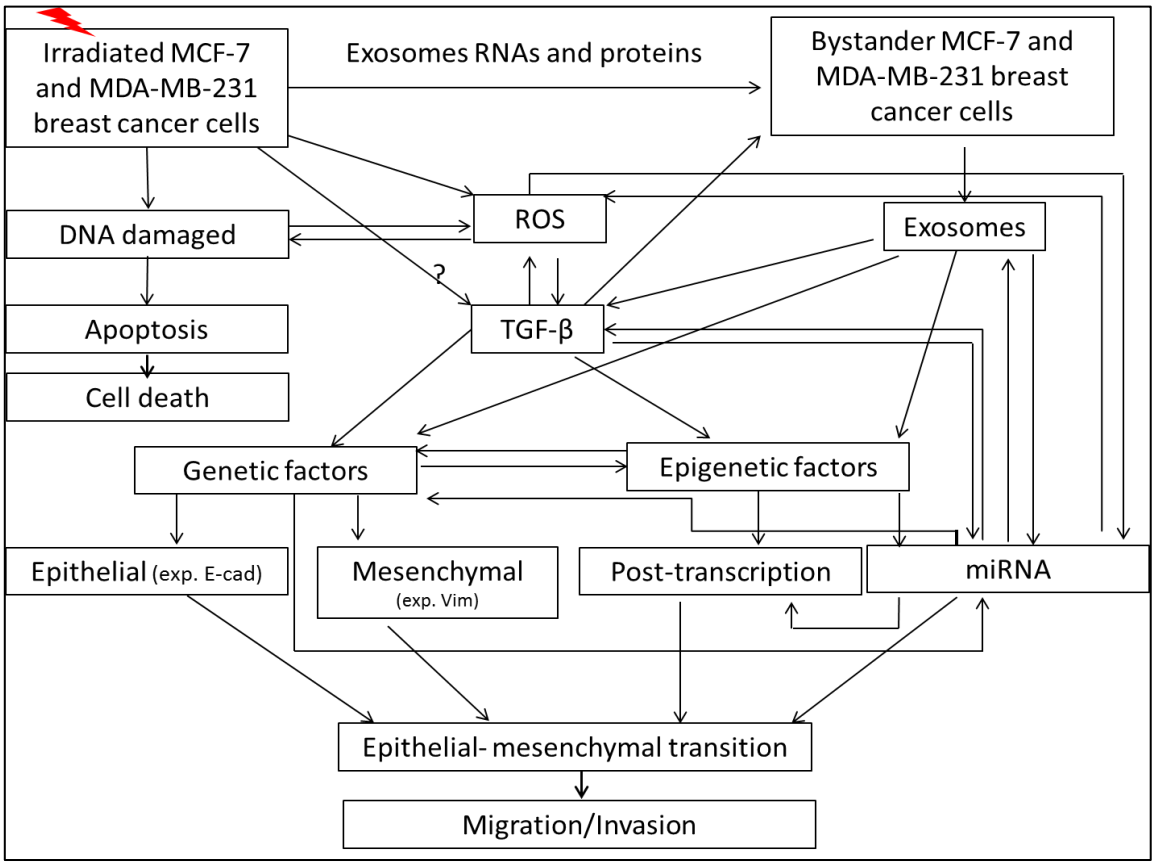


*Figure 6.1 A schematic diagram showing the possible mechanisms of migration/invasion of MCF-7 and MDA-MB-231 breast cancer cells following X-irradiation.*

Moreover, TGF-β could target other pathways that involve vimentin, E-cadherin and miRNA. This study showed that TGF-β is associated with increased vimentin and miR-9f expression and reduction in miR-30a and E-cadherin in MDA-MB-231 breast cancer cells. Meanwhile, the current study showed that the expression of TGF-β was associated with increased expression of miR-9f and vimentin and reduction in the expression of miR-200b and E-cadherin in MCF-7 cells.

These outcomes support the results of other studies. Cheng *et al.* (2012), reported that miR-30a could downregulate vimentin, inhibit EMT and reduce migration and invasion of both Hs578T and MDA-MB-231 breast cancer cells. Recent evidence has supported the finding, Yang *et al.* (2018b) demonstrated that miR-30a could downregulate TGF-β and inhibit metastasis of laryngeal carcinoma. Therefore, it can be suggested that X-irradiation may be able to inhibit expression of miR-30a in MDA-MB-231 cells, thereby causing an increase in TGF-β which ultimately results in activation of the SLUG/SNAIL pathway and

increase invasion of MDA-MB-231 breast cancer cells. Alternatively, miR-30a may target vimentin directly and prevent translation of vimentin mRNA to protein, resulting in repression of the invasion of breast cancer cells. It can be suggested that X-irradiation can downregulate miR-30a leading to an increase in the invasion of MDA-MB-231 breast cancer cells.

It has been reported that a functional role of miRNA is maintaining the balance of protein level in cells, either by blocking translation of mRNA or degrading protein (Cheng *et al.*, 2012). The downregulation of miR-30a following IR can be understood in the following way; miR-30a could target the vimentin gene in the 3' untranslated region of vimentin and prevent transcriptions of vimentin, resulting in a downregulation of vimentin protein (Cheng *et al.*, 2012). Another possible mechanism could involve miR-30a in the invasion of breast cancer cells by regulation of TGFβ expression. The current data in Section 4.2.10 and 4.2.17 showed an increase in the level of miR-30a and decreased in the level of TGF-β protein in MCF-7 following exosome transfer comparison to the TGF-β gene expression.

Meanwhile, a decrease in the level of miR-30a in MDA-MB-231 cells was associated with upregulation of the TGF-β gene and protein expression. Therefore, it could be suggested that exosomes derived from ICCM regulate expression of miR-30a and that could influence downregulation/upregulation of TGFβ and promote invasion of cancer cells. This suggestion supported by evidence by Zhou *et al.* (2013); they demonstrated that upregulation of miR-30a was associated with downregulation of TGF-β and inhibition of EMT of HMRSV 5, a human peritoneal mesothelial cell line.

In MCF-7 cells, X-irradiation induces ROS and subsequently increases expression of TGF-β, leading to inhibition of the miR-200 family as a result of decreased expression of E-cadherin, i.e. negative feedback from miR-200 downregulation of E-cadherin box genes (Kim *et al.*, 2014; Kurata *et al.*, 2018). Inhibition of miR-200 ultimately leads to increased invasion of breast cancer cells. Moreover, miR-9f has been reported to inhibit the expression of E-cadherin (Ma *et al.*, 2010). Therefore, X-irradiation induces expression of miR-9f, thereby

inhibiting E-cadherin, resulting in an increase in the invasive capacity of cancer cells.

From the current data, it can be suggested that X-irradiation either induces or inhibits expression of miRNA which activates several factors, including TGF-β and vimentin and leads to the promotion of invasiveness of breast cancer cells. However, the mechanisms controlling the induction or inhibition of miRNA are still obscure and require further study.

The results of qPCR, Figures (4.10 and 5.19) and the western blot assay, Figures 4.11 and 5.20, confirm the presence of miRNA and TGF-β in the exosomes that were isolated from irradiated and unirradiated cells. The expression of TGF-β gene was significantly higher following IR in both cell lines. However, the relative amount of TGF-β protein in MDA-MB-231 cells was higher than MCF-7, as presented in Figures 5.10 and 3.20, respectively. A possible mechanism that could explain the relationship between TGF-β, miRNA and invasion could be proposed as the following. It has been reported that miR-30a targets TGF-β, either through degradation of the protein or inhibition of translation of mRNA to protein (Yang *et al.*, 2018a). Therefore, an increase in miR-30a in MCF-7 cells following IR can reduce the significant induction of TGF-β protein comparison to the significant induction of TGF-β gene expression, as shown in Figure 4.9, 4.10 and 4.11. Meanwhile, downregulation of miR-30a in MDA-MB-231 cells keeps the level of TGF-β constant in terms of expression or protein as presented in Figures 5.17, 5.19 and 5.20.

Changes in the level of TGF-β in the exosomes derived from ICCM and that was associated with an increased in the invasive capacity of breast cancer cells, which confirm the role of the non-targeted effect of X-radiation / exosome bystander effects in breast cancer cells invasion and metastasis.

## 6.5: The role of GalNAc glycans in the invasion of breast cancer cells following IR

Data in Figures 3.18 and 5.8 showed that IR promotes expression of *GalNAc-T6* gene. This gene codes for the GalNAc-T6 enzyme, which is responsible for adding a GalNAc monosaccharide to the Serine (Ser) or Threonine (Thr) amino acid of a protein residue at the initiation of O-linked glycosylation. The current

data showed an increase in the expression of *GalNAc-T6* was associated with an increase in HPA positivity in MCF-7 and MDA-MB-231 breast cancer cells following X-irradiation. Increase in the HPA positivity was also associated with an increase in the number of invasive cells in both cell lines following irradiation or exosome transfer, as shown in Figures 3.14 and 5.5. Therefore, It could be suggested that GalNAc-glycans, recognised by HPA, may have a role in the invasion of cells through the Matrigel.

It has previously been reported that HPA-positive MCF-7 and ZR-75-1 breast cancer cells were more adhesive to endothelial monolayers (Bapu *et al.*, 2016). Meanwhile, Brooks and Hall (2002) showed there was no significant change in the adhesion of breast cancer cells to a Matrigel layer in a co-culture system following masking of the HPA-binding ligand using HPA lectin. However, the current data suggested there is a link between HPA positivity and the invasion and adhesion of breast cancer cells. The contradictory data can be explained in different ways. Firstly, although Brooks and Hall (2002) showed a non-significant change in the number of adhesive and invasive cells following masking the HPA-binding ligand, their data showed a decrease in the number of invasive cells in three breast cancer cell lines MDA-MB-434, MDA-MB-468 and ZR-75-1 when the HPA-binding glycans were masked. Secondly, the concentration of HPA (1 μg/ml) used by Brooks and Hall (2002) might be not sufficient to mask the HPA-binding glycan. Thirdly, the current study investigated the invasion capacity of MCF-7 and MDA-MB-231 breast cancer cells following IR, and that could induce specific factors, which can lead to increase in the invasion of these cells following irradiation. In this instance, IR promotes invasiveness capacity of irradiated cells, and that was associated with an increase in HPA positive cells. An increase in the HPA positivity could result from an increase in the GalNAc-T6, as shown in Figures 3.18 and 5.8.

Moreover, IR could increase expression of ST6GalNAc-1, which is responsible for adding sialic acid to the glycan and may cause an increase in the adhesion and invasion of cancer cells to the Matrigel. It has been reported that IR can promote expression of ST6GalNAc-1, and also an increase the number of adhesion and invasion of SW 480 colorectal cancer cells to the Matrigel in a co-

culture system (Lee *et al.*, 2010). They showed that SW 480 colorectal cancer cells that were exposed to 3.81 γ rays demonstrate an increase in sialylation of βI integrin and also adhesion of these cells to ECM components such as collagen, laminin and fibronectin.

The relationship between HPA positivity and the invasiveness of MDA-MB-231 and MCF-7 cell lines are is not completely clear. In other words, are HPA positive cells more invasive than HPA negative cells or *vice versa*? Thus, it was hypothesised that the physiological activity of cells could play a crucial role in the HPA positivity and negativity. Therefore, further experiments were set up using the Matrigel transwell co-culture system without irradiation.

As can be seen in Figure 3.9, it was difficult to count the HPA positive and negative MCF-7 cells in the upper surface of the Matrigel, and that may have given inaccurate results. Therefore, MDA-MB-231 cells were considered the best candidate to explore the role of HPA positivity and negativity in the invasiveness of breast cancer cells. There was a difference of around 80% in the proportion of HPA positive and negative cells between the upper and lower faces of the insert. Initially (after 4 hours), the percentage of HPA negative MDA-MB-231 cells was shown to have 5 fold than the positive cells in the lower face of the insert membrane. However, over time, the percentage of HPA negative cells decreased in preference to a gradual rise in the positively labelled cells, increased from 20% to approximately 40% after 8 hours incubation and this level was further maintained at subsequent time-points, as shown in Figure 5.2. As described later, HPA can detect GalNAc glycan. Therefore, data suggested the possible involvements of GalNAc glycan in the mechanism of cancer invasion. Cells can initially express a high level of GalNAc glycan and use it to attach to the top of the Matrigel membrane (upper layer of the insert) but over time this is then reduced to enable the cells to move and pass through the insert membrane. HPA positivity can be switched on and off during the cancer cell invasiveness mechanism.

However, the mechanisms underlying the control of glycosylation are still poorly understood. Data in Figures 3.18, 4.7, 5.8 and 5.15 confirmed the elevation of GalNAc-T6 expression post-X-irradiation or exosome transfer in both cell lines. The current data also showed an association between the HPA positive cells, as

shown in Figures 3.14, 4.5, 5.5 and 5.13, and GalNAc-T6 expression, as shown in Figures 3.18  4.7, 5.8 and 5.15. The results suggest that the increase in the HPA positive cells is due to an increase in the level of GalNAc-T6 following irradiation or following exosome transfer. It has been reported that initiation of O-linked glycosylation and biosynthesis of mucin-1 glycosylation is often controlled by the GalNAc-Ts family of enzymes (Bennett *et al.*, 2012). GalNAc-Ts including, GalNAc-T6, catalyse the synthesis of Tn antigen. In normal cells, Tn antigen is always elongated to form a range of normal O-glycans, as described in Section 1.5.3. However, alterations in glycosylation have been reported in cancer tissues (Oliveira-Ferrer, Legler and Milde-Langosch, 2017). It has been well reported that Tn antigen is highly expressed in more than 90% of breast cancer tissues, and it is also associated with high metastatic potential (Bennett *et al.*, 1999a; Freire *et al.*, 2004; Banford and Timson, 2017). Tn antigen can be detected using HPA lectin as described in Section 1.5.7. The current study can be considered as the first study to show the relationship between the increases in the level of GalNAc-T6 expression, HPA labelling and invasion of MCF-7 and MDA-MB-231 human breast cancer cells following X-irradiation. It could suggest that the increase of GalNAc-T6 expression may cause an increase in the level of Tn antigen and consequently increase in the HPA positivity. Increase in the level of Tn antigen may disturb adhesion of cancer cells to each other and promote invasion of breast cancer. It has been reported that re-localisation of GalNAc-Ts from Golgi apparatus to the endoplasmic reticulum (ER) associated with an increase in the level of Tn antigen in 7 breast cancer cell lines, including MDA-MB-231 (Gill *et al.*, 2013). They also showed an increase in the ER-ppGalNAc-T2 which is normally expressed in non-metastatic cancer cells and is associated with greater adhesion of cells to Matrigel. Meanwhile, GalNAc-T6 is reported to be more highly expressed in LSI74T metastatic colon cancer cells (Lavrsen *et al.*, 2018).

A characteristic of cancer cells is that they have immature O-glycans, such as Tn and sTn epitopes. The presence of these types of antigens is usually associated with poor prognosis of cancers (Brooks and Hall, 2002; Radhakrishnan *et al.*, 2014b) as described in detail in Section 1.5.3 and 1.5.9. ppGalNAc-Ts have been reported to have an important role in cell signalling, pro-protein processing and adhesion (Gessner *et al.*, 1993). The GalNAc-T6 seems to be expressed in most

types of cancer, including breast cancer (Berois *et al.*, 2006). Moreover, GalNAc-T6 may also be involved in TGF-β-induced EMT. Data from the current study showed an increase in the level of TGF-β to be associated with an increase in vimentin and a decrease in E-cadherin expression, also associated with an increase in the level of HPA positive cells. The work also demonstrated an increase in GalNAc-T6 expression in 2 Gy irradiated cells and the ICCM exosome treated cells compared to unirradiated cells or 0 Gy exosome treated cells, respectively. Results suggest that cells undergoing EMT showed a high level of vimentin and low level of E-cadherin and that was associated with an increase in the TGF-β and GalNAc-T6 gene expression. These ideas are supported by accumulating evidence that TGF-β and GalNAc-T6 have a crucial role in EMT and invasion of cancer cells. Freire-de-Lima *et al.* (2011) demonstrated that WPE and PNT1a human epithelial prostate cancer cell lines exhibit mesenchymal markers and up-regulation of oncofetal fibronectin expression when they are treated with TGF-β. Moreover, they demonstrated that changes in the morphology of cells were associated with an upregulation of GalNAc-T6 expression. It has also been reported that GalNAc-T6 is often involved in the induction of EMT, causing potential metastasis of mammary epithelial (Park *et al.*, 2011) and pancreatic cancer cells (Tarhan *et al.*, 2016).

Therefore, the high expression of GalNAc-T6 can increase the Tn antigen on cell surface proteins. Elevation in the Tn antigen can be detected by HPA binding. However, the mechanisms underlying the induction of GalNAc-T6 post-irradiation are not fully understood and need further studies.

To confirm the results of EMT markers (E-cadherin and vimentin) and CSCs markers (CD44 and CD24) a colourimetric base reading of positive and negative cells undertaken by a flow cytometry assay was used. The results of this assay confirmed that IR caused a decrease in the level of E-cadherin positivity and induced vimentin, as they are EMT markers. However, further, improvement may be to target other markers which could involve in EMT. For example, target other epithelial markers such as MUC-1 and cytokeratin, and mesenchymal markers including N-cadherin and β-catenin. In the argument of cancer stem cells markers it possible to target aldehyde dehydrogenase-1, CD133 (Szarynska *et al.*, 2018).

However, ALDH-1 and CD133 were found in CSC and normal stem cells (Vander Griend *et al.*, 2008; Tomita *et al.*, 2016).

## 6.6 Limitation of the current study

In the current study, a wide range of techniques was used to determine the role of IR on the invasive capacity of breast cancer cells. In this context, advantages and disadvantages have arisen. Immunocytochemistry and Biotinylated lectin techniques seem to be simple. Nevertheless, several factors are critical for the outcome, including the handling, preparation of the slides and interpretation of quantitative results. For example, long sample fixation time can lead to losing the antigenicity. The temperature of the laboratory can additionally alter the results of immunocytochemistry or Biotinylated lectin assays, as both are enzymatically based methods. Thus, the laboratory move, which was undertaken between the first and second experiments could affect some of parameters, (cool to a warmer laboratory). Moreover, nonspecific binding of avidin to the endogenous biotin visualised as a pale brown background, a problem in earlier experiments, represents the main limitation of biotinylated lectin. This problem was resolved by using endogenous peroxide blocking kit (Vector, SP-6000), and also running negative control (cells were not labelled with primary antibody), and positive control (cells showed positive results to HPA and primary antibody). Furthermore, it could be better to determine the activity of cancer cells following inhibition of GalNAc enzymes before X-irradiation. The method could also be further improved by using the protein-based fluorescent sensor assay prior to cell irradiation (Song, Bachert and Linstedt, 2016). The latter assay can determine the activity of GalNAc transferase in living cancer cells following inhibition of GalNAc enzymes.

Another critical issue of immunocytochemistry may come from the interpretation of the qualitative data. The positivity of EMT markers was based on the presence or absence of the brown colour substance reaction product within the cells. However, the decision often based on the location of brown colour within the cells; whether it is in the cytoplasm, nucleus or both?, which can be considered as a problematic issue in terms of immunocytochemistry (EMT) analysis, as has been reported by Radotra, ‘accordingly, the scientist argued about the clear definition of positive and negative results’ of EMT markers (Radotra *et al.*, 1994).

In contrast, recently, a considerable number of studies have confirmed that using the microscope and visual judgement can be considered a reliable method of the analysis of positivity and negativity of cells (Alonso-Alconada *et al.*, 2012; Jeeravongpanich *et al.*, 2014; Li *et al.*, 2017d).The results of immunocytochemistry and flow cytometry to detect the negative and positive cells are more likely to be qualitative rather than quantitative. In addition, flow cytometry showed the results of all cells rather than providing the identity of the distribution of molecules within the cell. Therefore, for future work, it may be interesting to present the data of flow cytometry in parallel with high-resolution imaging of living cells using a confocal microscope.

Accordingly, to confirm the change in the level of EMT markers, qPCR assay was applied to investigate the expression of E-cadherin and vimentin, as well as other transcription factors such as TGF-β and others, Table (2-2). These factors could play a crucial role in the invasion of cancer cells. However, these factors are not the only main players involved in EMT change of irradiated cells. For example, an increase in N-cadherin and β-catenin expression can induce EMT in neoplastic laryngeal carcinoma (Zhu *et al.*, 2018). Build up the network of factors involved in the invasion of cancer cells following IR needs further studies to understand the behaviour of cancer cells following irradiation. The critical issue about the results of qPCR may come from the fact that is not all transcript gene results can be converted to the protein. In fact, some of mRNA can be blocked by specific miRNA thereby preventing translation to protein. Moreover, some artefact of qPCR may be the result of technical error i.e. during transfer samples and reagents to 96 well plates, which could give a critical variation in the qPCR reading from one well to another. However, the variation of reading linked to the pipetting could be minimised by calculating the volume of cDNA/gDNA in the qPCR master mix to 40% of total reaction volume of master mix including a non-template control (Taylor *et al.*, 2019). Furthermore, to reduce the other artefact results, variable controls were run in parallel to the samples. To investigate a primer dimer, non-template control for each primer was run. To assess there is no contamination of gDNA in the isolated RNA, no reverse transcription control was also applied. RNA extraction and cDNA formation and storage could be a critical issue in qPCR results (Bustin *et al.*, 2015). However, the proper choice of

RNA extraction kit and direct production of cDNA and high quality of storage could also minimize the background contamination which could alter the validity of qPCR results (Kim *et al.*, 2007; Bustin *et al.*, 2015).

To confirm the results of qPCR, western blot was carried out to investigate the level of vimentin, E-cadherin and TGF-β proteins, as these proteins represent the main target in this study. However, the other factors, such as high expression of MMP-9 was detected by qPCR in this study, which could play a crucial role in the invasion of cancer cells (Brown, Recht and Strober, 2017), however, it needs to be confirmed by Western blot.

On the other hand, running a Western blot alone may be not enough to confirm the change in the level of proteins following irradiation. Thus, it would be advantageous to run a Coomassie Stain with Western blot in parallel to investigate whether the protein-loaded was equal amounts in each well (Welinder and Ekblad, 2011). However, this step has also some limitation by pipetting error. Therefore, further, an improvement would be to use a more sensitive technique such as enzyme-linked immune-sorbent assay (ELISA) to measure the level of proteins following irradiation. Though, using the ELISA technique could be useful with tiny amounts of protein such as enzymes. However, to determine the actual band of protein, western blot could be the best assay to follow (Frost *et al.*, 1998).

Centrifugation has routinely been used as a conventional method for exosomes isolation. Though, there are several other methods which could be used in its place. These include chemical isolation (polymer-based participation), HPLC + centrifugation, differential centrifugation and affinity beads (Zhang *et al.*, 2014). In this study, a combination of methods was used for exosome isolation and purification. Filtration + centrifugation + size-based chromatography was used to obtain purify and sterilise exosomes. Therefore, the yield of exosomes was low, and that was a critical issue compared to other methods. This method could be useful for isolating of exosomes from cell culture media, but it could be less efficient of investigating exosomal proteins from small samples. However, isolation of exosomes using combination method yields pure, sterilised and homogenous population of exosomes. Nevertheless, each method of exosome

isolation has advantages and disadvantages, and each method could be the best for a certain purpose of using. However, ultracentrifugation and size exclusion methods, which do not require incorporation of an extra compound to facilitate the pure exosomes isolation represent the optimum method for exosomes isolation (Li *et al.*, 2017b; Boriachek *et al.*, 2018).

The exosomal miRNA could have an impact on cancer cells invasion. Therefore, certain types of miRNAs were chosen to investigate the role of exosomal miRNA on the cancer cells invasion. However, it would be interesting if the whole hierarchy of exosomal miRNA would be investigated using miRNA microarray (Jiang *et al.*, 2013). Conversely, Camarillo and co-authors reported that qPCR can be considered as a good method for detection expression of specific miRNAs (Camarillo, Swerdel and Hart, 2011).

Moreover, using 3D dimension matrigel could be a useful technique to investigate the invasion of cancer cells *in vitro*. However, the matrigel represents four components of the basement membrane. The four components are clearly not the same component and structure barrier between the cancer cells and bloodstream. Therefore, an improved method would be to investigate the ability of breast cancer cells to invade other organs *in vivo*, for example using a mouse model. Three types of model have been used to investigate the metastasis of cancer cells *in vivo*, allograft, xenograft, and genetically engineered mouse model (GEMM). Allograph is a technique, which can transplant cells or organ from one animal to another animal in the same species. A xenograft is transplant cells or organ from organism to other organisms in different species. Meanwhile, GEMM is a mouse with altered genome using genetic engineering techniques, including gene mutation, deletion and editing (Zhou *et al.*, 2014). In this context, Gomez-Cuadrado *et al.* (2017) reported that using mouse models facilitates monitoring the interaction between the stromal cell in the site of the primary tumour, which could promote cancer cells invasion and metastasis. For example, tumour associated macrophage (TAM) are the most abundant cells in the site of cancer, which promote secretion of epidermal growth factor (EGF). The latter can activate the EGF receptor, and enhance the motility, invasion and metastasis of cancer cells *in vivo* (Zhou *et al.*, 2014).

Although these models have given understanding to the essential aspect of cancer biology including the complexity of invasion and metastasis; nevertheless, it is difficult to mimic metastasis of cancer cells in human, due to the lack of tissue specificity site and immune system problem (Kersten *et al.*, 2017). In addition, another limitation of GEMM is the low incidence of metastasis of cancer cells (Kabeer *et al.*, 2016).

Although this study was shown in parts to have limitations, it did show an increase in the invasiveness of cancer cells following irradiation, which could ultimately have future implications for further study of applied therapeutics of cancer.

## 6.7: Conclusion

The findings described in this thesis demonstrate that

1- A single therapeutic dose of X-irradiation can induce invasion of breast cancer cells by regulating EMT related factors, which are frequently associated with changes in glycosylation seen in GalNAc-T6 expression and HPA positivity.

2- Exosomes derived from irradiated cells that irradiated with a therapeutic dose of X-irradiation can increase the invasive capacity of unirradiated breast cancer cells.

3- MDA-MB-231 basal breast cancer cells have a greater invasive capacity than MCF-7 luminal breast cancer cells.

4- Exosomes derived from irradiated and unirradiated cancer cells can carry and transfer TGF-β and miRNA, which significantly influenced the invasion of breast cancer cells.

## 6.8: Future work

The relationship between IR, exosomes and cancer cell invasion needs more investigation and analysis. Unfortunately, at present, time and financial issues prevent this study from extending to involve miRNA microarray and proteomic techniques. These techniques can scan miRNAs and proteins that could be affected by irradiation and have an impact on cancer metastasis, as many types of proteins and miRNAs can be involved in the mechanisms of IR-induced

invasiveness, including structural, binding, enzyme regulating proteins, hydrolyses and transferases (Harris et al., 2015).

Furthermore, this study showed that IR increases HPA positivity and also increases the expression of GalNAc-T6, and that was associated with an increase in the invasion of cancer cells. However, the mechanisms that lead to the increased expression of GalNAc-T6 following X-irradiation are not fully understood and need further studies.

Moreover, there is a significant correlation between TGF-β, TWIST and other transcription factors that examined in this study such as vimentin, E-cadherin and ppGalNAc-1 and the invasion of breast cancer cells. Extension of this study to knock out the genes and proteins which could have an impact on the invasion of breast cancer cells would be extremely worthwhile. TGF-β protein plays a crucial role in the invasion of cancer cells.

However, due to the limitation of time in this current study, the downstream pathways that could involve in the invasion of cancer cells have not been explored. Further studies could explain all the mechanisms involved in the invasion of cancer cells such as TGF-β – ALIX pathway, TGF-β- MAPK/ERK pathway and TGF-β- Mitogen-Activated Protein Kinase Pathways.

Furthermore, exosomal TGF-β exhibit 2 bands, latent 46 kDa and active 12 kDa, ionising irradiation was shown to increase the active TGF-β in the exosomes rather than cells. Further experiments on the role of the active TGF-β exosome in cancer invasion and metastasis are warranted.

It has been well documented that cancer cell environment is hypoxic (Kidd, Shumaker and Ridge, 2014). Therefore, it would be interesting to explore the effect of hypoxia on invasive capacity and exosome secretion and measure associated EMT and glycosylation markers. A pilot study has been undertaken in this context. Therefore, repeating the study under the optimum hypoxic conditions in the hypoxic work station is highly recommended.

# References


Acheson, A., Sunshine, J. L. and Rutishauser, U. (1991) 'NCAM polysialic acid can regulate both cell-cell and cell-substrate interactions', *J Cell Biol,* 114(1), pp. 143-53.

Al-Hajj, M., Wicha, M. S., Benito-Hernandez, A., Morrison, S. J. and Clarke, M. F. (2003) 'Prospective identification of tumorigenic breast cancer cells', *Proc Natl Acad Sci U S A,* 100(7), pp. 3983-8. doi: 10.1073/pnas.0530291100.

Al-Mayah, A., Bright, S., Chapman, K., Irons, S., Luo, P., Carter, D., Goodwin, E. and Kadhim, M. (2015) 'The non-targeted effects of radiation are perpetuated by exosomes', *Mutat Res,* 772, pp. 38-45. doi: 10.1016/j.mrfmmm.2014.12.007.

Al-Mayah, A. H., Irons, S. L., Pink, R. C., Carter, D. R. and Kadhim, M. A. (2012) 'Possible role of exosomes containing RNA in mediating nontargeted effect of ionizing radiation', *Radiat Res,* 177(5), pp. 539-45.

Almeida, A. and Kolarich, D. (2016) 'The promise of protein glycosylation for personalised medicine', *Biochim Biophys Acta,* 1860(8), pp. 1583-95. doi: 10.1016/j.bbagen.2016.03.012.

Alonso-Alconada, D., Alvarez, A., Lacalle, J. and Hilario, E. (2012) 'Histological study of the protective effect of melatonin on neural cells after neonatal hypoxia-ischemia', *Histol Histopathol,* 27(6), pp. 771-83. doi: 10.14670/HH-27.771.

Altadill, T., Campoy, I., Lanau, L., Gill, K., Rigau, M., Gil-Moreno, A., Reventos, J., Byers, S., Colas, E. and Cheema, A. K. (2016) 'Enabling Metabolomics Based Biomarker Discovery Studies Using Molecular Phenotyping of Exosome-Like Vesicles', *PLoS One,* 11(3), pp. e0151339. doi: 10.1371/journal.pone.0151339.

Amo, L., Tamayo-Orbegozo, E., Maruri, N., Eguizabal, C., Zenarruzabeitia, O., Rinon, M., Arrieta, A., Santos, S., Monge, J., Vesga, M. A., Borrego, F. and Larrucea, S. (2014) 'Involvement of platelet-tumor cell interaction in immune evasion. Potential role of podocalyxin-like protein 1', *Front Oncol,* 4, pp. 245. doi: 10.3389/fonc.2014.00245.

An, Y., Gao, S., Zhao, W. C., Qiu, B. A., Xia, N. X., Zhang, P. J. and Fan, Z. P. (2018) 'Transforming growth factor-beta and peripheral regulatory cells are negatively correlated with the overall survival of hepatocellular carcinoma', *World J Gastroenterol,* 24(25), pp. 2733-2740. doi: 10.3748/wjg.v24.i25.2733.

Andarawewa, K. L., Erickson, A. C., Chou, W. S., Costes, S. V., Gascard, P., Mott, J. D., Bissell, M. J. and Barcellos-Hoff, M. H. (2007) 'Ionizing radiation predisposes nonmalignant human mammary epithelial cells to undergo transforming growth factor beta induced epithelial to mesenchymal transition', *Cancer Res,* 67(18), pp. 8662-70. doi: 10.1158/0008-5472.CAN-07-1294.

Annes, J. P., Munger, J. S. and Rifkin, D. B. (2003) 'Making sense of latent TGFbeta activation', *J Cell Sci,* 116(Pt 2), pp. 217-24.

Anzenberg, V., Chandiramani, S. and Coderre, J. A. (2008) 'LET-dependent bystander effects caused by irradiation of human prostate carcinoma cells with X rays or alpha particles', *Radiat Res,* 170(4), pp. 467-76.

Arab, M. R., Salari, S., Karimi, M. and Mofidpour, H. (2010) 'Lectin histochemical study of cell surface glycoconjugate in gastric carcinoma using helix pomatia agglutinin', *Acta Med Iran,* 48(4), pp. 209-13.

Arora, S., Heyza, J. R., Chalfin, E. C., Ruch, R. J. and Patrick, S. M. (2018) 'Gap Junction Intercellular Communication Positively Regulates Cisplatin Toxicity by Inducing DNA Damage through Bystander Signaling', *Cancers (Basel),* 10(10). doi: 10.3390/cancers10100368.

Arscott, W. T., Tandle, A. T., Zhao, S., Shabason, J. E., Gordon, I. K., Schlaff, C. D., Zhang, G., Tofilon, P. J. and Camphausen, K. A. (2013) 'Ionizing radiation and glioblastoma

exosomes: implications in tumor biology and cell migration', *Transl Oncol,* 6(6), pp. 638-48.

Asiedu, M. K., Beauchamp-Perez, F. D., Ingle, J. N., Behrens, M. D., Radisky, D. C. and Knutson, K. L. (2014) 'AXL induces epithelial-to-mesenchymal transition and regulates the function of breast cancer stem cells', *Oncogene,* 33(10), pp. 1316-24. doi: 10.1038/onc.2013.57.

Atienzar-Aroca, S., Flores-Bellver, M., Serrano-Heras, G., Martinez-Gil, N., Barcia, J. M., Aparicio, S., Perez-Cremades, D., Garcia-Verdugo, J. M., Diaz-Llopis, M., Romero, F. J. and Sancho-Pelluz, J. (2016) 'Oxidative stress in retinal pigment epithelium cells increases exosome secretion and promotes angiogenesis in endothelial cells', *J Cell Mol Med,* 20(8), pp. 1457-66. doi: 10.1111/jcmm.12834.

Azzam, E. I., Colangelo, N. W., Domogauer, J. D., Sharma, N. and de Toledo, S. M. (2016) 'Is Ionizing Radiation Harmful at any Exposure? An Echo That Continues to Vibrate', *Health Phys,* 110(3), pp. 249-51. doi: 10.1097/HP.0000000000000450.

Azzam, E. I., de Toledo, S. M., Gooding, T. and Little, J. B. (1998) 'Intercellular communication is involved in the bystander regulation of gene expression in human cells exposed to very low fluences of alpha particles', *Radiat Res,* 150(5), pp. 497-504.

Azzam, E. I., de Toledo, S. M., Gooding, T. and Little, J. B. (1998 ) 'Intercellular communication is involved in the bystander regulation of gene expression in human cells exposed to very low fluences of alpha particles', *Radiation Reaserch,* 150(5), pp. 497-504.

Azzam, E. I., de Toledo, S. M. and Little, J. B. (2003) 'Oxidative metabolism, gap junctions and the ionizing radiation-induced bystander effect', *Oncogene,* 22(45), pp. 7050-7. doi: 10.1038/sj.onc.1206961.

Azzam, E. I., De Toledo, S. M., Spitz, D. R. and Little, J. B. (2002) 'Oxidative metabolism modulates signal transduction and micronucleus formation in bystander cells from alpha-particle-irradiated normal human fibroblast cultures', *Cancer Res,* 62(19), pp. 5436-42.

Azzam, E. I., Jay-Gerin, J. P. and Pain, D. (2012) 'Ionizing radiation-induced metabolic oxidative stress and prolonged cell injury', *Cancer Lett,* 327(1-2), pp. 48-60. doi: 10.1016/j.canlet.2011.12.012.

Ballarini, F., Alloni, D., Facoetti, A., Mairani, A., Nano, R. and Ottolenghi, A. (2006) 'Modelling radiation-induced bystander effect and cellular communication', *Radiat Prot Dosimetry,* 122(1-4), pp. 244-51. doi: 10.1093/rpd/ncl446.

Banford, S. and Timson, D. J. (2017) 'UDP-N-acetyl-D-galactosamine:polypeptide N-acetylgalactosaminyltransferase- 6 (pp-GalNAc-T6): Role in Cancer and Prospects as a Drug Target', *Curr Cancer Drug Targets,* 17(1), pp. 53-61.

Banyard, J. and Bielenberg, D. R. (2015) 'The role of EMT and MET in cancer dissemination', *Connect Tissue Res,* 56(5), pp. 403-13. doi: 10.3109/03008207.2015.1060970.

Bapu, D., Runions, J., Kadhim, M. and Brooks, S. A. (2016) 'N-acetylgalactosamine glycans function in cancer cell adhesion to endothelial cells: A role for truncated O-glycans in metastatic mechanisms', *Cancer Lett,* 375(2), pp. 367-374. doi: 10.1016/j.canlet.2016.03.019.

Barnhill, R. L. and Lugassy, C. (2004) 'Angiotropic malignant melanoma and extravascular migratory metastasis: description of 36 cases with emphasis on a new mechanism of tumour spread', *Pathology,* 36(5), pp. 485-90. doi: 10.1080/00313020412331282708.

Bartek, J. and Lukas, J. (2003) 'Chk1 and Chk2 kinases in checkpoint control and cancer', *Cancer Cell,* 3(5), pp. 421-9.

Barthel, S. R., Gavino, J. D., Descheny, L. and Dimitroff, C. J. (2007) 'Targeting selectins and selectin ligands in inflammation and cancer', *Expert Opin Ther Targets,* 11(11), pp. 1473-91. doi: 10.1517/14728222.11.11.1473.

Baskar, R., Lee, K. A., Yeo, R. and Yeoh, K. W. (2012) 'Cancer and radiation therapy: current advances and future directions', *Int J Med Sci,* 9(3), pp. 193-9. doi: 10.7150/ijms.3635.

Bassaganas, S., Carvalho, S., Dias, A. M., Perez-Garay, M., Ortiz, M. R., Figueras, J., Reis, C. A., Pinho, S. S. and Peracaula, R. (2014) 'Pancreatic cancer cell glycosylation regulates cell adhesion and invasion through the modulation of alpha2beta1 integrin and E-cadherin function', *PLoS One,* 9(5), pp. e98595. doi: 10.1371/journal.pone.0098595.

Basu, D., Tian, L., Wang, W., Bobbs, S., Herock, H., Travers, A. and Showalter, A. M. (2015) 'A small multigene hydroxyproline-O-galactosyltransferase family functions in arabinogalactan-protein glycosylation, growth and development in Arabidopsis', *BMC Plant Biol,* 15, pp. 295. doi: 10.1186/s12870-015-0670-7.

Baum, B., Settleman, J. and Quinlan, M. P. (2008) 'Transitions between epithelial and mesenchymal states in development and disease', *Semin Cell Dev Biol,* 19(3), pp. 294-308. doi: 10.1016/j.semcdb.2008.02.001.

Beavon, I. R. (2000) 'The E-cadherin-catenin complex in tumour metastasis: structure, function and regulation', *Eur J Cancer,* 36(13 Spec No), pp. 1607-20.

Bennett, E. P., Hassan, H., Hollingsworth, M. A. and Clausen, H. (1999a) 'A novel human UDP-N-acetyl-D-galactosamine:polypeptide N-acetylgalactosaminyltransferase, GalNAc-T7, with specificity for partial GalNAc-glycosylated acceptor substrates', *FEBS Lett,* 460(2), pp. 226-30.

Bennett, E. P., Hassan, H., Mandel, U., Hollingsworth, M. A., Akisawa, N., Ikematsu, Y., Merkx, G., van Kessel, A. G., Olofsson, S. and Clausen, H. (1999b) 'Cloning and characterization of a close homologue of human UDP-N-acetyl-alpha-D-galactosamine:Polypeptide N-acetylgalactosaminyltransferase-T3, designated GalNAc-T6. Evidence for genetic but not functional redundancy', *J Biol Chem,* 274(36), pp. 25362-70.

Bennett, E. P., Mandel, U., Clausen, H., Gerken, T. A., Fritz, T. A. and Tabak, L. A. (2012) 'Control of mucin-type O-glycosylation: a classification of the polypeptide GalNAc-transferase gene family', *Glycobiology,* 22(6), pp. 736-56. doi: 10.1093/glycob/cwr182.

Bensimon, J., Altmeyer-Morel, S., Benjelloun, H., Chevillard, S. and Lebeau, J. (2013) 'CD24(-/low) stem-like breast cancer marker defines the radiation-resistant cells involved in memorization and transmission of radiation-induced genomic instability', *Oncogene,* 32(2), pp. 251-8. doi: 10.1038/onc.2012.31.

Berger, S. and Lavie, L. (2011) 'Endothelial progenitor cells in cardiovascular disease and hypoxia--potential implications to obstructive sleep apnea', *Transl Res,* 158(1), pp. 1-13. doi: 10.1016/j.trsl.2010.12.008.

Bernal, D., Trelis, M., Montaner, S., Cantalapiedra, F., Galiano, A., Hackenberg, M. and Marcilla, A. (2014) 'Surface analysis of Dicrocoelium dendriticum. The molecular characterization of exosomes reveals the presence of miRNAs', *J Proteomics,* 105, pp. 232-41. doi: 10.1016/j.jprot.2014.02.012.

Berois, N., Mazal, D., Ubillos, L., Trajtenberg, F., Nicolas, A., Sastre-Garau, X., Magdelenat, H. and Osinaga, E. (2006) 'UDP-N-acetyl-D-galactosamine: polypeptide N-acetylgalactosaminyltransferase-6 as a new immunohistochemical breast cancer marker', *J Histochem Cytochem,* 54(3), pp. 317-28. doi: 10.1369/jhc.5A6783.2005.

Bianco, N. R., Kim, S. H., Morelli, A. E. and Robbins, P. D. (2007) 'Modulation of the immune response using dendritic cell-derived exosomes', *Methods Mol Biol,* 380, pp. 443-55. doi: 10.1007/978-1-59745-395-0_28.

Bianco, N. R., Kim, S. H., Ruffner, M. A. and Robbins, P. D. (2009) 'Therapeutic effect of exosomes from indoleamine 2,3-dioxygenase-positive dendritic cells in collagen-induced arthritis and delayed-type hypersensitivity disease models', *Arthritis Rheum,* 60(2), pp. 380-9. doi: 10.1002/art.24229.

Biedermann, K. A., Sun, J. R., Giaccia, A. J., Tosto, L. M. and Brown, J. M. (1991) 'scid mutation in mice confers hypersensitivity to ionizing radiation and a deficiency in DNA double-strand break repair', *Proc Natl Acad Sci U S A,* 88(4), pp. 1394-7.

Blasiak, J., Hoser, G., Bialkowska-Warzecha, J., Pawlowska, E. and Skorski, T. (2015) 'Reactive Oxygen Species and Mitochondrial DNA Damage and Repair in BCR-ABL1 Cells Resistant to Imatinib', *Biores Open Access,* 4(1), pp. 334-42. doi: 10.1089/biores.2015.0022.

Bockhorn, M., Jain, R. K. and Munn, L. L. (2007) 'Active versus passive mechanisms in metastasis: do cancer cells crawl into vessels, or are they pushed?', *Lancet Oncol,* 8(5), pp. 444-8. doi: 10.1016/S1470-2045(07)70140-7.

Bodnarchuk, I. A. (2003) '[Modeling viability of mammalian cells exposed to ionizing radiation with different linear energy transfer]', *Biofizika,* 48(3), pp. 474-9.

Boelens, M. C., Wu, T. J., Nabet, B. Y., Xu, B., Qiu, Y., Yoon, T., Azzam, D. J., Twyman-Saint Victor, C., Wiemann, B. Z., Ishwaran, H., Ter Brugge, P. J., Jonkers, J., Slingerland, J. and Minn, A. J. (2014) 'Exosome transfer from stromal to breast cancer cells regulates therapy resistance pathways', *Cell,* 159(3), pp. 499-513. doi: 10.1016/j.cell.2014.09.051.

Boo, L., Ho, W. Y., Mohd Ali, N., Yeap, S. K., Ky, H., Chan, K. G., Yin, W. F., Satharasinghe, D. A., Liew, W. C., Tan, S. W., Cheong, S. K. and Ong, H. K. (2017) 'Phenotypic and microRNA transcriptomic profiling of the MDA-MB-231 spheroid-enriched CSCs with comparison of MCF-7 microRNA profiling dataset', *PeerJ,* 5, pp. e3551. doi: 10.7717/peerj.3551.

Boriachek, K., Islam, M. N., Moller, A., Salomon, C., Nguyen, N. T., Hossain, M. S. A., Yamauchi, Y. and Shiddiky, M. J. A. (2018) 'Biological Functions and Current Advances in Isolation and Detection Strategies for Exosome Nanovesicles', *Small,* 14(6). doi: 10.1002/smll.201702153.

Borrego-Soto, G., Ortiz-Lopez, R. and Rojas-Martinez, A. (2015) 'Ionizing radiation-induced DNA injury and damage detection in patients with breast cancer', *Genet Mol Biol,* 38(4), pp. 420-32. doi: 10.1590/S1415-475738420150019.

Boscher, C., Dennis, J. W. and Nabi, I. R. (2011) 'Glycosylation, galectins and cellular signaling', *Curr Opin Cell Biol,* 23(4), pp. 383-92. doi: 10.1016/j.ceb.2011.05.001.

Brinton, L. T., Sloane, H. S., Kester, M. and Kelly, K. A. (2015) 'Formation and role of exosomes in cancer', *Cell Mol Life Sci,* 72(4), pp. 659-71. doi: 10.1007/s00018-014-1764-3.

Brooks, S. A. (2000) 'The involvement of Helix pomatia lectin (HPA) binding N-acetylgalactosamine glycans in cancer progression', *Histol Histopathol,* 15(1), pp. 143-58. doi: 10.14670/HH-15.143.

Brooks, S. A., Carter, T. M., Royle, L., Harvey, D. J., Fry, S. A., Kinch, C., Dwek, R. A. and Rudd, P. M. (2008) 'Altered glycosylation of proteins in cancer: what is the potential for new anti-tumour strategies', *Anticancer Agents Med Chem,* 8(1), pp. 2-21.

Brooks, S. A. and Hall, D. M. (2002) 'Investigations into the potential role of aberrant N-acetylgalactosamine glycans in tumour cell interactions with basement membrane components', *Clin Exp Metastasis,* 19(6), pp. 487-93.

Brooks, S. A. and Leathem, A. J. (1991) 'Prediction of lymph node involvement in breast cancer by detection of altered glycosylation in the primary tumour', *Lancet,* 338(8759), pp. 71-4.

Brooks, S. A., Leathem, A. J., Camplejohn, R. S. and Gregory, W. (1993) 'Markers of prognosis in breast cancer--the relationship between binding of the lectin HPA and histological grade, SPF, and ploidy', *Breast Cancer Res Treat,* 25(3), pp. 247-56.

Brooks, S. A., Lomax-Browne, H. J., Carter, T. M., Kinch, C. E. and Hall, D. M. (2010) 'Molecular interactions in cancer cell metastasis', *Acta Histochem,* 112(1), pp. 3-25. doi: 10.1016/j.acthis.2008.11.022.

Brown, J. M., Recht, L. and Strober, S. (2017) 'The Promise of Targeting Macrophages in Cancer Therapy', *Clin Cancer Res,* 23(13), pp. 3241-3250. doi: 10.1158/1078-0432.CCR-16-3122.

Bryant, P. E., Jones, C., Armstrong, G., Frankenberg-Schwager, M. and Frankenberg, D. (2003) 'Induction of chromatid breaks by carbon K-shell ultrasoft X rays', *Radiat Res,* 159(2), pp. 247-50.

Brzozowa, M., Wyrobiec, G., Kolodziej, I., Sitarski, M., Matysiak, N., Reichman-Warmusz, E., Zaba, M. and Wojnicz, R. (2015) 'The aberrant overexpression of vimentin is linked to a more aggressive status in tumours of the gastrointestinal tract', *Prz Gastroenterol,* 10(1), pp. 7-11. doi: 10.5114/pg.2014.47502.

Bustin, S., Dhillon, H. S., Kirvell, S., Greenwood, C., Parker, M., Shipley, G. L. and Nolan, T. (2015) 'Variability of the reverse transcription step: practical implications', *Clin Chem,* 61(1), pp. 202-12. doi: 10.1373/clinchem.2014.230615.

Cabrera, M. C., Hollingsworth, R. E. and Hurt, E. M. (2015) 'Cancer stem cell plasticity and tumor hierarchy', *World J Stem Cells,* 7(1), pp. 27-36. doi: 10.4252/wjsc.v7.i1.27.

Camarillo, C., Swerdel, M. and Hart, R. P. (2011) 'Comparison of microarray and quantitative real-time PCR methods for measuring MicroRNA levels in MSC cultures', *Methods Mol Biol,* 698, pp. 419-29. doi: 10.1007/978-1-60761-999-4_30.

Campbell, I. D. and Humphries, M. J. (2011) 'Integrin structure, activation, and interactions', *Cold Spring Harb Perspect Biol,* 3(3). doi: 10.1101/cshperspect.a004994.

Cancer Research, U. K. (2018) *Breast cancer statistics avilable at (https://www.cancerresearchuk.org/health-professional/cancer-statistics/statistics-by-cancer-type/breast-cancer)* 193-9 (Accessed: 3/10/2018).

Cappello, F., Barresi, E. and Martorana, A. (2000) '[Breast cancer and lymph node metastasis: relation of lymph node dimensions and metastasis]', *Pathologica,* 92(1), pp. 5-8.

Carvalho, A. S., Harduin-Lepers, A., Magalhaes, A., Machado, E., Mendes, N., Costa, L. T., Matthiesen, R., Almeida, R., Costa, J. and Reis, C. A. (2010) 'Differential expression of alpha-2,3-sialyltransferases and alpha-1,3/4-fucosyltransferases regulates the levels of sialyl Lewis a and sialyl Lewis x in gastrointestinal carcinoma cells', *Int J Biochem Cell Biol,* 42(1), pp. 80-9. doi: 10.1016/j.biocel.2009.09.010.

Casas, E., Kim, J., Bendesky, A., Ohno-Machado, L., Wolfe, C. J. and Yang, J. (2011) 'Snail2 is an essential mediator of Twist1-induced epithelial mesenchymal transition and metastasis', *Cancer Res,* 71(1), pp. 245-54. doi: 10.1158/0008-5472.CAN-10-2330.

Catterall, J. B., Jones, L. M. and Turner, G. A. (1999) 'Membrane protein glycosylation and CD44 content in the adhesion of human ovarian cancer cells to hyaluronan', *Clin Exp Metastasis,* 17(7), pp. 583-91.

Chaffer, C. L., Thompson, E. W. and Williams, E. D. (2007) 'Mesenchymal to epithelial transition in development and disease', *Cells Tissues Organs,* 185(1-3), pp. 7-19. doi: 10.1159/000101298.

Chan, S. H. and Wang, L. H. (2015) 'Regulation of cancer metastasis by microRNAs', *J Biomed Sci,* 22, pp. 9. doi: 10.1186/s12929-015-0113-7.

Chandna, S. (2004) 'Single-cell gel electrophoresis assay monitors precise kinetics of DNA fragmentation induced during programmed cell death', *Cytometry A,* 61(2), pp. 127-33. doi: 10.1002/cyto.a.20071.

Chang, L., Guo, F., Huo, B., Lv, Y., Wang, Y. and Liu, W. (2015) 'Expression and clinical significance of the microRNA-200 family in gastric cancer', *Oncol Lett,* 9(5), pp. 2317-2324. doi: 10.3892/ol.2015.3028.

Chantarasrivong, C., Ueki, A., Ohyama, R., Unga, J., Nakamura, S., Nakanishi, I., Higuchi, Y., Kawakami, S., Ando, H., Imamura, A., Ishida, H., Yamashita, F., Kiso, M. and Hashida, M. (2017) 'Synthesis and Functional Characterization of Novel Sialyl LewisX Mimic-Decorated Liposomes for E-selectin-Mediated Targeting to Inflamed Endothelial Cells', *Mol Pharm,* 14(5), pp. 1528-1537. doi: 10.1021/acs.molpharmaceut.6b00982.

Chen, J., Chang, H., Peng, X., Gu, Y., Yi, L., Zhang, Q., Zhu, J. and Mi, M. (2016) '3,6-dihydroxyflavone suppresses the epithelial-mesenchymal transition in breast cancer cells by inhibiting the Notch signaling pathway', *Sci Rep,* 6, pp. 28858. doi: 10.1038/srep28858.

Chen, M. T., Sun, H. F., Li, L. D., Zhao, Y., Yang, L. P., Gao, S. P. and Jin, W. (2018) 'Downregulation of FOXP2 promotes breast cancer migration and invasion through TGFbeta/SMAD signaling pathway', *Oncol Lett,* 15(6), pp. 8582-8588. doi: 10.3892/ol.2018.8402.

Chen, T., Guo, J., Yang, M., Zhu, X. and Cao, X. (2011) 'Chemokine-containing exosomes are released from heat-stressed tumor cells via lipid raft-dependent pathway and act as efficient tumor vaccine', *J Immunol,* 186(4), pp. 2219-28. doi: 10.4049/jimmunol.1002991.

Cheng, C. W., Wang, H. W., Chang, C. W., Chu, H. W., Chen, C. Y., Yu, J. C., Chao, J. I., Liu, H. F., Ding, S. L. and Shen, C. Y. (2012) 'MicroRNA-30a inhibits cell migration and invasion by downregulating vimentin expression and is a potential prognostic marker in breast cancer', *Breast Cancer Res Treat,* 134(3), pp. 1081-93. doi: 10.1007/s10549-012-2034-4.

Chia, J., Tham, K. M., Gill, D. J., Bard-Chapeau, E. A. and Bard, F. A. (2014) 'ERK8 is a negative regulator of O-GalNAc glycosylation and cell migration', *Elife,* 3, pp. e01828. doi: 10.7554/eLife.01828.

Chugh, S., Meza, J., Sheinin, Y. M., Ponnusamy, M. P. and Batra, S. K. (2016) 'Loss of N-acetylgalactosaminyltransferase 3 in poorly differentiated pancreatic cancer: augmented aggressiveness and aberrant ErbB family glycosylation', *Br J Cancer,* 114(12), pp. 1376-86. doi: 10.1038/bjc.2016.116.

Circu, M. L. and Aw, T. Y. (2010) 'Reactive oxygen species, cellular redox systems, and apoptosis', *Free Radic Biol Med,* 48(6), pp. 749-62. doi: 10.1016/j.freeradbiomed.2009.12.022.

Clayton, A., Al-Taei, S., Webber, J., Mason, M. D. and Tabi, Z. (2011) 'Cancer exosomes express CD39 and CD73, which suppress T cells through adenosine production', *J Immunol,* 187(2), pp. 676-83. doi: 10.4049/jimmunol.1003884.

Clayton, A., Mitchell, J. P., Court, J., Mason, M. D. and Tabi, Z. (2007) 'Human tumor-derived exosomes selectively impair lymphocyte responses to interleukin-2', *Cancer Res,* 67(15), pp. 7458-66. doi: 10.1158/0008-5472.CAN-06-3456.

Cossarizza, A. and Chang, H. D. and Radbruch, A. and Akdis, M. and Andra, I. and Annunziato, F. and Bacher, P. and Barnaba, V. and Battistini, L. and Bauer, W. M. and Baumgart, S. and Becher, B. and Beisker, W. and Berek, C. and Blanco, A. and Borsellino, G. and Boulais, P. E. and Brinkman, R. R. and Buscher, M. and Busch, D. H. and Bushnell, T. P. and Cao, X. and Cavani, A. and Chattopadhyay, P. K. and Cheng, Q. and Chow, S. and Clerici, M. and Cooke, A. and Cosma, A. and Cosmi, L. and Cumano, A. and Dang, V. D. and Davies, D. and De Biasi, S. and Del Zotto, G. and Della Bella, S. and Dellabona, P. and Deniz, G. and Dessing, M. and Diefenbach, A. and Di Santo, J. and Dieli, F. and Dolf, A. and Donnenberg, V. S. and Dorner, T. and Ehrhardt, G. R. A. and Endl, E. and Engel, P. and Engelhardt, B. and Esser, C. and Everts, B. and Dreher, A. and Falk, C. S. and Fehniger, T. A. and Filby, A. and Fillatreau, S. and Follo, M. and Forster, I. and Foster, J. and Foulds, G. A. and Frenette, P. S. and Galbraith, D. and Garbi, N. and Garcia-Godoy, M. D. and Geginat, J. and Ghoreschi, K. and Gibellini, L. and Goettlinger, C. and Goodyear, C. S. and Gori, A. and Grogan, J. and Gross, M. and Grutzkau, A. and Grummitt, D. and Hahn, J. and Hammer, Q. and Hauser, A. E. and Haviland, D. L. and Hedley, D. and Herrera, G. and Herrmann, M. and Hiepe, F. and Holland, T. and Hombrink, P. and Houston, J. P. and Hoyer, B. F. and Huang, B. and Hunter, C. A. and Iannone, A. and Jack, H. M. and Javega, B. and Jonjic, S. and Juelke, K. and Jung, S. and Kaiser, T. and Kalina, T. and Keller, B. and Khan, S. and Kienhofer, D. and Kroneis, T. and Kunkel, D. and Kurts, C. and Kvistborg, P. and Lannigan, J. and Lantz, O. and Larbi, A. and LeibundGut-Landmann, S. and Leipold, M. D. and Levings, M. K. and Litwin, V. and Liu, Y. and Lohoff, M. and Lombardi, G. and Lopez, L. and Lovett-Racke, A. and Lubberts, E. and Ludewig, B. and Lugli, E. and Maecker, H. T. and Martrus, G. and Matarese, G. and Maueroder, C. and McGrath, M. and McInnes, I. and Mei, H. E. and Melchers, F. and Melzer, S. and Mielenz, D. and Mills, K. and Mirrer, D. and Mjosberg, J. and Moore, J. and Moran, B. and Moretta, A. and

Moretta, L. and Mosmann, T. R. and Muller, S. and Muller, W. and Munz, C. and Multhoff, G. and Munoz, L. E. and Murphy, K. M. and Nakayama, T. and Nasi, M. and Neudorfl, C. and Nolan, J. and Nourshargh, S. and O'Connor, J. E. and Ouyang, W. and Oxenius, A. and Palankar, R. and Panse, I. and Peterson, P. and Peth, C. and Petriz, J. and Philips, D. and Pickl, W. and Piconese, S. and Pinti, M. and Pockley, A. G. and Podolska, M. J. and Pucillo, C. and Quataert, S. A. and Radstake, T. and Rajwa, B. and Rebhahn, J. A. and Recktenwald, D. and Remmerswaal, E. B. M. and Rezvani, K. and Rico, L. G. and Robinson, J. P. and Romagnani, C. and Rubartelli, A. and Ruckert, B. and Ruland, J. and Sakaguchi, S. and Sala-de-Oyanguren, F. and Samstag, Y. and Sanderson, S. and Sawitzki, B. and Scheffold, A. and Schiemann, M. and Schildberg, F. and Schimisky, E. and Schmid, S. A. and Schmitt, S. and Schober, K. and Schuler, T. and Schulz, A. R. and Schumacher, T. and Scotta, C. and Shankey, T. V. and Shemer, A. and Simon, A. K. and Spidlen, J. and Stall, A. M. and Stark, R. and Stehle, C. and Stein, M. and Steinmetz, T. and Stockinger, H. and Takahama, Y. and Tarnok, A. and Tian, Z. and Toldi, G. and Tornack, J. and Traggiai, E. and Trotter, J. and Ulrich, H. and van der Braber, M. and van Lier, R. A. W. and Veldhoen, M. and Vento-Asturias, S. and Vieira, P. and Voehringer, D. and Volk, H. D. and von Volkmann, K. and Waisman, A. and Walker, R. and Ward, M. D. and Warnatz, K. and Warth, S. and Watson, J. V. and Watzl, C. and Wegener, L. and Wiedemann, A. and Wienands, J. and Willimsky, G. and Wing, J. and Wurst, P. and Yu, L. and Yue, A. and Zhang, Q. and Zhao, Y. and Ziegler, S. and Zimmermann, J. (2017) 'Guidelines for the use of flow cytometry and cell sorting in immunological studies', *Eur J Immunol,* 47(10), pp. 1584-1797. doi: 10.1002/eji.201646632.

Czarnomysy, R., Surazynski, A., Poplawska, B., Rysiak, E., Pawlowska, N., Czajkowska, A., Bielawski, K. and Bielawska, A. (2017) 'Synergistic action of cisplatin and echistatin in MDA-MB-231 breast cancer cells', *Mol Cell Biochem,* 427(1-2), pp. 13-22. doi: 10.1007/s11010-016-2894-8.

Czyz, J. (2008) 'The stage-specific function of gap junctions during tumourigenesis', *Cell Mol Biol Lett,* 13(1), pp. 92-102. doi: 10.2478/s11658-007-0039-5.

d'Adda di Fagagna, F., Reaper, P. M., Clay-Farrace, L., Fiegler, H., Carr, P., Von Zglinicki, T., Saretzki, G., Carter, N. P. and Jackson, S. P. (2003) 'A DNA damage checkpoint response in telomere-initiated senescence', *Nature,* 426(6963), pp. 194-8. doi: 10.1038/nature02118.

D'Ippolito, E., Plantamura, I., Bongiovanni, L., Casalini, P., Baroni, S., Piovan, C., Orlandi, R., Gualeni, A. V., Gloghini, A., Rossini, A., Cresta, S., Tessari, A., De Braud, F., Di Leva, G., Tripodo, C. and Iorio, M. V. (2016) 'miR-9 and miR-200 Regulate PDGFRbeta-Mediated Endothelial Differentiation of Tumor Cells in Triple-Negative Breast Cancer', *Cancer Res,* 76(18), pp. 5562-72. doi: 10.1158/0008-5472.CAN-16-0140.

Dai, X., Cheng, H., Bai, Z. and Li, J. (2017) 'Breast Cancer Cell Line Classification and Its Relevance with Breast Tumor Subtyping', *J Cancer,* 8(16), pp. 3131-3141. doi: 10.7150/jca.18457.

Dai, Y. H., Tang, Y. P., Zhu, H. Y., Lv, L., Chu, Y., Zhou, Y. Q. and Huo, J. R. (2012) 'ZEB2 promotes the metastasis of gastric cancer and modulates epithelial mesenchymal transition of gastric cancer cells', *Dig Dis Sci,* 57(5), pp. 1253-60. doi: 10.1007/s10620-012-2042-6.

Dall'Olio, F. and Trere, D. (1993) 'Expression of alpha 2,6-sialylated sugar chains in normal and neoplastic colon tissues. Detection by digoxigenin-conjugated Sambucus nigra agglutinin', *Eur J Histochem,* 37(3), pp. 257-65.

Dancea, H. C., Shareef, M. M. and Ahmed, M. M. (2009) 'Role of Radiation-induced TGF-beta Signaling in Cancer Therapy', *Mol Cell Pharmacol,* 1(1), pp. 44-56.

Dausset, J., Moullec, J. and Bernard, J. (1959) 'Acquired hemolytic anemia with polyagglutinability of red blood cells due to a new factor present in normal human serum (Anti-Tn)', *Blood,* 14, pp. 1079-93.

David, C. J., Huang, Y. H., Chen, M., Su, J., Zou, Y., Bardeesy, N., Iacobuzio-Donahue, C. A. and Massague, J. (2016) 'TGF-beta Tumor Suppression through a Lethal EMT', *Cell,* 164(5), pp. 1015-30. doi: 10.1016/j.cell.2016.01.009.

de Freitas Junior, J. C. and Morgado-Diaz, J. A. (2016) 'The role of N-glycans in colorectal cancer progression: potential biomarkers and therapeutic applications', *Oncotarget,* 7(15), pp. 19395-413. doi: 10.18632/oncotarget.6283.

de Jong, M. C., Pramana, J., van der Wal, J. E., Lacko, M., Peutz-Kootstra, C. J., de Jong, J. M., Takes, R. P., Kaanders, J. H., van der Laan, B. F., Wachters, J., Jansen, J. C., Rasch, C. R., van Velthuysen, M. L., Grenman, R., Hoebers, F. J., Schuuring, E., van den Brekel, M. W. and Begg, A. C. (2010) 'CD44 expression predicts local recurrence after radiotherapy in larynx cancer', *Clin Cancer Res,* 16(21), pp. 5329-38. doi: 10.1158/1078-0432.CCR-10-0799.

Delaney, G., Jacob, S., Featherstone, C. and Barton, M. (2005) 'The role of radiotherapy in cancer treatment: estimating optimal utilization from a review of evidence-based clinical guidelines', *Cancer,* 104(6), pp. 1129-37. doi: 10.1002/cncr.21324.

Demetriou, M., Nabi, I. R., Coppolino, M., Dedhar, S. and Dennis, J. W. (1995) 'Reduced contact-inhibition and substratum adhesion in epithelial cells expressing GlcNAc-transferase V', *J Cell Biol,* 130(2), pp. 383-92.

Dennis, J. W., Granovsky, M. and Warren, C. E. (1999a) 'Glycoprotein glycosylation and cancer progression', *Biochim Biophys Acta,* 1473(1), pp. 21-34.

Dennis, J. W., Granovsky, M. and Warren, C. E. (1999b) 'Protein glycosylation in development and disease', *Bioessays,* 21(5), pp. 412-21. doi: 10.1002/(SICI)1521-1878(199905)21:5<412::AID-BIES8>3.0.CO;2-5.

Devine, D. J., Rostas, J. W., Metge, B. J., Das, S., Mulekar, M. S., Tucker, J. A., Grizzle, W. E., Buchsbaum, D. J., Shevde, L. A. and Samant, R. S. (2014) 'Loss of N-Myc interactor promotes epithelial-mesenchymal transition by activation of TGF-beta/SMAD signaling', *Oncogene,* 33(20), pp. 2620-8. doi: 10.1038/onc.2013.215.

Dhasarathy, A., Phadke, D., Mav, D., Shah, R. R. and Wade, P. A. (2011) 'The transcription factors Snail and Slug activate the transforming growth factor-beta signaling pathway in breast cancer', *PLoS One,* 6(10), pp. e26514. doi: 10.1371/journal.pone.0026514.

Dhawan, A., Kohandel, M., Hill, R. and Sivaloganathan, S. (2014) 'Tumour control probability in cancer stem cells hypothesis', *PLoS One,* 9(5), pp. e96093. doi: 10.1371/journal.pone.0096093.

Diehn, M., Cho, R. W., Lobo, N. A., Kalisky, T., Dorie, M. J., Kulp, A. N., Qian, D., Lam, J. S., Ailles, L. E., Wong, M., Joshua, B., Kaplan, M. J., Wapnir, I., Dirbas, F. M., Somlo, G., Garberoglio, C., Paz, B., Shen, J., Lau, S. K., Quake, S. R., Brown, J. M., Weissman, I. L. and Clarke, M. F. (2009) 'Association of reactive oxygen species levels and radioresistance in cancer stem cells', *Nature,* 458(7239), pp. 780-3. doi: 10.1038/nature07733.

Ding, L. H., Shingyoji, M., Chen, F., Hwang, J. J., Burma, S., Lee, C., Cheng, J. F. and Chen, D. J. (2005) 'Gene expression profiles of normal human fibroblasts after exposure to ionizing radiation: a comparative study of low and high doses', *Radiat Res,* 164(1), pp. 17-26.

Dizdaroglu, M. and Jaruga, P. (2012) 'Mechanisms of free radical-induced damage to DNA', *Free Radic Res,* 46(4), pp. 382-419. doi: 10.3109/10715762.2011.653969.

Dizdaroglu, M., Jaruga, P., Birincioglu, M. and Rodriguez, H. (2002) 'Free radical-induced damage to DNA: mechanisms and measurement', *Free Radic Biol Med,* 32(11), pp. 1102-15.

dos-Santos, P. B., Zanetti, J. S., Vieira-de-Mello, G. S., Rego, M. B., Ribeiro-Silva, A. A. and Beltrao, E. I. (2014) 'Lectin histochemistry reveals SNA as a prognostic carbohydrate-dependent probe for invasive ductal carcinoma of the breast: a clinicopathological and immunohistochemical auxiliary tool', *Int J Clin Exp Pathol,* 7(5), pp. 2337-49.

Du, Z., Qin, R., Wei, C., Wang, M., Shi, C., Tian, R. and Peng, C. (2011) 'Pancreatic cancer cells resistant to chemoradiotherapy rich in "stem-cell-like" tumor cells', *Dig Dis Sci,* 56(3), pp. 741-50. doi: 10.1007/s10620-010-1340-0.

Dwek, M. V., Ross, H. A., Streets, A. J., Brooks, S. A., Adam, E., Titcomb, A., Woodside, J. V., Schumacher, U. and Leathem, A. J. (2001) 'Helix pomatia agglutinin lectin-binding oligosaccharides of aggressive breast cancer', *Int J Cancer,* 95(2), pp. 79-85.

Fan, Q., Qiu, M. T., Zhu, Z., Zhou, J. H., Chen, L., Zhou, Y., Gu, W., Wang, L. H., Li, Z. N., Xu, Y., Cheng, W. W., Wu, D. and Bao, W. (2015) 'Twist induces epithelial-mesenchymal transition in cervical carcinogenesis by regulating the TGF-beta/Smad3 signaling pathway', *Oncol Rep,* 34(4), pp. 1787-94. doi: 10.3892/or.2015.4143.

Fang, X., Zheng, P., Tang, J. and Liu, Y. (2010) 'CD24: from A to Z', *Cell Mol Immunol,* 7(2), pp. 100-3. doi: 10.1038/cmi.2009.119.

Feldman, L. E., Shin, K. C., Natale, R. B. and Todd, R. F., 3rd (1991) 'Beta 1 integrin expression on human small cell lung cancer cells', *Cancer Res,* 51(4), pp. 1065-70.

Fortuna-Costa, A., Gomes, A. M., Kozlowski, E. O., Stelling, M. P. and Pavao, M. S. (2014) 'Extracellular galectin-3 in tumor progression and metastasis', *Front Oncol,* 4, pp. 138. doi: 10.3389/fonc.2014.00138.

Francis-Oliveira, J., Vilar Higa, G. S., Mendonca Munhoz Dati, L., Carvalho Shieh, I. and De Pasquale, R. (2018) 'Metaplasticity in the Visual Cortex: Crosstalk Between Visual Experience and Reactive Oxygen Species', *J Neurosci,* 38(25), pp. 5649-5665. doi: 10.1523/JNEUROSCI.2617-17.2018.

Freire-de-Lima, L., Gelfenbeyn, K., Ding, Y., Mandel, U., Clausen, H., Handa, K. and Hakomori, S. I. (2011) 'Involvement of O-glycosylation defining oncofetal fibronectin in epithelial-mesenchymal transition process', *Proc Natl Acad Sci U S A,* 108(43), pp. 17690-5. doi: 10.1073/pnas.1115191108.

Freire, T., Fernandez, C., Chalar, C., Maizels, R. M., Alzari, P., Osinaga, E. and Robello, C. (2004) 'Characterization of a UDP-N-acetyl-D-galactosamine:polypeptide N-acetylgalactosaminyltransferase with an unusual lectin domain from the platyhelminth parasite Echinococcus granulosus', *Biochem J,* 382(Pt 2), pp. 501-10. doi: 10.1042/BJ20031877.

Frost, F. J., de la Cruz, A. A., Moss, D. M., Curry, M. and Calderon, R. L. (1998) 'Comparisons of ELISA and Western blot assays for detection of Cryptosporidium antibody', *Epidemiol Infect,* 121(1), pp. 205-11. doi: 10.1017/s0950268898008991.

Fukutomi, T., Itabashi, M., Tsugane, S., Yamamoto, H., Nanasawa, T. and Hirota, T. (1989) 'Prognostic contributions of Helix pomatia and carcinoembryonic antigen staining using histochemical techniques in breast carcinomas', *Jpn J Clin Oncol,* 19(2), pp. 127-34.

Galvan, J. A., Helbling, M., Koelzer, V. H., Tschan, M. P., Berger, M. D., Hadrich, M., Schnuriger, B., Karamitopoulou, E., Dawson, H., Inderbitzin, D., Lugli, A. and Zlobec, I. (2015) 'TWIST1 and TWIST2 promoter methylation and protein expression in tumor stroma influence the epithelial-mesenchymal transition-like tumor budding phenotype in colorectal cancer', *Oncotarget,* 6(2), pp. 874-85. doi: 10.18632/oncotarget.2716.

Gangopadhyay, S., Nandy, A., Hor, P. and Mukhopadhyay, A. (2013) 'Breast cancer stem cells: a novel therapeutic target', *Clin Breast Cancer,* 13(1), pp. 7-15. doi: 10.1016/j.clbc.2012.09.017.

Gerelchuluun, A., Manabe, E., Ishikawa, T., Sun, L., Itoh, K., Sakae, T., Suzuki, K., Hirayama, R., Asaithamby, A., Chen, D. J. and Tsuboi, K. (2015) 'The major DNA repair pathway after both proton and carbon-ion radiation is NHEJ, but the HR pathway is more relevant in carbon ions', *Radiat Res,* 183(3), pp. 345-56. doi: 10.1667/RR13904.1.

Gessner, P., Riedl, S., Quentmaier, A. and Kemmner, W. (1993) 'Enhanced activity of CMP-neuAc:Gal beta 1-4GlcNAc:alpha 2,6-sialyltransferase in metastasizing human colorectal tumor tissue and serum of tumor patients', *Cancer Lett,* 75(3), pp. 143-9.

Gibbs, B. F., Yasinska, I. M., Oniku, A. E. and Sumbayev, V. V. (2011) 'Effects of stem cell factor on hypoxia-inducible factor 1 alpha accumulation in human acute myeloid leukaemia and LAD2 mast cells', *PLoS One,* 6(7), pp. e22502. doi: 10.1371/journal.pone.0022502.

Gill, D. J., Tham, K. M., Chia, J., Wang, S. C., Steentoft, C., Clausen, H., Bard-Chapeau, E. A. and Bard, F. A. (2013) 'Initiation of GalNAc-type O-glycosylation in the endoplasmic reticulum promotes cancer cell invasiveness', *Proc Natl Acad Sci U S A,* 110(34), pp. E3152-61. doi: 10.1073/pnas.1305269110.

Gilles, C., Polette, M., Mestdagt, M., Nawrocki-Raby, B., Ruggeri, P., Birembaut, P. and Foidart, J. M. (2003) 'Transactivation of vimentin by beta-catenin in human breast cancer cells', *Cancer Res,* 63(10), pp. 2658-64.

Gimbrone, M. A., Jr., Leapman, S. B., Cotran, R. S. and Folkman, J. (1972) 'Tumor dormancy in vivo by prevention of neovascularization', *J Exp Med,* 136(2), pp. 261-76.

Giroldi, L. A., Bringuier, P. P., de Weijert, M., Jansen, C., van Bokhoven, A. and Schalken, J. A. (1997) 'Role of E boxes in the repression of E-cadherin expression', *Biochem Biophys Res Commun,* 241(2), pp. 453-8. doi: 10.1006/bbrc.1997.7831.

Gomez-Cuadrado, L., Tracey, N., Ma, R., Qian, B. and Brunton, V. G. (2017) 'Mouse models of metastasis: progress and prospects', *Dis Model Mech,* 10(9), pp. 1061-1074. doi: 10.1242/dmm.030403.

Graudenzi, A., Cava, C., Bertoli, G., Fromm, B., Flatmark, K., Mauri, G. and Castiglioni, I. (2017) 'Pathway-based classification of breast cancer subtypes', *Front Biosci (Landmark Ed),* 22, pp. 1697-1712.

Graves, J. A., Metukuri, M., Scott, D., Rothermund, K. and Prochownik, E. V. (2009) 'Regulation of reactive oxygen species homeostasis by peroxiredoxins and c-Myc', *J Biol Chem,* 284(10), pp. 6520-9. doi: 10.1074/jbc.M807564200.

Guarino, M. (2007) 'Epithelial-mesenchymal transition and tumour invasion', *Int J Biochem Cell Biol,* 39(12), pp. 2153-60. doi: 10.1016/j.biocel.2007.07.011.

Guerci, A. M., Dulout, F. N. and Seoane, A. I. (2004) 'DNA damage in Chinese hamster cells repeatedly exposed to low doses of X-rays', *Cytogenet Genome Res,* 104(1-4), pp. 173-7. doi: 10.1159/000077484.

Gwak, J. M., Kim, H. J., Kim, E. J., Chung, Y. R., Yun, S., Seo, A. N., Lee, H. J. and Park, S. Y. (2014) 'MicroRNA-9 is associated with epithelial-mesenchymal transition, breast cancer stem cell phenotype, and tumor progression in breast cancer', *Breast Cancer Res Treat,* 147(1), pp. 39-49. doi: 10.1007/s10549-014-3069-5.

Ha, M. and Kim, V. N. (2014) 'Regulation of microRNA biogenesis', *Nat Rev Mol Cell Biol,* 15(8), pp. 509-24. doi: 10.1038/nrm3838.

Hahn, S., Jackstadt, R., Siemens, H., Hunten, S. and Hermeking, H. (2013) 'SNAIL and miR-34a feed-forward regulation of ZNF281/ZBP99 promotes epithelial-mesenchymal transition', *EMBO J,* 32(23), pp. 3079-95. doi: 10.1038/emboj.2013.236.

Haimovitz-Friedman, A., Balaban, N., McLoughlin, M., Ehleiter, D., Michaeli, J., Vlodavsky, I. and Fuks, Z. (1994) 'Protein kinase C mediates basic fibroblast growth factor protection of endothelial cells against radiation-induced apoptosis', *Cancer Res,* 54(10), pp. 2591-7.

Hakomori, S. (1996) 'Tumor malignancy defined by aberrant glycosylation and sphingo(glyco)lipid metabolism', *Cancer Res,* 56(23), pp. 5309-18.

Hall, E. J. and Giaccia, A. J. (2012) *Radiobiology for the Radiologist.* 7th edn. Philadelphia, PA: Lippincott Williams & Wilkins.

Hall, E. J., Worgul, B. V., Smilenov, L., Elliston, C. D. and Brenner, D. J. (2006) 'The relative biological effectiveness of densely ionizing heavy-ion radiation for inducing ocular cataracts in wild type versus mice heterozygous for the ATM gene', *Radiat Environ Biophys,* 45(2), pp. 99-104. doi: 10.1007/s00411-006-0052-5.

Hallahan, D. E., Spriggs, D. R., Beckett, M. A., Kufe, D. W. and Weichselbaum, R. R. (1989) 'Increased tumor necrosis factor alpha mRNA after cellular exposure to ionizing radiation', *Proc Natl Acad Sci U S A,* 86(24), pp. 10104-7.

Hamidi, A., Song, J., Thakur, N., Itoh, S., Marcusson, A., Bergh, A., Heldin, C. H. and Landstrom, M. (2017) 'TGF-beta promotes PI3K-AKT signaling and prostate cancer cell migration through the TRAF6-mediated ubiquitylation of p85alpha', *Sci Signal,* 10(486). doi: 10.1126/scisignal.aal4186.

Hamill, K. J., Paller, A. S. and Jones, J. C. (2010) 'Adhesion and migration, the diverse functions of the laminin alpha3 subunit', *Dermatol Clin,* 28(1), pp. 79-87. doi: 10.1016/j.det.2009.10.009.

Han, L., Wang, W., Ding, W. and Zhang, L. (2017) 'MiR-9 is involved in TGF-beta1-induced lung cancer cell invasion and adhesion by targeting SOX7', *J Cell Mol Med,* 21(9), pp. 2000-2008. doi: 10.1111/jcmm.13120.

Hanahan, D. and Weinberg, R. A. (2011) 'Hallmarks of cancer: the next generation', *Cell,* 144(5), pp. 646-74. doi: 10.1016/j.cell.2011.02.013.

Handerson, T., Camp, R., Harigopal, M., Rimm, D. and Pawelek, J. (2005) 'Beta1,6-branched oligosaccharides are increased in lymph node metastases and predict poor outcome in breast carcinoma', *Clin Cancer Res,* 11(8), pp. 2969-73. doi: 10.1158/1078-0432.CCR-04-2211.

Harris, D. A., Patel, S. H., Gucek, M., Hendrix, A., Westbroek, W. and Taraska, J. W. (2015) 'Exosomes released from breast cancer carcinomas stimulate cell movement', *PLoS One,* 10(3), pp. e0117495. doi: 10.1371/journal.pone.0117495.

Hascoet, P., Chesnel, F., Le Goff, C., Le Goff, X. and Arlot-Bonnemains, Y. (2015) 'Unconventional Functions of Mitotic Kinases in Kidney Tumorigenesis', *Front Oncol,* 5, pp. 241. doi: 10.3389/fonc.2015.00241.

Hashiguchi, Y., Kasai, M., Fukuda, T., Ichimura, T., Yasui, T. and Sumi, T. (2016) 'Serum Sialyl-Tn (STN) as a Tumor Marker in Patients with Endometrial Cancer', *Pathol Oncol Res,* 22(3), pp. 501-4. doi: 10.1007/s12253-015-0030-9.

Hatzi, V. I., Laskaratou, D. A., Mavragani, I. V., Nikitaki, Z., Mangelis, A., Panayiotidis, M. I., Pantelias, G. E., Terzoudi, G. I. and Georgakilas, A. G. (2015) 'Non-targeted radiation effects in vivo: a critical glance of the future in radiobiology', *Cancer Lett,* 356(1), pp. 34-42. doi: 10.1016/j.canlet.2013.11.018.

Haugstad, K. E., Hadjialirezaei, S., Stokke, B. T., Brewer, C. F., Gerken, T. A., Burchell, J., Picco, G. and Sletmoen, M. (2016) 'Interactions of mucins with the Tn or Sialyl Tn cancer antigens including MUC1 are due to GalNAc-GalNAc interactions', *Glycobiology,* 26(12), pp. 1338-1350. doi: 10.1093/glycob/cww065.

Hauselmann, I. and Borsig, L. (2014) 'Altered tumor-cell glycosylation promotes metastasis', *Front Oncol,* 4, pp. 28. doi: 10.3389/fonc.2014.00028.

Hazan, R. B., Phillips, G. R., Qiao, R. F., Norton, L. and Aaronson, S. A. (2000) 'Exogenous expression of N-cadherin in breast cancer cells induces cell migration, invasion, and metastasis', *J Cell Biol,* 148(4), pp. 779-90.

Hazawa, M., Tomiyama, K., Saotome-Nakamura, A., Obara, C., Yasuda, T., Gotoh, T., Tanaka, I., Yakumaru, H., Ishihara, H. and Tajima, K. (2014) 'Radiation increases the cellular uptake of exosomes through CD29/CD81 complex formation', *Biochem Biophys Res Commun,* 446(4), pp. 1165-71. doi: 10.1016/j.bbrc.2014.03.067.

He, W. M., Yin, J. Q., Cheng, X. D., Lu, X., Ni, L., Xi, Y., Yin, G. D., Lu, G. Y., Sun, W. and Wei, M. G. (2018) 'Oleanolic acid attenuates TGF-β1-induced epithelial-mesenchymal transition in NRK-52E cells', *BMC Complementary and Alternative Medicine,* 18:205(205). doi: 10.17226/24743.

Hickman, A. W., Jaramillo, R. J., Lechner, J. F. and Johnson, N. F. (1994) 'Alpha-particle-induced p53 protein expression in a rat lung epithelial cell strain', *Cancer Res,* 54(22), pp. 5797-800.

Holliday, D. L. and Speirs, V. (2011) 'Choosing the right cell line for breast cancer research', *Breast Cancer Res,* 13(4), pp. 215. doi: 10.1186/bcr2889.

Hong, C. S., Funk, S., Muller, L., Boyiadzis, M. and Whiteside, T. L. (2016) 'Isolation of biologically active and morphologically intact exosomes from plasma of patients with cancer', *J Extracell Vesicles,* 5, pp. 29289. doi: 10.3402/jev.v5.29289.

Hu, W., Pei, H., Sun, F., Li, P., Nie, J., Li, B., Hei, T. K. and Zhou, G. (2018) 'Epithelial–mesenchymal transition in non-targeted lung tissues of Kunming mice exposed to X-rays is suppressed by celecoxib', *Journal of Radiation Research,* 59(5), pp. 583–587. doi: 10.1093/jrr/rry050.

Huber, M. A., Kraut, N. and Beug, H. (2005) 'Molecular requirements for epithelial-mesenchymal transition during tumor progression', *Curr Opin Cell Biol,* 17(5), pp. 548-58. doi: 10.1016/j.ceb.2005.08.001.

Hughes, C. S., Postovit, L. M. and Lajoie, G. A. (2010) 'Matrigel: a complex protein mixture required for optimal growth of cell culture', *Proteomics,* 10(9), pp. 1886-90. doi: 10.1002/pmic.200900758.

Hwang, W. L., Yang, M. H., Tsai, M. L., Lan, H. Y., Su, S. H., Chang, S. C., Teng, H. W., Yang, S. H., Lan, Y. T., Chiou, S. H. and Wang, H. W. (2011) 'SNAIL regulates interleukin-8 expression, stem cell-like activity, and tumorigenicity of human colorectal carcinoma cells', *Gastroenterology,* 141(1), pp. 279-91, 291 e1-5. doi: 10.1053/j.gastro.2011.04.008.

Iizuka, D., Sasatani, M., Barcellos-Hoff, M. H. and Kamiya, K. (2017) 'Hydrogen Peroxide Enhances TGFbeta-mediated Epithelial-to-Mesenchymal Transition in Human Mammary Epithelial MCF-10A Cells', *Anticancer Res,* 37(3), pp. 987-995. doi: 10.21873/anticanres.11408.

Iliopoulos, D., Hirsch, H. A. and Struhl, K. (2009) 'An epigenetic switch involving NF-kappaB, Lin28, Let-7 MicroRNA, and IL6 links inflammation to cell transformation', *Cell,* 139(4), pp. 693-706. doi: 10.1016/j.cell.2009.10.014.

Itkonen, H. M. and Mills, I. G. (2013) 'N-linked glycosylation supports cross-talk between receptor tyrosine kinases and androgen receptor', *PLoS One,* 8(5), pp. e65016. doi: 10.1371/journal.pone.0065016.

Jeeravongpanich, P., Chuangsuwanich, T., Komoltri, C. and Ratanawichitrasin, A. (2014) 'Histologic evaluation of sentinel and non-sentinel axillary lymph nodes in breast cancer by multilevel sectioning and predictors of non-sentinel metastasis', *Gland Surg,* 3(1), pp. 2-13. doi: 10.3978/j.issn.2227-684X.2014.02.01.

Jella, K. K., Garcia, A., McClean, B., Byrne, H. J. and Lyng, F. M. (2013) 'Cell death pathways in directly irradiated cells and cells exposed to medium from irradiated cells', *Int J Radiat Biol,* 89(3), pp. 182-90. doi: 10.3109/09553002.2013.734942.

Jella, K. K., Moriarty, R., McClean, B., Byrne, H. J. and Lyng, F. M. (2018) 'Reactive oxygen species and nitric oxide signaling in bystander cells', *PLoS One,* 13(4), pp. e0195371. doi: 10.1371/journal.pone.0195371.

Jella, K. K., Rani, S., O'Driscoll, L., McClean, B., Byrne, H. J. and Lyng, F. M. (2014) 'Exosomes are involved in mediating radiation induced bystander signaling in human keratinocyte cells', *Radiat Res,* 181(2), pp. 138-45. doi: 10.1667/RR13337.1.

Jelonek, K., Widlak, P. and Pietrowska, M. (2016) 'The Influence of Ionizing Radiation on Exosome Composition, Secretion and Intercellular Communication', *Protein Pept Lett,* 23(7), pp. 656-63.

Jelonek, K., Wojakowska, A., Marczak, L., Muer, A., Tinhofer-Keilholz, I., Lysek-Gladysinska, M., Widlak, P. and Pietrowska, M. (2015) 'Ionizing radiation affects protein composition of exosomes secreted in vitro from head and neck squamous cell carcinoma', *Acta Biochim Pol,* 62(2), pp. 265-72. doi: 10.18388/abp.2015_970.

Jia, Y., Wu, D., Yun, F., Shi, L., Luo, N., Liu, Z., Shi, Y., Sun, Q., Jiang, L., Wang, S. and Du, M. (2014) 'Transforming growth factor-beta1 regulates epithelial-mesenchymal transition in association with cancer stem-like cells in a breast cancer cell line', *Int J Clin Exp Med,* 7(4), pp. 865-72.

Jiang, L. H., Yang, N. Y., Yuan, X. L., Zou, Y. J., Jiang, Z. Q., Zhao, F. M., Chen, J. P., Wang, M. Y. and Lu, D. X. (2013) 'Microarray Analysis of mRNA and MicroRNA Expression Profile Reveals the Role of beta -Sitosterol-D-glucoside in the Proliferation of Neural Stem Cell', *Evid Based Complement Alternat Med,* 2013, pp. 360302. doi: 10.1155/2013/360302.

Jin, J., Krishnamachary, B., Mironchik, Y., Kobayashi, H. and Bhujwalla, Z. M. (2016) 'Phototheranostics of CD44-positive cell populations in triple negative breast cancer', *Sci Rep,* 6, pp. 27871. doi: 10.1038/srep27871.

Jing, X., Cui, X., Liang, H., Hao, C., Yang, Z., Li, X., Yang, X. and Han, C. (2018) 'CD24 is a Potential Biomarker for Prognosis in Human Breast Carcinoma', *Cell Physiol Biochem,* 48(1), pp. 111-119. doi: 10.1159/000491667.

Ju, T., Brewer, K., D'Souza, A., Cummings, R. D. and Canfield, W. M. (2002) 'Cloning and expression of human core 1 beta1,3-galactosyltransferase', *J Biol Chem,* 277(1), pp. 178-86. doi: 10.1074/jbc.M109060200.

Kabeer, F., Beverly, L. J., Darrasse-Jeze, G. and Podsypanina, K. (2016) 'Methods to Study Metastasis in Genetically Modified Mice', *Cold Spring Harb Protoc,* 2016(2), pp. pdb top069948. doi: 10.1101/pdb.top069948.

Kadhim, M., Salomaa, S., Wright, E., Hildebrandt, G., Belyakov, O. V., Prise, K. M. and Little, M. P. (2013) 'Non-targeted effects of ionising radiation--implications for low dose risk', *Mutat Res,* 752(2), pp. 84-98. doi: 10.1016/j.mrrev.2012.12.001.

Kadhim, M. A. and Hill, M. A. (2015) 'Non-targeted effects of radiation exposure: recent advances and implications', *Radiat Prot Dosimetry,* 166(1-4), pp. 118-24. doi: 10.1093/rpd/ncv167.

Kadhim, M. A., Lorimore, S. A., Townsend, K. M., Goodhead, D. T., Buckle, V. J. and Wright, E. G. (1995) 'Radiation-induced genomic instability: delayed cytogenetic aberrations and apoptosis in primary human bone marrow cells', *Int J Radiat Biol,* 67(3), pp. 287-93.

Kadhim, M. A., Macdonald, D. A., Goodhead, D. T., Lorimore, S. A., Marsden, S. J. and Wright, E. G. (1992) 'Transmission of chromosomal instability after plutonium alpha-particle irradiation', *Nature,* 355(6362), pp. 738-40. doi: 10.1038/355738a0.

Kadhim, M. A., Marsden, S. J. and Wright, E. G. (1998) 'Radiation-induced chromosomal instability in human fibroblasts: temporal effects and the influence of radiation quality', *Int J Radiat Biol,* 73(2), pp. 143-8.

Kahlert, C. and Kalluri, R. (2013) 'Exosomes in tumor microenvironment influence cancer progression and metastasis', *J Mol Med (Berl),* 91(4), pp. 431-7. doi: 10.1007/s00109-013-1020-6.

Kahlert, C., Melo, S. A., Protopopov, A., Tang, J., Seth, S., Koch, M., Zhang, J., Weitz, J., Chin, L., Futreal, A. and Kalluri, R. (2014) 'Identification of double-stranded genomic DNA spanning all chromosomes with mutated KRAS and p53 DNA in the serum exosomes of patients with pancreatic cancer', *J Biol Chem,* 289(7), pp. 3869-75. doi: 10.1074/jbc.C113.532267.

Kalluri, R. and Weinberg, R. A. (2009) 'The basics of epithelial-mesenchymal transition', *J Clin Invest,* 119(6), pp. 1420-8. doi: 10.1172/JCI39104.

Kanasugi, Y., Hamada, N., Wada, S., Funayama, T., Sakashita, T., Kakizaki, T., Kobayashi, Y. and Takakura, K. (2007) 'Role of DNA-PKcs in the bystander effect after low- or high-LET irradiation', *Int J Radiat Biol,* 83(2), pp. 73-80.

Kaup, S., Grandjean, V., Mukherjee, R., Kapoor, A., Keyes, E., Seymour, C. B., Mothersill, C. E. and Schofield, P. N. (2006) 'Radiation-induced genomic instability is associated with DNA

methylation changes in cultured human keratinocytes', *Mutat Res,* 597(1-2), pp. 87-97. doi: 10.1016/j.mrfmmm.2005.06.032.
Kaur, S., Singh, G. and Kaur, K. (2014) 'Cancer stem cells: an insight and future perspective', *J Cancer Res Ther,* 10(4), pp. 846-52. doi: 10.4103/0973-1482.139264.
Kawakami, K., Fujita, Y., Kato, T., Mizutani, K., Kameyama, K., Tsumoto, H., Miura, Y., Deguchi, T. and Ito, M. (2015) 'Integrin beta4 and vinculin contained in exosomes are potential markers for progression of prostate cancer associated with taxane-resistance', *Int J Oncol,* 47(1), pp. 384-90. doi: 10.3892/ijo.2015.3011.
Kersten, K., de Visser, K. E., van Miltenburg, M. H. and Jonkers, J. (2017) 'Genetically engineered mouse models in oncology research and cancer medicine', *EMBO Mol Med,* 9(2), pp. 137-153. doi: 10.15252/emmm.201606857.
Kidd, M. E., Shumaker, D. K. and Ridge, K. M. (2014) 'The role of vimentin intermediate filaments in the progression of lung cancer', *Am J Respir Cell Mol Biol,* 50(1), pp. 1-6. doi: 10.1165/rcmb.2013-0314TR.
Kilic, E., Tennstedt, P., Hogner, A., Lebok, P., Sauter, G., Bokemeyer, C., Izbicki, J. R. and Wilczak, W. (2016) 'The zinc-finger transcription factor SALL4 is frequently expressed in human cancers: association with clinical outcome in squamous cell carcinoma but not in adenocarcinoma of the esophagus', *Virchows Arch,* 468(4), pp. 483-92. doi: 10.1007/s00428-016-1908-y.
Kim, J., Wu, L., Zhao, J. C., Jin, H. J. and Yu, J. (2014) 'TMPRSS2-ERG gene fusions induce prostate tumorigenesis by modulating microRNA miR-200c', *Oncogene,* 33(44), pp. 5183-92. doi: 10.1038/onc.2013.461.
Kim, K. H., Choi, J. S., Kim, J. M., Choi, Y. L., Shin, Y. K., Lee, H. C., Seong, I. O., Kim, B. K., Chae, S. W. and Kim, S. H. (2009) 'Enhanced CD24 expression in endometrial carcinoma and its expression pattern in normal and hyperplastic endometrium', *Histol Histopathol,* 24(3), pp. 309-16. doi: 10.14670/HH-24.309.
Kim, S. J., Dix, D. J., Thompson, K. E., Murrell, R. N., Schmid, J. E., Gallagher, J. E. and Rockett, J. C. (2007) 'Effects of storage, RNA extraction, genechip type, and donor sex on gene expression profiling of human whole blood', *Clin Chem,* 53(6), pp. 1038-45. doi: 10.1373/clinchem.2006.078436.
Kim, S. J., Shin, J. Y., Lee, K. D., Bae, Y. K., Sung, K. W., Nam, S. J. and Chun, K. H. (2012) 'MicroRNA let-7a suppresses breast cancer cell migration and invasion through downregulation of C-C chemokine receptor type 7', *Breast Cancer Res,* 14(1), pp. R14. doi: 10.1186/bcr3098.
Kishikawa, T., Ghazizadeh, M., Sasaki, Y. and Springer, G. F. (1999) 'Specific role of T and Tn tumor-associated antigens in adhesion between a human breast carcinoma cell line and a normal human breast epithelial cell line', *Jpn J Cancer Res,* 90(3), pp. 326-32.
Kitajima, K., Varki, N. and Sato, C. (2015) 'Advanced Technologies in Sialic Acid and Sialoglycoconjugate Analysis', *Top Curr Chem,* 367, pp. 75-103. doi: 10.1007/128_2013_458.
Klungland, A. and Bjelland, S. (2007) 'Oxidative damage to purines in DNA: role of mammalian Ogg1', *DNA Repair (Amst),* 6(4), pp. 481-8. doi: 10.1016/j.dnarep.2006.10.012.
Kobayashi, T., Kim, H., Liu, X., Sugiura, H., Kohyama, T., Fang, Q., Wen, F. Q., Abe, S., Wang, X., Atkinson, J. J., Shipley, J. M., Senior, R. M. and Rennard, S. I. (2014) 'Matrix metalloproteinase-9 activates TGF-beta and stimulates fibroblast contraction of collagen gels', *Am J Physiol Lung Cell Mol Physiol,* 306(11), pp. L1006-15. doi: 10.1152/ajplung.00015.2014.
Koike, T., Kimura, N., Miyazaki, K., Yabuta, T., Kumamoto, K., Takenoshita, S., Chen, J., Kobayashi, M., Hosokawa, M., Taniguchi, A., Kojima, T., Ishida, N., Kawakita, M., Yamamoto, H., Takematsu, H., Suzuki, A., Kozutsumi, Y. and Kannagi, R. (2004) 'Hypoxia induces adhesion molecules on cancer cells: A missing link between Warburg effect and

induction of selectin-ligand carbohydrates', *Proc Natl Acad Sci U S A,* 101(21), pp. 8132-7. doi: 10.1073/pnas.0402088101.

Kokkinos, M. I., Wafai, R., Wong, M. K., Newgreen, D. F., Thompson, E. W. and Waltham, M. (2007) 'Vimentin and epithelial-mesenchymal transition in human breast cancer--observations in vitro and in vivo', *Cells Tissues Organs,* 185(1-3), pp. 191-203. doi: 10.1159/000101320.

Kondaveeti, Y., Guttilla Reed, I. K. and White, B. A. (2015) 'Epithelial-mesenchymal transition induces similar metabolic alterations in two independent breast cancer cell lines', *Cancer Lett,* 364(1), pp. 44-58. doi: 10.1016/j.canlet.2015.04.025.

Konge, J., Leteurtre, F., Goislard, M., Biard, D., Morel-Altmeyer, S., Vaurijoux, A., Gruel, G., Chevillard, S. and Lebeau, J. (2018) 'Breast cancer stem cell-like cells generated during TGFbeta-induced EMT are radioresistant', *Oncotarget,* 9(34), pp. 23519-23531. doi: 10.18632/oncotarget.25240.

Korsching, E., Packeisen, J., Liedtke, C., Hungermann, D., Wulfing, P., van Diest, P. J., Brandt, B., Boecker, W. and Buerger, H. (2005) 'The origin of vimentin expression in invasive breast cancer: epithelial-mesenchymal transition, myoepithelial histogenesis or histogenesis from progenitor cells with bilinear differentiation potential?', *J Pathol,* 206(4), pp. 451-7. doi: 10.1002/path.1797.

Kovacs, K., Decatur, C., Toro, M., Pham, D. G., Liu, H., Jing, Y., Murray, T. G., Lampidis, T. J. and Merchan, J. R. (2016) '2-Deoxy-Glucose Downregulates Endothelial AKT and ERK via Interference with N-Linked Glycosylation, Induction of Endoplasmic Reticulum Stress, and GSK3beta Activation', *Mol Cancer Ther,* 15(2), pp. 264-75. doi: 10.1158/1535-7163.MCT-14-0315.

Kowal, J., Arras, G., Colombo, M., Jouve, M., Morath, J. P., Primdal-Bengtson, B., Dingli, F., Loew, D., Tkach, M. and Thery, C. (2016) 'Proteomic comparison defines novel markers to characterize heterogeneous populations of extracellular vesicle subtypes', *Proc Natl Acad Sci U S A,* 113(8), pp. E968-77. doi: 10.1073/pnas.1521230113.

Kozlowski, J., Kozlowska, A. and Kocki, J. (2015) 'Breast cancer metastasis - insight into selected molecular mechanisms of the phenomenon', *Postepy Hig Med Dosw (Online),* 69, pp. 447-51.

Krakhmal, N. V., Zavyalova, M. V., Denisov, E. V., Vtorushin, S. V. and Perelmuter, V. M. (2015) 'Cancer Invasion: Patterns and Mechanisms', *Acta Naturae,* 7(2), pp. 17-28.

Krause, M., Dubrovska, A., Linge, A. and Baumann, M. (2017) 'Cancer stem cells: Radioresistance, prediction of radiotherapy outcome and specific targets for combined treatments', *Adv Drug Deliv Rev,* 109, pp. 63-73. doi: 10.1016/j.addr.2016.02.002.

Kruger, S., Abd Elmageed, Z. Y., Hawke, D. H., Worner, P. M., Jansen, D. A., Abdel-Mageed, A. B., Alt, E. U. and Izadpanah, R. (2014) 'Molecular characterization of exosome-like vesicles from breast cancer cells', *BMC Cancer,* 14, pp. 44. doi: 10.1186/1471-2407-14-44.

Kumar, D., Gupta, D., Shankar, S. and Srivastava, R. K. (2015a) 'Biomolecular characterization of exosomes released from cancer stem cells: Possible implications for biomarker and treatment of cancer', *Oncotarget,* 6(5), pp. 3280-91. doi: 10.18632/oncotarget.2462.

Kumar, L., Verma, S., Vaidya, B. and Gupta, V. (2015b) 'Exosomes: Natural Carriers for siRNA Delivery', *Curr Pharm Des,* 21(31), pp. 4556-65.

Kurata, A., Yamada, M., Ohno, S. I., Inoue, S., Hashimoto, H., Fujita, K., Takanashi, M. and Kuroda, M. (2018) 'Expression level of microRNA-200c is associated with cell morphology in vitro and histological differentiation through regulation of ZEB1/2 and E-cadherin in gastric carcinoma', *Oncol Rep,* 39(1), pp. 91-100. doi: 10.3892/or.2017.6093.

Kurrey, N. K., Jalgaonkar, S. P., Joglekar, A. V., Ghanate, A. D., Chaskar, P. D., Doiphode, R. Y. and Bapat, S. A. (2009) 'Snail and slug mediate radioresistance and chemoresistance by antagonizing p53-mediated apoptosis and acquiring a stem-like phenotype in ovarian cancer cells', *Stem Cells,* 27(9), pp. 2059-68. doi: 10.1002/stem.154.

Kurth, I., Hein, L., Mabert, K., Peitzsch, C., Koi, L., Cojoc, M., Kunz-Schughart, L., Baumann, M. and Dubrovska, A. (2015) 'Cancer stem cell related markers of radioresistance in head and neck squamous cell carcinoma', *Oncotarget,* 6(33), pp. 34494-509. doi: 10.18632/oncotarget.5417.

Lagadec, C., Vlashi, E., Della Donna, L., Dekmezian, C. and Pajonk, F. (2012) 'Radiation-induced reprogramming of breast cancer cells', *Stem Cells,* 30(5), pp. 833-44. doi: 10.1002/stem.1058.

Lai, R. C., Yeo, R. W., Padmanabhan, J., Choo, A., de Kleijn, D. P. and Lim, S. K. (2016) 'Isolation and Characterization of Exosome from Human Embryonic Stem Cell-Derived C-Myc-Immortalized Mesenchymal Stem Cells', *Methods Mol Biol,* 1416, pp. 477-94. doi: 10.1007/978-1-4939-3584-0_29.

Lange, T., Samatov, T. R., Tonevitsky, A. G. and Schumacher, U. (2014) 'Importance of altered glycoprotein-bound N- and O-glycans for epithelial-to-mesenchymal transition and adhesion of cancer cells', *Carbohydr Res,* 389, pp. 39-45. doi: 10.1016/j.carres.2014.01.010.

Languino, L. R., Singh, A., Prisco, M., Inman, G. J., Luginbuhl, A., Curry, J. M. and South, A. P. (2016) 'Exosome-mediated transfer from the tumor microenvironment increases TGFbeta signaling in squamous cell carcinoma', *Am J Transl Res,* 8(5), pp. 2432-7.

Lavrsen, K., Dabelsteen, S., Vakhrushev, S. Y., Levann, A. M. R., Haue, A. D., Dylander, A., Mandel, U., Hansen, L., Frodin, M., Bennett, E. P. and Wandall, H. H. (2018) 'De novo expression of human polypeptide N-acetylgalactosaminyltransferase 6 (GalNAc-T6) in colon adenocarcinoma inhibits the differentiation of colonic epithelium', *J Biol Chem,* 293(4), pp. 1298-1314. doi: 10.1074/jbc.M117.812826.

Leach, J. K., Van Tuyle, G., Lin, P. S., Schmidt-Ullrich, R. and Mikkelsen, R. B. (2001) 'Ionizing radiation-induced, mitochondria-dependent generation of reactive oxygen/nitrogen', *Cancer Res,* 61(10), pp. 3894-901.

Lee-Sayer, S. S. M., Dougan, M. N., Cooper, J., Sanderson, L., Dosanjh, M., Maxwell, C. A. and Johnson, P. (2018) 'CD44-mediated hyaluronan binding marks proliferating hematopoietic progenitor cells and promotes bone marrow engraftment', *PLoS One,* 13(4), pp. e0196011. doi: 10.1371/journal.pone.0196011.

Lee, H. A., Park, I., Byun, H. J., Jeoung, D., Kim, Y. M. and Lee, H. (2011) 'Metastasis suppressor KAI1/CD82 attenuates the matrix adhesion of human prostate cancer cells by suppressing fibronectin expression and beta1 integrin activation', *Cell Physiol Biochem,* 27(5), pp. 575-86. doi: 10.1159/000329979.

Lee, M., Lee, H. J., Seo, W. D., Park, K. H. and Lee, Y. S. (2010) 'Sialylation of integrin beta1 is involved in radiation-induced adhesion and migration in human colon cancer cells', *Int J Radiat Oncol Biol Phys,* 76(5), pp. 1528-36. doi: 10.1016/j.ijrobp.2009.11.022.

Lee, M. K., Pardoux, C., Hall, M. C., Lee, P. S., Warburton, D., Qing, J., Smith, S. M. and Derynck, R. (2007) 'TGF-beta activates Erk MAP kinase signalling through direct phosphorylation of ShcA', *EMBO J,* 26(17), pp. 3957-67. doi: 10.1038/sj.emboj.7601818.

Lee, S. Y., Jeong, E. K., Ju, M. K., Jeon, H. M., Kim, M. Y., Kim, C. H., Park, H. G., Han, S. I. and Kang, H. S. (2017) 'Induction of metastasis, cancer stem cell phenotype, and oncogenic metabolism in cancer cells by ionizing radiation', *Mol Cancer,* 16(1), pp. 10. doi: 10.1186/s12943-016-0577-4.

Legras, S., Levesque, J. P., Charrad, R., Morimoto, K., Le Bousse, C., Clay, D., Jasmin, C. and Smadja-Joffe, F. (1997) 'CD44-mediated adhesiveness of human hematopoietic progenitors to hyaluronan is modulated by cytokines', *Blood,* 89(6), pp. 1905-14.

Lemieux, E., Bergeron, S., Durand, V., Asselin, C., Saucier, C. and Rivard, N. (2009) 'Constitutively active MEK1 is sufficient to induce epithelial-to-mesenchymal transition in intestinal epithelial cells and to promote tumor invasion and metastasis', *Int J Cancer,* 125(7), pp. 1575-86. doi: 10.1002/ijc.24485.

Lescar, J., Sanchez, J. F., Audfray, A., Coll, J. L., Breton, C., Mitchell, E. P. and Imberty, A. (2007) 'Structural basis for recognition of breast and colon cancer epitopes Tn antigen and Forssman disaccharide by Helix pomatia lectin', *Glycobiology,* 17(10), pp. 1077-83. doi: 10.1093/glycob/cwm077.

Li, B., Chen, P., Chang, Y., Qi, J., Fu, H. and Guo, H. (2016a) 'Let-7a inhibits tumor cell growth and metastasis by directly targeting RTKN in human colon cancer', *Biochem Biophys Res Commun,* 478(2), pp. 739-45. doi: 10.1016/j.bbrc.2016.08.018.

Li, C., Heidt, D. G., Dalerba, P., Burant, C. F., Zhang, L., Adsay, V., Wicha, M., Clarke, M. F. and Simeone, D. M. (2007) 'Identification of pancreatic cancer stem cells', *Cancer Res,* 67(3), pp. 1030-7. doi: 10.1158/0008-5472.CAN-06-2030.

Li, F., Glinskii, O. V., Mooney, B. P., Rittenhouse-Olson, K., Pienta, K. J. and Glinsky, V. V. (2017a) 'Cell surface Thomsen-Friedenreich proteome profiling of metastatic prostate cancer cells reveals potential link with cancer stem cell-like phenotype', *Oncotarget,* 8(58), pp. 98598-98608. doi: 10.18632/oncotarget.21985.

Li, F., Zhou, K., Gao, L., Zhang, B., Li, W., Yan, W., Song, X., Yu, H., Wang, S., Yu, N. and Jiang, Q. (2016b) 'Radiation induces the generation of cancer stem cells: A novel mechanism for cancer radioresistance', *Oncol Lett,* 12(5), pp. 3059-3065. doi: 10.3892/ol.2016.5124.

Li, L., Xiao, B., Tong, H., Xie, F., Zhang, Z. and Xiao, G. G. (2012) 'Regulation of breast cancer tumorigenesis and metastasis by miRNAs', *Expert Rev Proteomics,* 9(6), pp. 615-25. doi: 10.1586/epr.12.64.

Li, P., Kaslan, M., Lee, S. H., Yao, J. and Gao, Z. (2017b) 'Progress in Exosome Isolation Techniques', *Theranostics,* 7(3), pp. 789-804. doi: 10.7150/thno.18133.

Li, S., Mo, C., Peng, Q., Kang, X., Sun, C., Jiang, K., Huang, L., Lu, Y., Sui, J., Qin, X. and Liu, Y. (2013) 'Cell surface glycan alterations in epithelial mesenchymal transition process of Huh7 hepatocellular carcinoma cell', *PLoS One,* 8(8), pp. e71273. doi: 10.1371/journal.pone.0071273.

Li, W., Ma, H., Zhang, J., Zhu, L., Wang, C. and Yang, Y. (2017c) 'Unraveling the roles of CD44/CD24 and ALDH1 as cancer stem cell markers in tumorigenesis and metastasis', *Sci Rep,* 7(1), pp. 13856. doi: 10.1038/s41598-017-14364-2.

Li, W., Wang, Z., Zha, L., Kong, D., Liao, G. and Li, H. (2017d) 'HMGA2 regulates epithelial-mesenchymal transition and the acquisition of tumor stem cell properties through TWIST1 in gastric cancer', *Oncol Rep,* 37(1), pp. 185-192. doi: 10.3892/or.2016.5255.

Li, W., Wei, W. and Ding, S. (2016) 'TGF-beta Signaling in Stem Cell Regulation', *Methods Mol Biol,* 1344, pp. 137-45. doi: 10.1007/978-1-4939-2966-5_8.

Li, W., Zhang, X., Wang, J., Li, M., Cao, C., Tan, J., Ma, D. and Gao, Q. (2017e) 'TGFβ1 in fibroblasts-derived exosomes promotes epithelial-mesenchymal transition of ovarian cancer cells.', *Oncotarget.,* 8(56), pp. 96035-96047. doi: doi: 10.18632/oncotarget.21635.

Li, Y., Zheng, Q., Bao, C., Li, S., Guo, W., Zhao, J., Chen, D., Gu, J., He, X. and Huang, S. (2015) 'Circular RNA is enriched and stable in exosomes: a promising biomarker for cancer diagnosis', *Cell Res,* 25(8), pp. 981-4. doi: 10.1038/cr.2015.82.

Lin, S., Kemmner, W., Grigull, S. and Schlag, P. M. (2002) 'Cell surface alpha 2,6 sialylation affects adhesion of breast carcinoma cells', *Exp Cell Res,* 276(1), pp. 101-10. doi: 10.1006/excr.2002.5521.

Lindsey, S. and Langhans, S. A. (2014) 'Crosstalk of Oncogenic Signaling Pathways during Epithelial-Mesenchymal Transition', *Front Oncol,* 4, pp. 358. doi: 10.3389/fonc.2014.00358.

List, M., Hauschild, A. C., Tan, Q., Kruse, T. A., Mollenhauer, J., Baumbach, J. and Batra, R. (2014) 'Classification of breast cancer subtypes by combining gene expression and DNA methylation data', *J Integr Bioinform,* 11(2), pp. 236. doi: 10.2390/biecoll-jib-2014-236.

Little, J. B. (2006) 'Cellular radiation effects and the bystander response', *Mutat Res,* 597(1-2), pp. 113-8. doi: 10.1016/j.mrfmmm.2005.12.001.

Liu, Y., Pan, Q., Zhao, Y., He, C., Bi, K., Chen, Y., Zhao, B., Chen, Y. and Ma, X. (2015) 'MicroRNA-155 Regulates ROS Production, NO Generation, Apoptosis and Multiple Functions of Human Brain Microvessel Endothelial Cells Under Physiological and Pathological Conditions', *J Cell Biochem,* 116(12), pp. 2870-81. doi: 10.1002/jcb.25234.

Lorimore, S. A., Coates, P. J. and Wright, E. G. (2003) 'Radiation-induced genomic instability and bystander effects: inter-related nontargeted effects of exposure to ionizing radiation', *Oncogene,* 22(45), pp. 7058-69. doi: 10.1038/sj.onc.1207044.

Lorimore, S. A., Kadhim, M. A., Pocock, D. A., Papworth, D., Stevens, D. L., Goodhead, D. T. and Wright, E. G. (1998) 'Chromosomal instability in the descendants of unirradiated surviving cells after alpha-particle irradiation', *Proc Natl Acad Sci U S A,* 95(10), pp. 5730-3.

Lorimore, S. A. and Wright, E. G. (2003) 'Radiation-induced genomic instability and bystander effects: related inflammatory-type responses to radiation-induced stress and injury? A review', *Int J Radiat Biol,* 79(1), pp. 15-25.

Lu, X., Kambe, F., Cao, X., Kozaki, Y., Kaji, T., Ishii, T. and Seo, H. (2008) '3beta-Hydroxysteroid-delta24 reductase is a hydrogen peroxide scavenger, protecting cells from oxidative stress-induced apoptosis', *Endocrinology,* 149(7), pp. 3267-73. doi: 10.1210/en.2008-0024.

Lu, Y., Lu, J., Li, X., Zhu, H., Fan, X., Zhu, S., Wang, Y., Guo, Q., Wang, L., Huang, Y., Zhu, M. and Wang, Z. (2014) 'MiR-200a inhibits epithelial-mesenchymal transition of pancreatic cancer stem cell', *BMC Cancer,* 14, pp. 85. doi: 10.1186/1471-2407-14-85.

Luo, H., Yang, A., Schulte, B. A., Wargovich, M. J. and Wang, G. Y. (2013) 'Resveratrol induces premature senescence in lung cancer cells via ROS-mediated DNA damage', *PLoS One,* 8(3), pp. e60065. doi: 10.1371/journal.pone.0060065.

Lutze, L. H., Cleaver, J. E., Morgan, W. F. and Winegar, R. A. (1993) 'Mechanisms involved in rejoining DNA double-strand breaks induced by ionizing radiation and restriction enzymes', *Mutat Res,* 299(3-4), pp. 225-32.

Lv, L., Li, C., Zhang, X., Ding, N., Cao, T., Jia, X., Wang, J., Pan, L., Jia, H., Li, Z., Zhang, J., Chen, F. and Zhang, Z. (2017) 'RNA Profiling Analysis of the Serum Exosomes Derived from Patients with Active and Latent Mycobacterium tuberculosis Infection', *Front Microbiol,* 8, pp. 1051. doi: 10.3389/fmicb.2017.01051.

Lv, N., Shan, Z., Gao, Y., Guan, H., Fan, C., Wang, H. and Teng, W. (2016) 'Twist1 regulates the epithelial-mesenchymal transition via the NF-kappaB pathway in papillary thyroid carcinoma', *Endocrine,* 51(3), pp. 469-77. doi: 10.1007/s12020-015-0714-7.

Lyng, F. M., Maguire, P., McClean, B., Seymour, C. and Mothersill, C. (2006) 'The involvement of calcium and MAP kinase signaling pathways in the production of radiation-induced bystander effects', *Radiat Res,* 165(4), pp. 400-9.

Lyng, F. M., Seymour, C. B. and Mothersill, C. (2000) 'Production of a signal by irradiated cells which leads to a response in unirradiated cells characteristic of initiation of apoptosis', *Br J Cancer,* 83(9), pp. 1223-30. doi: 10.1054/bjoc.2000.1433.

Ma, F., Li, W., Liu, C., Li, W., Yu, H., Lei, B., Ren, Y., Li, Z., Pang, D. and Qian, C. (2017) 'MiR-23a promotes TGF-beta1-induced EMT and tumor metastasis in breast cancer cells by directly targeting CDH1 and activating Wnt/beta-catenin signaling', *Oncotarget,* 8(41), pp. 69538-69550. doi: 10.18632/oncotarget.18422.

Ma, L., Young, J., Prabhala, H., Pan, E., Mestdagh, P., Muth, D., Teruya-Feldstein, J., Reinhardt, F., Onder, T. T., Valastyan, S., Westermann, F., Speleman, F., Vandesompele, J. and Weinberg, R. A. (2010) 'miR-9, a MYC/MYCN-activated microRNA, regulates E-cadherin and cancer metastasis', *Nat Cell Biol,* 12(3), pp. 247-56. doi: 10.1038/ncb2024.

Ma, Y., Zheng, X., Zhou, J., Zhang, Y. and Chen, K. (2015) 'ZEB1 promotes the progression and metastasis of cervical squamous cell carcinoma via the promotion of epithelial-mesenchymal transition', *Int J Clin Exp Pathol,* 8(9), pp. 11258-67.

Magalhaes, A., Duarte, H. O. and Reis, C. A. (2017) 'Aberrant Glycosylation in Cancer: A Novel Molecular Mechanism Controlling Metastasis', *Cancer Cell,* 31(6), pp. 733-735. doi: 10.1016/j.ccell.2017.05.012.

Mancuso, M., Pasquali, E., Leonardi, S., Tanori, M., Rebessi, S., Di Majo, V., Pazzaglia, S., Toni, M. P., Pimpinella, M., Covelli, V. and Saran, A. (2008) 'Oncogenic bystander radiation effects in Patched heterozygous mouse cerebellum', *Proc Natl Acad Sci U S A,* 105(34), pp. 12445-50. doi: 10.1073/pnas.0804186105.

Mao, L., Li, J., Chen, W. X., Cai, Y. Q., Yu, D. D., Zhong, S. L., Zhao, J. H., Zhou, J. W. and Tang, J. H. (2016) 'Exosomes decrease sensitivity of breast cancer cells to adriamycin by delivering microRNAs', *Tumour Biol,* 37(4), pp. 5247-56. doi: 10.1007/s13277-015-4402-2.

Marcos, N. T., Pinho, S., Grandela, C., Cruz, A., Samyn-Petit, B., Harduin-Lepers, A., Almeida, R., Silva, F., Morais, V., Costa, J., Kihlberg, J., Clausen, H. and Reis, C. A. (2004) 'Role of the human ST6GalNAc-I and ST6GalNAc-II in the synthesis of the cancer-associated sialyl-Tn antigen', *Cancer Res,* 64(19), pp. 7050-7. doi: 10.1158/0008-5472.CAN-04-1921.

Marshall, M., Gibson, J. A. and Holt, P. D. (1970) 'An analysis of the target theory of Lea with modern data', *Int J Radiat Biol Relat Stud Phys Chem Med,* 18(2), pp. 127-38.

Massague, J. (2008) 'TGFbeta in Cancer', *Cell,* 134(2), pp. 215-30. doi: 10.1016/j.cell.2008.07.001.

Mathivanan, S., Ji, H. and Simpson, R. J. (2010) 'Exosomes: extracellular organelles important in intercellular communication', *J Proteomics,* 73(10), pp. 1907-20. doi: 10.1016/j.jprot.2010.06.006.

Mehta, A., Comunale, M. A., Rawat, S., Casciano, J. C., Lamontagne, J., Herrera, H., Ramanathan, A., Betesh, L., Wang, M., Norton, P., Steel, L. F. and Bouchard, M. J. (2016) 'Intrinsic hepatocyte dedifferentiation is accompanied by upregulation of mesenchymal markers, protein sialylation and core alpha 1,6 linked fucosylation.

', *Scientific reports,* 22(6), pp. 27965. doi: 10.1038/srep27965.

Mendes, R. A., Carvalho, J. F. and van der Waal, I. (2010) 'Characterization and management of the keratocystic odontogenic tumor in relation to its histopathological and biological features', *Oral Oncol,* 46(4), pp. 219-25. doi: 10.1016/j.oraloncology.2010.01.012.

Mendez, M. G., Kojima, S. and Goldman, R. D. (2010) 'Vimentin induces changes in cell shape, motility, and adhesion during the epithelial to mesenchymal transition', *FASEB J,* 24(6), pp. 1838-51. doi: 10.1096/fj.09-151639.

Meng, Y., Eshghi, S., Li, Y. J., Schmidt, R., Schaffer, D. V. and Healy, K. E. (2010) 'Characterization of integrin engagement during defined human embryonic stem cell culture', *FASEB J,* 24(4), pp. 1056-65. doi: 10.1096/fj.08-126821.

Mi, Q., Ma, Y., Gao, X., Liu, R., Liu, P., Mi, Y., Fu, X. and Gao, Q. (2015) '2-Deoxyglucose conjugated platinum (II) complexes for targeted therapy: design, synthesis, and antitumor activity', *J Biomol Struct Dyn*, pp. 1-12. doi: 10.1080/07391102.2015.1114972.

Mishra, K. P. (2004) 'Cell membrane oxidative damage induced by gamma-radiation and apoptotic sensitivity', *J Environ Pathol Toxicol Oncol,* 23(1), pp. 61-6.

Mitchell, B. S., Brooks, S. A., Leathem, A. J. and Schumacher, U. (1998) 'Do HPA and PHA-L have the same binding pattern in metastasizing human breast and colon cancers?', *Cancer Lett,* 123(1), pp. 113-9.

Morgan, M. J. and Liu, Z. G. (2011) 'Crosstalk of reactive oxygen species and NF-kappaB signaling', *Cell Res,* 21(1), pp. 103-15. doi: 10.1038/cr.2010.178.

Morgan, W. F. (2003a) 'Non-targeted and delayed effects of exposure to ionizing radiation: I. Radiation-induced genomic instability and bystander effects in vitro', *Radiat Res,* 159(5), pp. 567-80.

Morgan, W. F. (2003b) 'Non-targeted and delayed effects of exposure to ionizing radiation: II. Radiation-induced genomic instability and bystander effects in vivo, clastogenic factors and transgenerational effects', *Radiat Res,* 159(5), pp. 581-96.
Morgan, W. F. (2012) 'Non-targeted and delayed effects of exposure to ionizing radiation: I. Radiation-induced genomic instability and bystander effects in vitro. 2003', *Radiat Res,* 178(2), pp. AV223-36.
Mothersill, C., Lyng, F., Mulford, A., Seymour, C., Cottell, D., Lyons, M. and Austin, B. (2001) 'Effect of low doses of ionizing radiation on cells cultured from the hematopoietic tissue of the Dublin Bay prawn, Nephrops norvegicus', *Radiat Res,* 156(3), pp. 241-50.
Mothersill, C., Rusin, A. and Seymour, C. (2017) 'Low doses and non-targeted effects in environmental radiation protection; where are we now and where should we go?', *Environ Res,* 159, pp. 484-490. doi: 10.1016/j.envres.2017.08.029.
Mothersill, C. and Seymour, C. B. (1998) 'Mechanisms and implications of genomic instability and other delayed effects of ionizing radiation exposure', *Mutagenesis,* 13(5), pp. 421-6.
Munich, S., Sobo-Vujanovic, A., Buchser, W. J., Beer-Stolz, D. and Vujanovic, N. L. (2012) 'Dendritic cell exosomes directly kill tumor cells and activate natural killer cells via TNF superfamily ligands', *Oncoimmunology,* 1(7), pp. 1074-1083. doi: 10.4161/onci.20897.
Munoz, P., Iliou, M. S. and Esteller, M. (2012) 'Epigenetic alterations involved in cancer stem cell reprogramming', *Mol Oncol,* 6(6), pp. 620-36. doi: 10.1016/j.molonc.2012.10.006.
Muraro, M. G., Mele, V., Daster, S., Han, J., Heberer, M., Cesare Spagnoli, G. and Iezzi, G. (2012) 'CD133+, CD166+CD44+, and CD24+CD44+ phenotypes fail to reliably identify cell populations with cancer stem cell functional features in established human colorectal cancer cell lines', *Stem Cells Transl Med,* 1(8), pp. 592-603. doi: 10.5966/sctm.2012-0003.
Mutschelknaus, L., Azimzadeh, O., Heider, T., Winkler, K., Vetter, M., Kell, R., Tapio, S., Merl-Pham, J., Huber, S. M., Edalat, L., Radulovic, V., Anastasov, N., Atkinson, M. J. and Moertl, S. (2017) 'Radiation alters the cargo of exosomes released from squamous head and neck cancer cells to promote migration of recipient cells', *Sci Rep,* 7(1), pp. 12423. doi: 10.1038/s41598-017-12403-6.
Mutschelknaus, L., Peters, C., Winkler, K., Yentrapalli, R., Heider, T., Atkinson, M. J. and Moertl, S. (2016) 'Exosomes Derived from Squamous Head and Neck Cancer Promote Cell Survival after Ionizing Radiation', *PLoS One,* 11(3), pp. e0152213. doi: 10.1371/journal.pone.0152213.
Muz, B., de la Puente, P., Azab, F. and Azab, A. K. (2015) 'The role of hypoxia in cancer progression, angiogenesis, metastasis, and resistance to therapy', *Hypoxia (Auckl),* 3, pp. 83-92. doi: 10.2147/HP.S93413.
Nagasawa, H. and Little, J. B. (1992) 'Induction of sister chromatid exchanges by extremely low doses of alpha-particles', *Cancer Res,* 52(22), pp. 6394-6.
Najafi, M., Fardid, R., Hadadi, G. and Fardid, M. (2014) 'The mechanisms of radiation-induced bystander effect', *J Biomed Phys Eng,* 4(4), pp. 163-72.
Nakamura, K., Terai, Y., Tanabe, A., Ono, Y. J., Hayashi, M., Maeda, K., Fujiwara, S., Ashihara, K., Nakamura, M., Tanaka, Y., Tanaka, T., Tsunetoh, S., Sasaki, H. and Ohmichi, M. (2017) 'CD24 expression is a marker for predicting clinical outcome and regulates the epithelial-mesenchymal transition in ovarian cancer via both the Akt and ERK pathways', *Oncol Rep,* 37(6), pp. 3189-3200. doi: 10.3892/or.2017.5583.
Nguyen, H. L., Kadam, P., Helkin, A., Cao, K., Wu, S., Samara, G. J., Zhang, Q., Zucker, S. and Cao, J. (2016) 'MT1-MMP Activation of TGF-beta Signaling Enables Intercellular Activation of an Epithelial-mesenchymal Transition Program in Cancer', *Curr Cancer Drug Targets,* 16(7), pp. 618-30.
Nias, A. H. (1990) 'Changes in relative biological effectiveness with depth of neutron beams', *Br J Radiol,* 63(746), pp. 149-50. doi: 10.1259/0007-1285-63-746-149-b.

Nosrati, A., Naghshvar, F., Maleki, I. and Salehi, F. (2016) 'Cancer stem cells CD133 and CD24 in colorectal cancers in Northern Iran', *Gastroenterol Hepatol Bed Bench,* 9(2), pp. 132-9.

O'Malley, Y., Zhao, W., Barcellos-Hoff, M. H. and Robbins, M. E. (1999) 'Radiation-induced alterations in rat mesangial cell Tgfb1 and Tgfb3 gene expression are not associated with altered secretion of active Tgfb isoforms', *Radiat Res,* 152(6), pp. 622-8.

Ogawa, T., Hirohashi, Y., Murai, A., Nishidate, T., Okita, K., Wang, L., Ikehara, Y., Satoyoshi, T., Usui, A., Kubo, T., Nakastugawa, M., Kanaseki, T., Tsukahara, T., Kutomi, G., Furuhata, T., Hirata, K., Sato, N., Mizuguchi, T., Takemasa, I. and Torigoe, T. (2017) 'ST6GALNAC1 plays important roles in enhancing cancer stem phenotypes of colorectal cancer via the Akt pathway', *Oncotarget,* 8(68), pp. 112550-112564. doi: 10.18632/oncotarget.22545.

Ogunbolude, Y., Dai, C., Bagu, E. T., Goel, R. K., Miah, S., MacAusland-Berg, J., Ng, C. Y., Chibbar, R., Napper, S., Raptis, L., Vizeacoumar, F., Vizeacoumar, F., Bonham, K. and Lukong, K. E. (2017) 'FRK inhibits breast cancer cell migration and invasion by suppressing epithelial-mesenchymal transition', *Oncotarget,* 8(68), pp. 113034-113065. doi: 10.18632/oncotarget.22958.

Okano, M., Konno, M., Kano, Y., Kim, H., Kawamoto, K., Ohkuma, M., Haraguchi, N., Yokobori, T., Mimori, K., Yamamoto, H., Sekimoto, M., Doki, Y., Mori, M. and Ishii, H. (2014) 'Human colorectal CD24+ cancer stem cells are susceptible to epithelial-mesenchymal transition', *Int J Oncol,* 45(2), pp. 575-80. doi: 10.3892/ijo.2014.2462.

Oliveira-Ferrer, L., Legler, K. and Milde-Langosch, K. (2017) 'Role of protein glycosylation in cancer metastasis', *Semin Cancer Biol,* 44, pp. 141-152. doi: 10.1016/j.semcancer.2017.03.002.

Pahlsson, P., Strindhall, J., Srinivas, U. and Lundblad, A. (1995) 'Role of N-linked glycosylation in expression of E-selectin on human endothelial cells', *Eur J Immunol,* 25(9), pp. 2452-9. doi: 10.1002/eji.1830250907.

Park, D., Brune, K. A., Mitra, A., Marusina, A. I., Maverakis, E. and Lebrilla, C. B. (2015) 'Characteristic Changes in Cell Surface Glycosylation Accompany Intestinal Epithelial Cell (IEC) Differentiation: High Mannose Structures Dominate the Cell Surface Glycome of Undifferentiated Enterocytes', *Mol Cell Proteomics,* 14(11), pp. 2910-21. doi: 10.1074/mcp.M115.053983.

Park, J. H., Katagiri, T., Chung, S., Kijima, K. and Nakamura, Y. (2011) 'Polypeptide N-acetylgalactosaminyltransferase 6 disrupts mammary acinar morphogenesis through O-glycosylation of fibronectin', *Neoplasia,* 13(4), pp. 320-6.

Park, J. H., Nishidate, T., Kijima, K., Ohashi, T., Takegawa, K., Fujikane, T., Hirata, K., Nakamura, Y. and Katagiri, T. (2010) 'Critical roles of mucin 1 glycosylation by transactivated polypeptide N-acetylgalactosaminyltransferase 6 in mammary carcinogenesis', *Cancer Res,* 70(7), pp. 2759-69. doi: 10.1158/0008-5472.CAN-09-3911.

Park, S. J., Kim, J. G., Kim, N. D., Yang, K., Shim, J. W. and Heo, K. (2016) 'Estradiol, TGF-β1 and hypoxia promote breast cancer stemness and EMT-mediated breast cancer migration.', *Oncology Letters,* 11(3), pp. 1895-1902.

Patani, N., Jiang, W. and Mokbel, K. (2008) 'Prognostic utility of glycosyltransferase expression in breast cancer', *Cancer Genomics Proteomics,* 5(6), pp. 333-40.

Patrie, S. M., Roth, M. J. and Kohler, J. J. (2013) 'Introduction to glycosylation and mass spectrometry', *Methods Mol Biol,* 951, pp. 1-17. doi: 10.1007/978-1-62703-146-2_1.

Peiris, D., Ossondo, M., Fry, S., Loizidou, M., Smith-Ravin, J. and Dwek, M. V. (2015) 'Identification of O-Linked Glycoproteins Binding to the Lectin Helix pomatia Agglutinin as Markers of Metastatic Colorectal Cancer', *PLoS One,* 10(10), pp. e0138345. doi: 10.1371/journal.pone.0138345.

Perry, K. T., Anthony, C. T. and Steiner, M. S. (1997) 'Immunohistochemical localization of TGF beta 1, TGF beta 2, and TGF beta 3 in normal and malignant human prostate', *Prostate,* 33(2), pp. 133-40.

Persson, H. L., Kurz, T., Eaton, J. W. and Brunk, U. T. (2005) 'Radiation-induced cell death: importance of lysosomal destabilization', *Biochem J,* 389(Pt 3), pp. 877-84. doi: 10.1042/BJ20050271.

Petrova, Y. I., Schecterson, L. and Gumbiner, B. M. (2016) 'Roles for E-cadherin cell surface regulation in cancer', *Mol Biol Cell,* 27(21), pp. 3233-3244. doi: 10.1091/mbc.E16-01-0058.

Pham, P. V., Phan, N. L., Nguyen, N. T., Truong, N. H., Duong, T. T., Le, D. V., Truong, K. D. and Phan, N. K. (2011) 'Differentiation of breast cancer stem cells by knockdown of CD44: promising differentiation therapy', *J Transl Med,* 9, pp. 209. doi: 10.1186/1479-5876-9-209.

Phillips, T. M., McBride, W. H. and Pajonk, F. (2006) 'The response of CD24(-/low)/CD44+ breast cancer-initiating cells to radiation', *J Natl Cancer Inst,* 98(24), pp. 1777-85. doi: 10.1093/jnci/djj495.

Phua, D. C., Humbert, P. O. and Hunziker, W. (2009) 'Vimentin regulates scribble activity by protecting it from proteasomal degradation', *Mol Biol Cell,* 20(12), pp. 2841-55. doi: 10.1091/mbc.E08-02-0199.

Pinho, S. S., Figueiredo, J., Cabral, J., Carvalho, S., Dourado, J., Magalhaes, A., Gartner, F., Mendonfa, A. M., Isaji, T., Gu, J., Carneiro, F., Seruca, R., Taniguchi, N. and Reis, C. A. (2013) 'E-cadherin and adherens-junctions stability in gastric carcinoma: functional implications of glycosyltransferases involving N-glycan branching biosynthesis, N-acetylglucosaminyltransferases III and V', *Biochim Biophys Acta,* 1830(3), pp. 2690-700. doi: 10.1016/j.bbagen.2012.10.021.

Pinho, S. S. and Reis, C. A. (2015) 'Glycosylation in cancer: mechanisms and clinical implications', *Nat Rev Cancer,* 15(9), pp. 540-55. doi: 10.1038/nrc3982.

Pirozzi, G., Tirino, V., Camerlingo, R., Franco, R., La Rocca, A., Liguori, E., Martucci, N., Paino, F., Normanno, N. and Rocco, G. (2011) 'Epithelial to mesenchymal transition by TGFbeta-1 induction increases stemness characteristics in primary non small cell lung cancer cell line', *PLoS One,* 6(6), pp. e21548. doi: 10.1371/journal.pone.0021548.

Ponnaiya, B., Jenkins-Baker, G., Randers-Pherson, G. and Geard, C. R. (2007) 'Quantifying a bystander response following microbeam irradiation using single-cell RT-PCR analyses', *Exp Hematol,* 35(4 Suppl 1), pp. 64-8. doi: 10.1016/j.exphem.2007.01.013.

Pouget, J. P., Georgakilas, A. G. and Ravanat, J. L. (2018) 'Targeted and Off-Target (Bystander and Abscopal) Effects of Radiation Therapy: Redox Mechanisms and Risk/Benefit Analysis', *Antioxid Redox Signal*. doi: 10.1089/ars.2017.7267.

Pozharskaya, V., Torres-Gonzalez, E., Rojas, M., Gal, A., Amin, M., Dollard, S., Roman, J., Stecenko, A. A. and Mora, A. L. (2009) 'Twist: a regulator of epithelial-mesenchymal transition in lung fibrosis', *PLoS One,* 4(10), pp. e7559. doi: 10.1371/journal.pone.0007559.

Prokop, O., Uhlenbruck, G. and Kohler, W. (1968) 'A new source of antibody-like substances having anti-blood group specificity. A discussion on the specificity of Helix agglutinins', *Vox Sang,* 14(5), pp. 321-33.

Radhakrishnan, P., Dabelsteen, S., Madsen, F., Francavilla, C., Kopp, K. L., C., S., S.Y., V., Olsen, J. V., Hansen, L., Bennett, E. P., Woetmann, A., Yin, G., Chen, L., Song, H., Bak, M., Hlady, R. A., Peters, S. L., Opavsky, R., Thode, C., Qvortrup, K., Schjoldager, K. T., Clausen, H., Hollingsworth, M. A. and H.H., W. (2014a) 'Immature truncated O-glycophenotype of cancer directly induces oncogenic features.

', *Proceedings of the National Academy of Sciences of the United States of America,* 111(39).

Radhakrishnan, P., Dabelsteen, S., Madsen, F. B., Francavilla, C., Kopp, K. L., Steentoft, C., Vakhrushev, S. Y., Olsen, J. V., Hansen, L., Bennett, E. P., Woetmann, A., Yin, G., Chen, L., Song, H., Bak, M., Hlady, R. A., Peters, S. L., Opavsky, R., Thode, C., Qvortrup, K.,

Schjoldager, K. T., Clausen, H., Hollingsworth, M. A. and Wandall, H. H. (2014b) 'Immature truncated O-glycophenotype of cancer directly induces oncogenic features', *Proc Natl Acad Sci U S A,* 111(39), pp. E4066-75. doi: 10.1073/pnas.1406619111.

Radotra, B. D., Joshi, K., Kak, V. K. and Banerjee, A. K. (1994) 'Choroid plexus tumours--an immunohistochemical analysis with review of literature', *Indian J Pathol Microbiol,* 37(1), pp. 9-19.

Rahman, M. A., Barger, J. F., Lovat, F., Gao, M., Otterson, G. A. and Nana-Sinkam, P. (2016) 'Lung cancer exosomes as drivers of epithelial mesenchymal transition', *Oncotarget*. doi: 10.18632/oncotarget.10243.

Rambaruth, N. D., Greenwell, P. and Dwek, M. V. (2012) 'The lectin Helix pomatia agglutinin recognizes O-GlcNAc containing glycoproteins in human breast cancer', *Glycobiology,* 22(6), pp. 839-48. doi: 10.1093/glycob/cws051.

Rao, G., Pierobon, M., Kim, I. K., Hsu, W. H., Deng, J., Moon, Y. W., Petricoin, E. F., Zhang, Y. W., Wang, Y. and Giaccone, G. (2017) 'Inhibition of AKT1 signaling promotes invasion and metastasis of non-small cell lung cancer cells with K-RAS or EGFR mutations', *Sci Rep,* 7(1), pp. 7066. doi: 10.1038/s41598-017-06128-9.

Reinhardt, H. C. and Yaffe, M. B. (2009) 'Kinases that control the cell cycle in response to DNA damage: Chk1, Chk2, and MK2', *Curr Opin Cell Biol,* 21(2), pp. 245-55. doi: 10.1016/j.ceb.2009.01.018.

Rodriguez, P. C., Zea, A. H. and Ochoa, A. C. (2003) 'Mechanisms of tumor evasion from the immune response', *Cancer Chemother Biol Response Modif,* 21, pp. 351-64.

Ronchini, C. and Capobianco, A. J. (2001) 'Induction of cyclin D1 transcription and CDK2 activity by Notch(ic): implication for cell cycle disruption in transformation by Notch(ic)', *Mol Cell Biol,* 21(17), pp. 5925-34.

Roth, V. (2006) *Doubling Time Computing*. Available from: http://www.doubling-time.com/compute.php.

Sahai, E. (2005) 'Mechanisms of cancer cell invasion', *Curr Opin Genet Dev,* 15(1), pp. 87-96. doi: 10.1016/j.gde.2004.12.002.

Sanchez-Madrid, F. and Barreiro, O. (2009) 'Leukocytes whisper to endothelial guards', *Blood,* 113(24), pp. 6048-9. doi: 10.1182/blood-2009-03-210336.

Sanchez, J. F., Lescar, J., Chazalet, V., Audfray, A., Gagnon, J., Alvarez, R., Breton, C., Imberty, A. and Mitchell, E. P. (2006) 'Biochemical and structural analysis of Helix pomatia agglutinin. A hexameric lectin with a novel fold', *J Biol Chem,* 281(29), pp. 20171-80. doi: 10.1074/jbc.M603452200.

Satelli, A., Batth, I. S., Brownlee, Z., Rojas, C., Meng, Q. H., Kopetz, S. and Li, S. (2016) 'Potential role of nuclear PD-L1 expression in cell-surface vimentin positive circulating tumor cells as a prognostic marker in cancer patients', *Sci Rep,* 6, pp. 28910. doi: 10.1038/srep28910.

Satelli, A. and Li, S. (2011) 'Vimentin in cancer and its potential as a molecular target for cancer therapy', *Cell Mol Life Sci,* 68(18), pp. 3033-46. doi: 10.1007/s00018-011-0735-1.

Schettino, G., Folkard, M., Michael, B. D. and Prise, K. M. (2005) 'Low-dose binary behavior of bystander cell killing after microbeam irradiation of a single cell with focused c(k) x rays', *Radiat Res,* 163(3), pp. 332-6.

Schwartz, J. L., Jordan, R., Sedita, B. A., Swenningson, M. J., Banath, J. P. and Olive, P. L. (1995) 'Different sensitivity to cell killing and chromosome mutation induction by gamma rays in two human lymphoblastoid cell lines derived from a single donor: possible role of apoptosis', *Mutagenesis,* 10(3), pp. 227-33.

Sears, P. and Wong, C. H. (1998) 'Enzyme action in glycoprotein synthesis', *Cell Mol Life Sci,* 54(3), pp. 223-52.

Sekihara, K., Saitoh, K., Yang, H., Kawashima, H., Kazuno, S., Kikkawa, M., Arai, H., Miida, T., Hayashi, N., Sasai, K. and Tabe, Y. (2018) 'Low-dose ionizing radiation exposure represses

the cell cycle and protein synthesis pathways in in vitro human primary keratinocytes and U937 cell lines', *PLoS One,* 13(6), pp. e0199117. doi: 10.1371/journal.pone.0199117.
Sengupta, P. K., Bouchie, M. P., Nita-Lazar, M., Yang, H. Y. and Kukuruzinska, M. A. (2013) 'Coordinate regulation of N-glycosylation gene DPAGT1, canonical Wnt signaling and E-cadherin adhesion', *J Cell Sci,* 126(Pt 2), pp. 484-96. doi: 10.1242/jcs.113035.
Sewell, R., Backstrom, M., Dalziel, M., Gschmeissner, S., Karlsson, H., Noll, T., Gatgens, J., Clausen, H., Hansson, G. C., Burchell, J. and Taylor-Papadimitriou, J. (2006) 'The ST6GalNAc-I sialyltransferase localizes throughout the Golgi and is responsible for the synthesis of the tumor-associated sialyl-Tn O-glycan in human breast cancer', *J Biol Chem,* 281(6), pp. 3586-94. doi: 10.1074/jbc.M511826200.
Seymour, C. and Mothersill, C. (1992) 'All colonies of CHO-K1 cells surviving gamma-irradiation contain non-viable cells', *Mutat Res,* 267(1), pp. 19-30.
Shankar, J. and Nabi, I. R. (2015) 'Actin cytoskeleton regulation of epithelial mesenchymal transition in metastatic cancer cells', *PLoS One,* 10(3), pp. e0119954. doi: 10.1371/journal.pone.0119954.
Shao, C., Folkard, M., Michael, B. D. and Prise, K. M. (2004) 'Targeted cytoplasmic irradiation induces bystander responses', *Proc Natl Acad Sci U S A,* 101(37), pp. 13495-500. doi: 10.1073/pnas.0404930101.
Shao, T., Song, P., Hua, H., Zhang, H., Sun, X., Kong, Q., Wang, J., Luo, T. and Jiang, Y. (2018) 'Gamma synuclein is a novel Twist1 target that promotes TGF-beta-induced cancer cell migration and invasion', *Cell Death Dis,* 9(6), pp. 625. doi: 10.1038/s41419-018-0657-z.
Shi, S., Zhang, Q., Xia, Y., You, B., Shan, Y., Bao, L., Li, L., You, Y. and Gu, Z. (2016) 'Mesenchymal stem cell-derived exosomes facilitate nasopharyngeal carcinoma progression', *Am J Cancer Res,* 6(2), pp. 459-72.
Shi, Y., Gong, H. L., Zhou, L., Tian, J. and Wang, Y. (2012) 'CD24: a novel cancer biomarker in laryngeal squamous cell carcinoma', *ORL J Otorhinolaryngol Relat Spec,* 74(2), pp. 78-85. doi: 10.1159/000335584.
Shilo, S., Roy, S., Khanna, S. and Sen, C. K. (2008) 'Evidence for the involvement of miRNA in redox regulated angiogenic response of human microvascular endothelial cells', *Arterioscler Thromb Vasc Biol,* 28(3), pp. 471-7. doi: 10.1161/ATVBAHA.107.160655.
Smit, M. A., Geiger, T. R., Song, J. Y., Gitelman, I. and Peeper, D. S. (2009) 'A Twist-Snail axis critical for TrkB-induced epithelial-mesenchymal transition-like transformation, anoikis resistance, and metastasis', *Mol Cell Biol,* 29(13), pp. 3722-37. doi: 10.1128/MCB.01164-08.
Song, L., Bachert, C. and Linstedt, A. D. (2016) 'Activity Detection of GalNAc Transferases by Protein-Based Fluorescence Sensors In Vivo', *Methods Mol Biol,* 1496, pp. 123-31. doi: 10.1007/978-1-4939-6463-5_10.
Springer, G. F. (1984) 'T and Tn, general carcinoma autoantigens', *Science,* 224(4654), pp. 1198-206.
Springer, G. F. (1995) 'T and Tn pancarcinoma markers: autoantigenic adhesion molecules in pathogenesis, prebiopsy carcinoma-detection, and long-term breast carcinoma immunotherapy', *Crit Rev Oncog,* 6(1), pp. 57-85.
Springer, G. F. (1997) 'Immunoreactive T and Tn epitopes in cancer diagnosis, prognosis, and immunotherapy', *J Mol Med (Berl),* 75(8), pp. 594-602.
Sprovieri, P. and Martino, G. (2018) 'The role of the carbohydrates in plasmatic membrane', *Physiol Res,* 67(1), pp. 1-11.
Sritananuwat, P., Sueangoen, N., Thummarati, P., Islam, K. and Suthiphongchai, T. (2017) 'Blocking ERK1/2 signaling impairs TGF-beta1 tumor promoting function but enhances its tumor suppressing role in intrahepatic cholangiocarcinoma cells', *Cancer Cell Int,* 17, pp. 85. doi: 10.1186/s12935-017-0454-2.

Stanley, P. and Okajima, T. (2010) 'Roles of glycosylation in Notch signaling', *Curr Top Dev Biol,* 92, pp. 131-64. doi: 10.1016/S0070-2153(10)92004-8.

Stewart, R. L., West, D., Wang, C., Weiss, H. L., Gal, T., Durbin, E., O'Connor, W., Chen, M. and O'Connor, K. L. (2016) 'Elevated integrin alpha6beta4 expression is associated with venous invasion and decreased overall survival in non-small cell lung cancer', *Hum Pathol*. doi: 10.1016/j.humpath.2016.04.003.

Stichel, D., Middleton, A. M., Muller, B. F., Depner, S., Klingmuller, U., Breuhahn, K. and Matthaus, F. (2017) 'An individual-based model for collective cancer cell migration explains speed dynamics and phenotype variability in response to growth factors', *NPJ Syst Biol Appl,* 3, pp. 5. doi: 10.1038/s41540-017-0006-3.

Storci, G., Sansone, P., Mari, S., D'Uva, G., Tavolari, S., Guarnieri, T., Taffurelli, M., Ceccarelli, C., Santini, D., Chieco, P., Marcu, K. B. and Bonafe, M. (2010) 'TNFalpha up-regulates SLUG via the NF-kappaB/HIF1alpha axis, which imparts breast cancer cells with a stem cell-like phenotype', *J Cell Physiol,* 225(3), pp. 682-91. doi: 10.1002/jcp.22264.

Su, H., Jin, X., Zhang, X., Zhao, L., Lin, B., Li, L., Fei, Z., Shen, L., Fang, Y., Pan, H. and Xie, C. (2015) 'FH535 increases the radiosensitivity and reverses epithelial-to-mesenchymal transition of radioresistant esophageal cancer cell line KYSE-150R', *J Transl Med,* 13, pp. 104. doi: 10.1186/s12967-015-0464-6.

Suarez, Y., Fernandez-Hernando, C., Pober, J. S. and Sessa, W. C. (2007) 'Dicer dependent microRNAs regulate gene expression and functions in human endothelial cells', *Circ Res,* 100(8), pp. 1164-73. doi: 10.1161/01.RES.0000265065.26744.17.

Suetsugu, A., Honma, K., Saji, S., Moriwaki, H., Ochiya, T. and Hoffman, R. M. (2013) 'Imaging exosome transfer from breast cancer cells to stroma at metastatic sites in orthotopic nude-mouse models', *Adv Drug Deliv Rev,* 65(3), pp. 383-90. doi: 10.1016/j.addr.2012.08.007.

Syn, N., Wang, L., Sethi, G., Thiery, J. P. and Goh, B. C. (2016) 'Exosome-Mediated Metastasis: From Epithelial-Mesenchymal Transition to Escape from Immunosurveillance', *Trends Pharmacol Sci,* 37(7), pp. 606-17. doi: 10.1016/j.tips.2016.04.006.

Szarynska, M., Olejniczak, A., Kobiela, J., Laski, D., Sledzinski, Z. and Kmiec, Z. (2018) 'Cancer stem cells as targets for DC-based immunotherapy of colorectal cancer', *Sci Rep,* 8(1), pp. 12042. doi: 10.1038/s41598-018-30525-3.

Szumiel, I. (2015) 'Ionizing radiation-induced oxidative stress, epigenetic changes and genomic instability: the pivotal role of mitochondria', *Int J Radiat Biol,* 91(1), pp. 1-12. doi: 10.3109/09553002.2014.934929.

Takahashi, R. U., Miyazaki, H. and Ochiya, T. (2014) 'The role of microRNAs in the regulation of cancer stem cells', *Front Genet,* 4, pp. 295. doi: 10.3389/fgene.2013.00295.

Takano, S., Kanai, F., Jazag, A., Ijichi, H., Yao, J., Ogawa, H., Enomoto, N., Omata, M. and Nakao, A. (2007) 'Smad4 is essential for down-regulation of E-cadherin induced by TGF-beta in pancreatic cancer cell line PANC-1', *J Biochem,* 141(3), pp. 345-51. doi: 10.1093/jb/mvm039.

Takebe, N., Harris, P. J., Warren, R. Q. and Ivy, S. P. (2011) 'Targeting cancer stem cells by inhibiting Wnt, Notch, and Hedgehog pathways', *Nat Rev Clin Oncol,* 8(2), pp. 97-106. doi: 10.1038/nrclinonc.2010.196.

Tamura, F., Sato, Y., Hirakawa, M., Yoshida, M., Ono, M., Osuga, T., Okagawa, Y., Uemura, N., Arihara, Y., Murase, K., Kawano, Y., Iyama, S., Takada, K., Hayashi, T., Sato, T., Miyanishi, K., Kobune, M., Takimoto, R. and Kato, J. (2016) 'RNAi-mediated gene silencing of ST6GalNAc I suppresses the metastatic potential in gastric cancer cells', *Gastric Cancer,* 19(1), pp. 85-97. doi: 10.1007/s10120-014-0454-z.

Tarhan, Y. E., Kato, T., Jang, M., Haga, Y., Ueda, K., Nakamura, Y. and Park, J. H. (2016) 'Morphological Changes, Cadherin Switching, and Growth Suppression in Pancreatic

Cancer by GALNT6 Knockdown', *Neoplasia,* 18(5), pp. 265-272. doi: 10.1016/j.neo.2016.03.005.

Tauro, B. J., Mathias, R. A., Greening, D. W., Gopal, S. K., Ji, H., Kapp, E. A., Coleman, B. M., Hill, A. F., Kusebauch, U., Hallows, J. L., Shteynberg, D., Moritz, R. L., Zhu, H. J. and Simpson, R. J. (2013) 'Oncogenic H-ras reprograms Madin-Darby canine kidney (MDCK) cell-derived exosomal proteins following epithelial-mesenchymal transition', *Mol Cell Proteomics,* 12(8), pp. 2148-59. doi: 10.1074/mcp.M112.027086.

Taylor, S. C., Nadeau, K., Abbasi, M., Lachance, C., Nguyen, M. and Fenrich, J. (2019) 'The Ultimate qPCR Experiment: Producing Publication Quality, Reproducible Data the First Time', *Trends Biotechnol,* 37(7), pp. 761-774. doi: 10.1016/j.tibtech.2018.12.002.

Tezcan, O. and Gunduz, U. (2014) 'Vimentin silencing effect on invasive and migration characteristics of doxorubicin resistant MCF-7 cells', *Biomed Pharmacother,* 68(3), pp. 357-64. doi: 10.1016/j.biopha.2014.01.006.

Thery, C., Duban, L., Segura, E., Veron, P., Lantz, O. and Amigorena, S. (2002) 'Indirect activation of naive CD4+ T cells by dendritic cell-derived exosomes', *Nat Immunol,* 3(12), pp. 1156-62. doi: 10.1038/ni854.

Thomas, L. J., Panneerselvam, K., Beattie, D. T., Picard, M. D., Xu, B., Rittershaus, C. W., Marsh, H. C., Jr., Hammond, R. A., Qian, J., Stevenson, T., Zopf, D. and Bayer, R. J. (2004) 'Production of a complement inhibitor possessing sialyl Lewis X moieties by in vitro glycosylation technology', *Glycobiology,* 14(10), pp. 883-93. doi: 10.1093/glycob/cwh112.

Tiwari, N., Gheldof, A., Tatari, M. and Christofori, G. (2012) 'EMT as the ultimate survival mechanism of cancer cells', *Semin Cancer Biol,* 22(3), pp. 194-207. doi: 10.1016/j.semcancer.2012.02.013.

Tomita, H., Tanaka, K., Tanaka, T. and Hara, A. (2016) 'Aldehyde dehydrogenase 1A1 in stem cells and cancer', *Oncotarget,* 7(10), pp. 11018-32. doi: 10.18632/oncotarget.6920.

Tong, L., Chuang, C. C., Wu, S. and Zuo, L. (2015) 'Reactive oxygen species in redox cancer therapy', *Cancer Lett,* 367(1), pp. 18-25. doi: 10.1016/j.canlet.2015.07.008.

Tran, D. T. and Ten Hagen, K. G. (2013) 'Mucin-type O-glycosylation during development', *J Biol Chem,* 288(10), pp. 6921-9. doi: 10.1074/jbc.R112.418558.

Tsukamoto, H., Shibata, K., Kajiyama, H., Terauchi, M., Nawa, A. and Kikkawa, F. (2007) 'Irradiation-induced epithelial-mesenchymal transition (EMT) related to invasive potential in endometrial carcinoma cells', *Gynecol Oncol,* 107(3), pp. 500-4. doi: 10.1016/j.ygyno.2007.08.058.

Tysnes, B. B. and Bjerkvig, R. (2007) 'Cancer initiation and progression: involvement of stem cells and the microenvironment', *Biochim Biophys Acta,* 1775(2), pp. 283-97. doi: 10.1016/j.bbcan.2007.01.001.

Ungar, D. (2009) 'Golgi linked protein glycosylation and associated diseases', *Semin Cell Dev Biol,* 20(7), pp. 762-9. doi: 10.1016/j.semcdb.2009.03.004.

Ungvari, Z., Tucsek, Z., Sosnowska, D., Toth, P., Gautam, T., Podlutsky, A., Csiszar, A., Losonczy, G., Valcarcel-Ares, M. N., Sonntag, W. E. and Csiszar, A. (2013) 'Aging-induced dysregulation of dicer1-dependent microRNA expression impairs angiogenic capacity of rat cerebromicrovascular endothelial cells', *J Gerontol A Biol Sci Med Sci,* 68(8), pp. 877-91. doi: 10.1093/gerona/gls242.

Van Deun, J., Mestdagh, P., Sormunen, R., Cocquyt, V., Vermaelen, K., Vandesompele, J., Bracke, M., De Wever, O. and Hendrix, A. (2014) 'The impact of disparate isolation methods for extracellular vesicles on downstream RNA profiling', *J Extracell Vesicles,* 3. doi: 10.3402/jev.v3.24858.

Van Slambrouck, S., Jenkins, A. R., Romero, A. E. and Steelant, W. F. (2009) 'Reorganization of the integrin alpha2 subunit controls cell adhesion and cancer cell invasion in prostate cancer', *Int J Oncol,* 34(6), pp. 1717-26.

Vander Griend, D. J., Karthaus, W. L., Dalrymple, S., Meeker, A., DeMarzo, A. M. and Isaacs, J. T. (2008) 'The role of CD133 in normal human prostate stem cells and malignant cancer-initiating cells', *Cancer Res,* 68(23), pp. 9703-11. doi: 10.1158/0008-5472.CAN-08-3084.

Varelas, X., Bouchie, M. P. and Kukuruzinska, M. A. (2014) 'Protein N-glycosylation in oral cancer: dysregulated cellular networks among DPAGT1, E-cadherin adhesion and canonical Wnt signaling', *Glycobiology,* 24(7), pp. 579-91. doi: 10.1093/glycob/cwu031.

Vares, G., Cui, X., Wang, B., Nakajima, T. and Nenoi, M. (2013) 'Generation of breast cancer stem cells by steroid hormones in irradiated human mammary cell lines', *PLoS One,* 8(10), pp. e77124. doi: 10.1371/journal.pone.0077124.

Varki, A., Kannagi, R. and Toole, B. P. (2009) 'Glycosylation Changes in Cancer', in Varki, A., Cummings, R.D., Esko, J.D., Freeze, H.H., Stanley, P., Bertozzi, C.R., Hart, G.W. & Etzler, M.E. (eds.) *Essentials of Glycobiology.* 2nd edn. Cold Spring Harbor (NY).

Varki, A. P., Baum, L. G., Bellis, S. L., Cummings, R. D., Esko, J. D., Hart, G. W., Linhardt, R. J., Lowe, J. B., McEver, R. P., Srivastava, A. and Sarkar, R. (2008) 'Working group report: the roles of glycans in hemostasis, inflammation and vascular biology', *Glycobiology,* 18(10), pp. 747-9. doi: 10.1093/glycob/cwn065.

Vazquez-Santillan, K., Melendez-Zajgla, J., Jimenez-Hernandez, L. E., Gaytan-Cervantes, J., Munoz-Galindo, L., Pina-Sanchez, P., Martinez-Ruiz, G., Torres, J., Garcia-Lopez, P., Gonzalez-Torres, C., Ruiz, V., Avila-Moreno, F., Velasco-Velazquez, M., Perez-Tapia, M. and Maldonado, V. (2016) 'NF-kappaB-inducing kinase regulates stem cell phenotype in breast cancer', *Sci Rep,* 7, pp. 44971. doi: 10.1038/srep44971.

Verbrugge, I., de Vries, E., Tait, S. W., Wissink, E. H., Walczak, H., Verheij, M. and Borst, J. (2008) 'Ionizing radiation modulates the TRAIL death-inducing signaling complex, allowing bypass of the mitochondrial apoptosis pathway', *Oncogene,* 27(5), pp. 574-84. doi: 10.1038/sj.onc.1210696.

Vesuna, F., Lisok, A., Kimble, B. and Raman, V. (2009) 'Twist modulates breast cancer stem cells by transcriptional regulation of CD24 expression', *Neoplasia,* 11(12), pp. 1318-28.

Vignard, J., Mirey, G. and Salles, B. (2013) 'Ionizing-radiation induced DNA double-strand breaks: a direct and indirect lighting up', *Radiother Oncol,* 108(3), pp. 362-9. doi: 10.1016/j.radonc.2013.06.013.

Vilenchik, M. M. and Knudson, A. G. (2006) 'Radiation dose-rate effects, endogenous DNA damage, and signaling resonance', *Proc Natl Acad Sci U S A,* 103(47), pp. 17874-9. doi: 10.1073/pnas.0607995103.

Vinken, M. (2012) 'Gap junctions and non-neoplastic liver disease', *J Hepatol,* 57(3), pp. 655-62. doi: 10.1016/j.jhep.2012.02.036.

Vouri, M., Croucher, D. R., Kennedy, S. P., An, Q., Pilkington, G. J. and Hafizi, S. (2016) 'Axl-EGFR receptor tyrosine kinase hetero-interaction provides EGFR with access to pro-invasive signalling in cancer cells', *Oncogenesis,* 5(10), pp. e266. doi: 10.1038/oncsis.2016.66.

Vulpis, E., Cecere, F., Molfetta, R., Soriani, A., Fionda, C., Peruzzi, G., Caracciolo, G., Palchetti, S., Masuelli, L., Simonelli, L., D'Oro, U., Abruzzese, M. P., Petrucci, M. T., Ricciardi, M. R., Paolini, R., Cippitelli, M., Santoni, A. and Zingoni, A. (2017) 'Genotoxic stress modulates the release of exosomes from multiple myeloma cells capable of activating NK cell cytokine production: Role of HSP70/TLR2/NF-kB axis', *Oncoimmunology,* 6(3), pp. e1279372. doi: 10.1080/2162402X.2017.1279372.

Vuong, D., Simpson, P. T., Green, B., Cummings, M. C. and Lakhani, S. R. (2014) 'Molecular classification of breast cancer', *Virchows Arch,* 465(1), pp. 1-14. doi: 10.1007/s00428-014-1593-7.

Vuoriluoto, K., Haugen, H., Kiviluoto, S., Mpindi, J. P., Nevo, J., Gjerdrum, C., Tiron, C., Lorens, J. B. and Ivaska, J. (2011) 'Vimentin regulates EMT induction by Slug and oncogenic H-Ras and migration by governing Axl expression in breast cancer', *Oncogene,* 30(12), pp. 1436-48. doi: 10.1038/onc.2010.509.

Wahid, F., Shehzad, A., Khan, T. and Kim, Y. Y. (2010) 'MicroRNAs: synthesis, mechanism, function, and recent clinical trials', *Biochim Biophys Acta,* 1803(11), pp. 1231-43. doi: 10.1016/j.bbamcr.2010.06.013.

Wakeford, R. (2004) 'The cancer epidemiology of radiation', *Oncogene,* 23(38), pp. 6404-28. doi: 10.1038/sj.onc.1207896.

Wang, J. L., Yu, J. P., Sun, Z. Q. and Sun, S. P. (2014a) 'Radiobiological characteristics of cancer stem cells from esophageal cancer cell lines', *World J Gastroenterol,* 20(48), pp. 18296-305. doi: 10.3748/wjg.v20.i48.18296.

Wang, K. and Tang, J. (2010) '[Tumour-derived exosomes and their roles in cancer]', *Zhong Nan Da Xue Xue Bao Yi Xue Ban,* 35(12), pp. 1288-92. doi: 10.3969/j.issn.1672-7347.2010.12.015.

Wang, K., Wu, X., Wang, J. and Huang, J. (2013a) 'Cancer stem cell theory: therapeutic implications for nanomedicine', *Int J Nanomedicine,* 8, pp. 899-908. doi: 10.2147/IJN.S38641.

Wang, L., Huang, X., Zheng, X., Wang, X., Li, S., Zhang, L., Yang, Z. and Xia, Z. (2013b) 'Enrichment of prostate cancer stem-like cells from human prostate cancer cell lines by culture in serum-free medium and chemoradiotherapy', *Int J Biol Sci,* 9(5), pp. 472-9. doi: 10.7150/ijbs.5855.

Wang, T., Liu, Y. P., Wang, T., Xu, B. Q. and Xu, B. (2017) 'ROS feedback regulates the microRNA-19-targeted inhibition of the p47phox-mediated LPS-induced inflammatory response', *Biochem Biophys Res Commun,* 489(4), pp. 361-368. doi: 10.1016/j.bbrc.2017.05.022.

Wang, W., Lin, H., Zhou, L., Zhu, Q., Gao, S., Xie, H., Liu, Z., Xu, Z., Wei, J., Huang, X. and Zheng, S. (2014b) 'MicroRNA-30a-3p inhibits tumor proliferation, invasiveness and metastasis and is downregulated in hepatocellular carcinoma', *Eur J Surg Oncol,* 40(11), pp. 1586-94. doi: 10.1016/j.ejso.2013.11.008.

Wang, Y., Liu, J., Ying, X., Lin, P. C. and Zhou, B. P. (2016) 'Twist-mediated Epithelial-mesenchymal Transition Promotes Breast Tumor Cell Invasion via Inhibition of Hippo Pathway', *Sci Rep,* 6, pp. 24606. doi: 10.1038/srep24606.

Warzecha, C. C. and Carstens, R. P. (2012) 'Complex changes in alternative pre-mRNA splicing play a central role in the epithelial-to-mesenchymal transition (EMT)', *Semin Cancer Biol,* 22(5-6), pp. 417-27. doi: 10.1016/j.semcancer.2012.04.003.

Wei, J., Xu, G., Wu, M., Zhang, Y., Li, Q., Liu, P., Zhu, T., Song, A., Zhao, L., Han, Z., Chen, G., Wang, S., Meng, L., Zhou, J., Lu, Y., Wang, S. and Ma, D. (2008) 'Overexpression of vimentin contributes to prostate cancer invasion and metastasis via src regulation', *Anticancer Res,* 28(1A), pp. 327-34.

Welinder, C. and Ekblad, L. (2011) 'Coomassie staining as loading control in Western blot analysis', *J Proteome Res,* 10(3), pp. 1416-9. doi: 10.1021/pr1011476.

Wellner, U., Schubert, J., Burk, U. C., Schmalhofer, O., Zhu, F., Sonntag, A., Waldvogel, B., Vannier, C., Darling, D., zur Hausen, A., Brunton, V. G., Morton, J., Sansom, O., Schuler, J., Stemmler, M. P., Herzberger, C., Hopt, U., Keck, T., Brabletz, S. and Brabletz, T. (2009) 'The EMT-activator ZEB1 promotes tumorigenicity by repressing stemness-inhibiting microRNAs', *Nat Cell Biol,* 11(12), pp. 1487-95. doi: 10.1038/ncb1998.

Wendt, M. K., Schiemann, B. J., Parvani, J. G., Lee, Y. H., Kang, Y. and Schiemann, W. P. (2013) 'TGF-beta stimulates Pyk2 expression as part of an epithelial-mesenchymal transition program required for metastatic outgrowth of breast cancer', *Oncogene,* 32(16), pp. 2005-15. doi: 10.1038/onc.2012.230.

Wicha, M. S., Liu, S. and Dontu, G. (2006) 'Cancer stem cells: an old idea--a paradigm shift', *Cancer Res,* 66(4), pp. 1883-90; discussion 1895-6. doi: 10.1158/0008-5472.CAN-05-3153.

Widel, M., Przybyszewski, W. M., Cieslar-Pobuda, A., Saenko, Y. V. and Rzeszowska-Wolny, J. (2012) 'Bystander normal human fibroblasts reduce damage response in radiation

targeted cancer cells through intercellular ROS level modulation', *Mutat Res,* 731(1-2), pp. 117-24. doi: 10.1016/j.mrfmmm.2011.12.007.

Wright, H. J., Hou, J., Xu, B., Cortez, M., Potma, E. O., Tromberg, B. J. and Razorenova, O. V. (2017) 'CDCP1 drives triple-negative breast cancer metastasis through reduction of lipid-droplet abundance and stimulation of fatty acid oxidation', *Proc Natl Acad Sci U S A*. doi: 10.1073/pnas.1703791114.

Wu, A., Wu, K., Li, J., Mo, Y., Lin, Y., Wang, Y., Shen, X., Li, S., Li, L. and Yang, Z. (2015) 'Let-7a inhibits migration, invasion and epithelial-mesenchymal transition by targeting HMGA2 in nasopharyngeal carcinoma', *J Transl Med,* 13, pp. 105. doi: 10.1186/s12967-015-0462-8.

Wu, D., Li, B., Liu, H., Yuan, M., Yu, M., Tao, L., Dong, S. and Tong, X. (2018) 'In vitro inhibited effect of gap junction composed of Cx43 in the invasion and metastasis of testicular cancer resistanced to cisplatin', *Biomed Pharmacother,* 98, pp. 826-833. doi: 10.1016/j.biopha.2018.01.016.

Wu, L. J., Randers-Pehrson, G., Xu, A., Waldren, C. A., Geard, C. R., Yu, Z. and Hei, T. K. (1999) 'Targeted cytoplasmic irradiation with alpha particles induces mutations in mammalian cells', *Proc Natl Acad Sci U S A,* 96(9), pp. 4959-64.

Xiao, Y. Q., Freire-de-Lima, C. G., Schiemann, W. P., Bratton, D. L., Vandivier, R. W. and Henson, P. M. (2008) 'Transcriptional and translational regulation of TGF-beta production in response to apoptotic cells', *J Immunol,* 181(5), pp. 3575-85.

Xuan, Y., Yang, H., Zhao, L., Lau, W. B., Lau, B., Ren, N., Hu, Y., Yi, T., Zhao, X., Zhou, S. and Wei, Y. (2015) 'MicroRNAs in colorectal cancer: small molecules with big functions', *Cancer Lett,* 360(2), pp. 89-105. doi: 10.1016/j.canlet.2014.11.051.

Xue, J., Lin, X., Chiu, W. T., Chen, Y. H., Yu, G., Liu, M., Feng, X. H., Sawaya, R., Medema, R. H., Hung, M. C. and Huang, S. (2014) 'Sustained activation of SMAD3/SMAD4 by FOXM1 promotes TGF-beta-dependent cancer metastasis', *J Clin Invest,* 124(2), pp. 564-79. doi: 10.1172/JCI71104.

Yahyapour, R., Motevaseli, E., Rezaeyan, A., Abdollahi, H., Farhood, B., Cheki, M., Najafi, M. and Villa, V. (2018) 'Mechanisms of Radiation Bystander and Non-Targeted Effects: Implications to Radiation Carcinogenesis and Radiotherapy', *Curr Radiopharm,* 11(1), pp. 34-45. doi: 10.2174/1874471011666171229123130.

Yamamoto, M., Sakane, K., Tominaga, K., Gotoh, N., Niwa, T., Kikuchi, Y., Tada, K., Goshima, N., Semba, K. and Inoue, J. I. (2017) 'Intratumoral bidirectional transitions between epithelial and mesenchymal cells in triple-negative breast cancer', *Cancer Sci,* 108(6), pp. 1210-1222. doi: 10.1111/cas.13246.

Yamashita, S., Miyagi, C., Fukada, T., Kagara, N., Che, Y. S. and Hirano, T. (2004) 'Zinc transporter LIVI controls epithelial-mesenchymal transition in zebrafish gastrula organizer', *Nature,* 429(6989), pp. 298-302. doi: 10.1038/nature02545.

Yan, J., Ma, C. and Gao, Y. (2017) 'MicroRNA-30a-5p suppresses epithelial-mesenchymal transition by targeting profilin-2 in high invasive non-small cell lung cancer cell lines', *Oncol Rep,* 37(5), pp. 3146-3154. doi: 10.3892/or.2017.5566.

Yan, T., Lin, Z., Jiang, J., Lu, S., Chen, M., Que, H., He, X., Que, G., Mao, J., Xiao, J. and Zheng, Q. (2015) 'MMP14 regulates cell migration and invasion through epithelial-mesenchymal transition in nasopharyngeal carcinoma', *Am J Transl Res,* 7(5), pp. 950-8.

Yan, Y., Zuo, X. and Wei, D. (2015) 'Concise Review: Emerging Role of CD44 in Cancer Stem Cells: A Promising Biomarker and Therapeutic Target', *Stem Cells Transl Med,* 4(9), pp. 1033-43. doi: 10.5966/sctm.2015-0048.

Yang, C., Kim, S. H., Bianco, N. R. and Robbins, P. D. (2011) 'Tumor-derived exosomes confer antigen-specific immunosuppression in a murine delayed-type hypersensitivity model', *PLoS One,* 6(8), pp. e22517. doi: 10.1371/journal.pone.0022517.

Yang, C. M., Ji, S., Li, Y., Fu, L. Y., Jiang, T. and Meng, F. D. (2017) 'Beta-Catenin promotes cell proliferation, migration, and invasion but induces apoptosis in renal cell carcinoma', *Onco Targets Ther,* 10, pp. 711-724. doi: 10.2147/OTT.S117933.

Yang, D., Elner, S. G., Bian, Z. M., Till, G. O., Petty, H. R. and Elner, V. M. (2007) 'Pro-inflammatory cytokines increase reactive oxygen species through mitochondria and NADPH oxidase in cultured RPE cells', *Exp Eye Res,* 85(4), pp. 462-72. doi: 10.1016/j.exer.2007.06.013.

Yang, J., Hou, Y., Zhou, M., Wen, S., Zhou, J., Xu, L., Tang, X., Du, Y. E., Hu, P. and Liu, M. (2016) 'Twist induces epithelial-mesenchymal transition and cell motility in breast cancer via ITGB1-FAK/ILK signaling axis and its associated downstream network', *Int J Biochem Cell Biol,* 71, pp. 62-71. doi: 10.1016/j.biocel.2015.12.004.

Yang, R., Hong, H., Wang, M. and Ma, Z. (2018a) 'Correlation Between Single-Nucleotide Polymorphisms Within miR-30a and Related Target Genes and Risk or Prognosis of Nephrotic Syndrome', *DNA Cell Biol,* 37(3), pp. 233-243. doi: 10.1089/dna.2017.4024.

Yang, Y., Lian, M., Feng, L., Wang, R., Shi, Q., Zhai, J., Liu, X. and Fang, J. (2018b) 'Array profiling identified dysregulated miRNAs and target genes and pathways in laryngeal squamous cell carcinoma', *Int J Clin Exp Med* 11(3), pp. 1973-1983.

Yen, E. Y., Miaw, S. C., Yu, J. S. and Lai, I. R. (2017) 'Exosomal TGF-β1 is correlated with lymphatic metastasis of gastric cancers

', *Am J Cancer Res* 7(11), pp. 2199-2208.

Yersal, O. and Barutca, S. (2014) 'Biological subtypes of breast cancer: Prognostic and therapeutic implications', *World J Clin Oncol,* 5(3), pp. 412-24. doi: 10.5306/wjco.v5.i3.412.

Yeung, T. M., Gandhi, S. C., Wilding, J. L., Muschel, R. and Bodmer, W. F. (2010) 'Cancer stem cells from colorectal cancer-derived cell lines', *Proc Natl Acad Sci U S A,* 107(8), pp. 3722-7. doi: 10.1073/pnas.0915135107.

Yin, H. L., Wu, C. C., Lin, C. H., Chai, C. Y., Hou, M. F., Chang, S. J., Tsai, H. P., Hung, W. C., Pan, M. R. and Luo, C. W. (2016) 'Beta 1 integrin as a prognostic and predictive marker in triple-negative breast cancer', *Int J Mol Sci,* 17(9). doi: 10.3390/ijms17091432.

Yoshino, H. and Kashiwakura, I. (2017) 'Involvement of reactive oxygen species in ionizing radiation-induced upregulation of cell surface Toll-like receptor 2 and 4 expression in human monocytic cells', *J Radiat Res,* 58(5), pp. 626-635. doi: 10.1093/jrr/rrx011.

Young, A. G. H. and Bennewith, K. L. (2017) 'Ionizing Radiation Enhances Breast Tumor Cell Migration In Vitro', *Radiat Res,* 188(4), pp. 381-391. doi: 10.1667/RR14738.1.

Yu, J. R., Tai, Y., Jin, Y., Hammell, M. C., Wilkinson, J. E., Roe, J. S., Vakoc, C. R. and Van Aelst, L. (2015) 'TGF-beta/Smad signaling through DOCK4 facilitates lung adenocarcinoma metastasis', *Genes Dev,* 29(3), pp. 250-61. doi: 10.1101/gad.248963.114.

Yu, Z., Zhao, S., Ren, L., Wang, L., Chen, Z., Hoffman, R. M. and Zhou, J. (2017) 'Pancreatic cancer-derived exosomes promote tumor metastasis and liver pre-metastatic niche formation', *Oncotarget*. doi: 10.18632/oncotarget.18831.

Zangar, R. C., Davydov, D. R. and Verma, S. (2004) 'Mechanisms that regulate production of reactive oxygen species by cytochrome P450', *Toxicol Appl Pharmacol,* 199(3), pp. 316-31. doi: 10.1016/j.taap.2004.01.018.

Zaravinos, A., Radojicic, J., Lambrou, G. I., Volanis, D., Delakas, D., Stathopoulos, E. N. and Spandidos, D. A. (2012) 'Expression of miRNAs involved in angiogenesis, tumor cell proliferation, tumor suppressor inhibition, epithelial-mesenchymal transition and activation of metastasis in bladder cancer', *J Urol,* 188(2), pp. 615-23. doi: 10.1016/j.juro.2012.03.122.

Zhang, F., Li, T., Han, L., Qin, P., Wu, Z., Xu, B., Gao, Q. and Song, Y. (2018) 'TGFbeta1-induced down-regulation of microRNA-138 contributes to epithelial-mesenchymal transition in

primary lung cancer cells', *Biochem Biophys Res Commun*. doi: 10.1016/j.bbrc.2018.01.164.

Zhang, L., Zhang, X. W., Liu, C. H., Lu, K., Huang, Y. Q., Wang, Y. D., Xing, L., Zhang, L. J., Liu, N., Jiang, H., Sun, C., Yang, Y., Chen, S. Q., Chen, M. and Xu, B. (2016) 'miRNA-30a functions as a tumor suppressor by downregulating cyclin E2 expression in castration-resistant prostate cancer', *Mol Med Rep,* 14(3), pp. 2077-84. doi: 10.3892/mmr.2016.5469.

Zhang, Z., Wang, C., Li, T., Liu, Z. and Li, L. (2014) 'Comparison of ultracentrifugation and density gradient separation methods for isolating Tca8113 human tongue cancer cell line-derived exosomes', *Oncol Lett,* 8(4), pp. 1701-1706. doi: 10.3892/ol.2014.2373.

Zhao, R., Wu, Z. and Zhou, Q. (2011) '[Epithelial-mesenchymal transition and tumor metastasis]', *Zhongguo Fei Ai Za Zhi,* 14(7), pp. 620-4. doi: 10.3779/j.issn.1009-3419.2011.07.11.

Zheng, G., Lyons, J. G., Tan, T. K., Wang, Y., Hsu, T. T., Min, D., Succar, L., Rangan, G. K., Hu, M., Henderson, B. R., Alexander, S. I. and Harris, D. C. (2009) 'Disruption of E-cadherin by matrix metalloproteinase directly mediates epithelial-mesenchymal transition downstream of transforming growth factor-beta1 in renal tubular epithelial cells', *Am J Pathol,* 175(2), pp. 580-91. doi: 10.2353/ajpath.2009.080983.

Zheng, J., Li, Y., Yang, J., Liu, Q., Shi, M., Zhang, R., Shi, H., Ren, Q., Ma, J., Guo, H., Tao, Y., Xue, Y., Jiang, N., Yao, L. and Liu, W. (2011) 'NDRG2 inhibits hepatocellular carcinoma adhesion, migration and invasion by regulating CD24 expression', *BMC Cancer,* 11, pp. 251:1-9. doi: 10.1186/1471-2407-11-251.

Zhou, L., Liu, F., Wang, X. and Ouyang, G. (2015) 'The roles of microRNAs in the regulation of tumor metastasis', *Cell Biosci,* 5, pp. 32. doi: 10.1186/s13578-015-0028-8.

Zhou, Q., Yang, M., Lan, H. and Yu, X. (2013) 'miR-30a negatively regulates TGF-beta1-induced epithelial-mesenchymal transition and peritoneal fibrosis by targeting Snai1', *Am J Pathol,* 183(3), pp. 808-19. doi: 10.1016/j.ajpath.2013.05.019.

Zhou, S., Fang, Z., Wang, G. and Wu, S. (2017) 'Gap junctional intercellular communication dysfunction mediates the cognitive impairment induced by cerebral ischemia-reperfusion injury: PI3K/Akt pathway involved', *Am J Transl Res,* 9(12), pp. 5442-5451.

Zhou, Y., Xia, L., Wang, H., Oyang, L., Su, M., Liu, Q., Lin, J., Tan, S., Tian, Y., Liao, Q. and Cao, D. (2018) 'Cancer stem cells in progression of colorectal cancer', *Oncotarget,* 9(70), pp. 33403-33415. doi: 10.18632/oncotarget.23607.

Zhou, Y. C., Liu, J. Y., Li, J., Zhang, J., Xu, Y. Q., Zhang, H. W., Qiu, L. B., Ding, G. R., Su, X. M., Mei, S. and Guo, G. Z. (2011) 'Ionizing radiation promotes migration and invasion of cancer cells through transforming growth factor-beta-mediated epithelial-mesenchymal transition', *Int J Radiat Oncol Biol Phys,* 81(5), pp. 1530-7. doi: 10.1016/j.ijrobp.2011.06.1956.

Zhou, Z. N., Sharma, V. P., Beaty, B. T., Roh-Johnson, M., Peterson, E. A., Van Rooijen, N., Kenny, P. A., Wiley, H. S., Condeelis, J. S. and Segall, J. E. (2014) 'Autocrine HBEGF expression promotes breast cancer intravasation, metastasis and macrophage-independent invasion in vivo', *Oncogene,* 33(29), pp. 3784-93. doi: 10.1038/onc.2013.363.

Zhu, B. and Zhou, X. (2011) '[The study of PI3K/AKT pathway in lung cancer metastasis and drug resistance]', *Zhongguo Fei Ai Za Zhi,* 14(8), pp. 689-94. doi: 10.3779/j.issn.1009-3419.2011.08.10.

Zhu, G. J., Song, P. P., Zhou, H., Shen, X. H., Wang, J. G., Ma, X. F., Gu, Y. J., Liu, D. D., Feng, A. N., Qian, X. Y. and Gao, X. (2018) 'Role of epithelial-mesenchymal transition markers E-cadherin, N-cadherin, beta-catenin and ZEB2 in laryngeal squamous cell carcinoma', *Oncol Lett,* 15(3), pp. 3472-3481. doi: 10.3892/ol.2018.7751.

Zhu, J., He, J., Liu, Y., Simeone, D. M. and Lubman, D. M. (2012) 'Identification of glycoprotein markers for pancreatic cancer CD24+CD44+ stem-like cells using nano-LC-MS/MS and tissue microarray', *J Proteome Res,* 11(4), pp. 2272-81. doi: 10.1021/pr201059g.

Zhu, Q. S., Rosenblatt, K., Huang, K. L., Lahat, G., Brobey, R., Bolshakov, S., Nguyen, T., Ding, Z., Belousov, R., Bill, K., Luo, X., Lazar, A., Dicker, A., Mills, G. B., Hung, M. C. and Lev, D. (2011a) 'Vimentin is a novel AKT1 target mediating motility and invasion', *Oncogene,* 30(4), pp. 457-70. doi: 10.1038/onc.2010.421.

Zhu, Q. S., Rosenblatt, k., Huang, K. L., Lahat, T., G., Brobey, R., Bolshakov, S., Nguyen, T., Ding, Z., Belousov, R., Bill, K., Luo, X., Lazar, A., Dicker, A., Mills, G. B., M.C., H. and Lev, D. (2011b) ' Vimentin is a novel AKT1 target mediating motility and invasion. ', *Oncogene,* 30, pp. 457-70.

Zhu, W., Leber, B. and Andrews, D. W. (2001) 'Cytoplasmic O-glycosylation prevents cell surface transport of E-cadherin during apoptosis', *EMBO J,* 20(21), pp. 5999-6007. doi: 10.1093/emboj/20.21.5999.

Zoller, M. (2015) 'CD44, Hyaluronan, the Hematopoietic Stem Cell, and Leukemia-Initiating Cells', *Front Immunol,* 6, pp. 235. doi: 10.3389/fimmu.2015.00235.